frontiers | Research Topics

Advances of endocrine and metabolic cardiovascular outcomes: From basic to clinical science, volume II

Edited by
Si Jin, Ye Ding, Chengqi Xu and Qiulun Lu

Published in
Frontiers in Endocrinology

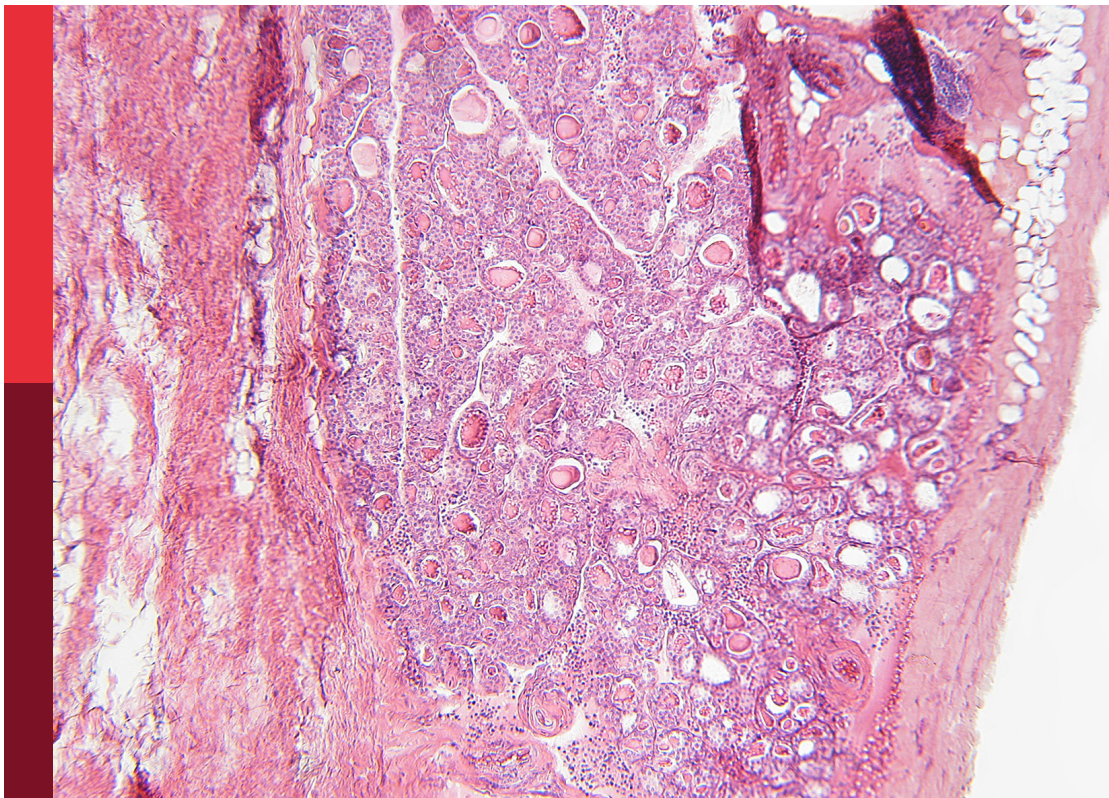

ISSN 1664-8714
ISBN 978-2-83251-465-8
DOI 10.3389/978-2-83251-465-8

About Frontiers

Frontiers is more than just an open access publisher of scholarly articles: it is a pioneering approach to the world of academia, radically improving the way scholarly research is managed. The grand vision of Frontiers is a world where all people have an equal opportunity to seek, share and generate knowledge. Frontiers provides immediate and permanent online open access to all its publications, but this alone is not enough to realize our grand goals.

Frontiers journal series

The Frontiers journal series is a multi-tier and interdisciplinary set of open-access, online journals, promising a paradigm shift from the current review, selection and dissemination processes in academic publishing. All Frontiers journals are driven by researchers for researchers; therefore, they constitute a service to the scholarly community. At the same time, the *Frontiers journal series* operates on a revolutionary invention, the tiered publishing system, initially addressing specific communities of scholars, and gradually climbing up to broader public understanding, thus serving the interests of the lay society, too.

Dedication to quality

Each Frontiers article is a landmark of the highest quality, thanks to genuinely collaborative interactions between authors and review editors, who include some of the world's best academicians. Research must be certified by peers before entering a stream of knowledge that may eventually reach the public - and shape society; therefore, Frontiers only applies the most rigorous and unbiased reviews. Frontiers revolutionizes research publishing by freely delivering the most outstanding research, evaluated with no bias from both the academic and social point of view. By applying the most advanced information technologies, Frontiers is catapulting scholarly publishing into a new generation.

What are Frontiers Research Topics?

Frontiers Research Topics are very popular trademarks of the *Frontiers journals series*: they are collections of at least ten articles, all centered on a particular subject. With their unique mix of varied contributions from Original Research to Review Articles, Frontiers Research Topics unify the most influential researchers, the latest key findings and historical advances in a hot research area.

Find out more on how to host your own Frontiers Research Topic or contribute to one as an author by contacting the Frontiers editorial office: frontiersin.org/about/contact

Advances of endocrine and metabolic cardiovascular outcomes: From basic to clinical science, volume II

Topic editors

Si Jin — Huazhong University of Science and Technology, China
Ye Ding — Georgia State University, United States
Chengqi Xu — Huazhong University of Science and Technology, China
Qiulun Lu — Nanjing Medical University, China

Citation

Jin, S., Ding, Y., Xu, C., Lu, Q., eds. (2023). *Advances of endocrine and metabolic cardiovascular outcomes: From basic to clinical science, volume II*.
Lausanne: Frontiers Media SA. doi: 10.3389/978-2-83251-465-8

Table of contents

frontiers | Frontiers in Endocrinology

TYPE Editorial
PUBLISHED 12 January 2023
DOI 10.3389/fendo.2022.1114632

OPEN ACCESS

EDITED AND REVIEWED BY
Ralf Jockers,
Université de Paris, France

*CORRESPONDENCE
Si Jin
Jinsi@hust.edu.cn

SPECIALTY SECTION
This article was submitted to Cellular Endocrinology, a section of the journal Frontiers in Endocrinology

RECEIVED 02 December 2022
ACCEPTED 27 December 2022
PUBLISHED 12 January 2023

CITATION
Cheng W, Ding Y, Xu C, Lu Q and Jin S (2023) Editorial: Advances of endocrine and metabolic cardiovascular outcomes: From basic to clinical science, volume II. *Front. Endocrinol.* 13:1114632. doi: 10.3389/fendo.2022.1114632

Editorial: Advances of endocrine and metabolic cardiovascular outcomes: From basic to clinical science, volume II

Wenzhuo Cheng[1], Ye Ding[2], Chengqi Xu[3], Qiulun Lu[4] and Si Jin[1]*

[1]Department of Endocrinology, Institute of Geriatric Medicine, Liyuan Hospital, Tongji Medical College, Huazhong University of Science and Technology, Wuhan, China, [2]Center for Molecular and Translational Medicine, Georgia State University, Atlanta, GA, United States, [3]Key Laboratory of Molecular Biophysics of the Ministry of Education, College of Life Science and Technology and Center for Human Genome Research, Huazhong University of Science and Technology, Wuhan, China, [4]Nanjing Medical University, Nanjing, China

KEYWORDS

ASCVD, metabolic diseases, diabetes, cardiovascular diseases, endocrine dysfunctions

Editorial on the Research Topic
Advances of endocrine and metabolic cardiovascular outcomes: From basic to clinical science, volume II

There is a growing body of research on the pathogenic mechanisms of atherosclerotic cardiovascular diseases (ASCVD), which continues to be the leading cause of mortality worldwide. Endocrine and metabolic diseases, including hyperglycemia, hyperlipidemia, hyperuricemia, hypertension, overweight or obesity, *etc.*, are the main risk factors for ASCVD (1, 2). Meanwhile, more and more anti-diabetic medicines, such as sodium-glucose transporter-2 inhibitors (SGLT2i), glucagon-like peptide-1 receptor agonists (GLP-1RAs), etc., are shown to have direct cardiovascular preventive benefits in addition to decreasing blood glucose levels, which were proved by the significant reduction in 3p MACE risks, independent of glucose-lowering glucose lowering effects. However, the specific regulatory mechanisms of endocrine and metabolic disorders affecting the occurrence and development of ASCVD are not fully understood. Therefore, there is an urgent need to study the pathogenesis of cardiovascular events associated with metabolic disorders in order to develop more effective therapies aimed at preventing and slowing down disease progression. In order to better value the cardiovascular results in the treatment of endocrine and metabolic diseases, this research topic (Volume II) aims to gather current developments emphasizing in this field, both in terms of basic and clinical aspects. We have collected 9 high-quality studies covering recent, novel, clinical significance in endocrine and metabolic cardiovascular diseases in our current research topics.

Diabetic cardiomyopathy (DCM) is a serious complication of diabetes mellitus and is the leading cause of cardiac death in diabetic patients. Therefore, it is crucial to explore the pathogenesis of DCM and find new effective therapeutic targets. Ferroptosis, a novel

mode of cell death, is not fully understood in the pathogenesis of DCM. Du et al. obtained DCM model by intraperitoneal injection of streptozotocin in C57BL6 mice. Subsequently, the DCM mice were divided into two groups by the canagliflozin intervention and key aspects relevant to ferroptosis, such as total iron, Fe^{2+}, transferrin receptor 1 (TfR1), ferritin heavy-chain (FTN-H), were investigated *in vivo* and *in vitro*. They found that canagliflozin attenuates the development of DCM by inhibiting ferroptosis. Through their research, we learned that ferroptosis may be involved in the process of DCM and prevention of ferroptosis may be effective in delaying the process of DCM. Moreover, Peng et al. focused on whether endothelial cell dysfunction is associated with DCM. The previous research discovered that an endogenous S-nitrosothiol produced by eNOS called S-nitroso-L-cysteine (CSNO), may be connected to the insulin signaling pathway. In the current study, they demonstrate that CSNO treatment promotes glucose uptake by activating the insulin signaling pathway, glucose transporter 4 (GLUT4) membrane translocation. CSNO mitigates cardiomyocyte injury by reducing oxidative stress, autophagy hyperactivation and mitochondrial damage. The data from these studies will improve our understanding of how DCM occurs and offer novel therapy alternatives.

With the in-depth study of the pathogenesis of diabetes, more and more glucose-lowering drugs are used in the clinic. However, it has been a great challenge to explore therapies with good efficacy and few side effects for the overall benefit of patients. Through clinical trials, Wu et al. recruited 20 diabetic patients and 175 normal controls to assess short-term and long-term glycemic and cardiovascular benefits after washed microbiota transplantation (WMT) treatment and they identify that WMT not only improves short- and long-term blood glucose levels, but also has a more significant cardiovascular benefit. Effective glucose lowering by WMT may provide a new means for the treatment of diabetes, which requires more and more in-depth mechanistic studies to provide a theoretical basis.

It is well known that nitric oxide (NO) is strongly associated with the development of vascular disease (3). However, in addition to NO, there are many other gas molecules in the blood that contribute to vascular disease, and research in this area is relatively lacking. A review by Zhu et al. systematically summarizes hydrogen sulfide (H_2S) in many diseases such as hypertension, atherosclerosis, inflammation, and angiogenesis. Notably, focusing on crosstalk between different gas transmitters in the control of vascular diseases contributes to our better understanding of the disease and to the development of new therapeutic approaches.

The development of disease prevention and treatment strategies depends on the identification of novel biomarkers for CVDs. By examining the expression of NIMA-related kinase 6 (NEK6) in head and neck squamous cell carcinoma (HNSCC), Yang et al. found that NEK6 upregulation in HNSCC. Analysis of the results by integrating several databases showed that NEK6 is mainly involved in the metabolism of extracellular matrix and EMT processes. The level of immune cell infiltration and the expression of different immunological checkpoints were correlated with an increase in NEK6 expression. Therefore, NEK6 may be a potential prognostic indicator and indicate how patients with HNSCC will respond to immunotherapy. Through the data analysis of several databases and verification by qRT-PCR, Wang et al. successfully identify that potential genes connected to pyroptosis that may contribute to the development of diabetic retinopathy are predicted, along with the lncRNAs and miRNAs that are linked to these genes. It is worth noting that the database analysis should be used as a screening method and the screened molecules should be further experimentally validated.

Melatonin (MT) is an important endogenous neuroendocrine hormone that is involved in a variety of physiological functions. Wang et al. identify that MT therapy could reduce the excitotoxicity model caused by glutamate in R28 cells as well as the retinal damage induced by N-methyl-D-aspartic acid (NMDA) in mice. Mechanistically, MT reduces ROS levels to achieve cytoprotective effects, and this process may be regulated by PI3K-AKT and JAK-STAT signaling pathways. This study provides us with a deeper understanding of the pathogenesis of glaucoma and offers new ideas for its treatment.

Finally, in recent years, there has been a growing number of studies on new antidiabetics, of which the most popular are SGLT2i, GLP-1RA and dipeptidyl peptidase-4 inhibitor (DPP-4). With the development of the economy, Li et al. found that there was a significant increase in the number of SGLT2i and GLP-1RA prescriptions in China from 2018 to 2021, and the preference for SGLIT2i over GLP-1RA is correlated with some patient socioeconomic and prescriber factors. Age, gender, and socioeconomic situation can all have an impact on the choice of glucose-lowering medications. Through Meta analysis, Pan et al. identified that compared with DPP4 inhibitor, higher exposure to GLP-1RAs may contribute to the incretin-based treatments' cardiovascular advantages. These studies will help people with diabetes choose the right medication for them.

Conclusion and prospects

The current research subject covers the recent advancements in the study of endocrine and metabolic cardiovascular disease, including the new clinical trial index and the unique molecular regulation of basic research. Based on these findings, a more

comprehensive understanding of endocrine and metabolic cardiovascular diseases can be achieved to provide mechanical insights in the pathogenesis and pathophysiology of ASCVD formation and more potential therapeutic targets may be identified. Regarding the close relationship between endocrine or metabolic disorders and downstream cardiovascular outcomes, a call for a new subspeciality in internal medicine, cardiometabolic or metabolic cardiovascular medicine, is indeed crucial in the future.

Author contributions

All authors listed, have reviewed and edited the manuscript, and approved it for publication.

Conflict of interest

The authors declare that the research was conducted in the absence of any commercial or financial relationships that could be construed as a potential conflict of interest.

Publisher's note

References

1. Pagidipati NJ, Zheng Y, Green JB, McGuire DK, Mentz RJ, Shah S, et al. Association of obesity with cardiovascular outcomes in patients with type 2 diabetes and cardiovascular disease: Insights from TECOS. *Am Heart J* (2020) 219:47–57. doi: 10.1016/j.ahj.2019.09.016

2. Czerniuk MR, Surma S, Romańczyk M, Nowak JM, Wojtowicz A, Filipiak KJ. Unexpected relationships: Periodontal diseases: Atherosclerosis-plaque destabilization? from the teeth to a coronary event. *Biology* (2022) 11(2):272. doi: 10.3390/biology11020272

3. Förstermann U, Xia N, Li H. Roles of vascular oxidative stress and nitric oxide in the pathogenesis of atherosclerosis. *Circ Res* (2017) 120(4):713–35. doi: 10.1161/CIRCRESAHA.116.309326

frontiers | Frontiers in Endocrinology

ORIGINAL RESEARCH
published: 26 May 2022
doi: 10.3389/fendo.2022.893971

Exposure–Response Analysis of Cardiovascular Outcome Trials With Incretin-Based Therapies

Qi Pan[1†], *Mingxia Yuan*[2†] *and Lixin Guo*[1*]

[1] Department of Endocrinology, Beijing Hospital, National Center of Gerontology, Institute of Geriatric Medicine, Chinese Academy of Medical Science, Beijing, China, [2] Department of Endocrinology, Beijing Friendship Hospital, Capital Medical University, Beijing, China

Our study aimed to evaluate the exposure–response relationship between incretin-based medications and the risk of major adverse cardiovascular events (MACE) using cardiovascular outcome trials (CVOTs). Eleven CVOTs with incretin-based medications were included. The median follow-up time, percentage of time exposure, and hazard ratio (HR) of MACE were obtained from each CVOT. The pharmacokinetic parameters of glucagon-like peptide-1 receptor agonists (GLP-1 RAs) and dipeptidyl peptidase-4 inhibitor (DPP-4) were obtained from published studies. Regression analysis was performed to assess the relationship between drug exposure and MACE HR. Cutoff values were determined from the ROC curves. The linear regression results indicated that log C_{max}, log $AUC_{0–24h}$, and log AUC_{CVOT} are negatively correlated with MACE HR (R^2 = 0.8494, R^2 = 0.8728, and R^2 = 0.8372, respectively; all $p < 0.0001$). The relationship between drug exposure (log C_{max}, log $AUC_{0–24h,}$ and log AUC_{CVOT}) and MACE HR strongly corresponded with the log (inhibitor) *vs*. response curve (R^2 = 0.8383, R^2 = 0.8430, and R^2 = 0.8229, respectively). The cutoff values in the ROC curves for log C_{max}, log $AUC_{0–24h}$, and log AUC_{CVOT}, were 2.556, 3.868, and 6.947, respectively (all p = 0.007). A Fisher's exact test revealed that these cutoff values were significantly related to cardiovascular benefits (all $p < 0.05$). Our study revealed a linear exposure–response relationship between drug exposure and MACE HR. We conclude that the cardiovascular benefits of incretin-based therapies may occur with higher doses of GLP-1 RAs and with increased exposure.

Keywords: type 2 diabetes mellitus, cardiovascular outcome trials, glucagon-like peptide-1 receptor agonist, dipeptidyl peptidase-4 inhibitor, incretin

OPEN ACCESS

Edited by:
Si Jin,
Huazhong University of Science and Technology, China

Reviewed by:
Zhelong Liu,
Huazhong University of Science and Technology, China
Guangda Xiang,
General Hospital of Central Theater Command, China

***Correspondence:**
Lixin Guo
glx1218@163.com

[†]These authors have contributed equally to this work

Specialty section:
This article was submitted to Cellular Endocrinology, a section of the journal Frontiers in Endocrinology

Received: *11 March 2022*
Accepted: *22 April 2022*
Published: *26 May 2022*

Citation:
Pan Q, Yuan M and Guo L (2022) Exposure–Response Analysis of Cardiovascular Outcome Trials With Incretin-Based Therapies. Front. Endocrinol. 13:893971. doi: 10.3389/fendo.2022.893971

INTRODUCTION

Type 2 diabetes (T2DM) is frequently accompanied by various cardiovascular complications. Further, cardiovascular complications are the leading cause of disability and death in patients with T2DM (1). Numerous *in vitro* studies and animal studies have investigated the effects of dipeptidyl peptidase-4 (DPP-4) inhibitors and GLP-1 receptor agonists (GLP-1 RAs) on the cardiovascular

system (2, 3). Considering the results of cardiovascular outcome trials (CVOTs) with incretin-based medications, significant heterogeneity in cardiovascular effects could be found between DPP-4 inhibitors and GLP-1 RAs. While the results obtained with DPP-4 inhibitors (alogliptin, saxagliptin, sitagliptin, and linagliptin) demonstrated cardiovascular safety (4–7), the majority of GLP-1 RAs (including liraglutide, albiglutide, dulaglutide, and subcutaneous semaglutide) significantly decreased the risk of major adverse cardiovascular events (MACE) (8–11). Furthermore, the meta-analysis results suggested that the GLP-1RA class could reduce the risk of MACE, cardiovascular mortality, and all-cause mortality (12). However, the results of the ELIXA study with lixisenatide (cardiovascular safety) (13), the PIONEER 6 study with oral semaglutide (cardiovascular safety) (14), and the EXSCEL study with extended exenatide (a trend toward reduction in MACE) (15), cast doubt on the existence of a class effect for GLP-1 RAs.

Although our overall understanding of the cardiovascular benefits of GLP-1RAs has evolved over time, head-to-head comparisons between different incretin-based drugs in the completed CVOTs have been lacking. Hence, differences in baseline characteristics/trial execution may account for the divergent MACE results. However, evidence from several studies suggest associations between cardiovascular risk reduction and HbA1c reduction (16), non-glycemic effects (17), or time of exposure to GLP-1 RAs (18). In the present study, we evaluated the exposure–response relationship of incretin-based medications by determining the effects of drug exposure on MACE risk in cardiovascular outcome trials.

RESEARCH DESIGN AND METHODS

In total, 11 CVOTs comparing add-on therapy using a DPP-4 inhibitor or GLP-1RA with a placebo were included. HbA1c reduction, weight loss, median follow-up time, percentage of time exposure to the trial drug, and hazard ratio (HR) of 3-point MACE in each individual CVOT were obtained from the records. Although the plasma concentration of GLP-1 RAs or GLP-1 was not measured in the CVOTs, the clinical pharmacokinetic and pharmacodynamic properties of these trial drugs have previously been established and published. The maximum observed plasma concentration of GLP-1 RA or active GLP-1 (C_{max}), the mean area under the curve (AUC_{0-24h}) with multiple doses, and the total AUC in CVOT (AUC_{CVOT}) were used to assess drug exposure (**Table 1**). AUC_{CVOT} was calculated by substituting the median follow-up time and percentage of time exposure to the trial drug using Eq. 1, as follows:

$$AUC_{CVOT} = AUC_{0-24h} \times \text{Median follow} - \text{up time} \times \text{Percentage of time exposure to trial drug} \quad (1)$$

Measurements of normalized cyclic adenosine monophosphate (cAMP) production, induced by GLP-1 RAs (19), was used to calibrate C_{max}, AUC_{0-24h}, and AUC_{CVOT}. Using the calibrated C_{max}, calibrated AUC_{0-24h}, and calibrated AUC_{CVOT}, a sensitivity analysis was conducted to assess the exposure–response relationship.

STATISTICAL ANALYSES

The values of C_{max}, AUC_{0-24h}, and AUC_{CVOT} were obtained as continuous variables and analyzed after natural logarithmic transformation. Linear regression analysis was used to assess the relationship between drug exposure (log C_{max}, log AUC_{0-24h}, or log AUC_{CVOT}) and MACE HR, HbA1c reduction, and weight loss. Nonlinear regression analysis was used to examine the exposure–response relationship by fitting a log (inhibitor) *vs.* response curve. Continuous variables were evaluated using receiver operating characteristic (ROC) curves. Cutoff values were determined following an assessment of the ROC curves. Fisher's exact tests were used to compare categorical variables. A p value < 0.05 was used to determine statistical significance. All analyses were performed using GraphPad Prism 6 (GraphPad Software, San Diego, CA, USA).

RESULTS

Drug Exposure

C_{max}, AUC_{0-24h}, and AUC_{CVOT} of GLP-1 RAs and native GLP-1 are reported in **Table 2**. According to the pharmacodynamic studies of alogliptin, saxagliptin, sitagliptin, and linagliptin, the DPP4 inhibitors significantly increased native GLP-1 levels in patients with T2DM (compared with placebo), yielding an average level of ≤ 19.0 pmol/L (**Table 2** and **Figure S1**) (20–23).

Pharmacokinetic studies of GLP-1 RAs revealed that the plasma concentrations of GLP-1 RAs in T2DM patients varied significantly. The peak plasma concentration of lixisenatide was 187.2 pg/mL (38.5 pmol/L) after multiple daily injections (24), while the steady-state plasma concentration of once-weekly exenatide reached 300 pg/mL (71.4 pmol/L) after multiple

TABLE 1 | Drug exposure related parameters.

Parameters	Description
C_{max}	The maximum observed plasma concentration of GLP-1 RA or active GLP-1 with multiple doses. C_{max} represents exposure concentration of drug.
AUC_{0-24h}	The mean drug exposure is expressed as the mean area under the curve from 0–24 hours. AUC_{0-24h} represents mean exposure concentration and time of drug.
AUC_{CVOT}	Total drug exposure is expressed as the area under the curve during the median follow-up period of the individual CVOT. AUC_{CVOT} represents total exposure concentration and time of drug.

TABLE 2 | Exposure–response related parameters.

	MACE HR	Mean follow up (years)	Percentage of time exposure to trial drug	C_{max} (pmol/L)	AUC_{0-24h} (pmol·h/L)	AUC_{CVOT} (pmol·h/L)
EXAMINE (Alogliptin) (4, 20)	0.96	1.5	0.97	14.2[ac]	132	70155
SAVOR-TIMI (Saxagliptin) (5, 21)	1.00	2.1	1.00	4.8 [acd]	72[d]	55188†
TECOS (Sitagliptin) (6, 22)	0.98	3.0	1.00	19.0 [ac]	191	208926
CARMELINA (Linagliptin) (7, 23)	1.02	2.2	0.86	11.8 [ac]	136	93643
ELIXA (Lixisenatide) (13, 24)	1.02	2.1	0.88	38.5 [ae]	175	117704
EXSCEL (Exenatide OW) (15, 25)	0.91	3.2	0.76	71.4[be]	1717	1523791
LEADER (Liraglutide) (8, 26)	0.87	3.8	0.84	22000.0[ae]	524000	610501920
HARMONY (Albiglutide) (9, 27)	0.78	1.6	0.87	29178.0 [be]	622309	316182858
SUSTAIN-6 (Semaglutide 1.0 mg) (11, 28)	0.71	2.1	0.87	30000.0[be]	719143	479564039
SUSTAIN-6 (Semaglutide 0.5 mg) (11, 28)	0.77	2.1	0.87	15800.0[be]	380429	253690714
REWIND (Dulaglutide) (10, 29)	0.88	5.4	0.82	1810.0[be]	31746	51308520
PIONEER 6 (Oral semaglutide) (14, 30)	0.79	1.3	1.00	14600.0[ac]	283700	137722165

[a]*once daily.*
[b]*once weekly.*
[c]*oral administration.*
[d]*the raw data were obtained from the visual graph of the published paper.*
[e]*subcutaneous injection.*

dosing (25). In contrast, several different pharmacokinetic studies have revealed that the steady-state concentrations of other GLP-1 RAs (including dulaglutide, liraglutide, albiglutide, subcutaneous semaglutide, and oral semaglutide) reach substantially higher (nanomolar) levels (**Table 2** and **Figure S1**) (26–30).

MACE Risk in CVOTs

According to the results of our statistical analysis of the primary outcomes in the CVOTs, several of the add-on therapies demonstrated cardiovascular noninferiority when compared with placebo. These included alogliptin [EXAMINE trial, HR, 0.96; $p < 0.001$ for noninferiority and $p = 0.32$ for superiority] (4), saxagliptin (SAVOR-TIMI 53 trial, HR, 1.00; $p < 0.001$ for noninferiority and $p = 0.99$ for superiority) (5), sitagliptin (TECOS trial, HR, 0.98; $p < 0.001$ for noninferiority and $p = 0.65$ for superiority) (6), linagliptin (CARMELINA trial, HR, 1.02; $p < 0.001$ for noninferiority and $p = 0.74$ for superiority) (7), lixisenatide (ELIXA trial, HR, 1.02; $p < 0.001$ for noninferiority and $p = 0.81$ for superiority) (13), once-weekly exenatide (EXSCEL trial, HR, 0.91; $p < 0.001$ for noninferiority and $p = 0.06$ for superiority) (15), and oral semaglutide (PIONEER 6 trial, HR, 0.79; $p < 0.001$ for noninferiority and $p = 0.17$ for superiority) (14).

Conversely, liraglutide (LEADER trial, HR, 0.87; $p < 0.001$ for noninferiority and $p = 0.01$ for superiority) (8), albiglutide (HARMONY trial, HR, 0.78; $p < 0.0001$ for noninferiority and $p = 0.0006$ for superiority) (9), dulaglutide (REWIND trial, HR, 0.88; $p = 0.026$ for superiority) (10), and subcutaneous semaglutide (SUSTAIN-6 trial, HR, 0.74; $p < 0.0001$ for noninferiority and $p = 0.02$ for superiority) (11) all demonstrated cardiovascular superiority over placebo (**Table 2**).

Exposure–Response Relationship

The linear regression results demonstrate that log C_{max}, log AUC_{0-24h}, and log AUC_{CVOT} negatively correlate with MACE HR ($R^2 = 0.8494$, $R^2 = 0.8728$, and $R^2 = 0.8372$, respectively; $p < 0.0001$; **Figures 1A–C**). The relationship between drug exposure (log C_{max}, log AUC_{0-24h}, or log AUC_{CVOT}) and MACE HR showed a good correspondence with the fitted curve ($R^2 = 0.8383$; $R^2 = 0.8430$; $R^2 = 0.8229$, respectively; **Figures 1D–F**). The ROC curve was used to evaluate drug exposure and define cutoff values (**Figure 2**). For the log C_{max}, log AUC_{0-24h}, and Log AUC_{CVOT} ROC curves, the cutoff values were 2.556, 3.868, and 6.947, respectively (all $p = 0.007$). Detailed results reporting areas under the curve, sensitivity, and specificity are shown in **Table 3**. These cutoff values were all significantly related to cardiovascular superiority (all $p < 0.05$, Fisher's exact test).

A similar correlation existed in the secondary prevention cohorts with a history of CVD ($p < 0.01$; **Figure S2**), but not in the primary prevention cohorts without a history of CVD (**Supplementary Figure S3**). The relationships between drug exposure and HbA1c reduction (compared with placebo) and between drug exposure and weight loss (compared with placebo) were also examined (**Supplementary Figures S4, S5**). In both instances, statistically significant relationships were observed ($p < 0.01$). A sensitivity analysis was also performed on calibrated C_{max}, calibrated AUC_{0-}

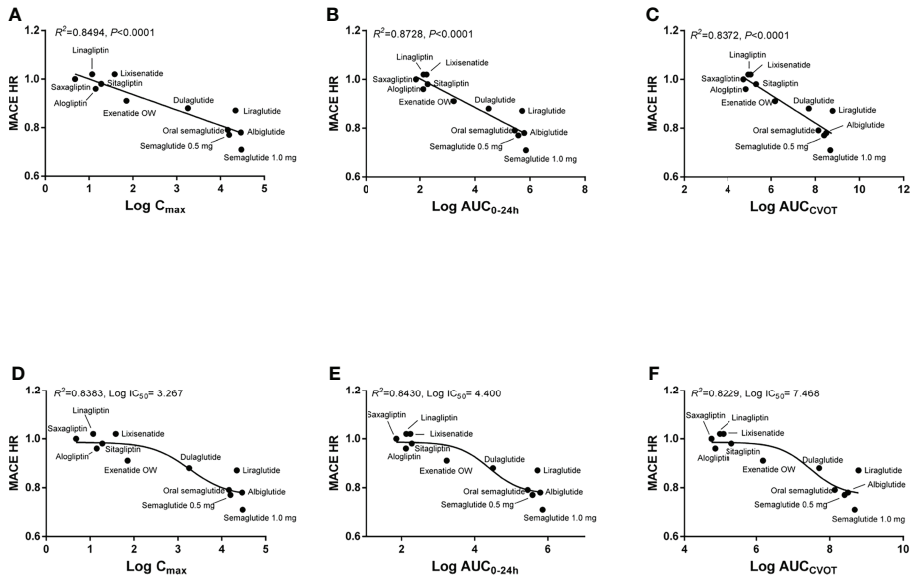

FIGURE 1 | Correlation between drug exposure and MACE HR. **(A)** Linear regression analysis between log C_{max} and MACE HR; **(B)** Linear regression analysis between log AUC_{0-24h} and MACE HR; **(C)** Linear regression analysis between log AUC_{CVOT} and MACE HR; **(D)** Nonlinear regression analysis between log C_{max} and MACE HR; **(E)** Nonlinear regression analysis between log AUC_{0-24h} and MACE HR; **(F)** Nonlinear regression analysis between log AUC_{CVOT} and MACE HR.

$_{24h}$, and calibrated AUC_{CVOT}. The results were generally consistent with the results of the aforementioned analysis (**Supplementary Figures S6–S10** and **Table S1**).

DISCUSSION

In healthy subjects, basal plasma levels of native GLP-1 are generally below 10 pmol/L, while postprandial levels of GLP-1 rise to 10–30 pmol/L (31–33). In comparison, prediabetes or T2DM subjects generally demonstrate lower basal GLP-1 levels, and/or a reduction in GLP-1 response to oral glucose load (33). DPP4 inhibitors reportedly raise the postprandial levels of native GLP-1 approximately 2–4 fold (20, 34). However, the concentrations of most GLP-1 RAs (except lixisenatide and once-weekly exenatide) are substantially higher than the reported physiological concentrations of GLP-1.

Our results indicate that the exposure concentrations of DPP4 inhibitor (lixisenatide) and once-weekly exenatide associated with cardiovascular safety are low, as the concentrations of these drugs were close to physiological levels (picomolar levels). In contrast, the exposure concentrations of other GLP-1 RAs (except oral semaglutide), which are associated with cardiovascular benefits, are higher (nanomolar levels). A strong relationship between the exposure concentration and MACE HR was demonstrated through regression analysis ($p < 0.0001$). Moreover, a good fit was obtained between the observed relationship and the theoretically constructed model. The exposure–response relationship of GLP-1 was also demonstrated in a cross-sectional study, and linear regression analysis showed that higher glucose-stimulated GLP-1 levels were associated with clinically relevant lower blood pressure (associated with beneficial effects on the cardiovascular system) (35). In addition, a strong relationship was demonstrated between the mean and total drug exposure and MACE HR.

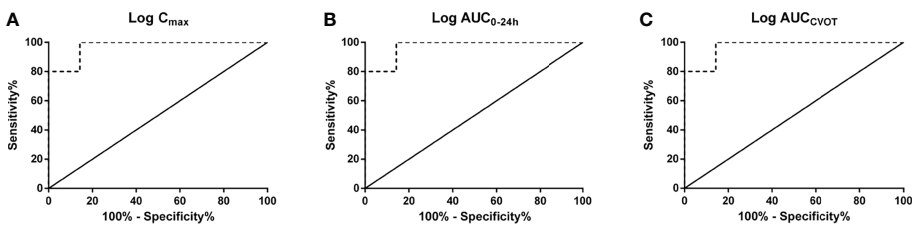

FIGURE 2 | Receiver operating characteristic (ROC) curves. **(A)** log C_{max}; **(B)** log AUC_{0-24h}; **(C)** log AUC_{CVOT}.

TABLE 3 | ROC Curves of all continuous variables.

Variable	Cutoff	P Value	Areas under the curve	Sensitivity	Specificity
Log C_{max}	2.556	0.007	0.971	100.0	85.7
Log AUC_{0-24h}	3.868	0.007	0.971	100.0	85.7
Log AUC_{CVOT}	6.947	0.007	0.971	100.0	85.7

Drug exposure is dependent on both concentration and time. When only concentration was considered, our ROC results suggest that log C_{max} > 2.556 (i.e., C_{max} > 359.7 pmol/L) could be a predictor for cardiovascular benefits. However, when both concentration and time were considered, our results indicate that log AUC_{0-24h} > 3.868 and log AUC_{CVOT} > 6.947 could be predictors for cardiovascular superiority. These results suggest that the drug should be continuously used at a steady-state C_{max} of 307.5 pmol/L per day for 3.29 years consecutively (the value was obtained by dividing AUC_{CVOT} by AUC_{0-24h}). Native GLP-1 levels when using DPP4 inhibitors and GLP-1 RA levels (lixisenatide and once-weekly exenatide) were both less than the predicted C_{max} values. Hence, these regimens show cardiovascular safety only. For PIONEER 6, the median exposure time was only 15.9 months. We predict that better results may be obtained by extending the exposure time with oral semaglutide.

The extent to which exendin-4-based agonists differ in cardiovascular effects from GLP-1-based agonists has been extensively debated. Although CVOTs do not provide evidence of any cardiovascular benefits of using exendin-4-based agonists, there is no evidence to suggest that exendin-4-based agonists attenuate activation of GLP-1 receptor signaling (2). The present study demonstrates significant associations between GLP-1 RA drug exposure and HbA1c reduction and between GLP-1 RA drug exposure and weight loss. HbA1c reduction and weight loss may both play important roles in mediating MACE benefits (16, 36). Compared with other GLP-1 RAs, the therapeutic benefits (HbA1c reduction, weight loss, and cardiovascular benefits) of using recommended and approved doses of lixisenatide or once-weekly exenatide, which reflect a tradeoff between the adverse effects and the therapeutic benefits (HbA1c reduction and weight loss) observed in phase 2–3 studies, are significantly reduced (37). Suboptimal GLP-1 RA drug exposure with exendin-4-based agonists may be a critical cause of their lack of cardiovascular benefits (similar time exposure, but lower dose exposure).

The importance of supraphysiological doses of GLP-1 was originally proposed by J.J. Holst (38). Holst considered moderately elevated GLP-1 concentrations to have a significant effect on pancreatic islets, higher concentrations to slow gastric emptying and reduce food intake, and much higher concentrations to lead to side effects (nausea, diarrhea, and vomiting) (38). Our study provides evidence to support the notion that higher GLP-1 RA drug exposure is associated with additional cardiovascular benefit.

This study has several limitations. The parameters for drug exposure were obtained from different studies and may be biased. Although the parameters for drug exposure were calibrated using normalized cAMP, a degree of bias may be inevitable. In addition, our study is based on trial level analyses using the published literature, and not on patient level analyses. Thus, some inferences based on these results may ultimately prove to be misleading.

In conclusion, our study demonstrates a good exposure–response relationship between drug exposure and MACE HR. Our results suggest that the cardiovascular benefits of incretin-based therapies may occur with higher exposure to GLP-1 RAs.

DATA AVAILABILITY STATEMENT

The original contributions presented in the study are included in the article/**Supplementary Material**. Further inquiries can be directed to the corresponding author.

AUTHOR CONTRIBUTIONS

QP, MY, contributed to data collection and analysis. LG contributed to the study design and interpretation. All authors approved the manuscript. All authors contributed to the article and approved the submitted version.

FUNDING

This work was supported by the China International Medical Foundation (grant Z-2017-26-1902).

ACKNOWLEDGMENTS

The authors acknowledge Dr. Yale Duan for his help in statistical analysis and medical writing.

SUPPLEMENTARY MATERIAL

The Supplementary Material for this article can be found online at: https://www.frontiersin.org/articles/10.3389/fendo.2022.893971/full#supplementary-material

REFERENCES

1. An Y, Zhang P, Wang J, Gong Q, Gregg EW, Yang W, et al. Cardiovascular and All-Cause Mortality Over a 23-Year Period Among Chinese With Newly Diagnosed Diabetes in the Da Qing IGT and Diabetes Study. *Diabetes Care* (2015) 38(7):1365–71. doi: 10.2337/dc14-2498
2. Drucker DJ. The Ascending GLP-1 Road From Clinical Safety to Reduction of Cardiovascular Complications. *Diabetes* (2018) 67(9):1710–9. doi: 10.2337/dbi18-0008
3. Bistola V, Lambadiari V, Dimitriadis G, Ioannidis I, Makrilakis K, Tentolouris N, et al. Possible Mechanisms of Direct Cardiovascular Impact of GLP-1 Agonists and DPP4 Inhibitors. *Heart Fail Rev* (2018) 23(3):377–88. doi: 10.1007/s10741-018-9674-3
4. White WB, Cannon CP, Heller SR, Nissen SE, Bergenstal RM, Bakris GL, et al. Alogliptin After Acute Coronary Syndrome in Patients With Type 2 Diabetes. *N Engl J Med* (2013) 369(14):1327–35. doi: 10.1056/NEJMoa1305889
5. Scirica BM, Bhatt DL, Braunwald E, Steg PG, Davidson J, Hirshberg B, et al. Saxagliptin and Cardiovascular Outcomes in Patients With Type 2 Diabetes Mellitus. *N Engl J Med* (2013) 369(14):1317–26. doi: 10.1056/NEJMoa1307684
6. Green JB, Bethel MA, Armstrong PW, Buse JB, Engel SS, Garg J, et al. Effect of Sitagliptin on Cardiovascular Outcomes in Type 2 Diabetes. *N Engl J Med* (2015) 373(3):232–42. doi: 10.1056/NEJMoa1501352
7. Rosenstock J, Perkovic V, Johansen OE, Cooper ME, Kahn SE, et al. Effect of Linagliptin vs Placebo on Major Cardiovascular Events in Adults With Type 2 Diabetes and High Cardiovascular and Renal Risk: The Carmelina Randomized Clinical Trial. *JAMA* (2019) 321(1):69–79. doi: 10.1001/jama.2018.18269
8. Marso SP, Daniels GH, Brown-Frandsen K, Kristensen P, Mann JF, Nauck MA, et al. Liraglutide and Cardiovascular Outcomes in Type 2 Diabetes. *N Engl J Med* (2016) 375(4):311–22. doi: 10.1056/NEJMoa1603827
9. Hernandez AF, Green JB, Janmohamed S, D'Agostino RB Sr, Granger CB, Jones NP, et al. Albiglutide and Cardiovascular Outcomes in Patients With Type 2 Diabetes and Cardiovascular Disease (Harmony Outcomes): A Double-Blind, Randomised Placebo-Controlled Trial. *Lancet* (2018) 392(10157):1519–29. doi: 10.1016/S0140-6736(18)32261-X
10. Gerstein HC, Colhoun HM, Dagenais GR, Diaz R, Lakshmanan M, Pais P, et al. Dulaglutide and Cardiovascular Outcomes in Type 2 Diabetes (REWIND): A Double-Blind, Randomised Placebo-Controlled Trial. *Lancet* (2019) 394 (10193):121–30. doi: 10.1016/S0140-6736(19)31149-3
11. Marso SP, Bain SC, Consoli A, Eliaschewitz FG, Jódar E, Leiter LA, et al. Semaglutide and Cardiovascular Outcomes in Patients With Type 2 Diabetes. *N Engl J Med* (2016) 375(19):1834–44. doi: 10.1056/NEJMoa1607141
12. Bethel MA, Patel RA, Merrill P, Lokhnygina Y, Buse JB, Mentz RJ, et al. Cardiovascular Outcomes With Glucagon-Like Peptide-1 Receptor Agonists in Patients With Type 2 Diabetes: A Meta-Analysis. *Lancet Diabetes Endocrinol* (2018) 6(2):105–13. doi: 10.1016/S2213-8587(17)30412-6
13. Pfeffer MA, Claggett B, Diaz R, Dickstein K, Gerstein HC, Køber LV, et al. Lixisenatide in Patients With Type 2 Diabetes and Acute Coronary Syndrome. *N Engl J Med* (2015) 373(23):2247–57. doi: 10.1056/NEJMoa1509225
14. Husain M, Birkenfeld AL, Donsmark M, Dungan K, Eliaschewitz FG, Franco DR, et al. Oral Semaglutide and Cardiovascular Outcomes in Patients With Type 2 Diabetes. *N Engl J Med* (2019) 381(9):841–51. doi: 10.1056/NEJMoa1901118
15. Holman RR, Bethel MA, Mentz RJ, Thompson VP, Lokhnygina Y, Buse JB, et al. Effects of Once-Weekly Exenatide on Cardiovascular Outcomes in Type 2 Diabetes. *N Engl J Med* (2017) 377(13):1228–39. doi: 10.1056/NEJMoa1612917
16. Giugliano D, Maiorino MI, Bellastella G, Chiodini P, Esposito K. Glycemic Control, Preexisting Cardiovascular Disease, and Risk of Major Cardiovascular Events in Patients With Type 2 Diabetes Mellitus: Systematic Review With Meta-Analysis of Cardiovascular Outcome Trials and Intensive Glucose Control Trials. *J Am Heart Assoc* (2019) 8(12):e012356. doi: 10.1161/JAHA.119.012356
17. Nauck MA, Meier JJ, Cavender MA, Abd El Aziz M, Drucker DJ. Cardiovascular Actions and Clinical Outcomes With Glucagon-Like Peptide-1 Receptor Agonists and Dipeptidyl Peptidase-4 Inhibitors. *Circulation* (2017) 136(9):849–70. doi: 10.1161/CIRCULATIONAHA.117.028136
18. Caruso I, Cignarelli A, Giorgino F. Heterogeneity and Similarities in GLP-1 Receptor Agonist Cardiovascular Outcomes Trials. *Trends Endocrinol Metab* (2019) 30(9):578–89. doi: 10.1016/j.tem.2019.07.004
19. Jones B, Buenaventura T, Kanda N, Chabosseau P, Owen BM, Scott R, et al. Targeting GLP-1 Receptor Trafficking to Improve Agonist Efficacy. *Nat Commun* (2018) 9(1):1602. doi: 10.1038/s41467-018-03941-2
20. Christopher R, Covington P, Davenport M, Fleck P, Mekki QA, Wann ER, et al. Pharmacokinetics, Pharmacodynamics, and Tolerability of Single Increasing Doses of the Dipeptidyl Peptidase-4 Inhibitor Alogliptin in Healthy Male Subjects. *Clin Ther* (2008) 30(3):513–27. doi: 10.1016/j.clinthera.2008.03.005
21. Henry RR, Smith SR, Schwartz SL, Mudaliar SR, Deacon CF, Holst JJ, et al. Effects of Saxagliptin on Beta-Cell Stimulation and Insulin Secretion in Patients With Type 2 Diabetes. *Diabetes Obes Metab* (2011) 13(9):850–8. doi: 10.1111/j.1463-1326.2011.01417.x
22. Murai K, Katsuno T, Miyagawa J, Matsuo T, Ochi F, Tokuda M, et al. Very Short-Term Effects of the Dipeptidyl Peptidase-4 Inhibitor Sitagliptin on the Secretion of Insulin, Glucagon, and Incretin Hormones in Japanese Patients With Type 2 Diabetes Mellitus: Analysis of Meal Tolerance Test Data. *Drugs R D* (2014) 14 (4):301–8. doi: 10.1007/s40268-014-0072-6
23. Nakamura Y, Tsuji M, Hasegawa H, Kimura K, Fujita K, Inoue M, et al. Anti-Inflammatory Effects of Linagliptin in Hemodialysis Patients With Diabetes. *Hemodial Int Int Symp Home Hemodial* (2014) 18(2):433–42. doi: 10.1111/hdi.12127
24. Barnett AH. Lixisenatide: Evidence for Its Potential Use in the Treatment of Type 2 Diabetes. *Core Evid* (2011) 6:67–79. doi: 10.2147/CE.S15525
25. Murphy CE. Review of the Safety and Efficacy of Exenatide Once Weekly for the Treatment of Type 2 Diabetes Mellitus. *Ann Pharmacot* (2012) 46(6):812–21. doi: 10.1345/aph.1Q722
26. Ingwersen SH, Petri KC, Tandon N, Yoon KH, Chen L, Vora J, et al. Liraglutide Pharmacokinetics and Dose-Exposure Response in Asian Subjects With Type 2 Diabetes From China, India and South Korea. *Diabetes Res Clin Pract* (2015) 108(1):113–9. doi: 10.1016/j.diabres.2015.01.001
27. Seino Y, Nakajima H, Miyahara H, Kurita T, Bush MA, Yang F, et al. Safety, Tolerability, Pharmacokinetics and Pharmacodynamics of Albiglutide, a Long-Acting GLP-1-Receptor Agonist, in Japanese Subjects With Type 2 Diabetes Mellitus. *Curr Med Res Opin* (2009) 25(12):3049–57. doi: 10.1185/03007990903372999
28. Carlsson Petri KC, Ingwersen SH, Flint A, Zacho J, Overgaard RV. Semaglutide s.c. Once-Weekly in Type 2 Diabetes: A Population Pharmacokinetic Analysis. *Diabetes Ther* (2018) 9(4):1533–47. doi: 10.1007/s13300-018-0458-5
29. Geiser JS, Heathman MA, Cui X, Martin J, Loghin C, Chien JY, et al. Clinical Pharmacokinetics of Dulaglutide in Patients With Type 2 Diabetes: Analyses of Data From Clinical Trials. *Clin Pharmacokinet* (2016) 55(5):625–34. doi: 10.1007/s40262-015-0338-3
30. Food and Drugs Administration. *Drug RYBELSUS: Drug Details: Label Information* (2019). Available at: https://www.accessdata.fda.gov/drugsatfda_docs/label/2019/213051s000lbl.pdf (Accessed 1 Aug 2020).
31. Alsalim W, Omar B, Pacini G, Bizzotto R, Mari A, Ahrén B. Incretin and Islet Hormone Responses to Meals of Increasing Size in Healthy Subjects. *J Clin Endocrinol Metab* (2015) 100(2):561–8. doi: 10.1210/jc.2014-2865
32. Herrmann C, Göke R, Richter G, Fehmann HC, Arnold R, Göke B, et al. Glucagon-Like Peptide-1 and Glucose-Dependent Insulin-Releasing Polypeptide Plasma Levels in Response to Nutrients. *Digestion* (1995) 56(2):117–26. doi: 10.1159/000201231
33. Færch K, Torekov SS, Vistisen D, Johansen NB, Witte DR, Jonsson A, et al. GLP-1 Response to Oral Glucose Is Reduced in Prediabetes, Screen-Detected Type 2 Diabetes, and Obesity and Influenced by Sex: The ADDITION-PRO Study. *Diabetes* (2015) 64(7):2513–25. doi: 10.2337/db14-1751
34. Drucker DJ, Nauck MA. The Incretin System: Glucagon-Like Peptide-1 Receptor Agonists and Dipeptidyl Peptidase-4 Inhibitors in Type 2 Diabetes. *Lancet* (2006) 368(9548):1696–705. doi: 10.1016/S0140-6736(06)69705-5
35. Lundgren JR, Færch K, Witte DR, Jonsson AE, Pedersen O, Hansen T, et al. Greater Glucagon-Like Peptide-1 Responses to Oral Glucose are Associated With Lower Central and Peripheral Blood Pressures. *Cardiovasc Diabetol* (2019) 18 (1):130. doi: 10.1186/s12933-019-0937-7
36. Yanagawa T. Strong Association Between Weight Reduction and Suppression of Cardiovascular Events in Recent Clinical Trials of DPP4 Inhibitors, GLP-1 Receptor Agonists, and SGLT2 Inhibitors. *J Clin Med Res* (2018) 10(10):796–7. doi: 10.14740/jocmr3587w
37. Nauck MA, Meier JJ. MANAGEMENT OF ENDOCRINE DISEASE: Are All GLP-1 Agonists Equal in the Treatment of Type 2 Diabetes? *Eur J Endocrinol* (2019) 181(6):R211–34. doi: 10.1530/EJE-19-0566

38. Holst JJ, Deacon CF, Vilsbøll T, Krarup T, Madsbad S. Glucagon-Like Peptide-1, Glucose Homeostasis and Diabetes. *Trends Mol Med* (2008) 14(4):161–8. doi: 10.1016/j.molmed.2008.01.003

Conflict of Interest: The authors declare that the research was conducted in the absence of any commercial or financial relationships that could be construed as a potential conflict of interest.

Publisher's Note: All claims expressed in this article are solely those of the authors and do not necessarily represent those of their affiliated organizations, or those of the publisher, the editors and the reviewers. Any product that may be evaluated in this article, or claim that may be made by its manufacturer, is not guaranteed or endorsed by the publisher.

frontiers | Frontiers in Endocrinology

ORIGINAL RESEARCH
published: 11 July 2022
doi: 10.3389/fendo.2022.943686

Predictive Role of NEK6 in Prognosis and Immune Infiltration in Head and Neck Squamous Cell Carcinoma

Zhi-Min Yang[1,2†], *Bing Liao*[1,2†], *Si-Si Yang*[1,3], *Tong Su*[1], *Jing Zhang*[1,2] *and Wei-Ming Wang*[1,2*]

[1] Department of Oral and Maxillofacial Surgery, Center of Stomatology, Xiangya Hospital, Central South University, Changsha, China, [2] Institute of Oral Precancerous Lesions, Central South University, Changsha, China, [3] Research Center of Oral and Maxillofacial Tumor, Xiangya Hospital, Central South University, Changsha, China

OPEN ACCESS

Edited by:
Qiulun Lu,
Nanjing Medical University, China

Reviewed by:
Chuan Ma,
Shandong University, China
Hairong Xu,
Yangzhou University, China

***Correspondence:**
Wei-Ming Wang
wwmasly10@csu.edu.cn

[†]These authors have contributed equally to this work

Specialty section:
This article was submitted to Cellular Endocrinology, a section of the journal Frontiers in Endocrinology

Received: 14 May 2022
Accepted: 14 June 2022
Published: 11 July 2022

Citation:
Yang Z-M, Liao B, Yang S-S, Su T, Zhang J and Wang W-M (2022) Predictive Role of NEK6 in Prognosis and Immune Infiltration in Head and Neck Squamous Cell Carcinoma. Front. Endocrinol. 13:943686. doi: 10.3389/fendo.2022.943686

Head and neck squamous cell carcinoma (HNSCC), as one of the common malignant tumors, seriously threatens human health. NEK6 (Never in Mitosis A (NIMA) related kinases 6), as a cyclin, promotes cancer cell proliferation and cancer progression. However, the prognostic value of NEK6 and its correlation with immune cell infiltration in HNSCC remain unclear. In this study, we comprehensively elucidated the prognostic role and potential function of NEK6 expression in HNSCC. The expression of NEK6 was significantly up-regulated by immunohistochemistry in HNSCC. Upregulation of NEK6 expression in gene expression studies predicts poor prognosis in HNSCC patients. The results of Gene Ontology (GO), Kyoto Encyclopedia of Genes and Genomes (KEGG) and Gene set variation analysis indicated that NEK6 is mainly involved in extracellular matrix metabolism and EMT processes. The expression of NEK6 increased with the level of immune cell infiltration and the expression of various immune checkpoints. In conclusion, NEK6 may serve as a candidate prognostic predictor and may predict the response of HNSCC patients to immunotherapy.

Keywords: NEK6, prognosis, immune infiltration, HNSCC, immune checkpoints

INTRODUCTION

Head and neck squamous cell carcinoma (HNSCC), as one of the common malignant tumors, seriously threatens human health (1). HNSCC metastasizes to lymph nodes *via* lymphatic channels at an early stage. Due to the lack of active treatment opportunities or the high recurrence and metastasis rate after treatment, the 5-year survival rate of advanced patients is less than 30% (2). In recent years, with the clinical application of new drugs (cetuximab and

immune checkpoint inhibitors), the survival of some HNSCC patients has been prolonged (3, 4). However, more than 70% of patients with advanced HNSCC still do not benefit from these drugs (3). Therefore, it is necessary to develop new valuable biomarkers to predict the therapeutic effect of HNSCC.

Previous studies have shown that cell cycle-related proteins promote tumor cell proliferation by regulating cell mitosis and promote invasion and therapy resistance (5). NEK6 (Never In Mitosis A (NIMA) related kinases 6), a cyclin, promotes the invasion and metastasis of various cancers by regulating cell proliferation and apoptosis (6). NEK6 is highly expressed in colorectal cancer, breast cancer, gastric cancer, prostate cancer, liver cancer, ovarian cancer, and thyroid cancer (6–11).

Since the first immune checkpoint inhibitor (ICI) drug, ipilimumab, was approved for clinical use by the US FDA in March 2011, ICIs (PD-1, PD-L1, and CTLA4) have shown promising therapeutic effects in a variety of tumors, suggesting that Inhibition of tumor-specific immunity prevents the occurrence and development of tumors (3, 12). However, only a minority of cancer patients have complete and durable responses to ICIs therapy, and most patients still do not benefit from ICIs therapy (13). Therefore, improving the response rate of immunotherapy in immunotherapy research is one of the research hotspots. Whether NEK6 expression in HNSCC is associated with immune cell infiltration has been poorly studied.

Therefore, in this study, a variety of bioinformatics methods and HNSCC tissue specimens were used to comprehensively measure the relationship between NEK6 expression and prognosis in HNSCC. The relationship between tumor immune cell infiltration and immune checkpoint molecule expression and NEK6 expression was also further analyzed. These results provide new insights into the function of NEK6 and new targets for the diagnosis and prognosis of HNSCC.

METHODS

Data Collection and Processing

Extracted pan-cancer sequencing data from The Cancer Genome Atlas (TCGA) and Broad Institute Cancer Cell Line Encyclopedia (CCLE) for analysis through their portals. Use the rma function in the R package (R studio version: 1.2.1335, R version: 3.6.1) (http://www.r-project.org/https://www.rstudio.com/) for the whole data set to filter. Missing and duplicated results were removed and transformed by log2 (TPM +1). Patients' age, gender, tumor stage, and clinical stage were retrieved from the portal, along with other clinical data.

Survival Analysis

In the R setting, Cox regression analysis was used to analyze the relationship between NEK6 expression and survival in HNSCC patients. After the patients were divided into NEK6 high-expression group and low-expression group by the optimal separation method, the Kaplan-Meier method was used to create the survival curve of HNSCC patients. Survival was studied using the Survival ROC and Survival in the R package (rdocumentation.org/packages/survival). Differences between curves were examined using the log-rank test, P values less than 0.05 were considered significant.

Immune Cell Infiltration Enrichment and Correlation Analysis of Immune Checkpoints

Tumor Immune Estimation Resource (TIMER) is a database-driven web application that calculates immune cell infiltration fractions for six major immune cell types, including B cells, CD4+, T cells, CD 8+, T cells, macrophages, Neutrophils and dendritic cells. Retrieve and examine infiltration data to see if there is a link between NEK6 expression and infiltration. Similarly, TIMER can also retrieve and examine whether there is a link between NEK6 expression and immune checkpoint gene expression.

NEK6-Related Gene Enrichment Analysis

We searched the STRING database (https://string-db.org/) using individual protein names ("NEK6") and organisms ("Homo sapiens"). After that, we set the following main parameters: the minimum interaction score required ["Low confidence (0.150)"], the meaning of the network edge ("evidence"), the maximum number of interactors to display ("No more than 50 interactors" " in the first shell) and an active interaction source ("experimental"). Finally, we searched for NEK6-binding proteins that had been determined experimentally. In addition, two sets of data (Kyoto Encyclopedia of Genes and Genomes) were integrated for KEGG pathway analysis. We collected data for functional annotation graphs by uploading gene lists to DAVID, a database for annotation, visualization, and integrated discovery, using parameters for the selected identifier ("OFFICIAL_GENE_SYMBOL") and species ("Homo sapiens"). Finally, enriched pathways are displayed using the R packages "tidyr" and "ggplot2". Additionally, we use the R package "clusterProfiler" to run GO.

Gene Set Variation Analysis

Gene set variation analysis (GSVA) was based on the MsigDB database (https://www.gsea-msigdb.org/gsea/msigdb/index.jsp) HALLMARK pathway dataset.

Immunohistochemistry

The present study was approved by the Medical Ethics Committee of Xiangya Hospital, Central South University (Hunan, China) and was performed according to the Declaration of Helsinki guidelines on experimentation involving human subjects. Written informed consent

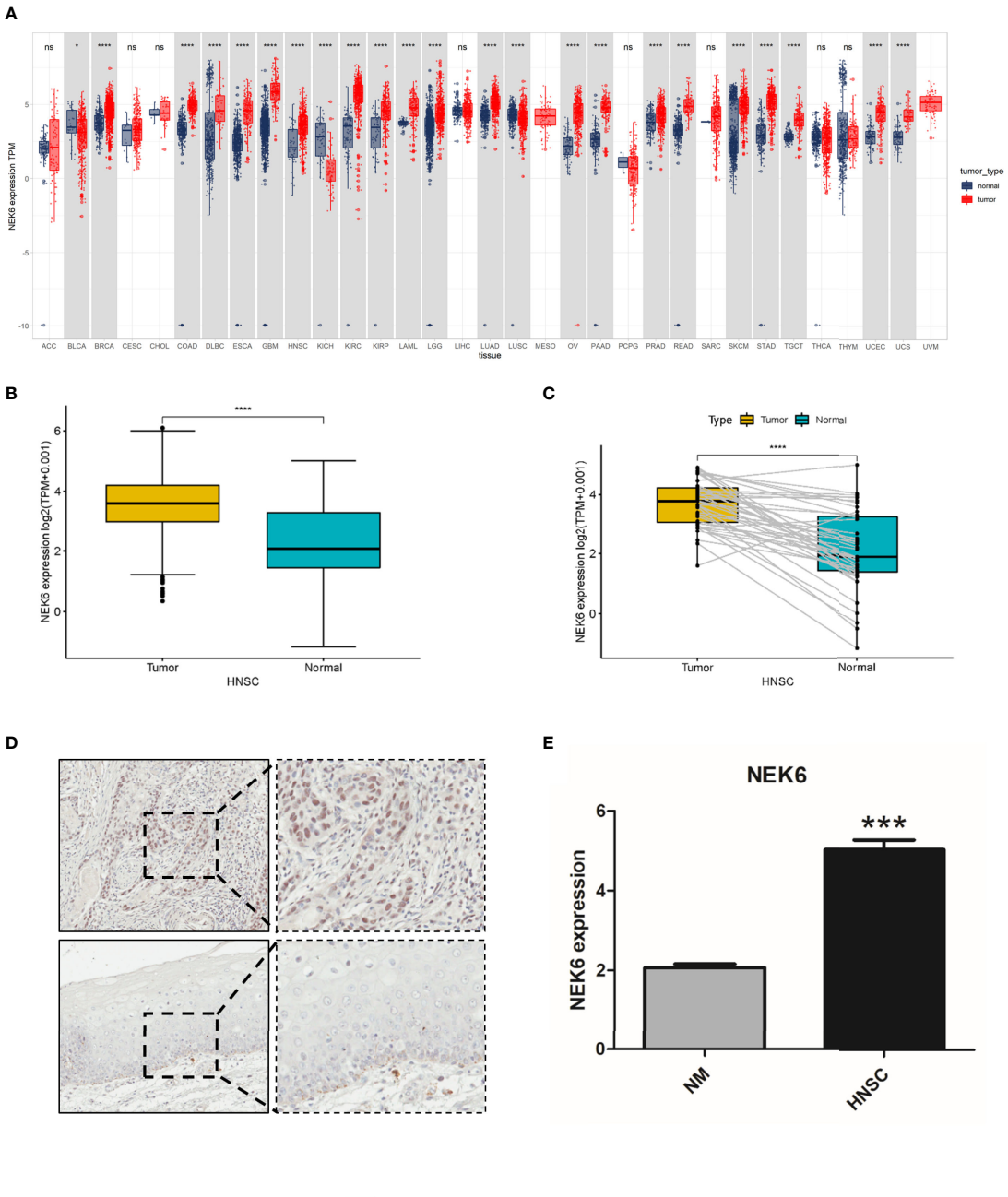

FIGURE 1 | Expression of NEK6 in HNSCC. **(A)** NEK6 expression in different types of cancer was investigated with the TIMER database. **(B)** Analysis of NEK6 expression in HNSCC and adjacent normal tissues in the TCGA database. **(C)** TCGA database and statistical analyses of HNSCC expression in HNSCC tissues and paired adjacent normal tissues. **(C)** Immunohistochemical staining of NEK6 was performed in HNSCC and normal mucosa. Representative images are shown. Scare bars, 50 mM. **(D, E)** The staining was quantified, as shown. ***p < 0.001.

was obtained from all participants. The sections of HNSCC were deparaffinized in xylene and rehydrated in a graded series of ethanol and double-distilled water before subjected to heat-induced antigen retrieval. After incubated with primary antibodies (NEK6 1:200 abcam, USA ab117986) overnight at 4°C, the secondary antibody was incubated at room temperature for 1 hr. Image-Pro Plus 6.0 (Media Cybernetics, Inc.) was used to calculate the density determination.

Statistical Analysis

Spearman's correlation test was used to analyze the association between NEK6 expression and targets. According to whether the

samples were paired or not, the comparison between normal tissue and cancer tissue was performed by two-group t-test. All graphics were created using R software. Data are reported as mean ± SD. Differences were defined as statistically significant if P-value < 0.05.

RESULTS

Increased NEK6 Expression in HNSCC

Compared with corresponding normal tissues (**Figure 1A**), the expression of NEK6 are increased in breast invasive carcinoma (BRCA), colon adenocarcinoma (COAD), Lymphoid Neoplasm Diffuse Large B-cell Lymphoma, esophageal carcinoma (ESCA), Glioblastoma multiforme(GBM), HNSCC, kidney chromophobe (KICH), and Kidney renal papillary cell carcinoma (KIRP). However, NEK6 expression are decreased in Bladder Urothelial Carcinoma (BLCA), renal chromophobe cells (KICH), and Lung squamous cell carcinoma(LUSC). Analysis of NEK6 expression in HNSCC samples and adjacent normal tissue using data gained directly from The Cancer Genome Atlas (TCGA). The results showed that the expression of NEK6 was significantly increased in HNSCC tissues compared to normal tissues (**Figure 1B**). Furthermore, the expression of NEK6 was significantly increased in HNSCC compared with paired normal samples (**Figure 1C**). Immunohistochemically results also showed similar results; the expression of NEK6 was significantly increased in HNSCC. (**Figures 1D, E**).

NEK6 Expression Was Associated With Prognosis in Patients With HNSCC

OS (overall survival), PFI (progression-free interval) and DSS (disease-related survival) of patients with high NEK6 gene expression in HNSCC were worse than those with low expression (**Figures 2A–C**) according to the Kaplan-Meier

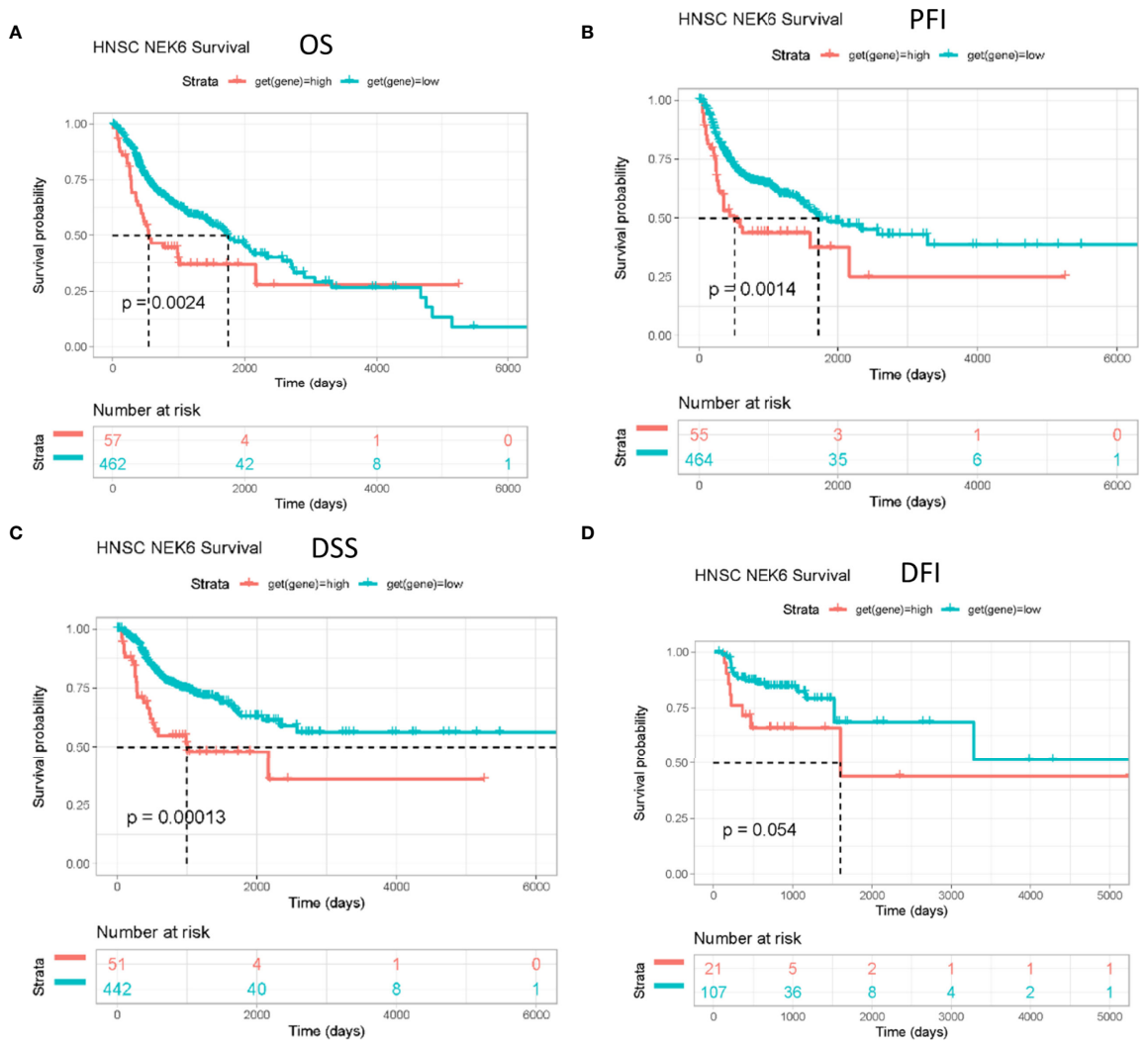

FIGURE 2 | Prognostic value of NEK6 in HNSCC. Survival curves for **(A)** OS, **(B)** PFI, **(C)** DSS, **(D)** DFI were displayed using a Kaplan-Meier plotter.

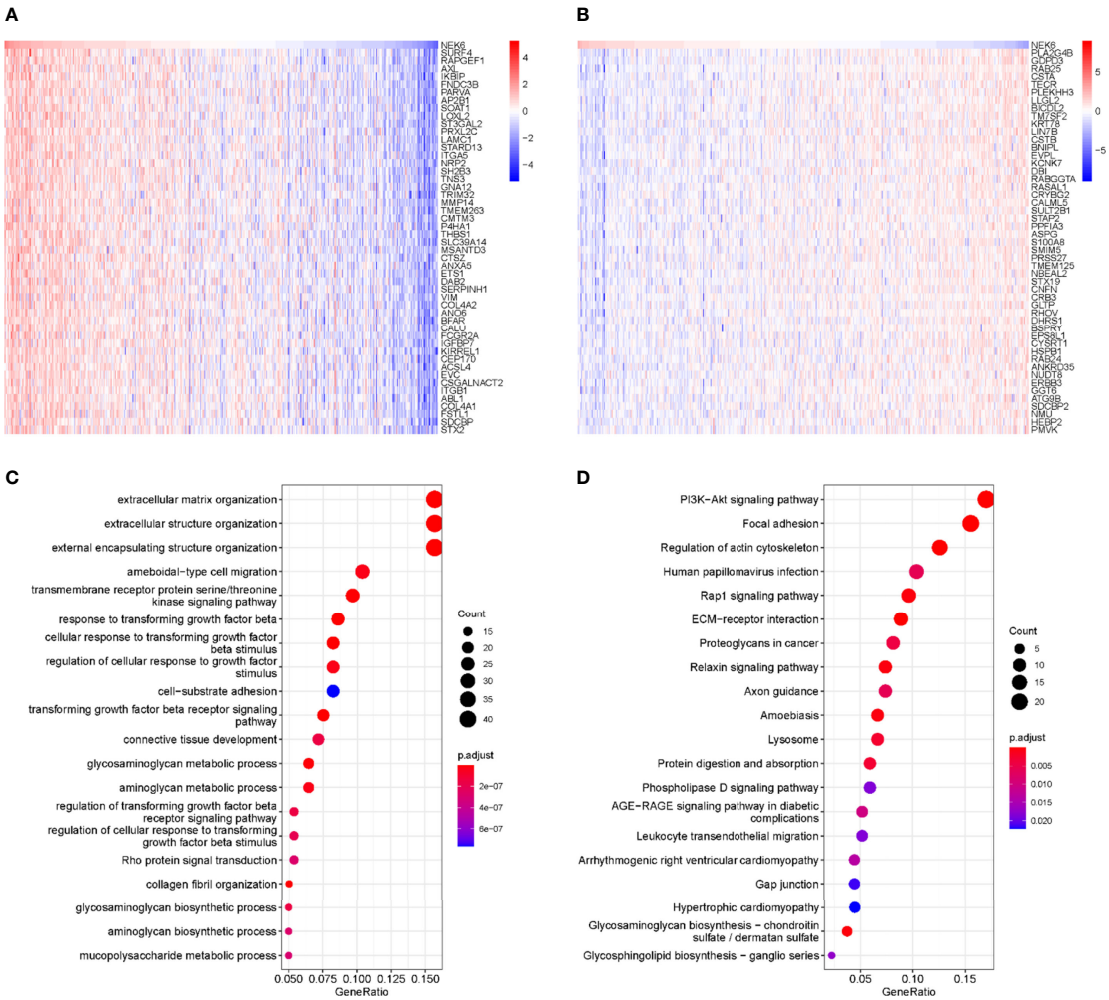

FIGURE 3 | GO and KEGG enrichment analysis of NEK6. **(A)** Top 50 genes negatively correlated with NEK expression levels in HNSCC. **(B)** Top 50 genes positively and negatively correlated with NEK expression levels in HNSCC. **(C)** Top 20 BP enrichment items in HNSCC. **(D)** Top 20 KEGG-enriched pathways in HNSCC.

plotter database. However, NEK6 expression was not correlated with DFI (disease free interval) (**Figure 2D**).

Analysis of NEK6 and Its Co-Expressed Genes in HNSCC

Figures 3A, B show the top 50 genes positively and negatively associated with NEK6 in HNSCC. KEGG and GO enrichment analysis was performed using 300 genes positively correlated with NEK6 to explore NEK6-related pathways and biological functions. In terms of BP, NEK6 was enriched in functions such as extracellular matrix organization, extracellular structure organization, external encapsulating structure organization, ameboidal-type cell migration (**Figure 3C**). The top 20 KEGG pathways of NEK6 and its related genes are shown in **Figure 3D**. The most significant correlation is the PI3K-Akt signaling pathway among these pathways. In addition, pathways such as focal adhesion and regulation of actin cytoskeleton were also significantly positively correlated with NEK6 expression.

Analysis of NEK6-Related Signaling Pathways by GSVA

The top 20 signaling pathways affected by NEK6 were mainly enriched in angiogenesis, epithelial mesenchymal transition, and TGFβ pathways (**Figure 4**). These results strongly implicate NEK6 in the regulation of HNSCC cell migration and motility

Correlation Analysis of NEK6 Expression and Infiltrating Immune Cells

NEK6 positively correlated with infiltrating levels of B cells, CD8+ T cells, neutrophil cells, mucosa-associated invariant T cells (MAIT), TEM cells, and Th17 cells, and negatively correlated with DCs, monocyte cells, nTreg cells, Macrophage, Tr1, CD4 T cells, iTreg cells, and NKT infiltration (**Figure 5**).

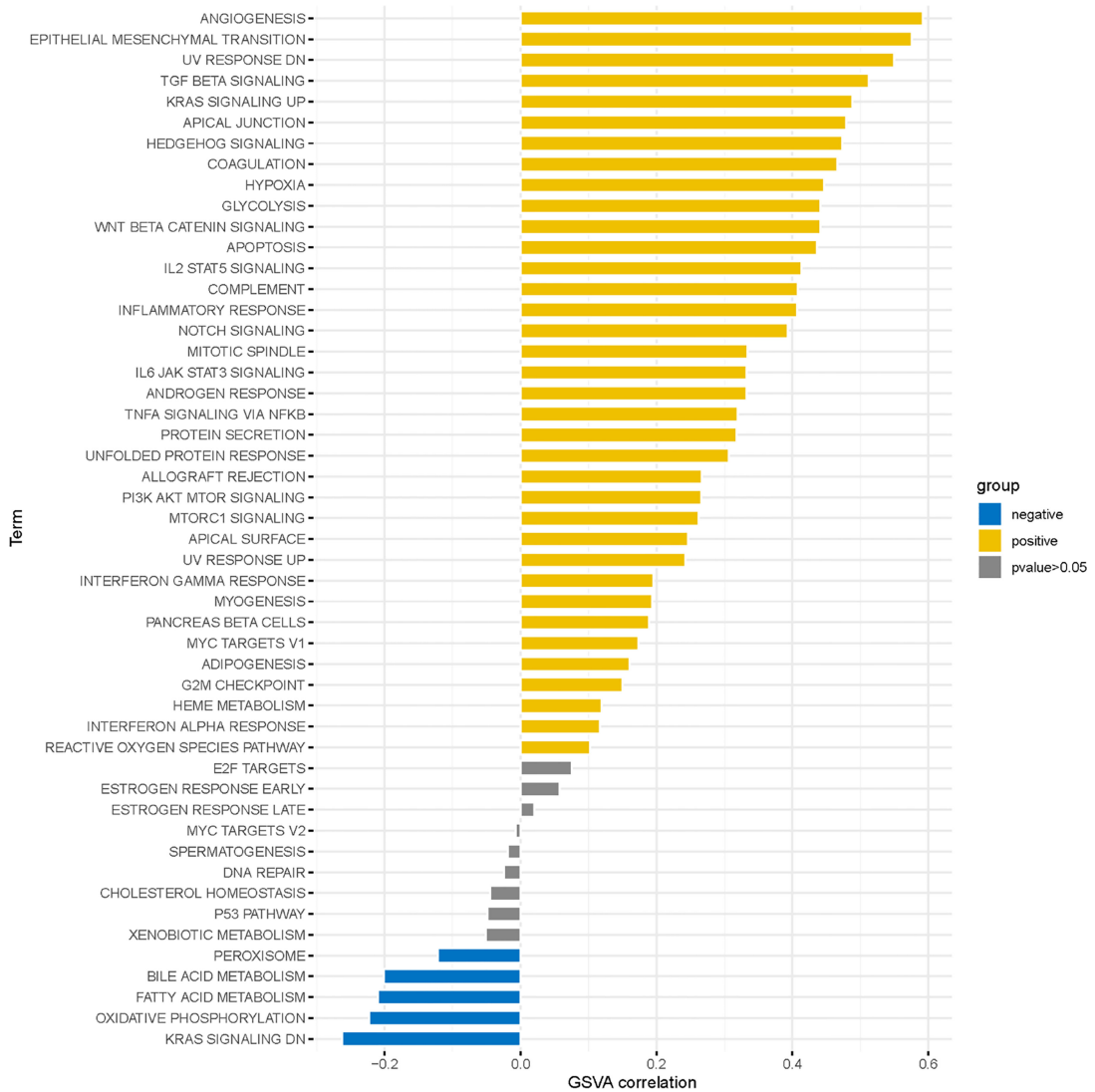

FIGURE 4 | GSVA enrichment analysis for NEK6.

Correlation of NEK6 Expression With Expression of Various Immune Checkpoints

We further investigated the correlation between NEK6 expression and well-known T-cell checkpoints such as LAG3, PDCD1, CD274, TIGIT, and CTLA-4 in the TIMER database. NEK6 expression was significantly correlated with the expression of LAG3, PDCD1, CD274, TIGIT and CTLA-4 in HNSCC (**Figures 6A–E**). These findings further suggest that NEK6 plays an important role in immune escape in the HNSCC microenvironment.

DISCUSSION

The treatment of HNSCC remains a challenge. Some patients have poor prognosis due to insufficient clinical treatment (14–16). It is necessary to find new genes related to the occurrence and development of HNSCC to improve the survival of patients. The discovery of new targeted genes enables treatments with greater specificity and sensitivity. In particular, finding new molecular targets related to immune infiltration is crucial for improving the therapeutic effect of HNSCC. Here, we aimed to investigate the function of NEK6 gene in HNSCC and its effect on tumor immune infiltration.

In our study, NEK6 was higher in multiple types of cancer tissues than in corresponding normal tissues. We further verified the high expression of NEK6 in HNSCC by immunohistochemistry. Furthermore, survival curves showed that NEK6 expression was an independent prognostic factor in HNSCC. Therefore, NEK6 has potential diagnostic value for HNSCC. Previews researches showed in liver cancer, breast cancer and gastric cancer the high expression of NEK6 is associated with poor prognosis of patients (6, 11, 17, 18).

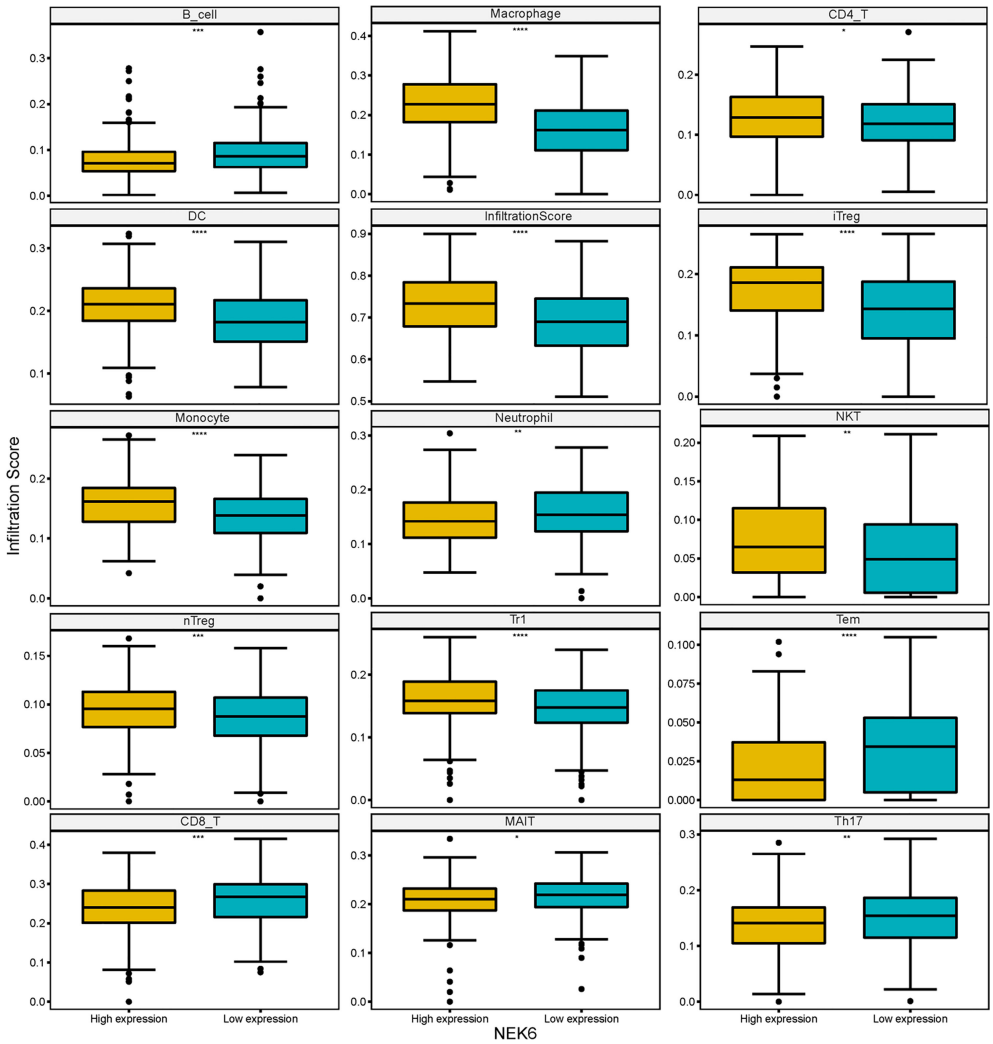

FIGURE 5 | Immune infiltrating cells associated with NEK expression in HNSCC.

Combined with previous studies and our findings, we speculate that high expression of NEK6 may predict poor prognosis in HNSCC patients in the real world. Our results showed that the transcript level of NEK6 was not correlated with the stage of HNSCC, suggesting NEK6 may have little relationship with cell proliferation. Its role in cancer cells may require further study.

We analyzed NEK6-related pathways in HNSCC to understand their oncogenic mechanisms. It was found that the functional network of NEK6 in HNSCC is mainly related to extracellular matrix organization, extracellular structure organization, external encapsulating structure organization, and ameboidal-type cell migration by GO and KEGG analysis. It also plays an important role in signaling pathways such as transmembrane receptor protein serine/threonine kinase signaling pathway activity, TGFβ response, and response to growth factor stimulation. KEGG pathway analysis showed that NEK6 gene was enriched in PI3K-Akt signaling pathway, focal adhesion and regulation of actin cytoskeleton. GSVA analysis showed that NEK6 was enriched in functions such as angiogenesis and epithelial mesenchymal transition. All these results suggest that NEK6 affects the degradation of extracellular matrix (19, 20), cell motility (21) and other aspects, mainly by affecting cell morphology such as EMT.

To further evaluate the potential immune mechanism of NEK6 in HNSCC, we analyzed the level of NEK6-related immune infiltration. The results showed that NEK6 was positively correlated with infiltration levels of CD8+ T cells, B cells, neutrophil cells, mucosa-associated invariant T cells (MAIT), TEM cells and Th17 cells. NEK6 was negatively correlated with DCs, monocyte cells, nTreg cells, Macrophage, Tr1, CD4 T cells, iTreg cells, NKTs. Some of these infiltrating cells contradict the function of NEK6, such as CD8+ T cells, mucosa-associated invariant T cells (MAIT), and Th17 cell infiltration is positively correlated with NEK6 expression.

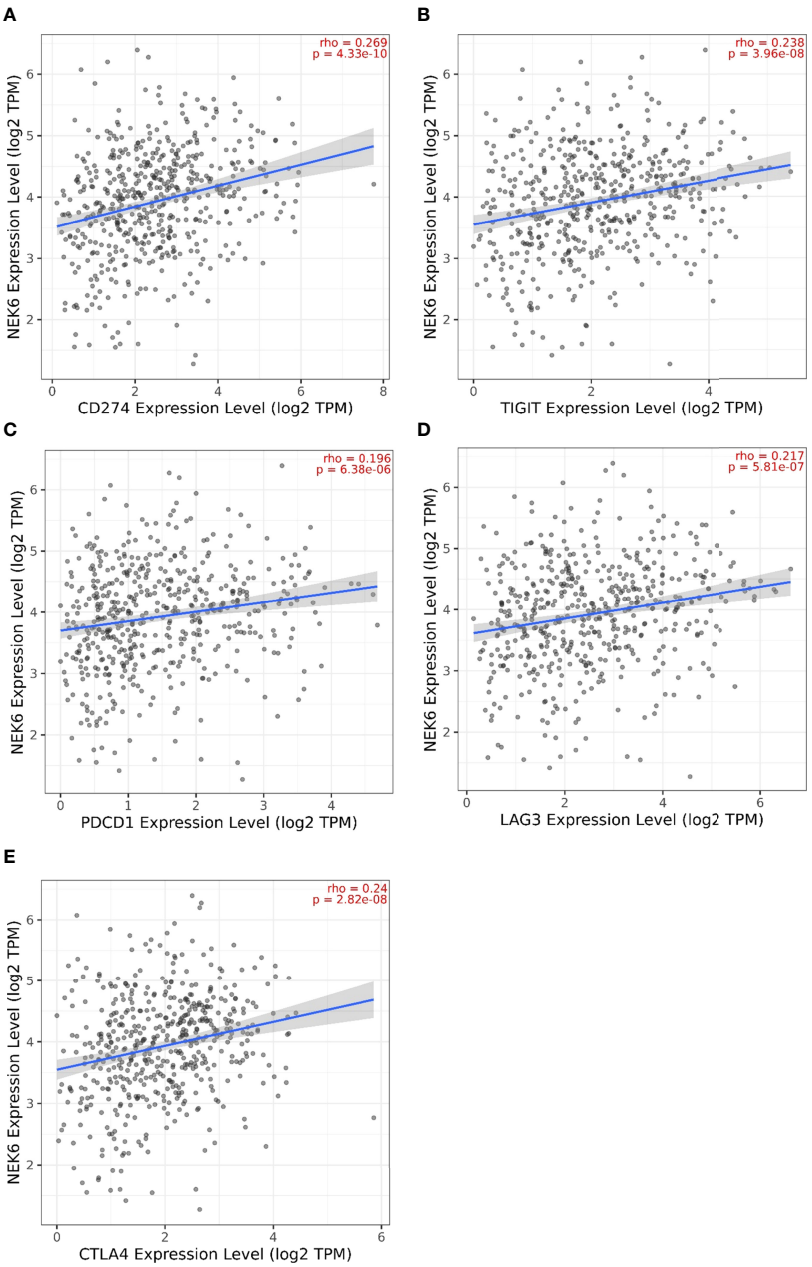

FIGURE 6 | Immune checkpoint marker associated with NEK expression in HNSCC. Scatterplots of the correlations between NEK6 expression and CD274 **(A)**, TIGIT **(B)**, PDCD1 **(C)**, LAG3 **(D)** and CTLA-4 **(E)** in HNSCC using the TIMER database.

Previous studies have shown that these cells inhibit cell invasion and metastasis in cancer (22–25). Therefore, the relationship between NEK6 expression and immune cell infiltration deserves to be further investigated in future work.

Most importantly, we investigated the correlation of NEK6 and immune checkpoint expression, including LAG3, PDCD1, CD274, TIGIT and CTLA-4, which correlate with response to ICB. These immune checkpoints are highly expressed in HNSCC (24, 26, 27). Furthermore, we found that NEK6 was positively co-expressed with these immune checkpoints, which may partially explain the cancer-promoting role of NEK6 by analyzing the correlation between immune checkpoints and NEK6.

Our study shows that immune cell infiltration recruited by NEK6 has both positive and negative effects on tumor patients. The mechanism of how NEK6 affects immune cell infiltration remains unclear. A limitation of this study is the large number of samples required to validate our results. In addition, underlying immune mechanisms should be explored and NEK6 investigated as a biomarker for predicting immune response rates in real-world HNSCC patients.

CONCLUSION

High expression of NEK6 in HNSCC predicts poor prognosis of patients, and NEK6 may play an important role in extracellular matrix degradation and cell motility. NEK6 alters clinical outcomes in patients with HNSCC by affecting molecular expression of immune checkpoints, and it may serve as a predictor of ICI therapy.

DATA AVAILABILITY STATEMENT

The original contributions presented in the study are included in the article/supplementary material. Further inquiries can be directed to the corresponding author.

ETHICS STATEMENT

The studies involving human participants were reviewed and approved by the Medical Ethics Committee of Xiangya Hospital, Central South University (Hunan, China). The patients/participants provided their written informed consent to participate in this study.

AUTHOR CONTRIBUTIONS

W-MW, Z-MY, and TS contributed to conception and design of the study. BL, S-SY organized the database. W-MW, Z-MY, BL performed the statistical analysis. BL, Z-MY wrote the first draft of the manuscript. S-SY, BL, JZ, and W-MW wrote sections of the manuscript. All authors contributed to manuscript revision, read, and approved the submitted version. All authors contributed to the article and approved the submitted version.

FUNDING

This study was funded by the National Natural Science Foundation of China (grant no.81702708, 81873717, 82170973), Natural Science Foundation of Hunan (grant no. 2018JJ3862), Open Research Fund Program of Hubei-MOST KLOS & KLOBME.

SUPPLEMENTARY MATERIAL

The Supplementary Material for this article can be found online at: https://www.frontiersin.org/articles/10.3389/fendo.2022.943686/full#supplementary-material

REFERENCES

1. Sung H, Ferlay J, Siegel RL, Laversanne M, Soerjomataram I, Jemal A, et al. Global Cancer Statistics 2020: GLOBOCAN Estimates of Incidence and Mortality Worldwide for 36 Cancers in 185 Countries. *CA Cancer J Clin* (2021) 71:209–49. doi: 10.3322/caac.21660
2. Chow LQM. Head and Neck Cancer. *N Engl J Med* (2020) 382:60–72. doi: 10.1056/NEJMra1715715
3. Veigas F, Mahmoud YD, Merlo J, Rinflerch A, Rabinovich GA, Girotti MR. Immune Checkpoints Pathways in Head and Neck Squamous Cell Carcinoma. *Cancers (Basel)* (2021) 13:1018. doi: 10.3390/cancers13051018
4. Pfister DG, Spencer S, Adelstein D, Adkins D, Anzai Y, Brizel DM, et al. Head and Neck Cancers, Version 2.2020, NCCN Clinical Practice Guidelines in Oncology. *J Natl Compr Canc Netw* (2020) 18:873–98. doi: 10.6004/jnccn.2020.0031
5. Malumbres M. Cyclin-Dependent Kinases. *Genome Biol* (2014) 15:122. doi: 10.1186/gb4184
6. Panchal NK, Evan Prince S. The NEK Family of Serine/Threonine Kinases as a Biomarker for Cancer. *Clin Exp Med* (2022). doi: 10.1007/s10238-021-00782-0
7. Chen F, Feng Z, Zhu J, Liu P, Yang C, Huang R, et al. Emerging Roles of circRNA_NEK6 Targeting miR-370-3p in the Proliferation and Invasion of Thyroid Cancer *via* Wnt Signaling Pathway. *Cancer Biol Ther* (2018) 19:1139–52. doi: 10.1080/15384047.2018.1480888
8. De Donato M, Righino B, Filippetti F, Battaglia A, Petrillo M, Pirolli D, et al. Identification and Antitumor Activity of a Novel Inhibitor of the NIMA-Related Kinase NEK6. *Sci Rep* (2018) 8:16047. doi: 10.1038/s41598-018-34471-y
9. Zuo J, Ma H, Cai H, Wu Y, Jiang W, Yu L. An Inhibitory Role of NEK6 in TGFbeta/Smad Signaling Pathway. *BMB Rep* (2015) 48:473–8. doi: 10.5483/BMBRep.2015.48.8.225
10. Han N, Zuo L, Chen H, Zhang C, He P, Yan H. Long non-Coding RNA Homeobox A11 Antisense RNA (HOXA11-AS) Promotes Retinoblastoma Progression *via* Sponging miR-506-3p. *Onco Targets Ther* (2019) 12:3509–17. doi: 10.2147/OTT.S195404
11. Ting G, Li X, Kwon HY, Ding T, Zhang Z, Chen Z, et al. microRNA-219-5p Targets NEK6 to Inhibit Hepatocellular Carcinoma Progression. *Am J Transl Res* (2020) 12:7528–41.
12. Tsai MS, Chen WC, Lu CH, Chen MF. The Prognosis of Head and Neck Squamous Cell Carcinoma Related to Immunosuppressive Tumor Microenvironment Regulated by IL-6 Signaling. *Oral Oncol* (2019) 91:47–55. doi: 10.1016/j.oraloncology.2019.02.027
13. Ribas A, Wolchok JD. Cancer Immunotherapy Using Checkpoint Blockade. *Science* (2018) 359:1350–5. doi: 10.1126/science.aar4060
14. Hayashi Y, Osawa K, Nakakaji R, Minamiyama S, Ohashi N, Ohya T, et al. Prognostic Factors and Treatment Outcomes of Advanced Maxillary Gingival Squamous Cell Carcinoma Treated by Intra-Arterial Infusion Chemotherapy Concurrent With Radiotherapy. *Head Neck* (2019) 41:1777–84. doi: 10.1002/hed.25607
15. Johnson DE, Burtness B, Leemans CR, Lui VWY, Bauman JE, Grandis JR. Head and Neck Squamous Cell Carcinoma. *Nat Rev Dis Primers* (2020) 6:92. doi: 10.1038/s41572-020-00224-3
16. Ren ZH, Hu CY, He HR, Li YJ, Lyu J. Global and Regional Burdens of Oral Cancer From 1990 to 2017: Results From the Global Burden of Disease Study. *Cancer Commun (Lond)* (2020) 40:81–92. doi: 10.1002/cac2.12009
17. He Z, Ni X, Xia L, Shao Z. Overexpression of NIMA-Related Kinase 6 (NEK6) Contributes to Malignant Growth and Dismal Prognosis in Human Breast Cancer. *Pathol Res Pract* (2018) 214:1648–54. doi: 10.1016/j.prp.2018.07.030
18. Orenay-Boyacioglu S, Kasap E, Gerceker E, Yuceyar H, Demirci U, Bilgic F, et al. Expression Profiles of Histone Modification Genes in Gastric Cancer Progression. *Mol Biol Rep* (2018) 45:2275–82. doi: 10.1007/s11033-018-4389-z
19. Li JJ, Mao XH, Tian T, Wang WM, Su T, Jiang CH, et al. Role of PFKFB3 and CD163 in Oral Squamous Cell Carcinoma Angiogenesis. *Curr Med Sci* (2019) 39:410–4. doi: 10.1007/s11596-019-2051-1
20. Yang JG, Wang WM, Xia HF, Yu ZL, Li HM, Ren JG, et al. Lymphotoxin-Alpha Promotes Tumor Angiogenesis in HNSCC by Modulating Glycolysis in a PFKFB3-Dependent Manner. *Int J Cancer* (2019) 145:1358–70. doi: 10.1002/ijc.32221

21. Morin C, Moyret-Lalle C, Mertani HC, Diaz JJ, Marcel V. Heterogeneity and Dynamic of EMT Through the Plasticity of Ribosome and mRNA Translation. *Biochim Biophys Acta Rev Cancer* (2022) 1877:188718. doi: 10.1016/j.bbcan.2022.188718
22. Maybruck BT, Pfannenstiel LW, Diaz-Montero M, Gastman BR. Tumor-Derived Exosomes Induce CD8(+) T Cell Suppressors. *J Immunother Cancer* (2017) 5:65. doi: 10.1186/s40425-017-0269-7
23. Oweida A, Hararah MK, Phan A, Binder D, Bhatia S, Lennon S, et al. Resistance to Radiotherapy and PD-L1 Blockade Is Mediated by TIM-3 Upregulation and Regulatory T-Cell Infiltration. *Clin Cancer Res* (2018) 24:5368–80. doi: 10.1158/1078-0432.CCR-18-1038
24. Yu GT, Bu LL, Zhao YY, Mao L, Deng WW, Wu TF, et al. CTLA4 Blockade Reduces Immature Myeloid Cells in Head and Neck Squamous Cell Carcinoma. *Oncoimmunology* (2016) 5:e1151594. doi: 10.1080/2162402X.2016.1151594
25. Germano G, Lu S, Rospo G, Lamba S, Rousseau B, Fanelli S, et al. CD4 T Cell-Dependent Rejection of Beta-2 Microglobulin Null Mismatch Repair-Deficient Tumors. *Cancer Discovery* (2021) 11:1844–59. doi: 10.1158/2159-8290.CD-20-0987
26. Gao A, Pan X, Yang X, Lin Z. Predictive Factors in the Treatment of Oral Squamous Cell Carcinoma Using PD-1/PD-L1 Inhibitors. *Invest New Drugs* (2021) 39:1132–8. doi: 10.1007/s10637-021-01082-w
27. Liu X, Li Q, Zhou Y, He X, Fang J, Lu H, et al. Dysfunctional Role of Elevated TIGIT Expression on T Cells in Oral Squamous Cell Carcinoma Patients. *Oral Dis* (2021) 27:1667–77. doi: 10.1111/odi.13703

Conflict of Interest: The authors declare that the research was conducted in the absence of any commercial or financial relationships that could be construed as a potential conflict of interest.

Publisher's Note: All claims expressed in this article are solely those of the authors and do not necessarily represent those of their affiliated organizations, or those of the publisher, the editors and the reviewers. Any product that may be evaluated in this article, or claim that may be made by its manufacturer, is not guaranteed or endorsed by the publisher.

frontiers | Frontiers in Endocrinology

TYPE Original Research
PUBLISHED 25 July 2022
DOI 10.3389/fendo.2022.918605

OPEN ACCESS

EDITED BY
Chengqi Xu,
Huazhong University of Science and Technology, China

REVIEWED BY
Xiaowu Gu,
Genentech, Inc., United States
Yang Gao,
Sun Yat-sen University, China

*CORRESPONDENCE
Siqi Xiong
petersage1221@126.com

†These authors have contributed equally to this work

SPECIALTY SECTION
This article was submitted to Cellular Endocrinology, a section of the journal Frontiers in Endocrinology

RECEIVED 12 April 2022
ACCEPTED 28 June 2022
PUBLISHED 25 July 2022

CITATION
Wang N, Ding L, Liu D, Zhang Q, Zheng G, Xia X and Xiong S (2022) Molecular investigation of candidate genes for pyroptosis-induced inflammation in diabetic retinopathy. *Front. Endocrinol.* 13:918605. doi: 10.3389/fendo.2022.918605

Molecular investigation of candidate genes for pyroptosis-induced inflammation in diabetic retinopathy

Nan Wang[1,2,3†], Lexi Ding[1,2,3†], Die Liu[1,2,3], Quyan Zhang[1,2,3], Guoli Zheng[1,2,3], Xiaobo Xia[1,2,3] and Siqi Xiong[1,2,3*]

[1]Eye Center of Xiangya Hospital, Central South University, Changsha, China, [2]Hunan Key Laboratory of Ophthalmology, Central South University, Changsha, China, [3]National Clinical Research Center for Geriatric Disorders, Xiangya Hospital, Central South University, Changsha, China

Background: Diabetic retinopathy is a diabetic microvascular complication. Pyroptosis, as a way of inflammatory death, plays an important role in the occurrence and development of diabetic retinopathy, but its underlying mechanism has not been fully elucidated. The purpose of this study is to identify the potential pyroptosis-related genes in diabetic retinopathy by bioinformatics analysis and validation in a diabetic retinopathy model and predict the microRNAs (miRNAs) and long non-coding RNAs (lncRNAs) interacting with them. Subsequently, the competing endogenous RNA (ceRNA) regulatory network is structured to explore their potential molecular mechanism.

Methods: We obtained mRNA expression profile dataset GSE60436 from the Gene Expression Omnibus (GEO) database and collected 51 pyroptosis-related genes from the PubMmed database. The differentially expressed pyroptosis-related genes were obtained by bioinformatics analysis with R software, and then eight key genes of interest were identified by correlation analysis, Gene Ontology (GO) enrichment analysis, Kyoto Encyclopedia of Genes and Genomes (KEGG) pathway analysis, and protein–protein interaction (PPI) network analysis. Then, the expression levels of these key pyroptosis-related genes were validated with quantitative real-time polymerase chain reaction (qRT-PCR) in human retinal endothelial cells with high glucose incubation, which was used as an *in vitro* model of diabetic retinopathy. Western blot was performed to measure the protein levels of gasdermin D (GSDMD), dasdermin E (GSDME) and cleaved caspase-3 in the cells. Moreover, the aforementioned genes were further confirmed with the validation set. Finally, the ceRNA regulatory network was structured, and the miRNAs and lncRNAs which interacted with CASP3, TLR4, and GBP2 were predicted.

Results: A total of 13 differentially expressed pyroptosis-related genes were screened from six proliferative diabetic retinopathy patients and three RNA samples from human retinas, including one downregulated gene and 12 upregulated genes. A correlation analysis showed that there was a

correlation among these genes. Then, KEGG pathway and GO enrichment analyses were performed to explore the functional roles of these genes. The results showed that the mRNA of these genes was mainly related to inflammasome complex, interleukin-1 beta production, and NOD-like receptor signaling pathway. In addition, eight hub genes—CASP3, TLR4, NLRP3, GBP2, CASP1, CASP4, PYCARD, and GBP1—were identified by PPI network analysis using Cytoscape software. High glucose increased the protein level of GSDMD and GSDME, as critical effectors of pyroptosis, in retinal vascular endothelial cells. Verified by qRT-PCR, the expression of all these eight hub genes in the *in vitro* model of diabetic retinopathy was consistent with the results of the bioinformatics analysis of mRNA chip. Among them, CASP4, GBP1, CASP3, TLR4, and GBP2 were further validated in the GSE179568 dataset. Finally, 20 miRNAs were predicted to target three key genes—CASP3, GBP2, and TLR4, and 22 lncRNAs were predicted to potentially bind to these 20 miRNAs. Then, we constructed a key ceRNA network that is expected to mediate cellular pyroptosis in diabetic retinopathy.

Conclusion: Through the data analysis of the GEO database by R software and verification by qRT-PCR and validation set, we successfully identified potential pyroptosis-related genes involved in the occurrence of diabetic retinopathy. The key ceRNA regulatory network associated with these genes was structured. These findings might improve the understanding of molecular mechanisms underlying pyroptosis in diabetic retinopathy.

KEYWORDS

pyroptosis, inflammatory death, diabetic retinopathy, competing endogenous RNA regulatory network, expression profiling by array

Introduction

Diabetic retinopathy is an irreversible blindness disease characterized by retinal microvascular dysfunction (1). As one of the most prominent microvascular complications in advanced diabetes mellitus (DM), its incidence has been increasing worldwide and become a global public health problem (2, 3). The occurrence of diabetic retinopathy is closely related to the duration of disease and blood glucose level. Chronic exposure to hyperglycemia and other risk factors will lead to pathological retinal changes, such as breakdown of the retinal–blood barrier and aberrant retinal angiogenesis, which cause vision function impairment or even vision loss. It not only affects the quality of life in diabetic patients but also imposes a significant financial burden on the society (4). At present, the therapeutic options for diabetic retinopathy depend on the severity of the disease. It includes retinal laser photocoagulation, intravitreal injection of anti-VEGF drugs (5) or implantation of dexamethasone sustained-release agent (Ozurdex), and vitreoretinal surgery (6). However, some of the patients still suffer from a continuous decline of visual acuity after the aforementioned treatments due to progression of diabetic retinopathy. Therefore, elucidating the pathogenesis of diabetic retinopathy and providing treatment according to it might offer better therapeutic effects.

Pyroptosis is a new way of programmed cell death mediated by gasdermin (7). Differently from other ways of cell death, such as apoptosis and necrosis, pyroptosis is characterized by dependence on inflammatory caspase and the release of a large number of pro-inflammatory factors (8). According to the activation mechanism, pyroptosis can be divided into two signal pathways. The canonical pathway is characterized by the direct activation of caspase-1. It can cleave the N-terminal sequence of gasdermin D (GSDMD) which forms pores on the cellular membrane, followed by cytoplasmic swelling and membrane rupture. Meanwhile, activated caspase-1 can promote the release of inflammatory factors such as IL-18 and IL-1β to induce inflammatory response (9–11). In the non-classical pathway, inflammatory stimulators, such as lipopolysaccharide (LPS), can directly activate caspase-4/5/11 and other members of the caspase family. It can process GSDMD and indirectly activate

caspase-1 to induce pyroptosis (12, 13). Under physiological conditions, pyroptosis is crucial for the maintenance of innate immunity and prevention of tumor occurrence (14), but accumulated dates have shown that abnormal pyroptosis is associated with cardiovascular diseases (15), nervous system disorders (16), and diabetic complications such as diabetic cardiomyopathy and diabetic retinopathy (17, 18). However, there is a little information concerning pyroptosis in diabetic retinopathy. Further exploration of the role of pyroptosis in diabetic retinopathy and uncovering the molecular mechanisms underlying it can provide a novel insight into the pathogenesis of diabetic retinopathy.

Ishikawa K et al. generated the dataset GSE60436 (19). They analyzed the gene profile expressed in the fibrovascular membranes (FVMs) associated with proliferative diabetic retinopathy by detecting the gene expression of the FVMs from patients with proliferative diabetic retinopathy. In this study, the GSE60436 dataset was used to explore potential pyroptosis-related genes associated with diabetic retinopathy. Through correlation analysis, Gene Ontology (GO) enrichment analysis, Kyoto Encyclopedia of Genes and Genomes (KEGG) pathway analysis, and protein–protein interaction (PPI) network analysis of differentially expressed genes (DEGs), we identified the pyroptosis-related genes that participate in diabetic retinopathy and verified them by the independent dataset GSE179568 and quantitative real-time polymerase chain reaction (qRT-PCR) in a diabetic model. Finally, we predicted the targeting microRNAs (miRNAs) and long non-coding RNAs (lncRNAs) that are correlated with the validated key pyroptosis-related genes and structured a competing endogenous RNA (ceRNA) regulatory network. It will lay the groundwork for revealing the mechanisms of pyroptosis in diabetic retinopathy and generate therapeutic insights (Figure 1).

Materials and methods

Microarray data and the exploration of PRGs

The GSE60436 microarray dataset deposited by Ishikawa K et al. was downloaded from the Gene Expression Omnibus (GEO) database (https://www.ncbi.nlm.nih.gov/geo/). The dataset contains three active FVMs and three inactive FVMs, which were obtained from proliferative diabetic retinopathy patients, and the RNAs from human retinas were purchased and were extracted from normal retinas pooled from 99 Caucasians. All samples were analyzed by GPL6884 platform (IlluminaHumanWG-6v3.0 expression beadchip), and R software (version 4.1.0) was used for data quality control, normalization, background correction, and subsequent analysis. The RNA-seq-based dataset GSE179568 was also obtained from GEO, including seven human retinal neovascularization (RNV) membranes, 10 macular pucker, and seven macular hole samples as controls. The search for pyroptosis-related genes was mainly carried out in the PubMed database (https://pubmed.ncbi.nlm.nih.gov/). Finally, 51 genes were collected (11, 20–26).

Differential expression analysis and correlation analysis

We used "limma" package in R software to screen the differential genes in FVM samples of proliferative diabetic retinopathy patients and control groups. Genes with an adjusted *P*-value <0.05 and $|\log_2$ fold change$|$ >0.5 were considered as differentially expressed genes, and one

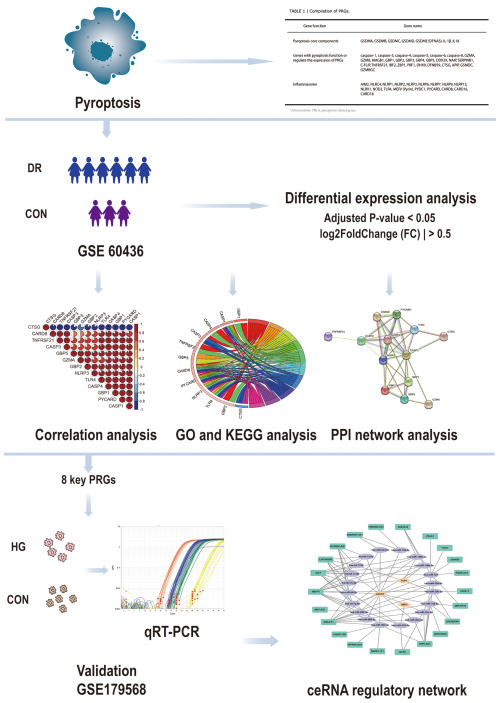

FIGURE 1
Design idea of this study. Downloaded GSE60436 dataset from the GEO database and 51 PRGs collected from the PubMed database. The R software was used to process the data, such as quality control, normalization, and background correction. A total of 13 differentially expressed PRGs in the dataset were identified by difference analysis, and GO and KEGG enrichment analyses were performed. At the same time, eight hub genes were identified by PPI analysis and then verified with qRT-PCR experiments and GSE179568. Finally, the specific mechanism of PRGs in DR was revealed by structuring a ceRNA regulatory network through multiMiR database and starbase database. GEO, Gene Expression Omnibus; PRGs, pyroptosis-related genes; PPI, protein–protein interaction; DR, diabetic retinopathy; qRT-PCR, quantitative real-time polymerase chain reaction; ceRNA, competing endogenous RNAs; GO, Gene Ontology; KEGG, Kyoto Encyclopedia of Genes and Genomes.

downregulated pyroptosis-related gene and 12 upregulated pyroptosis-related genes were identified. With *P*-value <0.05 and |$\log_2$ fold change| >1.0 as the threshold, 15 upregulated pyroptosis-related genes were obtained by analyzing the verification set GSE179568 with the same method. The correlation analysis of DEGs was carried out by using Spearman correlation in the "corrplot" package.

Functional and pathway enrichment analysis

In order to evaluate the function of differentially expressed pyroptosis-related genes, we used GO enrichment analysis and KEGG pathway analysis in R software for functional and pathway enrichment analysis and visualization. The adjusted *P*-value <0.05 was taken as the standard with statistical significance.

Construction of PPI network

The STRING database (https://string-db.org/) was used to construct the PPI network of DEG-encoded proteins (27), the threshold was set to a combined score ≥0.4, and the file in tsv format was downloaded. Then, Cytoscape software (version 3.9.0) was used to visualize the PPI network, and cytoHubba was used to excavate eight hub genes.

Construction of ceRNA-regulating network

The "multiMiR" package in R software combines 14 databases, including the mirTarbase database (https://maayanlab.cloud/Harmonizome/resource/MiRTarBase) with experimental methods to verify the relationship, and uses this tool to predict the miRNAs of the pyroptosis-related genes of interest. All the lncRNA–miRNA interaction data were obtained in the starbase database (https://starbase.sysu.edu.cn/), and the target lncRNA was screened according to clipExpNum >7. Finally, visualization was carried out in Cytoscape software.

Cell culture

Human retinal endothelial cells (HRECs) (CSC; Kirkland, WA, USA) were cultured in endothelial Complete Classic Medium (CSC; Kirkland, WA, USA) containing 10% fetal bovine serum (Gibco, USA). The culture medium was changed every 2 days. When the cells were 85–90% confluent, it was passaged at a ratio of 1:3. The *in vitro* diabetic model was induced by culturing HRECs with high-glucose medium containing 30 mM anhydrous glucose (Solarbio, Beijing, China) for 48 h, and the cells cultured in normal medium containing 5 mM glucose were used as control under the same conditions. In order to ensure the accuracy and stability of the results, 8–10 generations of cells were selected for follow-up study.

RNA Extraction and qRT-PCR

According to the manufacturer's plan, the total RNA of the experimental group and the control group was extracted by TRIzol reagent (Ambion, Carlsbad, CA). The concentration and the purity of RNA were measured by NanoDrop 2000c spectrophotometer (Thermo Fisher Scientific). Then, cDNA was reverse-transcribed from total RNA using UEIris II RT-PCR System (Suzhou Yuheng Biological Co., Ltd.) in strict accordance with the manufacturer's instructions, and qRT-PCR was performed using 2× SYBR Green qPCR Master Mix (Suzhou Yuheng Biological Co., Ltd.). The sequence of the qRT-PCR primers is shown in Supplementary Table S1. Gene expression was detected by the $2^{-\Delta\Delta Ct}$ method. β-actin mRNA was selected as the internal control.

Western blot analysis

HRECs were lysed with RIPA lysis buffer (Sangon Biotech, Shanghai, China) containing protease inhibitors and phosphatase inhibitors, and the protein concentrations were determined using the BCA kit (Thermo Fisher Scientific, Inc.). The samples were separated by 12% sodium dodecyl sulfate-polyacrylamide gel electrophoresis at 140 V and transferred to polyvinylidene membranes. Subsequently, the membranes were placed in 5% blocking buffer (bovine serum albumin) to block for 1 h, incubated with primary antibodies against CASP3 (Abcam, MA, USA), GSDMD (Abcam, MA, USA), GSDME (Abcam, MA, USA), and GAPDH (Abcam, MA, USA) at 4°C overnight, followed by horseradish peroxidase-labeled secondary antibodies (Abcam, MA, USA) for 1 h at room temperature, and finally developed with an enhanced chemiluminescence kit for visualization. The collected images were examined using ImageJ software (version 6.0; Media Cybernetics, Inc.).

Statistical analysis

Each *in vitro* experiment was repeated at least three times. Statistical analysis was performed using GraphPad Prism software (version 8.2.1). On the basis of the homogeneity of the variance test, Student's *t*-test was performed, and *P* <0.05 was considered significant and statistically significant.

Results

Differential expression of pyroptosis-related genes in the FVMs of proliferative diabetic retinopathy patients and the retina of normal individuals

After quality control, normalization, and background correction of the data in the GSE60436 dataset, 3,188 genes with significant changes were obtained by using adjusted *P*-value <0.05 and |$\log_2$ fold change| >0.5 as thresholds, including 1,640 upregulated genes and 1,548 downregulated genes as shown in the volcano plot (Figure 2A). Due to the lack of a systematic database of pyroptosis-related genes, we collected 51 pyroptosis-related genes from PubMed database, including reported pyroptosis core components, genes with pyroptosis function or genes that regulate the expression of pyroptosis-related genes, and inflammasome that play an important role in cell pyroptosis, which were listed in Table 1 (11, 20–26). One downregulated pyroptosis-related gene CTSG and 12 upregulated pyroptosis-related genes—CASP4, TNFRSF21, PYCARD, CASP1, CASP3, GBP1, TLR4, CARD8, NLRP3,

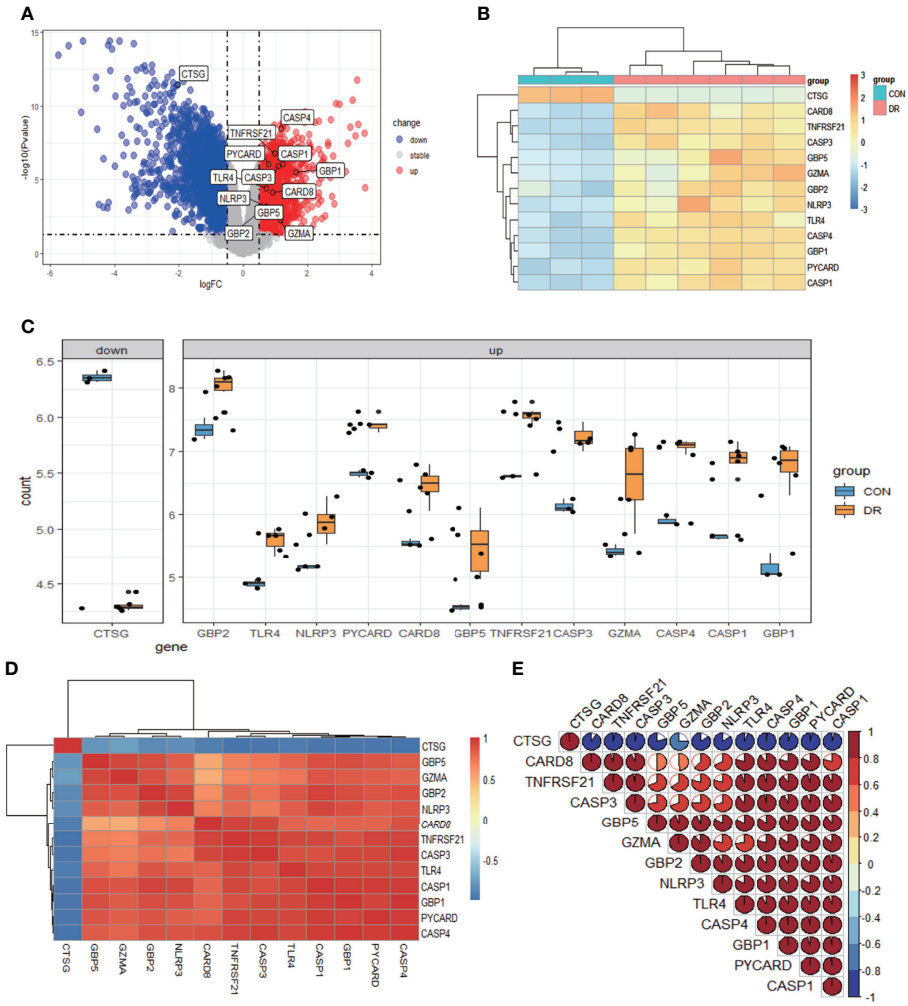

FIGURE 2
Differentially expressed PRGs in PDR and normal samples. **(A)** Volcano plot of 3,188 differentially expressed genes in the GSE60436 dataset. It contains 1,640 significantly upregulated genes, represented by red dots, and 1,548 significantly downregulated genes, represented by blue dots, whereas gray dots represent stably expressed genes. **(B)** Heatmap of 13 differentially expressed PRGs in the GSE60436 dataset. It contains one significantly downregulated gene and 12 significantly upregulated genes. The green bars represent control specimens from human retinas, denoted by "CON", and the red bars represent specimens from PDR patients, denoted by "DR". **(C)** Boxplot of 13 differentially expressed PRGs in FVM tissues of PRD patients and in RNA samples from human retinas. The blue bars represent control specimens from normal individuals, denoted by "CON", and the yellow bars represent specimens from PDR patients, denoted by "DR". Adjusted *P*-value <0.05 and |$\log_2$ fold change| >0.5. **(D, E)** Correlation analysis of 13 differentially expressed PRGs. There was a strong correlation among the 12 upregulated genes. PRGs, pyroptosis-related genes; PDR, proliferative diabetic retinopathy; FVM, fibrovascular membrane.

10.3389/fendo.2022.918605

TABLE 1 Compilation of pyroptosis-related genes.

Gene function	Gene symbol	Gene name
Pyroptosis core components	GSDMA	gasdermin A
	GSDMB	gasdermin B
	GSDMC	gasdermin C
	GSDMD	gasdermin D
	GSDME (DFNA5)	gasdermin E (DFNA5)
	IL-1β	interleukin 1 beta
	IL18	interleukin 18
Genes with pyroptosis function or regulate the expression of PRGs	CASP1	caspase-1
	CASP3	caspase-3
	CASP4	caspase-4
	CASP5	caspase-5
	CASP6	caspase-6
	CASP8	caspase-8
	GZMA	granzyme A
	GZMB	granzyme B
	HMGB1	high mobility group box 1
	GBP1	guanylate binding protein 1
	GBP2	guanylate binding protein 2
	GBP3	guanylate binding protein 3
	GBP4	guanylate binding protein 4
	GBP5	guanylate binding protein 5
	DDX3X	DEAD-box helicase 3 X-linked
	NAIP	NLR family apoptosis inhibitory protein
	SERPINB1	serpin family B member 1
	C-FLIP	cellular FADD-like interleukin-1β converting enzyme inhibitory protein TNF receptor superfamily member 21
	TNFRSF21	interferon regulatory factor 2
	IRF2	Z-DNA binding protein 1
	ZBP1	perforin 1
	PRF1	DExH-box helicase 9
	DHX9	guanylate binding protein 5
	DFNB59 (PJVK)	DFNB59 (pejvakin)
	CTSG	cathepsin G
	APIP	APAF1 interacting protein
Inflammasome	AIM2	absent in melanoma 2
	NLRC4	NLR family CARD domain containing 4
	NLRP1	NLR family pyrin domain containing 1
	NLRP2	NLR family pyrin domain containing 2
	NLRP3	NLR family pyrin domain containing 3
	NLRP6	NLR family pyrin domain containing 6
	NLRP7	NLR family pyrin domain containing 7
	NLRP9	NLR family pyrin domain containing 9
	NLRP12	NLR family pyrin domain containing 12
	NLRX1	NLR family member X1
	NOD2	nucleotide binding oligomerization domain containing 2
	TLR4	toll like receptor 4

(Continued)

TABLE 1 Continued

Gene function	Gene symbol	Gene name
	MEFV (Pyrin)	MEFV innate immuity regulator (Pyrin)
	PYDC1	pyrin domain containing 1
	PYCARD	PYD and CARD domain containing
	CARD8	caspase recruitment domain family member 8
	CARD16	caspase recruitment domain family member 16
	CARD18	caspase recruitment domain family member 18

51 pyroptosis-related genes were collected from the PubMed database (11, 20–26).

GBP2, GBP5, and GZMA—were screened by intersecting these pyroptosis-related genes with genes in the GSE60436 database. These genes are annotated in the volcano plot (Figure 2A) and organized in Table 2. The expression of these genes was plotted as heatmap and box plot (Figures 2B, C). At the same time, we discussed the correlation of these genes, and the results showed that there was a correlation among the 13 pyroptosis-related genes (Figures 2D, E). Then, we further analyzed the differentially expressed genes between active FVMs and inactive FVMs according to the same thresholds and found an upregulated gene GZMB, indicating that GZMB may play an important regulatory role in different states of proliferative diabetic retinopathy.

Functional and pathway enrichment analysis of differentially expressed pyroptosis-related genes

The enrichment analysis was performed on the differentially expressed pyroptosis-related genes to further understand their potential molecular functions and signaling pathways. The GO analysis showed that 383 GO terms were significantly enriched, including 331 biological processes, five cellular components, and 47 molecular functions, involving interleukin-1 beta production, inflammasome complex, and CARD domain binding, indicating that these pyroptosis-related genes play a role in diabetic retinopathy through pyroptosis and inflammatory response (Figures 3A–D). Subsequently, we analyzed the relationship between these pathways, and the result is shown in Figure 4A. Then, we further analyzed the common genes of the first three pathways to clarify the relationship between the differentially expressed pyroptosis-related genes and these pathways (Figure 4B). The heatmap-like functional classification showed the specific enrichment of these genes in the first eight pathways (Figure 4C). At the same time, 67 significantly enriched pathways were obtained by KEGG analysis, indicating that these differentially expressed pyroptosis-related genes may play a key role in NOD-like receptor signaling pathway and other pathways (Figure 5). The most significant pathways obtained by GO analysis and KEGG analysis were shown in Table 3.

TABLE 2 The 13 differentially expressed pyroptosis-related genes in diabetic retinopathy samples compared to normal samples.

Gene symbol	logFC	Changes	P-value	Adjusted P-value	Gene id
CTSG	-2.04863800	Down	3.474745e-12	3.535901e-09	1511
CASP4	1.18248927	Up	3.190990e-09	5.237341e-07	837
TNFRSF21	0.97602261	Up	1.671004e-07	8.553391e-06	27242
PYCARD	0.77897161	Up	8.722862e-07	2.709519e-05	29108
CASP1	1.23521922	Up	8.987948e-07	2.748238e-05	834
CASP3	1.08640598	Up	1.156639e-06	3.351356e-05	836
GBP1	1.64253837	Up	3.128202e-06	6.727089e-05	2633
TLR4	0.71026963	Up	3.722308e-05	4.113837e-04	7099
CARD8	0.91154823	Up	7.318641e-05	6.827511e-04	22900
NLRP3	0.72061228	Up	6.323034e-04	3.673396e-03	114548
GBP2	0.67696609	Up	6.970046e-04	3.974848e-03	2634
GBP5	0.96463926	Up	2.668633e-03	1.181312e-02	115362
GZMA	1.16170618	Up	5.368367e-03	2.079660e-02	3001

PRGs, pyroptosis-related genes; DR, diabetic retinopathy; FC, fold change.

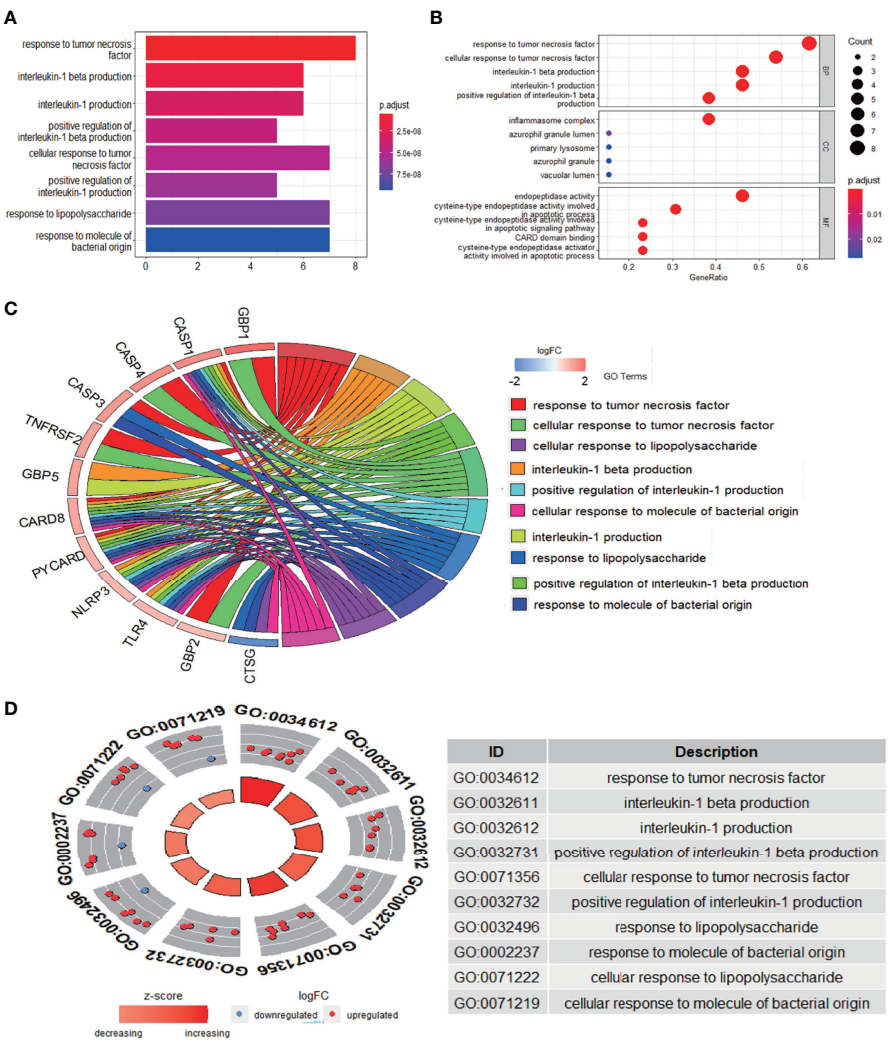

ID	Description
GO:0034612	response to tumor necrosis factor
GO:0032611	interleukin-1 beta production
GO:0032612	interleukin-1 production
GO:0032731	positive regulation of interleukin-1 beta production
GO:0071356	cellular response to tumor necrosis factor
GO:0032732	positive regulation of interleukin-1 production
GO:0032496	response to lipopolysaccharide
GO:0002237	response to molecule of bacterial origin
GO:0071222	celluar response to lipopolysaccharide
GO:0071219	cellular response to molecule of bacterial origin

FIGURE 3
GO enrichment analysis of 13 differentially expressed PRGs. **(A)** Bar plot of enriched GO terms. **(B)** Bubble plot of enriched GO terms. **(C)** Chordal graph of enriched GO terms. **(D)** Eight diagrams of enriched GO terms. It contains three aspects—BPs, CCs, and MFs—and shows the specific genes involved in each GO term. GO, Gene Ontology; PRGs, pyroptosis-related genes; BPs, biological processes; CCs, cellular components; MFs, molecular functions.

Construction of PPI network

The PPI network is composed of individual proteins through the interaction between each other, which is of great significance for understanding protein function and interaction (27). In order to further explore the differentially expressed pyroptosis-related genes, we carried out PPI analysis. Firstly, the network files sorted out in R software are uploaded to String database, which is a network tool for exploring known and predicted protein–protein interactions (28). A PPI network with 13 nodes and 35 sides is obtained, and the average node degree is 5.38 (Figure 6A). Then, we used the cytoHubba in CytoScape software for further analysis, sequenced these differentially expressed pyroptosis-related genes by MCC mode, and screened the first eight hub genes, namely: CASP1, NLRP3, CASP4, PYCARD, TLR4, CASP3, GBP2, and GBP1 (Figure 6B, Table 4).

Validation of pyroptosis-related genes

To ensure the reliability of the results of the GSE60436 dataset analysis, we use qRT-PCR experiments and RNA-seq-based dataset GSE179568 for validation. Firstly, the expression levels of the eight key differentially expressed pyroptosis-related genes were further identified by qRT-PCR in the *in*

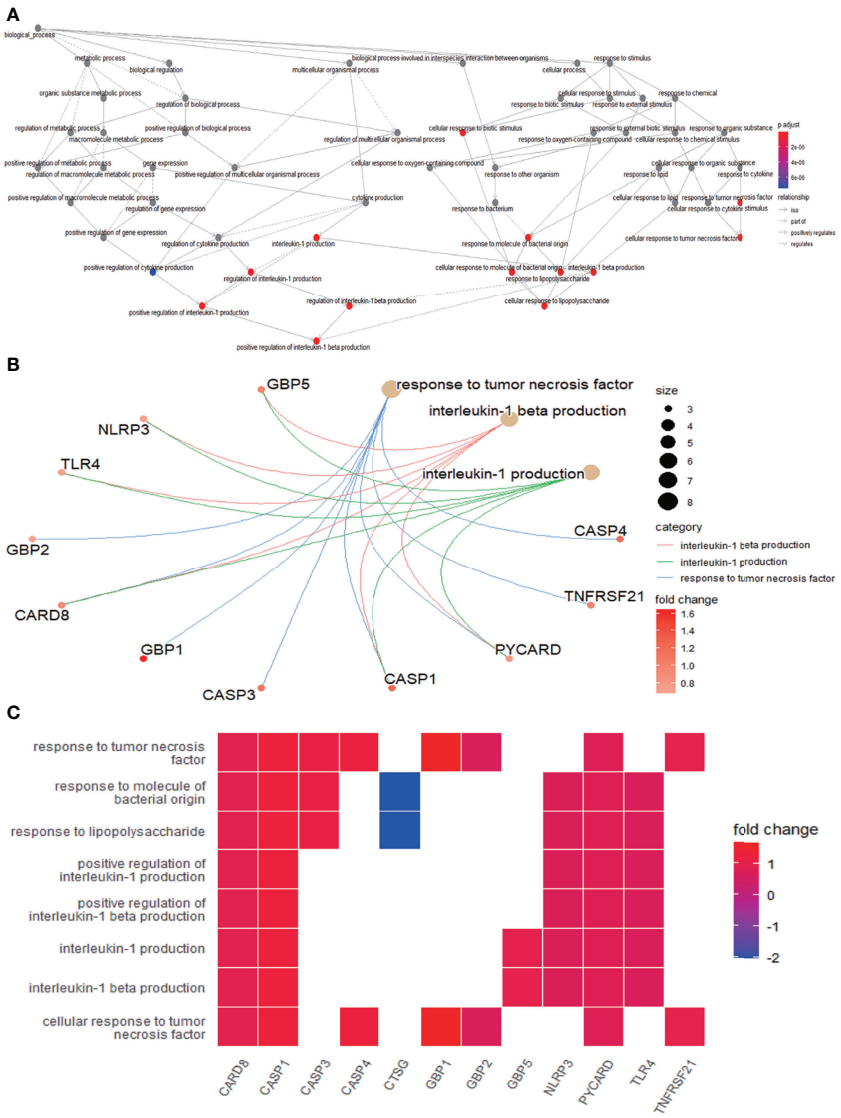

FIGURE 4
Further analysis of the results obtained by GO enrichment analysis. **(A)** Relationship between the pathways obtained by GO enrichment analysis. **(B)** Common genes among the three most prominent pathways. Each path is represented by lines of different colors. **(C)** Heatmap-like functional classification. The enrichment relationships of differentially expressed PRGs in the eight most significant pathways are shown. GO, Gene Ontology; PRGs, pyroptosis-related genes.

vitro model of diabetic retinopathy. HRECs were cultured in high glucose medium (30 mmol/L anhydrous glucose) or normal-glucose medium. High-glucose-exposed HRECs were used as an *in vitro* model of diabetic retinopathy. Similar to the results of mRNA chip in the GSE60436 dataset, high glucose treatment significantly increased the mRNA expression levels of CASP3, TLR4, GBP2, CASP4, and GBP1 in HRECs. In addition, the expression levels of NLRP3, CASP1, and PYCARD were also increased (Figure 7). These results were in accordance with the bioinformatics analysis. Then, as described previously, we analyzed the 51 pyroptosis-related genes in the verification set with $|\log_2$ fold change$| > 1.0$ as the threshold, and the trend of five pyroptosis-related genes was consistent with that of the hub genes analyzed by the GSE60436 dataset, including CASP4, GBP1, CASP3, TLR4, and GBP2 (Figure 8). In general, the results between the training set and the validation set are relatively consistent. Next, we detected the expression of caspase-3 and gasdermin proteins, the key executor of pyroptosis, in the *in vitro* model of diabetic retinopathy by western blotting. It showed that the protein levels of cleaved caspase-3, GSDMD, and gasdermin E (GSDME) were increased in human retinal endothelial cells

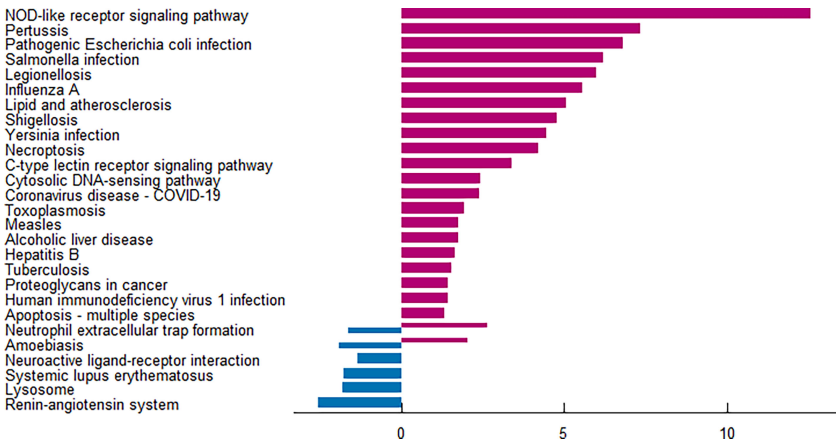

FIGURE 5
KEGG pathway analysis of 13 differentially expressed PRGs. According to the adjusted *P*-value, a total of 67 pathways were reported. KEGG, Kyoto Encyclopedia of Genes and Genomes; PRGs, pyroptosis-related genes.

after high glucose incubation, suggesting the occurrence of pyroptosis (Figure 9).

Construction of ceRNA-regulating network

In order to further explore the interaction between lncRNA, miRNA, and mRNA in diabetic retinopathy, we structured a ceRNA regulatory network. MultiMiR is a new miRNA–target interaction R package and database, which combines human and mouse records from 14 databases and includes mirTarbase databases with experimental methods to verify the interactions (29). Through this database, not only the miRNA that interacts with mRNA but also the targeted mRNA of miRNA can be predicted. We used the luciferase reporter assay as the screening criterion and used this tool to predict 20 miRNAs, including hsa-let-7a-5p, hsa-miR-433-3p, and so on (Table 5). Then, based on

TABLE 3 Top 7 GO terms and top 3 KEGG pathway analyses for the differentially expressed PRGs.

Pathway id	Category	Description	Count	Genes	P-value
GO:0061702	CC	inflammasome complex	5	CASP4, PYCARD, CASP1, CARD8, NLRP3	3.36E-13
GO:0034612	BP	cysteine-type endopeptidase activity involved in apoptotic process	8	CASP4, TNFRSF21, PYCARD, CASP1, CASP3, GBP1, CARD8, GBP2	7.52E-12
GO:0032611	BP	interleukin-1 beta production	6	PYCARD, CASP1, TLR4, CARD8, NLRP3, GBP5	5.09E-11
GO:0032612	BP	interleukin-1 production	6	PYCARD, CASP1, TLR4, CARD8, NLRP3, GBP5	1.30E-10
GO:0097153	MF	cysteine-type endopeptidase activity involved in apoptotic process	4	CASP4, PYCARD, CASP1, CASP3	2.06E-10
GO:0032731	BP	positive regulation of interleukin-1 beta production	5	PYCARD, CASP1, TLR4, CARD8, NLRP3	2.43E-10
GO:0071356	BP	cellular response to tumor necrosis factor	7	CASP4, TNFRSF21, , CASP1, GBP1, CARD8, GBP2	3.46E-10
hsa04621	KEGG	NOD-like receptor signaling pathway	9	CASP4, PYCARD, CASP1, GBP1, TLR4, CARD8, NLRP3, GBP2, GBP5	8.37E-13
hsa05133	KEGG	Pertussis	5	PYCARD, CASP1, CASP3, TLR4, NLRP3	7.53E-08
hsa05130	KEGG	Pathogenic Escherichia coli infection	6	CASP4, PYCARD, CASP1, CASP3, TLR4, NLRP3	2.77E-07

*GO, Gene Ontology; KEGG, Kyoto Encyclopedia ofGenes and Genomes; PRGs, pyroptosis-related genes.

10.3389/fendo.2022.918605

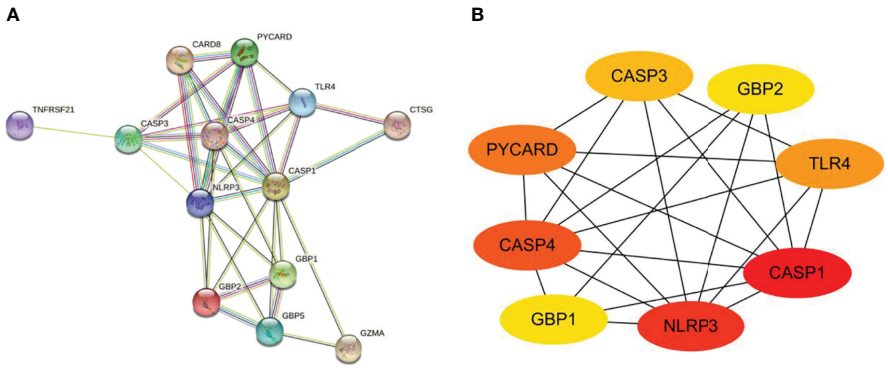

FIGURE 6
Construction of PPI network and identification of hub genes. **(A)** The PPI network of 13 differentially expressed PRGs was constructed by using String database. It contains 13 nodes and 35 edges. The average node degree is 5.38, and the PPI enrichment *P*-value is less than 1.0e-16. **(B)** First eight hub genes of the PPI network. First eight genes with the highest degree identified by Cytoscape software and CytoHubba. These genes are ranked in descending order from red to yellow. PPI, protein–protein interaction; PRGs, pyroptosis-related genes.

these miRNAs, we obtained 22 targeted lncRNAs through the starbase database. Finally, the three mRNAs, 20 miRNAs, and 22 lncRNAs were used to structure the ceRNA regulatory network, and the visualization was carried out in the CytoScape software (Figure 10).

Discussion

It has been demonstrated that leukostasis, infiltration of neutrophil and macrophage, and activation of complements and microglial cells were found in the retinas of patients or animal model with diabetic retinopathy. Meanwhile, elevated levels of inflammatory cytokines and chemokines were detected in vitreous or aqueous humor from diabetic patients, indicating a critical role of inflammation in diabetic retinopathy (30, 31). Pyroptosis, known as cell inflammatory death, is accompanied by the release of a large number of pro-inflammatory factors, which is closely related to the pathogenesis of various chronic inflammatory diseases (8). Diabetic retinopathy is currently considered a chronic inflammatory disease. Thus, the involvement of pyroptosis-induced inflammation in diabetic retinopathy draws more and more attention. However, the molecular mechanisms underlying pyroptosis in diabetic retinopathy are unclear and need further investigations (32).

Bioinformatics methods have been widely used for the exploration of key pathogenic factors and potential therapeutic targets in diabetic retinopathy (33–35). To the best of our knowledge, bioinformatics analysis of pyroptosis-related genes in diabetic retinopathy has not been reported. In the current study, 13 differentially expressed pyroptosis-related genes in diabetic retinopathy were identified by bioinformatics for the first time, and eight of the most critical genes were identified by PPI analysis. At the same time, we performed GO analysis and KEGG analysis on these 13 differentially expressed pyroptosis-related genes to clarify the enrichment relationship between these genes and related pathways. The results showed that these genes were enriched in inflammasome complex, interleukin-1 beta production, and other pathways, confirming the role of pyroptosis in diabetic retinopathy.

TABLE 4 PPI network of the top 8 hub genes.

Rank	Gene symbol	Score	Gene id	Gene name
1	CASP1	196	834	caspase-1
2	NLRP3	192	114548	NLR family pyrin domain containing 3 caspase-4
3	CASP4	168	837	PYD and CARD domain containing toll like receptor 4
4	PYCARD	144	29108	NLR family pyrin domain containing 3 caspase-4
5	TLR4	122	7099	PYD and CARD domain containing toll like receptor 4
6	CASP3	121	836	caspase-3
7	GBP2	48	2634	guanylate binding protein 2
8	GBP1	48	2633	guanylate binding protein 1

PPI, protein-protein interaction.

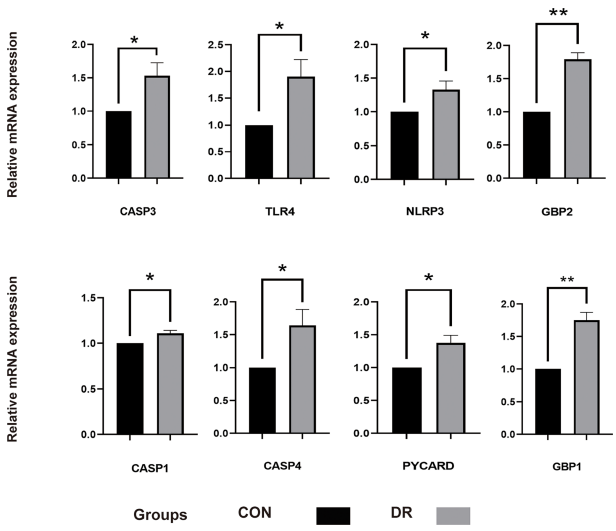

FIGURE 7
qRT-PCR experiment to verify the expression of PRGs of interest in the *in vitro* model. HRECs exposed to high glucose for 48 h were used as DR model, and HRECs cultured on normal culture medium were used as control. The *P*-values were calculated using a two-sided unpaired Student's *t*-test. *$P < 0.05$; **$P < 0.01$. qRT-PCR, quantitative real-time polymerase chain reaction; PRGs, pyroptosis-related genes; HRECs, human retinal endothelial cells; DR, diabetic retinopathy.

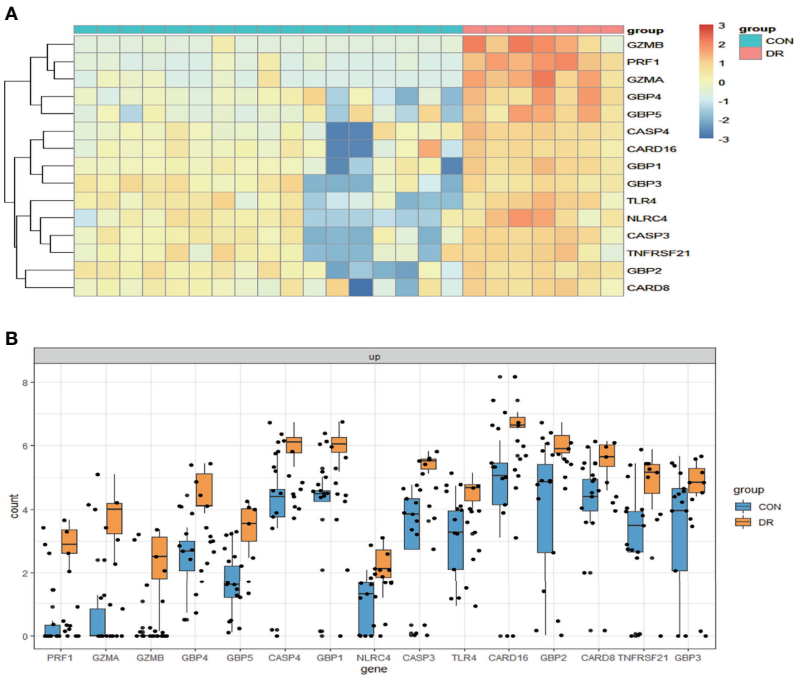

FIGURE 8
Validation of PRGs in the GSE179568 dataset. **(A)** Heatmap of 15 differentially expressed PRGs in the GSE60436 dataset. **(B)** Box plot of 15 differentially expressed PRGs in the RNV membranes of PRD patients and in the epiretinal membranes of macular pucker and macular hole samples. Adjusted *P*-value <0.05 and $|\log_2$ fold change$|$ >1.0. PRGs, pyroptosis-related genes; RNV, retinal neovascularization; PDR, proliferative diabetic retinopathy.

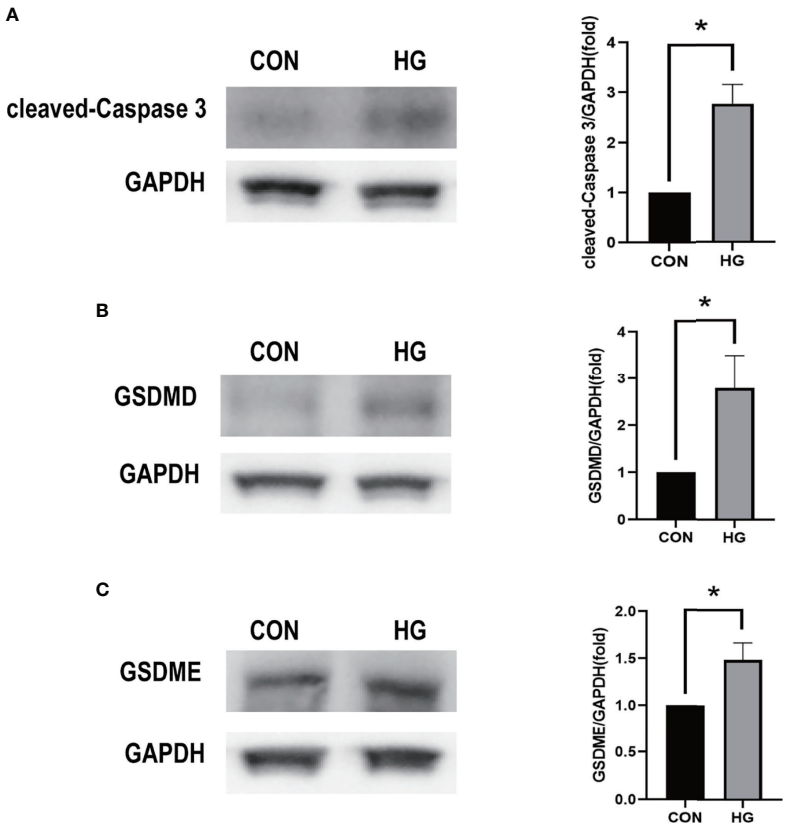

FIGURE 9
Western blot analysis of caspase-3 and gasdermin proteins in *in vitro* models. **(A)** Cleaved caspase-3 (17 kDa) was tested. GAPDH (36 kDa) was used as a control. **(B)** GSDMD (31 kDa) was examined. GAPDH was used as a control. **(C)** GSDME (55 kDa) was examined. GAPDH was used as a control. The experiments were repeated independently at least three times. *$P < 0.05$. CON, control group; HG, high-glucose group; GSDMD, gasdermin D; GSDME, gasdermin E.

Based on the results of the bioinformatics analysis, we identified eight most interesting pyroptosis-related genes according to PPI analysis and enrichment analysis. HRECs were incubated with high-glucose medium to mimic diabetic retinopathy *in vitro*. qRT-PCR was used for the verification of selected pyroptosis-related genes in a diabetic retinopathy model. The results showed that the change of mRNA level of CASP3, TLR4, NLRP3, GBP2, CASP1, CASP4, PYCARD, and GBP1 was consistent with that of the bioinformatics analysis of the mRNA chip. Among them, CASP3, TLR4, GBP2, CASP4, and GBP1 are verified in the validation set. We also showed that the cleaved CASP3 was upregulated in the *in vitro* model of diabetic retinopathy (Figure 9A). Several reports have shown that hyperglycemia can trigger the retinal inflammatory responses by abnormal metabolic pathways. It is accompanied by the activation of inflammasomes such as NLRP3 and TLR4, which play an important role in cell pyroptosis (36–38). Meanwhile, it has been reported that these potential pyroptosis-related genes mediated pyroptosis mainly due to the release of inflammatory cytokines such as IL-1β and IL-18 and lactate dehydrogenase, and the activation of GSDMD promotes pore formation in cells. Pyroptosis is associated with the damage of retinal vascular endothelial cells, retinal pericytes, and retinal

TABLE 5 miRNAs and specic targeted mRNAs in ceRNA regulatory network.

mRNA	miRNA
CASP3	hsa-miR-421, hsa-let-7g-5p, hsa-miR-30e-5p, hsa-let-7c-5p, hsa-let-7a-5p, hsa-miR-363-3p, hsa-miR-30c-5p, hsa-miR-138-5p, hsa-miR-98-5p, hsa-miR-224-5p, hsa-miR-155-5p, hsa-miR-30d-5p, hsa-miR-582-5p, hsa-miR-885-5p
TLR4	hsa-let-7i-5p, hsa-miR-146b-5p, hsa-miR-26b-5p, hsa-let-7b-5p, hsa-miR-146a-5p
GBP2	hsa-miR-433-3p

miRNAs, microRNAs; ceRNA, competing endogenous RNAs.

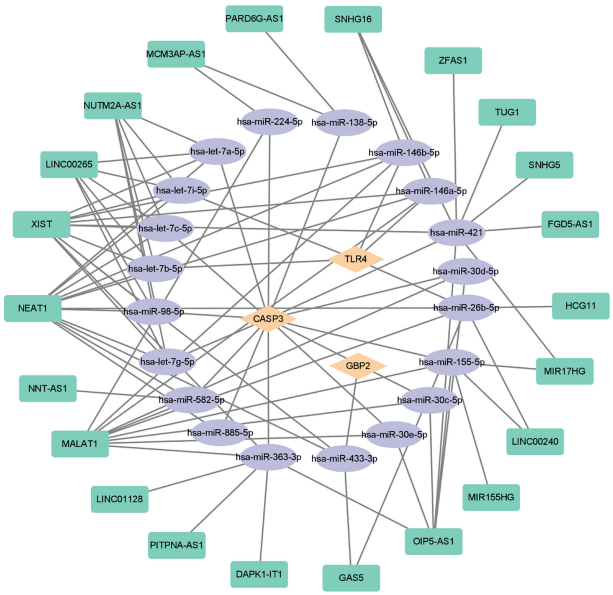

FIGURE 10
ceRNA-regulating networks. The yellow diamond represents the protein coding genes, the purple circle represents miRNAs, and the green rectangle represents lncRNAs. The black lines indicate the interaction of lncRNA–miRNA–mRNA. ceRNA, competing endogenous RNAs; miRNAs, microRNAs; lncRNAs, long non-coding RNAs.

pigment epithelium (RPE) cells in diabetic retinopathy (39–44). In the current study, both GSDMD and GSDME were increased in the high-glucose-treated retinal vascular endothelial cells, which is consistent with previous findings, indicating that hyperglycemia can trigger pyroptosis in retinal vascular endothelial cells. Destruction of retinal vascular endothelial cells by hyperglycemia leads to blood–retinal barrier damage and occlusion of the retinal capillary, which cause macular edema and pathological retinal neovascularization (45, 46). Rescuing the disrupted retinal vascular endothelial cells is the therapeutic strategy for diabetic retinopathy. Therefore, further elucidating the function of the aforementioned pyroptosis-related genes in retinal vascular endothelial cells will provide a deep insight into the mechanism underlying diabetic retinopathy.

Recently, increasing data demonstrated that lncRNA- and miRNA-mediated pyroptosis is involved in the occurrence of diabetic retinopathy. miRNA miR-590-3p, which has been proved to play an active role in inflammation (47), could directly target NLRP1 and NOX4 and inhibit pyroptosis in diabetic retinopathy through the NOX4/ROS/TXNIP/NLRP3 pathway (42). METTL3, as the key methyltransferase for m^6A RNA methylation, reduced the pyroptosis level in a diabetic model by targeting the miR-25-3p/PTEN/Akt signal cascade with the assistance of DGCR8 (43). CircZNF532 could also regulate pyroptosis in RPE cells from diabetic retinopathy patients by targeting the miR-20b-5p/STAT3 axis (44). Another study found that lncRNA MIAT was significantly upregulated in human retinal pericytes and promoted human retinal pericyte pyroptosis by regulating miR-342-3p targeting CASP1 (41). Therefore, we constructed the ceRNA-regulating network to figure out the reciprocal interaction between lncRNA and miRNA and its function in regulating pyroptosis-related gene expression. By using multiMiR database, we predicted 20 miRNAs to be involved in the modulation of three essential pyroptosis-related genes, such as CASP3, TLR4, and GBP2. Subsequently, we found a possible interaction between 22 lncRNAs and these 20 miRNAs. Based on these findings, we created the ceRNA-regulating network through the aforementioned 22 lncRNAs, 20 miRNAs, and three target mRNAs. Among these genes, TLR4 as a pattern recognition receptor is very important for the activation of NLRP3 inflammatory bodies (48). After activation, inflammatory bodies can bind to pro-caspase-1 through the binding protein ASC, activate caspase-1, and induce cell pyroptosis through the classical pathway. At the same time, in the non-classical pathway, although caspase-4/5/11 can be directly activated by LPS without the participation of receptors, it still needs to be completed with the assistance of caspase-1 activated by NLRP3. Both classical and non-classical pathways will induce pyroptosis by cleaving GSDMD (49, 50). GBP2 plays a dual role in the occurrence of pyroptosis. It not only promotes the activation of AIM2 inflammatory cytokines but also controls the recruitment of caspase-4 (51, 52). In recent years, accumulated evidence have shown that caspase-3, which is usually regarded as a marker of apoptosis, can play an important role in pyroptosis by cleaving GSDME, which is another new pathway of pyroptosis that is

different from the classical and non-classical pathways (8, 53, 54). In this study, we confirmed that high glucose could upregulate the expression of caspase-3 and GSDME in the diabetic model, suggesting that CASP3-mediated pyroptosis is involved in the development of diabetic retinopathy, which has not been explored. Further studies are required to uncover it.

Conclusions

In this study, the key pyroptosis-related genes in diabetic retinopathy, such as CASP3, GBP2, and TLR4, were preliminarily identified by bioinformatics analysis and confirmed by GSE179568 and qRT-PCR in a diabetic model. lncRNAs and miRNAs that are associated with these genes were further predicted (Figure 10). It provides a novel insight into the molecular mechanism of pyroptosis in the pathogenesis of diabetic retinopathy.

Data availability statement

The dataset presented in this study can be found in online repositories. The names of the repository/repositories and accession number(s) can be found in the article/**Supplementary Material**.

Author contributions

NW and LD analyzed the data and drafted the manuscript. DL, XX, QZ, and GZ edited and provided comments to improve the manuscript. SX designed this experiment and reviewed and revised the manuscripts. All the authors contributed to the article and approved the final manuscript.

Funding

This study was financially supported by the National Natural Science Foundation of China (no. 81974137 to SX), the National Natural Science Foundation of China (no. 82070966 to LD), the Natural Science Foundation of Hunan Province (no. 2019JJ40507 to SX), and the Science and Technology Innovation Program of Hunan Province (no. 2021RC3026 to LD).

Conflict of interest

The authors declare that the research was conducted in the absence of any commercial or financial relationships that could be construed as a potential conflict of interest.

Publisher's note

All claims expressed in this article are solely those of the authors and do not necessarily represent those of their affiliated organizations, or those of the publisher, the editors and the reviewers. Any product that may be evaluated in this article, or claim that may be made by its manufacturer, is not guaranteed or endorsed by the publisher.

Supplementary material

The Supplementary Material for this article can be found online at: https://www.frontiersin.org/articles/10.3389/fendo.2022.918605/full#supplementary-material

References

1. Amoaku WM, Ghanchi F, Bailey C, Banerjee S, Banerjee S, Downey L, et al. Diabetic retinopathy and diabetic macular oedema pathways and management: Uk consensus working group. *Eye (Lond)* (2020) 34(Suppl 1):1–51. doi: 10.1038/s41433-020-0961-6

2. Wang CF, Yuan JR, Qin D, Gu JF, Zhao BJ, Zhang L, et al. Protection of tauroursodeoxycholic acid on high glucose-induced human retinal microvascular endothelial cells dysfunction and streptozotocin-induced diabetic retinopathy rats. *J Ethnopharmacol* (2016) 185:162–70. doi: 10.1016/j.jep.2016.03.026

3. Teo ZL, Tham YC, Yu M, Chee ML, Rim TH, Cheung N, et al. Global prevalence of diabetic retinopathy and projection of burden through 2045: Systematic review and meta-analysis. *Ophthalmology* (2021) 128(11):1580–91. doi: 10.1016/j.ophtha.2021.04.027

4. Wong TY, Cheung CM, Larsen M, Sharma S, Simó R. Diabetic retinopathy. *Nat Rev Dis Primers* (2016) 2:16012. doi: 10.1038/nrdp.2016.12

5. Simó R, Hernández C. Intravitreous anti-vegf for diabetic retinopathy: Hopes and fears for a new therapeutic strategy. *Diabetologia* (2008) 51(9):1574–80. doi: 10.1007/s00125-008-0989-9

6. Campochiaro PA, Hafiz G, Mir TA, Scott AW, Zimmer-Galler I, Shah SM, et al. Pro-permeability factors in diabetic macular edema; the diabetic macular edema treated with ozurdex trial. *Am J Ophthalmol* (2016) 168:13–23. doi: 10.1016/j.ajo.2016.04.017

7. Shi J, Gao W, Shao F. Pyroptosis: Gasdermin-mediated programmed necrotic cell death. *Trends Biochem Sci* (2017) 42(4):245–54. doi: 10.1016/j.tibs.2016.10.004

8. Wang Y, Gao W, Shi X, Ding J, Liu W, He H, et al. Chemotherapy drugs induce pyroptosis through caspase-3 cleavage of a gasdermin. *Nature* (2017) 547 (7661):99–103. doi: 10.1038/nature22393

9. Shi J, Zhao Y, Wang K, Shi X, Wang Y, Huang H, et al. Cleavage of gsdmd by inflammatory caspases determines pyroptotic cell death. *Nature* (2015) 526 (7575):660–5. doi: 10.1038/nature15514

10. Ding J, Wang K, Liu W, She Y, Sun Q, Shi J, et al. Pore-forming activity and structural autoinhibition of the gasdermin family. *Nature* (2016) 535(7610):111–6. doi: 10.1038/nature18590

11. Vande Walle L, Lamkanfi M. Pyroptosis. *Curr Biol* (2016) 26(13):R568–r72. doi: 10.1016/j.cub.2016.02.019

12. Kayagaki N, Stowe IB, Lee BL, O'Rourke K, Anderson K, Warming S, et al. Caspase-11 cleaves gasdermin d for non-canonical inflammasome signalling. *Nature* (2015) 526(7575):666–71. doi: 10.1038/nature15541

13. Kayagaki N, Warming S, Lamkanfi M, Vande Walle L, Louie S, Dong J, et al. Non-canonical inflammasome activation targets caspase-11. *Nature* (2011) 479 (7371):117–21. doi: 10.1038/nature10558

14. Tan Y, Chen Q, Li X, Zeng Z, Xiong W, Li G, et al. Pyroptosis: A new paradigm of cell death for fighting against cancer. *J Exp Clin Cancer Res* (2021) 40 (1):153. doi: 10.1186/s13046-021-01959-x

15. Zhaolin Z, Guohua L, Shiyuan W, Zuo W. Role of pyroptosis in cardiovascular disease. *Cell Prolif* (2019) 52(2):e12563. doi: 10.1111/cpr.12563

16. Tan CC, Zhang JG, Tan MS, Chen H, Meng DW, Jiang T, et al. Nlrp1 inflammasome is activated in patients with medial temporal lobe epilepsy and contributes to neuronal pyroptosis in amygdala kindling-induced rat model. *J Neuroinflamm* (2015) 12:18. doi: 10.1186/s12974-014-0233-0

17. Jeyabal P, Thandavarayan RA, Joladarashi D, Suresh Babu S, Krishnamurthy S, Bhimaraj A, et al. Microrna-9 inhibits hyperglycemia-induced pyroptosis in human ventricular cardiomyocytes by targeting Elavl1. *Biochem Biophys Res Commun* (2016) 471(4):423–9. doi: 10.1016/j.bbrc.2016.02.065

18. Meng C, Gu C, He S, Su T, Lhamo T, Draga D, et al. Pyroptosis in the retinal neurovascular unit: New insights into diabetic retinopathy. *Front Immunol* (2021) 12:763092. doi: 10.3389/fimmu.2021.763092

19. Ishikawa K, Yoshida S, Kobayashi Y, Zhou Y, Nakama T, Nakao S, et al. Microarray analysis of gene expression in fibrovascular membranes excised from patients with proliferative diabetic retinopathy. *Invest Ophthalmol Vis Sci* (2015) 56 (2):932–46. doi: 10.1167/iovs.14-15589

20. Wang Q, Liu Q, Qi S, Zhang J, Liu X, Li X, et al. Comprehensive pan-cancer analyses of pyroptosis-related genes to predict survival and immunotherapeutic outcome. *Cancers (Basel)* (2022) 14(1) 237. doi: 10.3390/cancers14010237

21. Chen X, Chen H, Yao H, Zhao K, Zhang Y, He D, et al. Turning up the heat on non-immunoreactive tumors: Pyroptosis influences the tumor immune microenvironment in bladder cancer. *Oncogene* (2021) 40(45):6381–93. doi: 10.1038/s41388-021-02024-9

22. Shao W, Yang Z, Fu Y, Zheng L, Liu F, Chai L, et al. The pyroptosis-related signature predicts prognosis and indicates immune microenvironment infiltration in gastric cancer. *Front Cell Dev Biol* (2021) 9:676485. doi: 10.3389/fcell.2021.676485

23. Loveless R, Bloomquist R, Teng Y. Pyroptosis at the forefront of anticancer immunity. *J Exp Clin Cancer Res* (2021) 40(1):264. doi: 10.1186/s13046-021-02065-8

24. Hachim MY, Khalil BA, Elemam NM, Maghazachi AA. Pyroptosis: The missing puzzle among innate and adaptive immunity crosstalk. *J Leukoc Biol* (2020) 108(1):323–38. doi: 10.1002/jlb.3mir0120-625r

25. Yogarajah T, Ong KC, Perera D, Wong KT. Aim2 inflammasome-mediated pyroptosis in enterovirus A71-infected neuronal cells restricts viral replication. *Sci Rep* (2017) 7(1):5845. doi: 10.1038/s41598-017-05589-2

26. Du T, Gao J, Li P, Wang Y, Qi Q, Liu X, et al. Pyroptosis, metabolism, and tumor immune microenvironment. *Clin Transl Med* (2021) 11(8):e492. doi: 10.1002/ctm2.492

27. Szklarczyk D, Gable AL, Lyon D, Junge A, Wyder S, Huerta-Cepas J, et al. String V11: Protein-protein association networks with increased coverage, supporting functional discovery in genome-wide experimental datasets. *Nucleic Acids Res* (2019) 47(D1):D607–d13. doi: 10.1093/nar/gky1131

28. Szklarczyk D, Gable AL, Nastou KC, Lyon D, Kirsch R, Pyysalo S, et al. The string database in 2021: Customizable protein-protein networks, and functional characterization of user-uploaded Gene/Measurement sets. *Nucleic Acids Res* (2021) 49(D1):D605–d12. doi: 10.1093/nar/gkaa1074

29. Ru Y, Kechris KJ, Tabakoff B, Hoffman P, Radcliffe RA, Bowler R, et al. The multimir r package and database: Integration of microrna-target interactions along with their disease and drug associations. *Nucleic Acids Res* (2014) 42(17):e133. doi: 10.1093/nar/gku631

30. Hotamisligil GS. Inflammation and metabolic disorders. *Nature* (2006) 444 (7121):860–7. doi: 10.1038/nature05485

31. Forrester JV, Kuffova L, Delibegovic M. The role of inflammation in diabetic retinopathy. *Front Immunol* (2020) 11:583687. doi: 10.3389/fimmu.2020.583687

32. Al Mamun A, Mimi AA, Zaeem M, Wu Y, Monalisa I, Akter A, et al. Role of pyroptosis in diabetic retinopathy and its therapeutic implications. *Eur J Pharmacol* (2021) 904:174166. doi: 10.1016/j.ejphar.2021.174166

33. Miao A, Lu J, Wang Y, Mao S, Cui Y, Pan J, et al. Identification of the aberrantly methylated differentially expressed genes in proliferative diabetic retinopathy. *Exp Eye Res* (2020) 199:108141. doi: 10.1016/j.exer.2020.108141

34. Huang J, Zhou Q. Identification of the relationship between hub genes and immune cell infiltration in vascular endothelial cells of proliferative diabetic retinopathy using bioinformatics methods. *Dis Markers* (2022) 2022:7231046. doi: 10.1155/2022/7231046

35. Cao NJ, Liu HN, Dong F, Wang W, Sun W, Wang G. Integrative analysis of competitive endogenous rna network reveals the regulatory role of non-coding rnas in high-Glucose-Induced human retinal endothelial cells. *PeerJ* (2020) 8:e9452. doi: 10.7717/peerj.9452

36. Zhou X, Xia XB, Xiong SQ. Neuro-protection of retinal stem cells transplantation combined with copolymer-1 immunization in a rat model of glaucoma. *Mol Cell Neurosci* (2013) 54:1–8. doi: 10.1016/j.mcn.2012.12.001

37. Schroder K, Zhou R, Tschopp J. The Nlrp3 inflammasome: A sensor for metabolic danger? *Science* (2010) 327(5963):296–300. doi: 10.1126/science.1184003

38. Bayan N, Yazdanpanah N, Rezaei N. Role of toll-like receptor 4 in diabetic retinopathy. *Pharmacol Res* (2022) 175:105960. doi: 10.1016/j.phrs.2021.105960

39. Homme RP, Singh M, Majumder A, George AK, Nair K, Sandhu HS, et al. Remodeling of retinal architecture in diabetic retinopathy: Disruption of ocular physiology and visual functions by inflammatory gene products and pyroptosis. *Front Physiol* (2018) 9:1268. doi: 10.3389/fphys.2018.01268

40. Gan J, Huang M, Lan G, Liu L, Xu F. High glucose induces the loss of retinal pericytes partly *Via* Nlrp3-Caspase-1-Gsdmd-Mediated pyroptosis. *BioMed Res Int* (2020) 2020:4510628. doi: 10.1155/2020/4510628

41. Yu X, Ma X, Lin W, Xu Q, Zhou H, Kuang H. Long noncoding rna miat regulates primary human retinal pericyte pyroptosis by modulating mir-342-3p targeting of Casp1 in diabetic retinopathy. *Exp Eye Res* (2021) 202:108300. doi: 10.1016/j.exer.2020.108300

42. Gu C, Draga D, Zhou C, Su T, Zou C, Gu Q, et al. Mir-590-3p inhibits pyroptosis in diabetic retinopathy by targeting Nlrp1 and inactivating the Nox4 signaling pathway. *Invest Ophthalmol Vis Sci* (2019) 60(13):4215–23. doi: 10.1167/iovs.19-27825

43. Zha X, Xi X, Fan X, Ma M, Zhang Y, Yang Y. Overexpression of Mettl3 attenuates high-glucose induced rpe cell pyroptosis by regulating mir-25-3p/Pten/Akt signaling cascade through Dgcr8. *Aging (Albany NY)* (2020) 12(9):8137–50. doi: 10.18632/aging.103130

44. Liang GH, Luo YN, Wei RZ, Yin JY, Qin ZL, Lu LL, et al. Circznf532 knockdown protects retinal pigment epithelial cells against high glucose-induced apoptosis and pyroptosis by regulating the mir-20b-5p/Stat3 axis. *J Diabetes Investig* (2021) 13(5):781–95. doi: 10.1111/jdi.13722

45. Beltramo E, Porta M. Pericyte loss in diabetic retinopathy: Mechanisms and consequences. *Curr Med Chem* (2013) 20(26):3218–25. doi: 10.2174/09298673113209990022

46. Sorrentino FS, Matteini S, Bonifazzi C, Sebastiani A, Parmeggiani F. Diabetic retinopathy and endothelin system: Microangiopathy versus endothelial dysfunction. *Eye (Lond)* (2018) 32(7):1157–63. doi: 10.1038/s41433-018-0032-4

47. Mussbacher M, Salzmann M, Brostjan C, Hoesel B, Schoergenhofer C, Datler H, et al. Cell type-specific roles of nf-κb linking inflammation and thrombosis. *Front Immunol* (2019) 10:85. doi: 10.3389/fimmu.2019.00085

48. He Y, Hara H, Núñez G. Mechanism and regulation of Nlrp3 inflammasome activation. *Trends Biochem Sci* (2016) 41(12):1012–21. doi: 10.1016/j.tibs.2016.09.002

49. Man SM, Kanneganti TD. Gasdermin d: The long-awaited executioner of pyroptosis. *Cell Res* (2015) 25(11):1183–4. doi: 10.1038/cr.2015.124

50. Broz P. Immunology: Caspase target drives pyroptosis. *Nature* (2015) 526 (7575):642–3. doi: 10.1038/nature15632

51. Yang Y, Wang H, Kouadir M, Song H, Shi F. Recent advances in the mechanisms of Nlrp3 inflammasome activation and its inhibitors. *Cell Death Dis* (2019) 10(2):128. doi: 10.1038/s41419-019-1413-8

52. Rathinam VA, Fitzgerald KA. Inflammasome complexes: Emerging mechanisms and effector functions. *Cell* (2016) 165(4):792–800. doi: 10.1016/j.cell.2016.03.046

53. Yu J, Li S, Qi J, Chen Z, Wu Y, Guo J, et al. Cleavage of gsdme by caspase-3 determines lobaplatin-induced pyroptosis in colon cancer cells. *Cell Death Dis* (2019) 10(3):193. doi: 10.1038/s41419-019-1441-4

54. Li Y, Yuan Y, Huang ZX, Chen H, Lan R, Wang Z, et al. Gsdme-mediated pyroptosis promotes inflammation and fibrosis in obstructive nephropathy. *Cell Death Differ* (2021) 28(8):2333–50. doi: 10.1038/s41418-021-00755-6

frontiers | Frontiers in Endocrinology

TYPE Mini Review
PUBLISHED 10 August 2022
DOI 10.3389/fendo.2022.934231

OPEN ACCESS

EDITED BY
Chengqi Xu,
Huazhong University of Science and Technology, China

REVIEWED BY
Rongfeng Zhang,
Dalian Medical University, China
Huiying Liu,
307th Hospital of Chinese People's Liberation Army, China

*CORRESPONDENCE
Ranji Cui
cuiranji@jlu.edu.cn
Kexiang Liu
kxliu64@hotmail.com

†These authors have contributed equally to this work and share first authorship

SPECIALTY SECTION
This article was submitted to Cellular Endocrinology, a section of the journal Frontiers in Endocrinology

RECEIVED 02 May 2022
ACCEPTED 11 July 2022
PUBLISHED 10 August 2022

CITATION
Zhu C, Liu Q, Li X, Wei R, Ge T, Zheng X, Li B, Liu K and Cui R (2022) Hydrogen sulfide: A new therapeutic target in vascular diseases. *Front. Endocrinol.* 13:934231. doi: 10.3389/fendo.2022.934231

Hydrogen sulfide: A new therapeutic target in vascular diseases

Cuilin Zhu[1,2†], Qing Liu[3†], Xin Li[2], Ran Wei[1], Tongtong Ge[2], Xiufen Zheng[4], Bingjin Li[2], Kexiang Liu[1*] and Ranji Cui[2*]

[1]Department of Cardiovascular Surgery, The Second Hospital of Jilin University, Changchun, China, [2]Jilin Provincial Key Laboratory on Molecular and Chemical Genetic, The Second Hospital of Jilin University, Changchun, China, [3]Department of Cardiovascular Medicine, University of Tokyo, Tokyo, Japan, [4]Department of Surgery, Western University, London, ON, Canada

Hydrogen sulfide (H_2S) is one of most important gas transmitters. H_2S modulates many physiological and pathological processes such as inflammation, oxidative stress and cell apoptosis that play a critical role in vascular function. Recently, solid evidence show that H_2S is closely associated to various vascular diseases. However, specific function of H_2S remains unclear. Therefore, in this review we systemically summarized the role of H_2S in vascular diseases, including hypertension, atherosclerosis, inflammation and angiogenesis. In addition, this review also outlined a novel therapeutic perspective comprising crosstalk between H_2S and smooth muscle cell function. Therefore, this review may provide new insight inH_2S application clinically.

KEYWORDS

hydrogen sulfide, vascular, hypertension, angiogenesis, atherosclerosis

Introduction

Hydrogen sulfide (H_2S) is recently recognized as the third gas signaling transmitter after nitric oxide (NO) and carbon monoxide (CO) despite it was once considered as toxic gas. Endogenous H_2S production is mainly mediated by cystathionine-b-synthase (CBS), cystathionine-c-lyase (CSE), 3-mercaptopyruvate sulfur transferase (3-MST), which are the most pre-dominant enzymes of H_2S production (1–3). Exogenous administration of H_2S is mainly performed with NaHS salts and H_2S related compounds.

Recent studies have proved H_2S to be vasculoprotective by participating different cellular pathways and interfering with a variety of vascular diseases (4–7). H_2S is endogenously produced by vascular cells or exogenously administered by H_2S releasing donors. In the vasculature, H_2S regulates the proliferation and migration of endothelial cells and vascular smooth muscle cell, regulates the apoptosis, oxidative stress and inflammation of vascular cells. Furthermore, H_2S has been widely proved to regulate

many vascular diseases, including hypertension, atherosclerosis (AS) and angiogenesis (8). Although the beneficial effects of H_2S have widely been recognized, the mechanisms into the molecular pathways largely remained unknown. Deeper understanding of the working mechanisms will help put their way into further clinical application.

In this review, we review the recent findings about H_2S in vascular diseases, including hypertension, AS and angiogenesis, as well as recent working mechanisms. The role of H_2S will be separately discussed endogenously and exogenously here. Finally, we will discuss the possible perspectives of H_2S in the future.

H_2S in hypertension

Hypertension has been a worldwide disease, accounting for 30-40% of the whole population, posing great danger to people's health (9, 10). It is reported that H_2S plays a role in blood pressure regulation. Despite emerging evidence from experimental studies targeting H_2S to protect against hypertension, these results need further clinical research.

Endogenous H_2S in hypertension

The concentration of H_2S in human blood has been reported within a normal range under physical conditions. However, the change of H_2S concentration has been reported to be reduced in high blood pressure (HBP) patients, suggesting the potential regulatory role of H_2S in HBP (11, 12). Several clinical studies have reported the relationship between H_2S and hypertension related disorders (13). Additionally, decreased H_2S plasmatic levels were also found in lead-induced HBP patients (14).

Furthermore, the three major generating enzymes, CSE, CBS and 3-MST were reported to be reduced in HBP patients, suggesting the endogenous synthesis of H_2S may participate in the pathogenesis of HBP (15). Aging is an important predisposing factor for HBP. Loss of 3-MST using a genetic mouse model recuses the mouse cardiovascular system from aging-dependent disorders, thus regulating progression of HBP (16). Innate immune and adoptive immune cells are essential in the genesis and target-organ damage of hypertension. In a recent study, Cui reported that CSE-derived H_2S promotes Treg differentiation and proliferation in an adenosine monophosphate activated protein kinase (AMPK) dependent pathway, which attenuates the vascular immune-inflammation, thereby preventing hypertension (17). Furthermore, DL-propargylgycine (PPG), a CSE inhibitor, was reported to increase BP in Wistar-Kyoto rats and to promote vascular remodeling, indicating the potential regulatory role of CSE in maintaining normal BP (18). Interestingly, in another study, treatment of Sprague-Dawley rats with CSE inhibitor, DL-propargylglycine (PAG) or CBS inhibitor, aminooxyacetic acid alone, did not alter the BP levels, while treatment with both inhibitors would significantly increase mean arterial pressure. This finding could partly explain the interaction of different H_2S producing enzymes in regulating BP (19).

As important gas transmitters, H_2S and NO share crosstalk in regulating pathological and physical conditions (20, 21). In hypertension, endogenous H_2S production regulated by CSE, inhibits endogenous endothelial NO bioavailability, therefore contributing to blood pressure control (22). Sodium nitroprusside (SNP), a NO donor, was reported to increase H_2S production *via* upregulating the CSE or CBS activity, suggesting the crosstalk between the endogenous production of two gases (23). However, the details of two gases interaction regulating blood pressure remain to be elucidated.

Taken together, endogenous H_2S production acts as an important physiological mediator that regulates BP homeostasis and H_2S deficiency will contribute to the progress of HBP.

Exogenous H_2S in hypertension

Apart from endogenous regulation of H_2S in HBP, exogenous administration of H_2S would regulate the process of HBP. The effects of exogenous H_2S donors have been widely studied in animals in different experimental settings.

NaHS was the most widely used H_2S donor for examining the effects in treating HBP. It is reported that early treatment with sodium hydrosulfide (NaHS) (14umol/Kg/day daily intraperitoneal injection for 4 weeks) was proved to prevent the transition from pre-hypertension to hypertension in spontaneously hypertensive rats (SHRs) (24). In another study, NaHS was reported to improve endothelial dysfunction by inhibiting the NLRP3 inflammasome and oxidative stress in SHRs. However, the protective effects were abolished by knocking out Nrf2 (25). The protective effects of NaHS was also testified in an Ang-II induced HBP model, suggesting the universal effects of H_2S in treating HBP (26). Xiao and colleagues reported that 20-week administration of NaHS lowered the arterial pressure and increased the production of NO, enhancing eNOS phosphorylation through the activation of peroxisome proliferator-activated receptor/protein kinase B/AMP-activated protein kinase (PPAR-d/Akt/AMPK) signaling pathway (27). Administration of NaHS exerted anti-hypertensive effects, promoted non-NO-mediated relaxation, and decreased oxidative stress in rats with plumbum-induced hypertension (14). Injection of NaHS was demonstrated to ameliorate soluble FMS-like tyrosine kinase 1 (sFlt1)-induced hypertension, proteinuria, and glomerular endotheliosis in rats by increasing vascular endothelial growth factor (VEGF) expression (28). NaHS administration in SHRs were proven to reduce hypertensive related inflammation, partly through

regulation of T cell subsets balance by Connexin (Cx) 40/Cx43 expressions inhibition (29). These experiment results demonstrate that NaHS dramatically suppressed the progression of HBP in different experimental settings *via* different mechanisms.

GYY4137 was synthesized in 2018, characterized as a novel, water-soluble and long-releasing hydrogen sulfide-releasing molecule (30). GYY4137 has been reported to have anti-hypertensive effects, due to upregulating the expression of VEGFR2 (31). In another study, GYY4137 reversed blood pressure increase after Ang-II inducement, which was accompanied by upregulation of microRNA-129 (32). Exogenous GYY4137 supplementation in the paraventricular nucleus (PVN) attenuated sympathetic activity and hypertensive response, partly due to decrease of reactive oxygen species (ROS) and pro-inflammatory cytokines within the PVN in high salt-induced hypertension (33).

Apart from GYY4137 and NaHS, various H_2S releasing organic compounds have been shown to exhibit protective effects in treating HBP. Allicin, which comprised a variety of sulfur-containing compounds, has been reported to exert anti-hypertensive effects in an endothelium dependent pathway (34). Sodium thiosulfate, a reversible oxidation product of H_2S, has vasodilating and anti-oxidative properties in a N-ω-nitro-L-arginine (L-NNA) induced hypertension model (35). N-phenylthiourea (PTU) and N,N'-diphenylthiourea (DPTU) compounds have been investigated as potential H_2S-donors, and also demonstrated typical H_2S-mediated vascular properties (36). This experimental evidence advocates more extensive discovery of new H_2S donors to exert more extensive application in treating HBP.

H_2S does share interplay with NO and CO, regulating the pathogenesis of HBP. H_2S and NO are both vasodilating mediators. H_2S donors were reported to induce vasorelaxation and promote NO-donor induced vasorelaxation in rat thoracic aorta, showing the possible interaction between NO and H_2S in vascular regulation (37). In $_L$-NAME induced hypertensive rats a dysfunctional H_2S pathway was revealed and exogenous H_2S attenuated the elevated blood pressure in this model (38). Reducing CO levels in Brown-Norway rats increases H_2S generation and prevents hypoxia-induced pulmonary edema. Increasing CO levels in SHR has been found to enhance carotid H2S generation, prevent hypersensitivity to hypoxia and control hypertension in SHR (39). H2S has also been demonstrated to exert protective effects for acute CO poisoning patients (40).

As for the mechanisms of H_2S in regulating HBP, they share similar functions and several similar pathways to regulate hypertension. The possible mechanisms of H_2S on vascular tone include: KATP- channel dependent relaxation, other K^+ channels, PKG activation, hyperpolarization, eNOS inhibition, inhibition of cytochrome C oxidase and anti-oxidant effects (21, 41–47).

H_2S not only exert anti-hypertensive effects in systematic hypertension, it also has a regulatory role in pulmonary hypertension (PHT). PHT is characterized by blood pressure increased in pulmonary artery, associated with high incidence of mortality and morbidity (48). H_2S was reported to exert anti-hypertensive effects in pulmonary hypertension *via* vaso-relaxative actions (49, 50). H_2S has been proven to effectively inhibit hypoxia-induced increase in cell proliferation, migration, and oxidative stress in pulmonary artery smooth muscle cells (PASMCs) in an endoplasmic reticulum (ER) -dependent pathway, therefore exerting protective effects in PHT (51). Rashid et al. demonstrated that the relaxation response of to NaHS in porcine lungs was reduced in the presence of a high concentration of K^+, indicating that the mechanism of relaxation depends, in part, on K^+ channel activity (52). Du group showed that H2S treatment attenuated the oxidative stress accompanied by PHT, by reducing oxidized glutathione content (53). It was also reported that endogenous sulfur dioxide pathway was down-regulated in rats with PHT, indicating the involvement of sulfur dioxide/aspartate aminotransferase 2 pathway (54).

To summarize, due to the complexity of HBP management and lack of adequate therapy, H_2S is gaining increasingly attention as a potential therapeutic target. Therefore, we summarized the role of H_2S in regulating hypertension in Table 1. However, the effects and mechanisms by which H_2S regulates HBP are complicated and still remaining largely unknown.

H_2S and atherosclerosis

Atherosclerosis (AS) is a long-term, chronic inflammatory disease of the vessel wall, which is widely recognized as a high risk for cardiovascular diseases (55). The progression of AS is extremely complex, involving numerous pathophysiological processes, including endothelial dysfunction, oxidative stress, inflammation, vascular smooth muscle cell proliferation and migration (56).

H_2S has been reported to be a vaso-relaxant agent, which processes the property of ameliorating vascular dysfunction and mitigating the progression of AS. The potential therapeutic effects in anti-AS include maintaining endothelial cell dysfunction, inhibiting inflammation, suppressing vascular smooth muscle cell (VSMC) proliferation, migration and mitigating oxidative stress (57). However, the mechanisms of H_2S to be protective against AS have not been fully elucidated and the therapeutic potential of H_2S for AS treatment needs further exploration. Herein, we will review the recent findings of H_2S in anti-AS from two main perspectives: endothelial cell dysfunction and inflammation.

Endothelial cell dysfunction

The endothelial cell represents a fundamental barrier for the maintenance of vascular homeostasis. Dysfunction in the

TABLE 1 Role of H_2S in Regulating Hypertension.

Source	Gene/ Compound	Effects	Mechanism	Reference
Endogenous	CSE	Inhibit inflammation	Dependent on AMPK pathway	(17)
	CSE inhibitor	Increase hypertension	Not applicable	(18)
	CSE inhibitor or CBS inhibitor	Increase hypertension	Not applicable	(19)
Exogenous	NaHS	Prevent HBP	restores NO bioavailability, and blocks the RAS system in the kidney	(22)
		Prevent hypertension in SHR	improve endothelial dysfunction by inhibiting the NLRP3 inflammasome and oxidative stress	(25)
		Protective in Ang II induced HBP mice	reduces blood pressure, endothelial dysfunction and vascular oxidative stress	(26)
		Protective in HBP	increased the production of NO, enhancing eNOS phosphorylation *via* PPAR-d/Akt/AMPK pathway.	(27)
		anti-hypertensive in plumbum-induced hypertension	promoted non-NO-mediated relaxation, and decreased oxidative stress	(14)
		anti-hypertensive	Ameliorate proteinuria, and glomerular endotheliosis by increasing VEGF expression	(28)
		reduce hypertensive related inflammation	regulation of T cell subsets balance by Cx 40/Cx43 expressions inhibition	(29)
	GYY4137	anti-hypertensive	upregulating the expression of VEGF receptor 2	(31)
		anti-hypertensive after Ang-II inducement	upregulating of micro RNA-129	(32)
		attenuated sympathetic activity and hypertensive response in the paraventricular nucleus	decrease of reactive oxygen species and pro-inflammatory cytokines	(33)
	Allicin	exert anti-hypertensive effects	Dependent on endothelium	(34)
	Sodium thiosulfate	Protective in HBP	vasodilating and anti-oxidative properties	(35)
	thiourea	vasorelaxing effects	membrane hyperpolarization, mediated by activation of KATP and Kv7 potassium channels.	(36)

CSE, cystathionine-c-lyase; CBS, cystathionine-b-synthase; HBP, high blood pressure; AMPK, adenosine monophosphate activated protein kinase; RAS, renin-angiotensin system; NLPR3, Nucleotide-binding oligomerization domain, leucine-rich repeat and pyrin domain-containing 3; NO, nitric oxide; eNOS, endothelial nitric oxide synthase; Cx, Connexin; VEGF, vascular endothelial growth factor; KATP, ATP-sensitive potassium channel.

endothelium may lead to several cardiovascular diseases (58, 59). Therefore, protecting the vascular endothelium from damage is one of the key factors against AS and AS related disorders.

Endogenous regulation of H_2S are observed to play a role in regulating AS. The concentration of H_2S was found to be decreased in AS mice, indicating the potential regulatory role of H_2S in AS (60). As mentioned previously, the synthesis of H_2S are regulated by 3 enzymes: CBS, CSE, and 3-MST. Loss of enzyme functions may lead to endothelial dysfunction in AS. For example, CSE/H_2S pathway is reported to involve in AS *via* the H_2S/CSE-TXNIP-NLRP3-IL-18/IL-1β-nitric oxide (NO) signaling pathway (61). Furthermore, Tian and colleagues observed that H_2S deficiency derived from CSE depletion contributes to the development of endothelial dysfunction. In their study, MAPK/TXNIP (thioredoxin interacting protein signaling) is positively involved in CSE/H_2S deficiency-associated endothelial dysfunction (62). CSE/H_2S pathway may be protective against the formation of uremia accelerated atherosclerosis (UAAS) by affecting the expression of downstream molecule endothelial nitric oxide synthase (eNOS), which may be mediated by conventional protein kinase C (PKC) βII/Akt signaling pathway (63). Besides CSE, CBS was also observed to play a role in the process of AS. Mutations in the CBS gene are known to cause endothelial dysfunction responsible for cardiovascular and neurovascular diseases, and CBS/H_2S pathway interacts with mitochondrial function and ER-mitochondrial tethering, therefore interfering with endothelial cell dysfunction-related pathologies (64). However, the role of 3-MST in maintain endothelial cell function in AS needs to be investigated. Collectively, the level of H_2S and CSE/CSB/3-MST level can be considered as potential biomarkers and therapeutic targets for AS patients.

Numerous studies have demonstrated that exogenous H_2S supplementation is another source contributing to the anti-AS effects. For instance, NaHS was proved to be protective against AS by upregulating angiotensin converting enzyme 2 (ACE2) expression in endothelial cells (65). Besides, H_2S can reverse the endothelial dysfunction induced by AngII in HUVECs by ER stress pathway (66). Furthermore, H_2S can enhance activator protein 1 (AP-1 binding) activity with the sirtuins 3 (SIRT3) promoter, thereby upregulating SIRT3 expression and ultimately reducing oxidant-provoked vascular endothelial dysfunction (67). Also Ford reported that NaHS treatment significantly reduced endothelial dysfunction and inhibited vascular

superoxide generation in high-fat diet ApoE$^{(-/-)}$ mice, and therefore impaired atherosclerotic lesion development (68).

Apart from supplementation of traditional donors, administration of organic H_2S donors would also be protective in maintaining EC function against AS. GYY4137 can induce autophagy and can protect ECs from Ox-LDL-induced apoptosis by activating Sirt1 (69). AP39 and AP123, the newly synthesized mitochondria-target H_2S donors, are reported to protect endothelial cells from highglycemia-induced injury *via* preserving mitochondria function (70). With the development of pharmacy technology, the synthesis of new H_2S releasing compounds are promising against AS.

There is crosstalk between H_2S and NO in regulating the pathogenesis of AS. H_2S was reported to increase NO production and upregulated the expression of inducible nitric oxide synthase (iNOS) (71). ApoE$^{-/-}$ mice fed with PAG was found with enhanced atherosclerotic lesion area, and with decreased NO levels, suggesting H_2S could regulate atherosclerosis progression through NO crosstalk. H_2S partially restores aortic endothelium-dependent relaxation in ApoE$^{-/-}$ mice, which may be related to increased phosphorylation of eNOS in the aorta (72).

To summarize, large numbers of studies have demonstrated the protective role of H_2S in anti-AS *via* maintaining normal EC function, however, the mechanisms need deeper understanding. As a result, this will further facilitate the development of drug therapy for treating AS.

Inflammation

AS is a chronic vascular inflammatory disease and inflammation exists at all stages of AS (73). H_2S has been reported to have anti-inflammatory effects, further regulating the pathogenesis of AS. Deeper understating of the protective effects of H_2S donors *via* inhibiting inflammation will help provide a new way for future AS treatment.

Endogenous H_2S production has been reported to regulate inflammation in AS by its producing enzymes. Alterations of CSE/H_2S pathway may thus be involved in atherosclerosis pathogenesis (74). However, the underlying mechanisms are poorly understood. Endogenous CSE/H_2S can directly sulfhydrate SIRT1, promote its deacetylation activity, and increase SIRT1 stability, thus reducing atherosclerotic plaque formation, by reducing vascular related inflammation (75). In another study, zofenopril at, the active metabolite of zofenopril has been reported to exert anti-inflammatory activity in vascular cells through its ability to increase H_2S availability, therefore providing a potential target for treating AS (76). Moreover, CSE/H_2S pathway has been reported to play an anti-inflammatory role in oxidized low-density lipoprotein (ox-LDL)-stimulated macrophage by suppressing c-Jun N-terminal kinase (JNK)/NF-κB signaling pathway (74). Furthermore, high fat diet is a predisposing factor for the progression of AS. It is reported that high fat diet might cause impaired function of CSE/H_2S pathway, aggravating inflammation and posing risks to the development of AS (77). Apart from CSE regulation pathway, it is shown that deletion of CBS would impair endogenous H_2S production and promote inflammatory reaction in AS-susceptible mice (78). This provided evidence that H_2S releasing diet may help protect against AS.

Apart from endogenous H_2S in regulating AS related inflammation, exogenous H_2S administration also had an important role in AS. NaHS was originally the most widely used H_2S donor in studying the effects of H_2S in anti-AS. Numerous studies have demonstrated NaHS to be protective against AS by reducing inflammation (74, 75, 79, 80). In addition to traditional H_2S releasing salts, new synthesized H_2S donors have shown great potential with physiological properties. Whiteman and et al. demonstrated that GYY4137 could significantly inhibit lipopolysaccharide (LPS) -induced release of pro-inflammatory mediators and promoted the release of the anti-inflammatory chemokines. While NaHS exerted a bidirectional effect at high concentrations. This finding can partly explain the complex regulation system of H_2S in inflammation (81). GYY4137, has also been proved to be protective against the development of diabetes-accelerated AS by preventing the activation of NLPR3 inflammasome (82). Furthermore, H_2S rich compounds are reported to upregulate the expression of glutathione (GSH) and glutamate-cysteine ligase catalytic (GCLC) subunit, inhibiting inflammation, and exerting beneficial effects of mitigating AS (83). The effects of endogenous H_2S and exogenous H_2S in AS were listed in Table 2.

H_2S and angiogenesis

Angiogenesis is a process of new vessel formation from the existing vasculature (84). It is found that H_2S might be a pro-angiogenic factor, promoting angiogenesis in different diseases and increase the expression of angiogenesis related biomarkers, including diabetes mellitus (DM), ischemic diseases and cancer (85).

H_2S and DM related angiogenesis

DM is the leading cause of mortality worldwide, causing a variety of vascular complications (86). Impaired angiogenesis is a strong feature of DM and it can commonly induce refractory wound lesions. Therefore, promoting angiogenesis is of crucial importance for DM patients.

DM patients are reported with lower concentration of H_2S in serum and in curtenous tissues, indicating the impaired synthesis of H_2S production in DM patients (87, 88). Therefore, regulation of endogenous H_2S production and production enzymes are a potential treatment for DM related wound healing. CSE down-

TABLE 2 Effects of Endogenous H_2S and Exogenous H_2S in AS.

Source	Gene/ Compound	Effects	Mechanism	Reference
Endogenous	CSE	CSE deficiency upregulated the levels of IL-1β and IL-18 inflammatory cytokines	*Via* activating TXNIP-NLRP3-IL-18/IL-1β-NO signaling pathway	(47)
		CSE depletion contributes to the development of endothelial dysfunction in AS	*Via* activating MAPK/TXNIP pathway	(48)
		protective against the formation of uremia accelerated atherosclerosis	*Via* activating eNOS/PKC βII/Akt signaling pathway	(49)
		reducing atherosclerotic plaque formation, by reducing vascular related inflammation	sulfhydrate SIRT1, promote its deacetylation activity, and increase SIRT1 stability	(59)
		anti-inflammatory role in ox-LDL-stimulated macrophage	suppressing JNK/NF-κB signaling pathway	(58)
Exogenous	NaHS	protective in endothelial cells	upregulating ACE2 expression	(51)
	NaHS	reverse the endothelial dysfunction induced by AngII in HUVECs	*via* ER stress pathway	(52)
	NaHS	improve vascular function by reducing vascular superoxide generation and impairing atherosclerotic lesion development	reducing endothelial dysfunction and inhibiting vascular superoxide generation	(54)
	GYY4137	reducing oxidant-provoked vascular endothelial dysfunction	upregulate activator protein 1 activity with the SIRT3 promoter	(53)
	GYY4137	protect endothelial cells from Ox-LDL-induced apoptosis by activating Sirt1	induce autophagy	(55)
	GYY4137	inhibit lipopolysaccharide -induced release of pro-inflammatory mediators and promoted the release of the anti-inflammatory chemokines	Not applicable	(65)
	GYY4137	be protective against the development of diabetes-accelerated AS	preventing the activation of NLPR3 inflammasome	(66)
	AP39 and AP123	protect endothelial cells from highglycemia-induced injury	preserving mitochondria function	(56)
	zofenoprilat	exert anti-inflammatory activity in vascular cells	In a CSE/H_2S-mediated manner	(60)

CSE, cystathionine-c-lyase; NO, nitric oxide; TXNIP, thioredoxin-interacting protein; NLPR3, Nucleotide-binding oligomerization domain, leucine-rich repeat and pyrin domain-containing 3; NO, nitric oxide; MAPK, mitogen-activated protein kinase; eNOS, endothelial nitric oxide synthase; PKC, protein kinase C; SIRT, Sirtuin; ox-LDL, oxidized low-density lipoprotein; JNK, c-Jun N-terminal kinase; ACE2, angiotensin converting enzyme 2; ER, endoplasmic reticulum; HUVEC, human umbilical vein endothelial cell.

regulation is reported to play a role in the pathogenesis of diabetic impaired wound healing (89). Danhong, a traditional Chinese herb medicine, has been reported to promote angiogenesis in the diabetic hind limb ischemia model through activation of local CSE-H_2S-vascular endothelial growth factor (VEGF) axis (90). Furthermore, DM leads to the dysfunction of 3-MST/H_2S and 3-MST might be a therapeutic target for DM patients (91). Besides, 3-MST/H_2S axis was also reported to exert pro-angiogeneic effects *via* modulating mitochondrial respiration and increasing mitochondrial adenosine triphosphate (ATP) production (92).

Numerous studies have proved H_2S to be a pro-angiogenetic factor (89, 93, 94). For example, H_2S has been reported to increase angiogenesis in injured ischemic adductor muscle and to promote the ischemic diabetic wound healing in type 2 diabetic db/db mice (95). H_2S improves wound healing by restoration of endothelial progenitor cell (EPC) functions and activation of Ang-1 in type 2 diabetic mice (94). H_2S can also improve diabetic impaired wound healing by attenuating inflammation and increasing angiogenesis (96). These findings together imply that H_2S played a role in DM mediated angiogenesis.

Apart from traditional widely-know H_2S releasing donors, new and effective donors containing H_2S moiety have been synthesized and utilized in DM related diseases. HA-JK1 and SA/JK-1 have been synthesized as examples. For HA-JK1, an *in situ* forming biomimetic hyaluronic acid (HA) hydrogel was used as a matrix to dope a pH-controllable H_2S donor, JK1, to form a novel HA-JK1 hybrid system. This HA-JK1 hydrogel was designed as an ideal delivery scaffold for JK1 with pH-dependent prolonged H_2S releasing profile (97). For SA/JK-1, which was capable of releasing H_2S consistently under acidic pH conditions by absorbing exudate at the wound interface. The SA/JK-1 sponge exhibited biocompatibility to fibroblasts and promoted cell migration *in vitro*, and exhibited obviously positive influence on wound healing, therefore providing an effective treatment for non-healing wound (98). Interestingly, microparticles containing NaHS, have been synthesized using the emulsion technique, called NaHS@MPs. It can sustainably release H_2S under physiological conditions and promote angiogenesis, further accelerating the healing of full-thickness wounds in diabetic mice (99).

Collectively, the role of H_2S in DM related angiogenesis is gaining increasingly attention. However, there remains large space to be explored to clinical practice.

H_2S and angiogenesis in ischemic diseases

Ischemic diseases are accompanied by shortage of blood supply. Angiogenesis would potentially increase the blood flow, therefore exerting the treating effects.

Modulation of endogenous H_2S generation has a role in angiogenesis. CBS, CSE and 3-MST responded differently to angiogenesis. CSE is reported to promote VEGF-dependent angiogenesis through H_2S generation under amino acid restriction (100). However, in another study, Tao and et al. found that CBS could promote vascular endothelial cell migration both under normoxic and minor hypoxia conditions (10% oxygen), while CSE had the opposite effects. 3-MST can accelerate the migration of endothelial cells in hypoxia, while no such effect was observed under normoxic conditions. They further found that 3-MST can modulate the endothelial cell migration, rather than CSE or CBS. Their study highlighted the need to get deeper understanding of the different functions of the H_2S producing enzymes under different conditions (101). Furthermore, thiosulfate, one of the products formed during oxidative H_2S metabolism, has surprisingly demonstrated inhibitory effects on VEGF-dependent endothelial cell proliferation, combined with reduction of CSE expression level (102). Therefore, the role of endogenous H_2S on angiogenesis is controversial and requires more study to elucidate the potential mechanisms.

GYY4137 was reported to promote HHcy-mediated neoangiogenesis impairment in the ischemic hind limbs of post femoral artery ligation model *via* peroxisome proliferator-activated receptor (PPAR)-γ/VEGF axis (103). DATS, an organic polysulfide releasing H_2S, has been demonstrated to promote angiogenesis in hindlimb ischemia *via* Akt-eNOS signaling pathway (104). Furthermore, NaHS could increase NO bioavailability and promote angiogenesis in ischemia hindlimb (105). NaHS exert proangiogeneic effect mediated by interaction between the upregulated VEGF in the skeletal muscle cells and the VEGF receptor 2 (106). In another report, NaHS exerts pro-angiogeneic effects through dependent on activation of Akt (107).

Recently, with the development of material synthesis technology, various H_2S releasing compounds have been synthesized to enhance H_2S releasing properties. For instance, A poly (D, L-lactic-co-glycolic acid) microparticle system that contains DATS, called DATS@MPs, possess the property of slow and long-term H_2S release. DATS@MPs have been reported to promote therapeutic angiogenesis in an ischemic mouse limb model through activating nuclear respiratory factor 2 (Nrf2) translocation, thus providing therapeutic potential in treating ischemic diseases (108). Moreover, ZYZ-803, a novel synthetic H_2S-NO hybrid molecule, which can slowly release H_2S and NO, has been reported to exert pro-angiogenetic effects *via* SIRT1 dependent pathway. The pro-angiogenetic effects of H_2S are also dependent on CSE and eNOS expression *via* cross-talk between signal transducer and activator of transcription 3 (STAT3) and Ca^{2+}/CaM-dependent protein kinase II (CaMKII) activation (109, 110).

Apart from ischemic limb diseases, myocardial infarction (MI) is another serious ischemic disease, which poses great danger to people's health. GYY4137 was reported to exert pro-angiogenic effects following MI *via* endogenous natriuretic peptide activation (111). Diallyl trisulfide, a long-lasting H_2S donor, can mitigate left ventricular dysfunction *via* inducing angiogenesis in over-loaded heart failure (112). NaHS was reported to increase angiogenesis and improve left ventricular function after MI (113). Besides, NaHS was also reported to promote angiogenesis, and mitigating the progression of heart failure by inducing matrix metalloproteinase (MMP)-2 activation and inhibiting MMP-9 and tissue inhibitor of matrix metalloproteinase (TIMP)-3 expression (114).

Newly and novel H_2S releasing compounds have been synthesized, with the aim to over the limitations of traditional H_2S releasing donors. Liang and et al. developed a macromolecular H_2S prodrug. The compound comprised of a 2-aminopyridine-5-thiocarboxamide (a small-molecule H_2S donor) on partially oxidized alginate (ALG-CHO), to obtain the slow and continuous release of endogenous H_2S. They further formed a stem cell-loaded conductive H_2S-releasing hydrogel through the Schiff base reaction between ALG-CHO and gelatin. They utilized the hydrogel in treating MI, demonstrating a dramatical improvement of the cardiac functions in rats (115). Moreover, S-Propargyl-Cysteine (SPRC), a novel water-soluble modulator of endogenous H_2S production, has been demonstrated to exhibit pro-angiogenetic effects *via* the activation of STAT3. SPRC therefore provides a novel therapeutic strategy for ischemia heart diseases (116).

H_2S and NO shared interactions in regulating angiogenesis. Aortic rings harvested from eNOS−/− mice exhibited no microvessel outgrowth in response to NaHS, compared with wild-type controls, demonstrating that NO was essential for the pro-angiogenic effect of H_2S. Besides, chemical inhibition of CSE attenuated NO-mediated cGMP angiogenesis (44). Apart from this, NO donors increased CSE dependent H_2S biogenesis in a cGMP-dependent manner. Pre-treating NO donors increased CSE mRNA and protein levels in smooth muscle cells increased H_2S production (117). Taken together, NO and H_2S contributed mutually in regulating angiogenesis.

In summary, H_2S plays an important role in different vascular diseases. The structure of normal artery consisted of 3 layers. The inner layer lined by a monolayer of ECs is closely contacted with blood; the middle layer composed of VSMCs is located at the complex extracellular matrix; and the outer layer of arteries is composed of mast cells, nerve endings, and microvessels. Imbalance and dysfunction of the 3 layers lead to the pathogenesis of vascular diseases, especially dysfunction of EC and SMC (7). This indicates the universal functions of H_2S in regulating different vascular diseases. Studied have focused on the effects of H_2S from endogenous H_2S production and exogenous H2S administration. However, the application of H_2S in vascular diseases is still in the basic research stage. Studies and experiments of H_2S in treating vascular diseases are required.

Future research should focus on the role and mechanism of H_2S and different H_2S releasing donors in treating vascular diseases. Synthetic H_2S donors have been developed to

overcome the disadvantages of traditional H_2S donors. They can be categorized by their class of triggering mechanisms, possessing their specific delivery system and H_2S releasing properties (118). Continuous improvements in the interaction and crosstalk between different gas transmitters in the control of vascular diseases. Exploring the therapeutic potential in regulating vascular diseases will be promising in the near future.

Author contributions

CZ and QL wrote the first draft. XL, RW, TG, XZ and BL provided the organization and framework of the article. KL and RC provided critical revisions. All authors contributed to the article and approved the submitted version.

Funding

The study was supported by Natural Science Foundation of China (82000390), China Postdoctoral Science Foundation (2020M681048), and Special Fund of Jilin Province (2020SC2T038). Jilin Provincial Finance Department, China (2020SCZT091). The Jilin Science and Technology Agency funds in China, China (20210402003GH).

Conflict of interest

The authors declare that the research was conducted in the absence of any commercial or financial relationships that could be construed as a potential conflict of interest.

Publisher's note

References

1. Li L, Rose P, Moore PK. Hydrogen sulfide and cell signaling. *Annu Rev Pharmacol Toxicol* (2011) 51:169–87. doi: 10.1146/annurev-pharmtox-010510-100505

2. Mustafa AK, Gadalla MM, Sen N, Kim S, Mu W, Gazi SK, et al. H2S signals through protein s-sulfhydration. *Sci Signal* (2009) 2:ra72. doi: 10.1126/scisignal.2000464

3. Wallace JL, Wang R. Hydrogen sulfide-based therapeutics: exploiting a unique but ubiquitous gasotransmitter. *Nat Rev Drug Discov* (2015) 14:329–45. doi: 10.1038/nrd4433

4. Lv B, Chen S, Tang C, Jin H, Du J and Huang Y. Hydrogen sulfide and vascular regulation - an update. *J Adv Res* (2021) 27:85–97. doi: 10.1016/j.jare.2020.05.007

5. Yuan S, Kevil CG. Nitric oxide and hydrogen sulfide regulation of ischemic vascular remodeling. *Microcirculation* (2016) 23:134–45. doi: 10.1111/micc.12248

6. Yang G, Wang R. H2S and blood vessels: An overview. *Handb Exp Pharmacol* (2015) 230:85–110. doi: 10.1007/978-3-319-18144-8_4

7. Kanagy NL. Szabo c and papapetropoulos a. vascular biology of hydrogen sulfide. *Am J Physiol Cell Physiol* (2017) 312:C537–49. doi: 10.1152/ajpcell.00329.2016

8. Tian X, Zhou D, Zhang Y, Song Y, Zhang Q, Bu D, et al. Persulfidation of transcription factor FOXO1 at cysteine 457: A novel mechanism by which H2S inhibits vascular smooth muscle cell proliferation. *J Adv Res* (2021) 27:155–64. doi: 10.1016/j.jare.2020.06.023

9. Dong N, Piao H, Li B, Xu J, Wei S, Liu K. Poor management of hypertension is an important precipitating factor for the development of acute aortic dissection. *J Clin Hypertens (Greenwich)* (2019) 21:804–12. doi: 10.1111/jch.13556

10. Mancia G, Fagard R, Narkiewicz K, Redon J, Zanchetti A, Bohm M, et al. 2013 ESH/ESC guidelines for the management of arterial hypertension: the task force for the management of arterial hypertension of the European society of hypertension (ESH) and of the European society of cardiology (ESC). *J Hypertens* (2013) 31:1281–357. doi: 10.1097/01.hjh.0000431740.32696.cc

11. Kutz JL, Greaney JL, Santhanam L, Alexander LM. Evidence for a functional vasodilatatory role for hydrogen sulphide in the human cutaneous microvasculature. *J Physiol* (2015) 593:2121–9. doi: 10.1113/JP270054

12. Sun NL, Xi Y, Yang SN, Ma Z, Tang CS. Plasma hydrogen sulfide and homocysteine levels in hypertensive patients with different blood pressure levels and complications. *Zhonghua Xin Xue Guan Bing Za Zhi* (2007) 35:1145–8.

13. Shi MM, Wang JL, Zhang LQ, Qin M, Huang YW. Association between hydrogen sulfide and OSA-associated hypertension: a clinical study. *Sleep Breath* (2020) 24:745–50. doi: 10.1007/s11325-019-01997-y

14. Possomato-Vieira JS, Goncalves-Rizzi VH, do Nascimento RA, Wandekin RR, Caldeira-Dias M, Chimini JS, et al. Clinical and experimental evidences of hydrogen sulfide involvement in lead-induced hypertension. *BioMed Res Int* (2018) 2018:4627391. doi: 10.1155/2018/4627391

15. Aminzadeh MA, Vaziri ND. Downregulation of the renal and hepatic hydrogen sulfide (H2S)-producing enzymes and capacity in chronic kidney disease. *Nephrol Dial Transplant* (2012) 27:498–504. doi: 10.1093/ndt/gfr560

16. Peleli M, Bibli SI, Li Z, Chatzianastasiou A, Varela A, Katsouda A, et al. Cardiovascular phenotype of mice lacking 3-mercaptopyruvate sulfurtransferase. *Biochem Pharmacol* (2020) 176:113833. doi: 10.1016/j.bcp.2020.113833

17. Cui C, Fan J, Zeng Q, Cai J, Chen Y, Chen Z, et al. CD4(+) T-cell endogenous cystathionine gamma lyase-hydrogen sulfide attenuates hypertension by sulfhydrating liver kinase B1 to promote T regulatory cell differentiation and proliferation. *Circulation* (2020) 142:1752–69. doi: 10.1161/CIRCULATIONAHA.119.045344

18. Yan H, Du J, Tang C. The possible role of hydrogen sulfide on the pathogenesis of spontaneous hypertension in rats. *Biochem Biophys Res Commun* (2004) 313:22–7. doi: 10.1016/j.bbrc.2003.11.081

19. Roy A, Khan AH, Islam MT, Prieto MC, Majid DS. Interdependency of cystathione gamma-lyase and cystathione beta-synthase in hydrogen sulfide-induced blood pressure regulation in rats. *Am J Hypertens* (2012) 25:74–81. doi: 10.1038/ajh.2011.149

20. Li L, Hsu A, Moore PK. Actions and interactions of nitric oxide, carbon monoxide and hydrogen sulphide in the cardiovascular system and in inflammation–a tale of three gases! *Pharmacol Ther* (2009) 123:386–400. doi: 10.1016/j.pharmthera.2009.05.005

21. Ali MY, Ping CY, Mok YY, Ling L, Whiteman M, Bhatia M, et al. Regulation of vascular nitric oxide *in vitro* and *in vivo*; a new role for endogenous hydrogen sulphide? *Br J Pharmacol* (2006) 149:625–34. doi: 10.1038/sj.bjp.0706906

22. Szijarto IA, Marko L, Filipovic MR, Miljkovic JL, Tabeling C, Tsvetkov D, et al. Cystathionine gamma-Lyase-Produced hydrogen sulfide controls endothelial NO bioavailability and blood pressure. *Hypertension* (2018) 71:1210–7. doi: 10.1161/HYPERTENSIONAHA.117.10562

23. Zhao W, Ndisang JF, Wang R. Modulation of endogenous production of H2S in rat tissues. *Can J Physiol Pharmacol* (2003) 81:848–53. doi: 10.1139/y03-077

24. Tain YL, Hsu CN, Lu PC. Early short-term treatment with exogenous hydrogen sulfide postpones the transition from prehypertension to hypertension in spontaneously hypertensive rat. *Clin Exp Hypertens* (2018) 40:58–64. doi: 10.1080/10641963.2017.1313847

25. Li J, Teng X, Jin S, Dong J, Guo Q, Tian D, et al. Hydrogen sulfide improves endothelial dysfunction by inhibiting the vicious cycle of NLRP3 inflammasome and oxidative stress in spontaneously hypertensive rats. *J Hypertens* (2019) 37:1633–43. doi: 10.1097/HJH.0000000000002101

26. Al-Magableh MR, Kemp-Harper BK, Hart JL. Hydrogen sulfide treatment reduces blood pressure and oxidative stress in angiotensin II-induced hypertensive mice. *Hypertens Res* (2015) 38:13–20. doi: 10.1038/hr.2014.125

27. Xiao L, Dong JH, Teng X, Jin S, Xue HM, Liu SY, et al. Hydrogen sulfide improves endothelial dysfunction in hypertension by activating peroxisome proliferator-activated receptor delta/endothelial nitric oxide synthase signaling. *J Hypertens* (2018) 36:651–65. doi: 10.1097/HJH.0000000000001605

28. Holwerda KM, Burke SD, Faas MM, Zsengeller Z, Stillman IE, Kang PM, et al. Hydrogen sulfide attenuates sFlt1-induced hypertension and renal damage by upregulating vascular endothelial growth factor. *J Am Soc Nephrol* (2014) 25:717–25. doi: 10.1681/ASN.2013030291

29. Ni X, Zhang L, Peng M, Shen TW, Yu XS, Shan LY, et al. Hydrogen sulfide attenuates hypertensive inflammation *via* regulating connexin expression in spontaneously hypertensive rats. *Med Sci Monit* (2018) 24:1205–18. doi: 10.12659/MSM.908761

30. Li L, Whiteman M, Guan YY, Neo KL, Cheng Y, Lee SW, et al. Characterization of a novel, water-soluble hydrogen sulfide-releasing molecule (GYY4137): new insights into the biology of hydrogen sulfide. *Circulation* (2008) 117:2351–60. doi: 10.1161/CIRCULATIONAHA.107.753467

31. Zhu ML, Zhao FR, Zhu TT, Wang QQ, Wu ZQ, Song P, et al. The antihypertension effect of hydrogen sulfide (H2S) is induced by activating VEGFR2 signaling pathway. *Life Sci* (2021) 267:118831. doi: 10.1016/j.lfs.2020.118831

32. Weber GJ, Pushpakumar SB, Sen U. Hydrogen sulfide alleviates hypertensive kidney dysfunction through an epigenetic mechanism. *Am J Physiol Heart Circ Physiol* (2017) 312:H874–85. doi: 10.1152/ajpheart.00637.2016

33. Liang YF, Zhang DD, Yu XJ, Gao HL, Liu KL, Qi J, et al. Hydrogen sulfide in paraventricular nucleus attenuates blood pressure by regulating oxidative stress and inflammatory cytokines in high salt-induced hypertension. *Toxicol Lett* (2017) 270:62–71. doi: 10.1016/j.toxlet.2017.02.004

34. Cui T, Liu W, Chen S, Yu C, Li Y, Zhang JY. Antihypertensive effects of allicin on spontaneously hypertensive rats *via* vasorelaxation and hydrogen sulfide mechanisms. *BioMed Pharmacother* (2020) 128:110240. doi: 10.1016/j.biopha.2020.110240

35. Nguyen ITN, Klooster A, Minnion M, Feelisch M, Verhaar MC, van Goor H, et al. Sodium thiosulfate improves renal function and oxygenation in l-NNA-induced hypertension in rats. *Kidney Int* (2020) 98:366–77. doi: 10.1016/j.kint.2020.02.020

36. Citi V, Martelli A, Bucci M, Piragine E, Testai L, Vellecco V, et al. Searching for novel hydrogen sulfide donors: The vascular effects of two thiourea derivatives. *Pharmacol Res* (2020) 159:105039. doi: 10.1016/j.phrs.2020.105039

37. Hosoki R, Matsuki N, Kimura H. The possible role of hydrogen sulfide as an endogenous smooth muscle relaxant in synergy with nitric oxide. *Biochem Biophys Res Commun* (1997) 237:527–31. doi: 10.1006/bbrc.1997.6878

38. Zhong G, Chen F, Cheng Y, Tang C, Du J. The role of hydrogen sulfide generation in the pathogenesis of hypertension in rats induced by inhibition of nitric oxide synthase. *J Hypertens* (2003) 21:1879–85. doi: 10.1097/00004872-200310000-00015

39. Peng YJ, Makarenko VV, Nanduri J, Vasavda C, Raghuraman G, Yuan G, et al. Inherent variations in CO-H2S-mediated carotid body O2 sensing mediate hypertension and pulmonary edema. *Proc Natl Acad Sci U S A* (2014) 111:1174–9. doi: 10.1073/pnas.1322172111

40. Yu YP, Li ZG, Wang DZ, Zhan X, Shao JH. Hydrogen sulfide as an effective and specific novel therapy for acute carbon monoxide poisoning. *Biochem Biophys Res Commun* (2011) 404:6–9. doi: 10.1016/j.bbrc.2010.11.113

41. Mustafa AK, Sikka G, Gazi SK, Steppan J, Jung SM, Bhunia AK, et al. Hydrogen sulfide as endothelium-derived hyperpolarizing factor sulfhydrates potassium channels. *Circ Res* (2011) 109:1259–68. doi: 10.1161/CIRCRESAHA.111.240242

42. Jiang B, Tang G, Cao K, Wu L, Wang R. Molecular mechanism for H(2)S-induced activation of K(ATP) channels. *Antioxid Redox Signal* (2010) 12:1167–78. doi: 10.1089/ars.2009.2894

43. Bautista-Nino PK, van der Stel M, Batenburg WW, de Vries R, Roks AJM, Danser AHJ. Endothelium-derived hyperpolarizing factor and protein kinase G ialpha activation: H2O2 versus s-nitrosothiols. *Eur J Pharmacol* (2018) 827:112–6. doi: 10.1016/j.ejphar.2018.03.019

44. Coletta C, Papapetropoulos A, Erdelyi K, Olah G, Modis K, Panopoulos P, et al. Hydrogen sulfide and nitric oxide are mutually dependent in the regulation of angiogenesis and endothelium-dependent vasorelaxation. *Proc Natl Acad Sci U S A* (2012) 109:9161–6. doi: 10.1073/pnas.1202916109

45. Kiss L, Deitch EA, Szabo C. Hydrogen sulfide decreases adenosine triphosphate levels in aortic rings and leads to vasorelaxation *via* metabolic inhibition. *Life Sci* (2008) 83:589–94. doi: 10.1016/j.lfs.2008.08.006

46. Hedegaard ER, Gouliaev A, Winther AK, Arcanjo DD, Aalling M, Renaltan NS, et al. Involvement of potassium channels and calcium-independent mechanisms in hydrogen sulfide-induced relaxation of rat mesenteric small arteries. *J Pharmacol Exp Ther* (2016) 356:53–63. doi: 10.1124/jpet.115.227017

47. Szabo C, Ransy C, Modis K, Andriamihaja M, Murghes B, Coletta C, et al. Regulation of mitochondrial bioenergetic function by hydrogen sulfide. part i. biochemical and physiological mechanisms. *Br J Pharmacol* (2014) 171:2099–122. doi: 10.1111/bph.12369

48. Nair A. Pharmacologic therapy for pulmonary artery hypertension. *Curr Opin Cardiol* (2020) 35:643–56. doi: 10.1097/HCO.0000000000000796

49. Ariyaratnam P, Loubani M, Morice AH. Hydrogen sulphide vasodilates human pulmonary arteries: a possible role in pulmonary hypertension? *Microvasc Res* (2013) 90:135–7. doi: 10.1016/j.mvr.2013.09.002

50. Castro-Piedras I, Perez-Zoghbi JF. Hydrogen sulphide inhibits Ca2+ release through InsP3 receptors and relaxes airway smooth muscle. *J Physiol* (2013) 591:5999–6015. doi: 10.1113/jphysiol.2013.257790

51. Wu J, Pan W, Wang C, Dong H, Xing L, Hou J, et al. H2S attenuates endoplasmic reticulum stress in hypoxia-induced pulmonary artery hypertension. *Biosci Rep* (2019) 39:1-13. doi: 10.1042/BSR20190304

52. Rashid S, Heer JK, Garle MJ, Alexander SP, Roberts RE. Hydrogen sulphide-induced relaxation of porcine peripheral bronchioles. *Br J Pharmacol* (2013) 168:1902–10. doi: 10.1111/bph.12084

53. Wei HL, Zhang CY, Jin HF, Tang CS, Du JB. Hydrogen sulfide regulates lung tissue-oxidized glutathione and total antioxidant capacity in hypoxic pulmonary hypertensive rats. *Acta Pharmacol Sin* (2008) 29:670–9. doi: 10.1111/j.1745-7254.2008.00796.x

54. Luo L, Liu D, Tang C, Du J, Liu AD, Holmberg L, et al. Sulfur dioxide upregulates the inhibited endogenous hydrogen sulfide pathway in rats with pulmonary hypertension induced by high pulmonary blood flow. *Biochem Biophys Res Commun* (2013) 433:519–25. doi: 10.1016/j.bbrc.2013.03.014

55. Taleb S. Inflammation in atherosclerosis. *Arch Cardiovasc Dis* (2016) 109:708–15. doi: 10.1016/j.acvd.2016.04.002

56. Liu Q, Zhang H, Lin J, Zhang R, Chen S, Liu W, et al. C1q/TNF-related protein 9 inhibits the cholesterol-induced vascular smooth muscle cell phenotype switch and cell dysfunction by activating AMP-dependent kinase. *J Cell Mol Med* (2017) 21:2823–36. doi: 10.1111/jcmm.13196

57. Wang ZJ, Wu J, Guo W, Zhu YZ. Atherosclerosis and the hydrogen sulfide signaling pathway - therapeutic approaches to disease prevention. *Cell Physiol Biochem* (2017) 42:859–75. doi: 10.1159/000478628

58. Lee DY, Chiu JJ. Atherosclerosis and flow: roles of epigenetic modulation in vascular endothelium. *J BioMed Sci* (2019) 26:56. doi: 10.1186/s12929-019-0551-8

59. Theodorou K, Boon RA. Endothelial cell metabolism in atherosclerosis. *Front Cell Dev Biol* (2018) 6:82. doi: 10.3389/fcell.2018.00082

60. Mani S, Li H, Untereiner A, Wu L, Yang G, Austin RC, et al. Decreased endogenous production of hydrogen sulfide accelerates atherosclerosis. *Circulation* (2013) 127:2523–34. doi: 10.1161/CIRCULATIONAHA.113.002208

61. Yue LM, Gao YM, Han BH. Evaluation on the effect of hydrogen sulfide on the NLRP3 signaling pathway and its involvement in the pathogenesis of atherosclerosis. *J Cell Biochem* (2019) 120:481–92. doi: 10.1002/jcb.27404

62. Tian D, Dong J, Jin S, Teng X, Wu Y. Endogenous hydrogen sulfide-mediated MAPK inhibition preserves endothelial function through TXNIP signaling. *Free Radic Biol Med* (2017) 110:291–9. doi: 10.1016/j.freeradbiomed.2017.06.016

63. Xiong R, Lu X, Song J, Li H, Wang S. Molecular mechanisms of hydrogen sulfide against uremic accelerated atherosclerosis through cPKCbetaII/Akt signal pathway. *BMC Nephrol* (2019) 20:358. doi: 10.1186/s12882-019-1550-4

64. Rao G, Murphy B, Dey A, Dwivedi SKD, Zhang Y, Roy RV, et al. Cystathionine beta synthase regulates mitochondrial dynamics and function in endothelial cells. *FASEB J* (2020) 34:9372–92. doi: 10.1096/fj.202000173R

65. Lin Y, Zeng H, Gao L, Gu T, Wang C, Zhang H. Hydrogen sulfide attenuates atherosclerosis in a partially ligated carotid artery mouse model *via* regulating angiotensin converting enzyme 2 expression. *Front Physiol* (2017) 8:782. doi: 10.3389/fphys.2017.00782

66. Hu HJ, Jiang ZS, Qiu J, Zhou SH, Liu QM. Protective effects of hydrogen sulfide against angiotensin II-induced endoplasmic reticulum stress in HUVECs. *Mol Med Rep* (2017) 15:2213–22. doi: 10.3892/mmr.2017.6238

67. Xie L, Feng H, Li S, Meng G, Liu S, Tang X, et al. SIRT3 mediates the antioxidant effect of hydrogen sulfide in endothelial cells. *Antioxid Redox Signal* (2016) 24:329–43. doi: 10.1089/ars.2015.6331

68. Ford A, Al-Magableh M, Gaspari TA, Hart JL. Chronic NaHS treatment is vasoprotective in high-Fat-Fed ApoE(-/-) mice. *Int J Vasc Med* (2013) 2013:915983. doi: 10.1155/2013/915983

69. Zhu L, Duan W, Wu G, Zhang D, Wang L, Chen D, et al. Protective effect of hydrogen sulfide on endothelial cells through Sirt1-FoxO1-mediated autophagy. *Ann Transl Med* (2020) 8:1586. doi: 10.21037/atm-20-3647

70. Gero D, Torregrossa R, Perry A, Waters A, Le-Trionnaire S, Whatmore JL, et al. The novel mitochondria-targeted hydrogen sulfide (H2S) donors AP123 and AP39 protect against hyperglycemic injury in microvascular endothelial cells *in vitro*. *Pharmacol Res* (2016) 113:186–98. doi: 10.1016/j.phrs.2016.08.019

71. Lin Y, Chen Y, Zhu N, Zhao S, Fan J, Liu E. Hydrogen sulfide inhibits development of atherosclerosis through up-regulating protein s-nitrosylation. *BioMed Pharmacother* (2016) 83:466–76. doi: 10.1016/j.biopha.2016.07.003

72. Liu Z, Han Y, Li L, Lu H, Meng G, Li X, et al. The hydrogen sulfide donor, GYY4137, exhibits anti-atherosclerotic activity in high fat fed apolipoprotein e(-/-) mice. *Br J Pharmacol* (2013) 169:1795–809. doi: 10.1111/bph.12246

73. Libby P. Inflammation in atherosclerosis. *Arterioscler Thromb Vasc Biol* (2012) 32:2045–51. doi: 10.1161/ATVBAHA.108.179705

74. Wang XH, Wang F, You SJ, Cao YJ, Cao LD, Han Q, et al. Dysregulation of cystathionine gamma-lyase (CSE)/hydrogen sulfide pathway contributes to ox-LDL-induced inflammation in macrophage. *Cell Signal* (2013) 25:2255–62. doi: 10.1016/j.cellsig.2013.07.010

75. Du C, Lin X, Xu W, Zheng F, Cai J, Yang J, et al. Sulfhydrated sirtuin-1 increasing its deacetylation activity is an essential epigenetics mechanism of anti-atherogenesis by hydrogen sulfide. *Antioxid Redox Signal* (2019) 30:184–97. doi: 10.1089/ars.2017.7195

76. Monti M, Terzuoli E, Ziche M, Morbidelli L. H2S dependent and independent anti-inflammatory activity of zofenoprilat in cells of the vascular wall. *Pharmacol Res* (2016) 113:426–37. doi: 10.1016/j.phrs.2016.09.017

77. Peh MT, Anwar AB, Ng DS, Atan MS, Kumar SD, Moore PK. Effect of feeding a high fat diet on hydrogen sulfide (H2S) metabolism in the mouse. *Nitric Oxide* (2014) 41:138–45. doi: 10.1016/j.niox.2014.03.002

78. Zhang D, Jiang X, Fang P, Yan Y, Song J, Gupta S, et al. Hyperhomocysteinemia promotes inflammatory monocyte generation and accelerates atherosclerosis in transgenic cystathionine beta-synthase-deficient mice. *Circulation* (2009) 120:1893–902. doi: 10.1161/CIRCULATIONAHA.109.866889

79. Xu S, Liu Z, Liu P. Targeting hydrogen sulfide as a promising therapeutic strategy for atherosclerosis. *Int J Cardiol* (2014) 172:313–7. doi: 10.1016/j.ijcard.2014.01.068

80. Liu YH, Lu M, Hu LF, Wong PT, Webb GD, Bian JS. Hydrogen sulfide in the mammalian cardiovascular system. *Antioxid Redox Signal* (2012) 17:141–85. doi: 10.1089/ars.2011.4005

81. Whiteman M, Li L, Rose P, Tan CH, Parkinson DB, Moore PK. The effect of hydrogen sulfide donors on lipopolysaccharide-induced formation of inflammatory mediators in macrophages. *Antioxid Redox Signal* (2010) 12:1147–54. doi: 10.1089/ars.2009.2899

82. Zheng Q, Pan L, Ji Y. H_2S protects against diabetes-accelerated atherosclerosis by preventing the activation of NLRP3 inflammasome. *J BioMed Res* (2019) 34:94–102. doi: 10.7555/JBR.33.20190071

83. Jain SK, Huning L, Micinski D. Hydrogen sulfide upregulates glutamate-cysteine ligase catalytic subunit, glutamate-cysteine ligase modifier subunit, and glutathione and inhibits interleukin-1beta secretion in monocytes exposed to high glucose levels. *Metab Syndr Relat Disord* (2014) 12:299–302. doi: 10.1089/met.2014.0022

84. Carmeliet P. Mechanisms of angiogenesis and arteriogenesis. *Nat Med* (2000) 6:389–95. doi: 10.1038/74651

85. Terzuoli E, Monti M, Vellecco V, Bucci M, Cirino G, Ziche M, et al. Characterization of zofenoprilat as an inducer of functional angiogenesis through increased H2 s availability. *Br J Pharmacol* (2015) 172:2961–73. doi: 10.1111/bph.13101

86. Gregg EW, Williams DE, Geiss L. Changes in diabetes-related complications in the united states. *N Engl J Med* (2014) 371:286–7. doi: 10.1056/NEJMc1406009

87. Jain SK, Bull R, Rains JL, Bass PF, Levine SN, Reddy S, et al. Low levels of hydrogen sulfide in the blood of diabetes patients and streptozotocin-treated rats causes vascular inflammation? *Antioxid Redox Signal* (2010) 12:1333–7. doi: 10.1089/ars.2009.2956

88. Brancaleone V, Roviezzo F, Vellecco V, De Gruttola L, Bucci M, Cirino G. Biosynthesis of H2S is impaired in non-obese diabetic (NOD) mice. *Br J Pharmacol* (2008) 155:673–80. doi: 10.1038/bjp.2008.296

89. Cheng Z, Shen X, Jiang X, Shan H, Cimini M, Fang P, et al. Hyperhomocysteinemia potentiates diabetes-impaired EDHF-induced vascular relaxation: Role of insufficient hydrogen sulfide. *Redox Biol* (2018) 16:215–25. doi: 10.1016/j.redox.2018.02.006

90. Wu F, He Z, Ding R, Huang Z, Jiang Q, Cui H, et al. Danhong promotes angiogenesis in diabetic mice after critical limb ischemia by activation of CSE-h 2 s-VEGF axis. *Evid Based Complement Alternat Med* (2015) 2015:276263. doi: 10.1155/2015/276263

91. Coletta C, Modis K, Szczesny B, Brunyanszki A, Olah G, Rios EC, et al. Regulation of vascular tone, angiogenesis and cellular bioenergetics by the 3-mercaptopyruvate Sulfurtransferase/H2S pathway: Functional impairment by hyperglycemia and restoration by DL-alpha-Lipoic acid. *Mol Med* (2015) 21:1–14. doi: 10.2119/molmed.2015.00035

92. Abdollahi Govar A, Toro G, Szaniszlo P, Pavlidou A, Bibli SI, Thanki K, et al. 3-mercaptopyruvate sulfurtransferase supports endothelial cell angiogenesis and bioenergetics. *Br J Pharmacol* (2020) 177:866–83. doi: 10.1111/bph.14574

93. Yang HB, Liu HM, Yan JC, Lu ZY. Effect of diallyl trisulfide on ischemic tissue injury and revascularization in a diabetic mouse model. *J Cardiovasc Pharmacol* (2018) 71:367–74. doi: 10.1097/FJC.0000000000000579

94. Liu F, Chen DD, Sun X, Xie HH, Yuan H, Jia W, et al. Hydrogen sulfide improves wound healing *via* restoration of endothelial progenitor cell functions and activation of angiopoietin-1 in type 2 diabetes. *Diabetes* (2014) 63:1763–78. doi: 10.2337/db13-0483

95. Wang GG, Li W. Hydrogen sulfide improves vessel formation of the ischemic adductor muscle and wound healing in diabetic db/db mice. *Iran J Basic Med Sci* (2019) 22:1192–7. doi: 10.22038/ijbms.2019.36551.8709

96. Zhao H, Lu S, Chai J, Zhang Y, Ma X, Chen J, et al. Hydrogen sulfide improves diabetic wound healing in ob/ob mice *via* attenuating inflammation. *J Diabetes Complications* (2017) 31:1363–9. doi: 10.1016/j.jdiacomp.2017.06.011

97. Wu J, Chen A, Zhou Y, Zheng S, Yang Y, An Y, et al. Novel H2S-releasing hydrogel for wound repair *via in situ* polarization of M2 macrophages. *Biomaterials* (2019) 222:119398. doi: 10.1016/j.biomaterials.2019.119398

98. Zhao X, Liu L, An T, Xian M, Luckanagul JA, Su Z, et al. A hydrogen sulfide-releasing alginate dressing for effective wound healing. *Acta Biomater* (2020) 104:85–94. doi: 10.1016/j.actbio.2019.12.032

99. Lin WC, Huang CC, Lin SJ, Li MJ, Chang Y, Lin YJ, et al. *In situ* depot comprising phase-change materials that can sustainably release a gasotransmitter H2S to treat diabetic wounds. *Biomaterials* (2017) 145:1–8. doi: 10.1016/j.biomaterials.2017.08.023

100. Longchamp A, Mirabella T, Arduini A, MacArthur MR, Das A, Trevino-Villarreal JH, et al. Amino acid restriction triggers angiogenesis *via* GCN2/ATF4 regulation of VEGF and H2S production. *Cell* (2018) 173:117–29.e14. doi: 10.1016/j.cell.2018.03.001

101. Tao B, Wang R, Sun C, Zhu Y. 3-mercaptopyruvate sulfurtransferase, not cystathionine beta-synthase nor cystathionine gamma-lyase, mediates hypoxia-induced migration of vascular endothelial cells. *Front Pharmacol* (2017) 8:657. doi: 10.3389/fphar.2017.00657

102. Leskova A, Pardue S, Glawe JD, Kevil CG, Shen X. Role of thiosulfate in hydrogen sulfide-dependent redox signaling in endothelial cells. *Am J Physiol Heart Circ Physiol* (2017) 313:H256–64. doi: 10.1152/ajpheart.00723.2016

103. Majumder A, Singh M, George AK, Behera J, Tyagi N, Tyagi SC. Hydrogen sulfide improves postischemic neoangiogenesis in the hind limb of cystathionine-beta-synthase mutant mice *via* PPAR-gamma/VEGF axis. *Physiol Rep* (2018) 6:e13858. doi: 10.14814/phy2.13858

104. Hayashida R, Kondo K, Morita S, Unno K, Shintani S, Shimizu Y, et al. Diallyl trisulfide augments ischemia-induced angiogenesis *via* an endothelial nitric oxide synthase-dependent mechanism. *Circ J* (2017) 81:870–8. doi: 10.1253/circj.CJ-16-1097

105. Bir SC, Kolluru GK, McCarthy P, Shen X, Pardue S, Pattillo CB, et al. Hydrogen sulfide stimulates ischemic vascular remodeling through nitric oxide synthase and nitrite reduction activity regulating hypoxia-inducible factor-1alpha and vascular endothelial growth factor-dependent angiogenesis. *J Am Heart Assoc* (2012) 1:e004093. doi: 10.1161/JAHA.112.004093

106. Wang MJ, Cai WJ, Li N, Ding YJ, Chen Y, Zhu YC. The hydrogen sulfide donor NaHS promotes angiogenesis in a rat model of hind limb ischemia. *Antioxid Redox Signal* (2010) 12:1065–77. doi: 10.1089/ars.2009.2945

107. Cai WJ, Wang MJ, Moore PK, Jin HM, Yao T, Zhu YC. The novel proangiogenic effect of hydrogen sulfide is dependent on akt phosphorylation. *Cardiovasc Res* (2007) 76:29–40. doi: 10.1016/j.cardiores.2007.05.026

108. Hsieh MH, Tsai HW, Lin KJ, Wu ZY, Hu HY, Chang Y, et al. An *in situ* slow-releasing H2S donor depot with long-term therapeutic effects for treating ischemic diseases. *Mater Sci Eng C Mater Biol Appl* (2019) 104:109954. doi: 10.1016/j.msec.2019.109954

109. Hu Q, Wu D, Ma F, Yang S, Tan B, Xin H, et al. Novel angiogenic activity and molecular mechanisms of ZYZ-803, a slow-releasing hydrogen sulfide-nitric oxide hybrid molecule. *Antioxid Redox Signal* (2016) 25:498–514. doi: 10.1089/ars.2015.6607

110. Xiong Y, Chang LL, Tran B, Dai T, Zhong R, Mao YC, et al. ZYZ-803, a novel hydrogen sulfide-nitric oxide conjugated donor, promotes angiogenesis *via* cross-talk between STAT3 and CaMKII. *Acta Pharmacol Sin* (2020) 41:218–28. doi: 10.1038/s41401-019-0255-3

111. Lilyanna S, Peh MT, Liew OW, Wang P, Moore PK, Richards AM, et al. GYY4137 attenuates remodeling, preserves cardiac function and modulates the natriuretic peptide response to ischemia. *J Mol Cell Cardiol* (2015) 87:27–37. doi: 10.1016/j.yjmcc.2015.07.028

112. Polhemus D, Kondo K, Bhushan S, Bir SC, Kevil CG, Murohara T, et al. Hydrogen sulfide attenuates cardiac dysfunction after heart failure *via* induction of angiogenesis. *Circ Heart Fail* (2013) 6:1077–86. doi: 10.1161/CIRCHEARTFAILURE.113.000299

113. Qipshidze N, Metreveli N, Mishra PK, Lominadze D, Tyagi SC. Hydrogen sulfide mitigates cardiac remodeling during myocardial infarction *via* improvement of angiogenesis. *Int J Biol Sci* (2012) 8:430–41. doi: 10.7150/ijbs.3632

114. Givvimani S, Munjal C, Gargoum R, Sen U, Tyagi N, Vacek JC, et al. Hydrogen sulfide mitigates transition from compensatory hypertrophy to heart failure. *J Appl Physiol (1985)* (2011) 110:1093–100. doi: 10.1152/japplphysiol.01064.2010

115. Liang W, Chen J, Li L, Li M, Wei X, Tan B, et al. Conductive hydrogen sulfide-releasing hydrogel encapsulating ADSCs for myocardial infarction treatment. *ACS Appl Mater Interfaces* (2019) 11:14619–29. doi: 10.1021/acsami.9b01886

116. Kan J, Guo W, Huang C, Bao G, Zhu Y, Zhu YZ. S-propargyl-cysteine, a novel water-soluble modulator of endogenous hydrogen sulfide, promotes angiogenesis through activation of signal transducer and activator of transcription 3. *Antioxid Redox Signal* (2014) 20:2303–16. doi: 10.1089/ars.2013.5449

117. Cheng Y, Ndisang JF, Tang G, Cao K, Wang R. Hydrogen sulfide-induced relaxation of resistance mesenteric artery beds of rats. *Am J Physiol Heart Circ Physiol* (2004) 287:H2316–23. doi: 10.1152/ajpheart.00331.2004

118. Powell CR, Dillon KM, Matson JB. A review of hydrogen sulfide (H2S) donors: Chemistry and potential therapeutic applications. *Biochem Pharmacol* (2018) 149:110–23. doi: 10.1016/j.bcp.2017.11.014

frontiers | Frontiers in Endocrinology

TYPE Original Research
PUBLISHED 23 September 2022
DOI 10.3389/fendo.2022.985636

OPEN ACCESS

EDITED BY
Si Jin,
Huazhong University of Science and Technology, China

REVIEWED BY
Ting Zhang,
Shanghai Jiao Tong University, China
Xiao Ding,
The Chinese University of Hong Kong, China

*CORRESPONDENCE
Xing-Xiang He
hexingxiang@gdpu.edu.cn
Qing-Ping Wu
wuqp203@163.com

†These authors have contributed equally to this work

SPECIALTY SECTION
This article was submitted to Cellular Endocrinology, a section of the journal Frontiers in Endocrinology

RECEIVED 04 July 2022
ACCEPTED 08 September 2022
PUBLISHED 23 September 2022

CITATION
Wu L, Li M-Q, Xie Y-T, Zhang Q, Lu X-J, Liu T, Lin W-Y, Xu J-T, Wu Q-P and He X-X (2022) Washed microbiota transplantation improves patients with high blood glucose in South China. *Front. Endocrinol.* 13:985636. doi: 10.3389/fendo.2022.985636

Washed microbiota transplantation improves patients with high blood glucose in South China

Lei Wu[1,2,3†], Man-Qing Li[1†], Ya-Ting Xie[1†], Qing Zhang[1†], Xin-Jian Lu[1], Tao Liu[1], Wen-Ying Lin[1], Jia-Ting Xu[1], Qing-Ping Wu[2*] and Xing-Xiang He[1*]

[1]Department of Gastroenterology, Research Center for Engineering Techniques of Microbiota-Targeted Therapies of Guangdong Province, The First Affiliated Hospital of Guangdong Pharmaceutical University, Guangzhou, China, [2]Guangdong Provincial Key Laboratory of Microbial Safety and Health, State Key Laboratory of Applied Microbiology Southern China, Institute of Microbiology, Guangdong Academy of Sciences, Guangzhou, China, [3]School of Biology and Biological Engineering, South China University of Technology, Guangzhou, China

Background and Aims: Although fecal microbiota transplantation (FMT) from healthy donors has been shown to have hypoglycemic effects in animal models of diabetes, its clinical impact in patients with abnormal blood glucose metabolism is unclear, especially in southern Chinese populations. The aim of this study was to investigate the feasibility and efficacy of washed microbiota transplantation (WMT) in the treatment of abnormal blood glucose metabolism in a population in southern China.

Methods: The clinical data of patients with different indications who received 1-3 treatments of WMT were retrospectively collected. The changes of blood glucose, blood lipids, blood pressure, liver function and blood routine before and after WMT were compared, such as fasting blood glucose (FBG), glycosylated hemoglobin (HbA1c), total cholesterol (TC), triglyceride (TG), systolic blood pressure (SBP), white blood cells (WBC), lymphocytes (LY) and platelets (PLT), etc.

Results: A total of 195 patients were included in the First Affiliated Hospital of Guangdong Pharmaceutical University, including 20 patients with high blood glucose and 175 patients with normal blood glucose. WMT has a significant effect in reducing short term blood glucose level (FBG) in patients with high blood glucose ($p < 0.05$). The fasting blood glucose (FBG) of 72.22% of patients with high blood glucose decreased to normal in a short term (about 1 month) ($p < 0.001$); In the medium term (about 2 months), there was a significant hypolipidemic (TG) ($p = 0.043$) effect, long term (about 6 months) significant blood pressure lowering (SBP, $p = 0.048$) effect. Overall, WMT significantly reduced the risk of high risk classes of Atherosclerotic Cardiovascular Disease (ASCVD) in the short term ($p = 0.029$) and medium term ($p = 0.050$).

Conclusion: WMT can significantly improve blood glucose in patients with high blood glucose, and there is no long-term elevated risk of blood glucose and ASCVD. FBG levels were significantly reduced in both the short and medium term in patients with high blood glucose treated with WMT. Therefore, the regulation of gut microbiota by WMT may provide a new clinical approach for the treatment of abnormal blood glucose metabolism.

KEYWORDS

fecal microbiota transplantation, washed microbiota transplantation (WMT), abnormal blood glucose metabolism, high blood glucose, fasting blood glucose

Introduction

Diabetes mellitus, a chronic disease characterized by relative or absolute insulin deficiency leading to hyperglycemia, is one of the largest global public health problems. The prevalence of diabetes has continued to increase in most developed and developing countries in recent decades (1, 2). To date, the International Diabetes Federation (IDF) estimates that approximately 451 million adults (aged 18-99) were living with diabetes worldwide in 2017, and this is expected to increase to 693 million by 2045 if effective prevention methods are not taken (3). In China, the prevalence of diabetes is still rising, with the prevalence increased rapidly to 10.9% - 12.8% from 2010 to 2018. Diabetes awareness (36.5%), treatment (32.2%) and control (49.2%) rates have improved but remain low (4). The prevalence of diabetes was significantly higher in urban areas than in rural areas (12.0% vs 8.9%), and higher in men than in women (11.1% vs 9.6%) (5, 6). Type 2 diabetes mellitus (T2DM) accounts for more than 90% of the diabetic population, and the prevalence of diabetes in the elderly over 60 years old is close to or exceeds 20% (7). At the same time, diabetes is one of the top ten causes of death in the world, and people with diabetes mainly die of diabetes-related complications rather than diabetes itself (8). A large number of these premature deaths can potentially be prevented through prevention or early detection, and improved management of diabetes and these complications.

T2DM patients often have one or more components of metabolic syndrome, such as hypertension, dyslipidemia, obesity, etc., which significantly increase the risk, progression speed and harm of T2DM complications. Therefore, a scientific and reasonable T2DM treatment strategy should be comprehensive, including the control of blood glucose, blood pressure, blood lipids, and body weight, antiplatelet therapy and lifestyle improvement measures. These treatment strategies are mainly lifestyle intervention and drug therapy. A variety of drugs are used to treat T2DM and can be divided into five main categories: drugs that stimulate insulin production by beta cells (sulfonylureas), improve insulin action (thiazolidinediones), delay carbohydrate uptake in the gut (alpha-glucosidase inhibitors), reduce hepatic glucose production (metformin) or target the glucagon-like peptide (GLP-1) axis (GLP-1 receptor agonists or DPP-4 inhibitors) (9). However, long term use of drug therapy can have significant side effects. Therefore, it is of great significance to comprehensively analyze the related factors of diabetes and find a treatment method with less side effects.

Gut microbiota has emerged as an important factor associated with human disease (10, 11). Numerous studies have demonstrated changes in the gut microbiota of T2DM patients by comparing the gut microbiota of T2DM patients with healthy individuals (12, 13). Dietary fiber selectively promotes gut bacteria to alleviate T2DM (14), suggesting that gut microbiota plays an important role in T2DM. In animal models of T2DM, Fecal microbiota transplantation (FMT) can improve HOMA-IR and insulin sensitivity (15), and repair damaged pancreatic islets (16), providing a potential strategy for the treatment of T2DM (17). FMT is a new treatment approach that uses healthy microbial profiles to replace the patient's own microbiota (18). FMT is of increasing interest (19) and have been successfully used to treat a variety of human diseases, such as inflammatory bowel disease (20), obesity (21), as well as metabolic syndrome (22) and functional bowel disease (23, 24). Whether FMT can improve abnormal blood glucose metabolism is a topic to be explored in clinical medicine.

Washed microbiota transplantation (WMT) is safe, quality-controlled (25), and effective (26) for the treatment of gut microbiota disorders. We attempted to investigate whether WMT could improve blood glucose metabolism in patients undergoing WMT. We hypothesized that WMT could safely and consistently affect patients across a variety of indications, improving abnormal blood glucose metabolism without side effects. Therefore, we conducted a retrospective trial to collect medical data from patients with abnormal blood glucose metabolism treated with WMT.

Materials and methods

Patients

This study was approved by the Ethics Committee of the First Affiliated Hospital of Guangdong Pharmaceutical University, Guangzhou, China according to the Declaration of Helsinki (no. 2017-98). Written informed consent was obtained and reviewed from all patients. This study included patients who completed 2-4 courses of WMT in our hospital from December 7, 2016 to April 30, 2022. Inclusion criteria: older than 18 years, informed consent, and those who received WMT. Exclusion criteria: pregnant women, patients taking antibiotics, hormones and probiotics during the first 3 months of WMT and during transplantation, and patients taking hypoglycemic drugs after WMT. In the end, a total of 195 people met the requirements.

WMT procedure

The procedure of WMT was in accordance with the Nanjing Consensus on the Methodology of Washed Microbiota Transplantation (26). All healthy fecal donors between the ages of 18 and 25 undergo rigorous consultation, psychological and physical examination, biochemical testing and infectious disease screening. To prepare the washed microbiota, each 100 g of feces and 500 mL of 0.9% saline was used to prepare a homogeneous fecal suspension. The fecal suspension was then subjected to microfiltration (to remove fecal particles, parasite eggs, and fungi) using a smart microbial separation system (GenFMTer; FMT Medical, Nanjing, China). After microfiltration, the fecal supernatant was centrifuged at 1100 × g for 3 min at room temperature. Then, the supernatant obtained after centrifugation was discarded. The microbiota pellet was resuspended in saline, then the microbiota pellet was centrifuged and resuspended 3 times. In the final resuspension, 100 mL of saline was added to the microbiota pellet obtained from 100 g of feces (25). Then, according to each patient's physical condition and wishes, the fecal suspension was injected into the patient through a nasojejunal tube (upper gastrointestinal tract) or a colonic transendoscopic enteral tube (lower gastrointestinal tract). A WMT course of 3 days, once a day, once a 120ml (27). The results of blood tests and other tests before the first course of treatment are the baseline values, and relevant indicators will be obtained before each subsequent course of treatment. According to the standard treatment time of WMT, short term: about 1 month interval from the first course of WMT; medium term: about 2 months interval from the first course of WMT; long term: about 6 months interval from the first course of WMT. All patients received at least 2 courses of WMT and completed follow-up.

Data collection

The medical records of the patients before treatment (baseline value), short term efficacy, medium term efficacy, and long-term efficacy were collected. Data included age, sex, body mass index (BMI), blood glucose at admission, blood pressure, disease or indication for WMT, and laboratory test results. Blood glucose indicators, namely fasting blood glucose (FBG), glycosylated hemoglobin (HbA1c). Insulin indicators, namely fasting insulin (FI), homeostasis model assessment of insulin resistance (HOMA-IR). Blood lipid indicators, namely total cholesterol (TC), triglyceride (TG), low density lipoprotein cholesterol (LDL-c), high density lipoprotein cholesterol (HDL-c), apolipoprotein B (ApoB), non-high density lipoprotein (non-HDL-c), lipoprotein (LIP). Blood pressure indicators, namely systolic blood pressure (SBP) on admission, diastolic blood pressure (DBP) on admission. Liver function indicators, namely alanine aminotransferase (ALT), aspartate aminotransferase (AST), serum albumin (ALB), total protein (TP), Albumin/globulin ratio (A/G), leucine aminopeptidase (LAP), glutamyl transpeptidase (GT), glutathione reductase (GR), Direct bilirubin (DBIL), indirect bilirubin (IBIL), total bilirubin (TBIL). Blood routine, that is, red blood cell count (RBC), hemoglobin concentration (HGB), white blood cell count (WBC), lymphocyte count (LY), platelet count (PLT), etc. HOMA-IR values were calculated as previously described (28). According to the Chinese Guidelines for the Prevention and Treatment of Type 2 Diabetes (2020 Edition), patients with high blood glucose were diagnosed (4), and all eligible patients were divided into 2 groups: high blood glucose group, 6.1mmol/L≤FBG or 6.1%<HbA1c and no hypoglycemic drugs, or FBG ≥7.0mmol/L was diagnosed as diabetic but without hypoglycemic drugs. Diagnosed with diabetes and the use of hypoglycemic drugs were excluded. Normal blood glucose group, 3.9mmol/L≤FBG<6.1mmol/L. Hospital-defined hyperlipidemia (TC ≥ 6.2 mmol/L or TG ≥ 2.3 mmol/L or LDL-c ≥ 4.1 mmol/L), hypolipidemia (TC < 3.6 mmol/L or TG < 0.33 mmol/L or LDL-c < 2.07 mmol/L or HDL < 0.91 mmol/L). Hypertension was defined as SBP ≥140 mmHg and/or DBP ≥90 mmHg (29). With reference to the Chinese cardiovascular disease prevention guidelines (2017 edition) (30), ASCVD risk stratification was performed according to baseline and blood lipid status: Those who meet one of the following conditions were directly classified as high-risk groups (1): Diabetes (age ≥ 40 years old) (2). Individuals with extremely high levels of a single risk factor, including: ① LDL-c ≥ 4.9 mmol/L (190 mg/dl) or TC ≥ 7.2 mmol/L (280 mg/dl); ② Grade 3 hypertension; ③ Heavy smoking (≥ 30 sticks/d). According to the 10-year average risk of ASCVD in different combinations, it was defined as low risk, intermediate risk and high risk according to < 5%, 5%-9% and ≥ 10%, respectively. Obese (≥ 28.0), overweight (24.0-28.0), normal weight (18.5-24.0), and underweight (< 18.5) were

defined according to BMI (kg/m^2) (31). Definition of serious adverse events (AEs): increased frequency of defecation, fever, abdominal pain, flatulence, hematochezia, vomiturition, bloating and herpes zoster, etc (25). All patients were divided into 2 groups according to the above definitions. After all patients received 1-3 WMT treatments and completed follow-up, statistical analysis and evaluation of blood glucose, blood lipids, blood pressure, liver function and blood routine results were performed.

Statistical analysis

Statistical analysis was performed using SPSS 22.0 (IBM Corp., Armonk, NY, USA) and Prism 8 (GraphPad, San Diego, CA, USA). Results are expressed as frequencies and percentages for categorical variables, mean and standard deviation for continuous variables with a normal distribution. Categorical variables were analyzed using chi-square or Fisher's exact test. For comparison of continuous variables between two independent groups, an unpaired Student's-t test (normally distributed variables) can be used. Paired data were compared using paired Student's-t test (normally distributed variables). Two-tailed p-values ≤ 0.05 were considered statistically significant.

Results

Clinical characteristics of patients who underwent WMT

WMT was completed in the First Affiliated Hospital of Guangdong Pharmaceutical University from December 2016 to April 2022. A total of 195 patients met the inclusion criteria (20 in the high blood glucose group and 175 in the normal blood glucose group). Among them, 98 (50.26%) were male and 97 (49.74%) were female, with an average age of 52.59 ± 14.36 years (Figure 1). Table 1 shows the main six disease characteristics of patients undergoing WMT, which are functional bowel disease (n=112, 57.44%, including irritable bowel syndrome, functional constipation), ulcerative colitis (n=21, 10.77%), gastroesophageal reflux disease (n=16, 8.21%), gouty arthritis (n=7, 3.59%), atopic dermatitis (n=6, 3.08%), chemotherapy-related diarrhea (n=6, 3.08%), hyperlipidemia (n=6, 3.08%). Due to the different compliance of patients, WMT treatment may not be completed on schedule. In this study, the time interval of WMT in the enrolled patients was counted, and the number of days was expressed as the median (25%-75%). The blood test results of the patients before the first course of treatment were the baseline values, and the interval between 3 treatments was 35 days (32-42 days) in the short term, 77 days (67-97.75 days) in the medium term, and 183 days (145-202.25 days) in the long term.

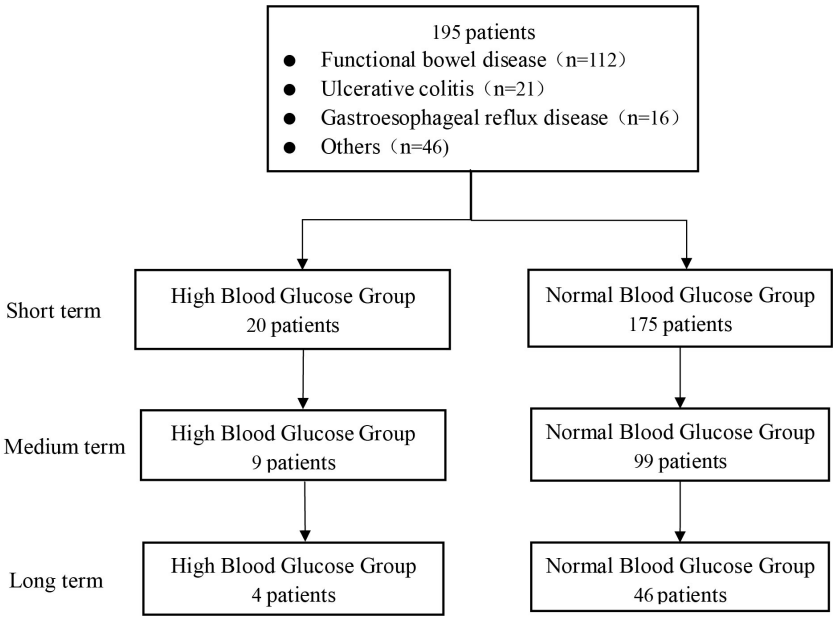

FIGURE 1
Flow chart of this study.

10.3389/fendo.2022.985636

TABLE 1 The main diagnoses of patients receiving washed microbiota transplantation.

Primary cause of WMT	Number (n)	Percentage (%)
Functional bowel disease	112	57.44%
Ulcerative colitis	21	10.77%
Gastroesophageal reflux disease	16	8.21%
Gouty arthritis	7	3.59%
Atopic dermatitis	6	3.08%
Chemotherapy-associated diarrhea	6	3.08%
Hyperlipidemia	6	3.08%
Radiation enteritis	5	2.56%
Hyperuricemia	3	1.54%
Hepatitis B cirrhosis	1	0.51%
Hyperlipidemic pancreatitis	1	0.51%
Functional dysphagia	1	0.51%
Senile tremor	1	0.51%
Epilepsy	1	0.51%
Duodenal stasis	1	0.51%
Crohn's disease	1	0.51%
Chronic urticaria	1	0.51%
Depression	1	0.51%
Parkinson's syndrome	1	0.51%
Bipolar disorder	1	0.51%
Psoriasis vulgaris	1	0.51%
Perianal eczema	1	0.51%
Total	195	100%

The demographic and clinical characteristics of high blood glucose group versus normal blood glucose group patients are compared in Table 2. Due to different compliance, not all patients have complete data, so the number of patients in each group is different for each indicator. There was no significant difference in age, gender ratio, and BMI between high blood glucose group and normal blood glucose group, indicating that the basic conditions of the study population were not significantly different, reducing the confounding factors of this study. The mean FBG of the high blood glucose group was 6.6 ± 1.67mmol/L higher than the definition in Materials and methods, and the mean FBG of the normal blood glucose group was 4.62 ± 0.48mmol/L. There was a significant difference in FBG between the two groups. The average TG in the high blood glucose group was 3.33 ± 4.75mmol/L, which was higher than the definition of hyperlipidemia, and that in the normal blood glucose group was 1.2 ± 0.78mmol/L. There was a significant difference in TG between the two groups. This indicated that the high blood glucose group was accompanied by symptoms of hyperlipidemia in addition to the higher FBG. HbA1c (6.02 ± 0.78 vs 5.41 ± 0.30%), FI (14.71 ± 10.86 vs 8.12 ± 4.93 μU/mL), HOMA-IR (4.26 ± 3.3 vs 1.7 ± 1.1), non-HDL-c (4.15 ± 1.65 vs 3.4 ± 0.98 mmol/L), AST (26.1 ± 11.53 vs 20.98 ± 7.12 U/L), LAP (33.2 ± 8.93 vs 29.71 ± 4.8 U/L), GT (60.34 ± 80.04 vs 23.88 ± 14.04U/L), DBIL (5.82 ± 10.41 vs 4.25 ± 1.85 μmol/L), TBIL (15.08 ± 24.8 vs 13.16 ± 5.62μmol/L), WBC (7.58 ± 3.22 vs 5.66 ± 1.69 10^9/L), PLT (256.6 ± 102.96 vs 224.36 ± 56.79 10^9/L), these indicators were significantly higher in the high blood glucose group than in the normal blood glucose group. There were only 10 AEs (1.82%) among the 548 times undergoing WMT treatment, mainly diarrhea (3 patients, 0.55%), sore throat (2 patients, 0.36%), and anal pain (2 patients, 0.36%)), nausea (1 patient, 0.18%), dizziness (1 patient, 0.18%), joint soreness (1 patient, 0.18%). There were no serious AEs, and it resolved itself within a few days.

Comparative analysis of each index after WMT treatment and baseline

Table 3 and Figure 2 show the effects of WMT on blood glucose, blood lipids, blood pressure, liver function and blood routine in patients with abnormal blood glucose metabolism. The results showed that WMT had a significant reducing effect on FBG in the short term (from 6.70 ± 1.65 to 5.29 ± 0.99mmol/L, $p = 0.006$) and medium term (from 6.58 ± 1.20 to 5.56 ± 0.95mmol/L, $p = 0.025$) in the high blood glucose group ($p < 0.05$), and also showed a decreasing effect in the long term (from 6.27 ± 0.08 to 4.80 ± 1.56mmol/L), but because the number of people was too small, it was not significant in the long term ($p = 0.425$). In the high blood glucose group, HbA1c decreased from 7.05 ± 0.49 to 6.95 ± 0.21mmol/L in the short term. FI decreased from 15.77 ± 10.3 to 11.88 ± 5.78 μU/mL in the short term and from 13.91 ± 11.8 to 11.98 ± 2.48 μU/mL in the long term. The HOMA-IR decreased from 4.73 ± 3.27 to 2.54 ± 1.36 in the short term and from 3.85 ± 3.25 to 2.64 ± 1.36 in the long term, but it was not significant. Overall, WMT has a good effect on improving blood glucose metabolism in patients with abnormal blood glucose metabolism.

At the same time, in the high blood glucose group, WMT significantly reduced TG (from 7.22 ± 7.83 to 3.09 ± 3.21mmol/L, $p = 0.043$) in the mid-term ($p < 0.05$), indicating that WMT has the effect of reducing blood lipids. There was a significant long term reduction ($p < 0.05$) on SBP (from 128.67 ± 3.51 to 119.00 ± 7.00mmHg, $p = 0.048$), indicating that WMT has a blood pressure lowering effect. There was a significant short term reduction ($p < 0.05$) on WBC (from 6.97 ± 1.76 to 6.04 ± 1.58 109/L, $p = 0.016$), indicating that WMT may have the function of inhibiting inflammatory response. Significantly decreased LY (from 1.98 ± 0.62 to 1.63 ± 0.53 109/L, $p = 0.019$) in the medium term ($p < 0.05$), indicating that WMT may have an immunomodulatory effect. There was a significant reduction ($p < 0.05$) in the short term (from 238.47 ± 65.23 to 217.11 ± 58.10 109/L, $p = 0.037$) and mid-term (from 275.89 ± 136.38 to 230.11 ± 106.85 109/L, $p = 0.031$) of PLT, indicating that WMT may have a role in regulating cardiovascular disease. There was no significant change in FBG, HbA1c, FI, HOMA-IR, etc. in the short term, medium term and long term in the normal blood glucose group by WMT, that is, WMT had no effect on normoglycemic patients. But for TC

10.3389/fendo.2022.985636

TABLE 2 Demographics and clinical characteristics of patients at baseline.

	High blood glucose group (20)	Normal blood glucose group (175)	p-Value
Age (year)	54.8 ± 13.42 (n = 20)	50.38 ± 15.29 (n = 175)	0.275
Male n (%)	48.57	65	0.164
BMI (kg/m^2)	24.75 ± 5.56 (n = 17)	22.07 ± 3.94 (n = 174)	0.423
FBG (mmol/L)	6.6 ± 1.67 (n = 20)	4.62 ± 0.48 (n = 175)	<0.001
HbA1c (%)	6.02 ± 0.78 (n = 11)	5.41 ± 0.30 (n=12)	0.007
FI (μU/mL)	14.71 ± 10.86 (n = 11)	8.12 ± 4.93 (n =94)	<0.001
HOMA-IR	4.26 ± 3.3 (n = 11)	1.7 ± 1.1 (n = 94)	<0.001
TC (mmol/L)	5.24 ± 1.45 (n = 17)	4.73 ± 1.03 (n = 157)	0.206
TG (mmol/L)	3.33 ± 4.75 (n = 17)	1.2 ± 0.78 (n = 157)	<0.001
LDL-c (mmol/L)	2.82 ± 0.94 (n = 17)	2.87 ± 0.91 (n = 157)	0.511
HDL-c (mmol/L)	1.09 ± 0.3 (n = 17)	1.32 ± 0.32 (n = 157)	0.827
ApoB (g/L)	1.04 ± 0.31 (n = 17)	0.91 ± 0.23 (n = 157)	0.741
non-HDL-c (mmol/L)	4.15 ± 1.65 (n = 17)	3.4 ± 0.98 (n = 157)	0.029
LIP (mmol/L)	193.34 ± 228.31 (n = 8)	160.31 ± 235.92 (n = 49)	0.366
SBP (mmHg)	130.2 ± 19.87 (n = 20)	121.5 ± 13.08 (n = 175)	0.130
DBP (mmHg)	78.75 ± 10.84 (n = 20)	77.11 ± 9.7 (n = 175)	0.592
ALT (U/L)	23.55 ± 13.14 (n = 20)	20.54 ± 16.57 (n=174)	0.817
AST (U/L)	26.1 ± 11.53 (n = 20)	20.98 ± 7.12 (n = 174)	0.015
ALB (g/L)	38.01 ± 6.29 (n = 20)	40.7 ± 4.32 (n=174)	0.307
TP (g/L)	67.87 ± 5.1 (n = 20)	68.3 ± 6.01 (n = 174)	0.219
A/G	1.33 ± 0.36 (n = 20)	1.53 ± 0.33 (n = 174)	0.972
LAP (U/L)	33.2 ± 8.93 (n = 12)	29.71 ± 4.8 (n = 133)	0.006
GT (U/L)	60.34 ± 80.04 (n = 11)	23.88 ± 14.04 (n = 142)	<0.001
GR (U/L)	59.66 ± 16.49 (n = 17)	56.51 ± 12.7 (n = 128)	0.105
DBIL (μmol/L)	5.82 ± 10.41 (n = 20)	4.25 ± 1.85 (n = 174)	<0.001
IBIL (μmol/L)	7.98 ± 7.87 (n = 20)	8.83 ± 4.02 (n = 174)	0.393
TBIL (μmol/L)	15.08 ± 24.8 (n = 20)	13.16 ± 5.62 (n = 174)	0.001
RBC (10^{12}/L)	4.41 ± 0.8 (n = 20)	4.32 ± 0.62 (n = 164)	0.242
HGB (g/L)	130.05 ± 24.19 (n = 20)	128.06 ± 18.22 (n = 164)	0.222
WBC (10^9/L)	7.58 ± 3.22 (n = 20)	5.66 ± 1.69 (n = 164)	0.013
LY (10^9/L)	2 ± 0.71 (n = 20)	1.74 ± 0.59 (n = 164)	0.142
PLT (10^9/L)	256.6 ± 102.96 (n = 20)	224.36 ± 56.79 (n = 164)	0.021

Data presented as mean ± standard deviation, or n (%).
BMI (kg/m^2), Body mass index; FBG (mmol/L), Fasting blood glucose; HbA1c (%), Glycated hemoglobin; FI (μU/mL), Fasting insulin; HOMA-IR, Homeostasis model assessment of insulin resistance; TC (mmol/L), Total cholesterol; TG (mmol/L), Triglyceride; LDL-c (mmol/L), Low-density lipoprotein cholesterol; HDL-c (mmol/L), High-density lipoprotein cholesterol; ApoB (g/L), Apolipoprotein B; non-HDL-c (mmol/L), Non-HDL cholesterol; LIP (mmol/L), Lipoprotein; SBP (mmHg), Systolic blood pressure; DBP (mmHg), Diastolic blood pressure; ALT (U/L), Alanine aminotransferase; AST (U/L), Aspartate aminotransferase; ALB (g/L), Serum albumin; TP (g/L), Total protein; A/G, Albumin/globulin; LAP (U/L), Leucine aminopeptidase; GT (U/L), glutamyl transpeptidase; GR (U/L), Glutathione Reductase; DBIL (μmol/L), Direct bilirubin; IBIL (μmol/L), Indirect bilirubin; TBIL (μmol/L), Total bilirubin; RBC (10^{12}/L), Red blood cell; HGB (g/L), Hemoglobin; WBC (10^9/L), White blood cell; LY (10^9/L), Lymphocyte; PLT (10^9/L), Platelet.

($p = 0.039$) and TG ($p = 0.030$) were significantly decreased ($p < 0.05$). Both the high blood glucose group and the normal blood glucose group had a decreasing trend in BMI before and after treatment, but there was no significant change.

Correlation analysis of WMT on indicators affecting blood glucose regulation

Earlier we found that during the treatment process, WMT had a significant improvement effect on FBG, TG, SBP, WBC, LY and PLT in the high blood glucose group. In order to find the relevant factors that affect the regulation of blood glucose by WMT, correlation analysis was carried out on the above-mentioned indicators with significant regulation effect. As shown in Figure 3, we found that in high blood glucose levels, FBG was positively correlated with TG (r=0.973), SBP (r=0.866), WBC (r=0.926), and LY (r=0.089); FBG was negatively correlated with PLT (r=-0.069). Our data show that during WMT treatment, blood pressure, blood lipids, anti-inflammatory response and immune function are simultaneously affected while improving blood glucose, and there is an interaction link. This provides us with a good treatment idea for the treatment of patients with

10.3389/fendo.2022.985636

TABLE 3 The comparison values of each index in high blood glucose group and normal blood glucose group in the short term, medium term and long term with baseline during the treatment of washed microbiota transplantation.

Items	Baseline	Short term	p-Value	Baseline	Medium term	p-Value	Baseline	Long term	p-Value
High blood glucose group									
BMI (kg/m^2)	24.75 ± 5.56 (n = 17)	24.32 ± 5.37 (n = 17)	0.303	23.54 ± 4.12 (n = 7)	22.62 ± 4.26 (n = 7)	0.067	21.11 ± 5.38 (n = 2)	19.85 ± 3.25 (n = 2)	0.557
FBG (mmol/L)	6.70 ± 1.65 (n = 18)	5.29 ± 0.99 (n = 18)	0.006	6.58 ± 1.20 (n = 8)	5.56 ± 0.95 (n = 8)	0.025	6.27 ± 0.08 (n = 2)	4.80 ± 1.56 (n = 2)	0.425
HbA1c (%)	7.05 ± 0.49 (n = 2)	6.95 ± 0.21 (n = 2)	0.874	/	/	/	/	/	/
FI (μU/mL)	15.77 ± 10.36 (n = 7)	11.88 ± 5.78 (n = 7)	0.359	/	/	/	13.91 ± 11.85 (n = 2)	11.98 ± 2.48 (n = 2)	0.820
HOMA-IR	4.73 ± 3.27 (n = 7)	2.54 ± 1.36 (n = 7)	0.134	/	/	/	3.85 ± 3.25 (n = 2)	2.64 ± 1.36 (n = 2)	0.532
TC (mmol/L)	5.36 ± 1.56 (n = 14)	4.98 ± 1.09 (n = 14)	0.338	6.68 ± 1.87 (n = 5)	5.24 ± 1.09 (n = 5)	0.136	/	/	/
TG (mmol/L)	3.78 ± 5.16 (n = 14)	2.62 ± 3.03 (n = 14)	0.198	7.22 ± 7.83 (n = 5)	3.09 ± 3.21 (n = 5)	0.043	/	/	/
LDL-c (mmol/L)	2.81 ± 1.00 (n = 14)	2.86 ± 1.13 (n = 14)	0.860	3.16 ± 1.29 (n = 5)	2.78 ± 1.26 (n = 5)	0.366	/	/	/
HDL-c (mmol/L)	1.06 ± 0.29 (n = 14)	1.09 ± 0.27 (n = 14)	0.575	0.83 ± 0.21 (n = 5)	1.06 ± 0.21 (n = 5)	0.082	/	/	/
ApoB (g/L)	1.07 ± 0.32 (n = 14)	1.03 ± 0.20 (n = 14)	0.676	1.28 ± 0.41 (n = 5)	1.04 ± 0.15 (n = 5)	0.314	/	/	/
non-HDL-c (mmol/L)	4.30 ± 1.75 (n = 14)	3.90 ± 1.07 (n = 14)	0.327	5.85 ± 2.05 (n = 5)	4.18 ± 1.21 (n = 5)	0.103	/	/	/
LIP (mmol/L)	198.64 ± 228.59 (n = 5)	228.54 ± 250.33 (n = 5)	0.168	/	/	/	/	/	/
SBP (mmHg)	130.20 ± 19.87 (n = 20)	127.00 ± 20.83 (n = 20)	0.315	124.11 ± 15.66 (n = 9)	124.22 ± 14.47 (n = 9)	0.984	128.67 ± 3.51 (n = 3)	119.00 ± 7.00 (n = 3)	0.048
DBP (mmHg)	78.75 ± 10.84 (n = 20)	76.30 ± 11.47 (n = 20)	0.275	75.22 ± 10.98 (n = 9)	79.78 ± 9.50 (n = 9)	0.243	75.33 ± 0.58 (n = 3)	73.00 ± 5.20 (n = 3)	0.556
ALT (U/L)	23.84 ± 13.43 (n = 19)	24.21 ± 13.96 (n = 19)	0.907	30.25 ± 13.66 (n = 8)	22.75 ± 14.5 (n = 8)	0.266	32.25 ± 13.15 (n = 4)	23.00 ± 9.70 (n = 4)	0.334
AST (U/L)	26.42 ± 11.75 (n = 19)	26.84 ± 12.97 (n = 19)	0.884	31.13 ± 13.44 (n = 8)	24.00 ± 9.93 (n = 8)	0.217	37.25 ± 17.23 (n = 4)	36.75 ± 20.97 (n = 4)	0.938
ALB (g/L)	38.00 ± 6.46 (n = 19)	39.03 ± 5.54 (n = 19)	0.455	36.08 ± 9.11 (n = 8)	39.27 ± 8.03 (n = 8)	0.220	32.33 ± 14.35 (n = 3)	38.13 ± 13.11 (n = 3)	0.058
TP (g/L)	67.94 ± 5.23 (n = 19)	67.92 ± 5.58 (n = 19)	0.991	65.41 ± 4.09 (n = 8)	67.74 ± 6.93 (n = 8)	0.385	62.17 ± 5.51 (n = 3)	73.80 ± 8.25 (n = 3)	0.121
A/G	1.33 ± 0.37 (n = 19)	1.42 ± 0.39 (n = 19)	0.323	1.34 ± 0.54 (n = 8)	1.49 ± 0.53 (n = 8)	0.435	1.26 ± 0.82 (n = 3)	1.31 ± 0.85 (n = 3)	0.586
LAP (U/L)	32.84 ± 9.27 (n = 11)	33.16 ± 8.21 (n = 11)	0.848	35.82 ± 11.72 (n = 5)	36.68 ± 10.63 (n = 5)	0.828	46.05 ± 13.93 (n = 2)	49.35 ± 6.29 (n = 2)	0.856
GT (U/L)	58.27 ± 84.05 (n = 10)	47.62 ± 53.10 (n = 10)	0.316	75.62 ± 119.66 (n = 5)	54.08 ± 71.22 (n = 5)	0.379	149.00 ± 197.99 (n = 2)	102.70 ± 133.93 (n = 2)	0.493
GR (U/L)	61.08 ± 15.92 (n = 16)	59.23 ± 12.02 (n = 16)	0.610	65.03 ± 18.02 (n = 6)	56.18 ± 10.62 (n = 6)	0.230	59.00 ± 31.11 (n = 2)	65.50 ± 0.71 (n = 2)	0.821
DBIL (μmol/L)	6.01 ± 10.66 (n = 19)	5.87 ± 9.35 (n = 19)	0.801	10.00 ± 16.08 (n = 8)	6.96 ± 10.58 (n = 8)	0.191	18.23 ± 27.08 (n = 3)	12.72 ± 15.57 (n = 3)	0.494
IBIL (μmol/L)	8.28 ± 7.97 (n = 19)	8.22 ± 5.70 (n = 19)	0.952	11.14 ± 11.98 (n = 8)	11.43 ± 13.10 (n = 8)	0.828	16.93 ± 20.45 (n = 3)	14.75 ± 9.63 (n = 3)	0.760
TBIL (μmol/L)	15.54 ± 25.39 (n = 19)	14.09 ± 14.67 (n = 19)	0.593	24.11 ± 38.83 (n = 8)	18.39 ± 23.64 (n = 8)	0.336	45.87 ± 64.33 (n = 3)	19.83 ± 11.95 (n = 3)	0.480
RBC (10^{12}/L)	4.43 ± 0.82 (n = 19)	4.38 ± 0.77 (n = 19)	0.575	4.17 ± 1.03 (n = 9)	4.52 ± 0.73 (n = 9)	0.070	3.53 ± 1.30 (n = 4)	4.40 ± 1.10 (n = 4)	0.077

(Continued)

TABLE 3 Continued

Items	Baseline	Short term	p-Value	Baseline	Medium term	p-Value	Baseline	Long term	p-Value
HGB (g/L)	132.42 ± 22.34 (n = 19)	130.84 ± 16.43 (n = 19)	0.577	123.44 ± 33.19 (n = 9)	131.56 ± 23.08 (n = 9)	0.203	103.00 ± 42.65 (n = 4)	122.50 ± 32.28 (n = 4)	0.246
WBC (10^9/L)	6.97 ± 1.76 (n = 19)	6.04 ± 1.58 (n = 19)	0.016	7.70 ± 4.33 (n = 9)	5.77 ± 1.60 (n = 9)	0.151	9.21 ± 6.63 (n = 4)	5.7 ± 2.51 (n = 4)	0.230
LY (10^9/L)	2.03 ± 0.71 (n = 19)	1.93 ± 0.63 (n = 19)	0.358	1.98 ± 0.62 (n = 9)	1.63 ± 0.53 (n = 9)	0.019	1.56 ± 0.33 (n = 4)	2.03 ± 1.10 (n = 4)	0.498
PLT (10^9/L)	238.47 ± 65.23 (n = 19)	217.11 ± 58.10 (n = 19)	0.037	275.89 ± 136.38 (n = 9)	230.11 ± 106.85 (n = 9)	0.031	346.00 ± 187.35 (n = 4)	249.75 ± 118.42 (n = 4)	0.099
Normal blood glucose group									
BMI (kg/m^2)	22.09 ± 3.94 (n = 172)	21.99 ± 3.89(n = 172)	0.386	21.7 ± 3.67(n = 96)	21.51 ± 3.7 (n = 96)	0.375	22.07 ± 3.99 (n = 45)	21.98 ± 4.04(n = 45)	0.787
FBG (mmol/L)	4.63 ± 0.48 (n = 154)	4.59 ± 0.78 (n = 154)	0.538	4.63 ± 0.5 (n = 86)	4.54 ± 0.82(n = 86)	0.261	4.77 ± 0.55 (n = 42)	4.79 ± 0.83 (n = 42)	0.893
HbA1c (%)	5.15 ± 0.50 (n = 2)	5.20 ± 0.71 (n = 2)	0.795	/	/	/	/	/	/
FI (μU/mL)	8.52 ± 5.31 (n=53)	8.80 ± 5.46 (n=53)	0.624	8.98 ± 5.48 (n=29)	8.95 ± 5.8 (n=29)	0.960	11.49 ± 6.36 (n=15)	10.97 ± 6.7 (n=15)	0.667
HOMA-IR	1.77 ± 1.16 (n=53)	1.87 ± 1.45 (n=53)	0.489	1.90 ± 1.28 (n=29)	1.95 ± 1.44 (n=29)	0.729	2.46 ± 1.5 (n=15)	2.33 ± 1.57 (n=15)	0.615
TC (mmol/L)	4.76 ± 1.06 (n=110)	4.66 ± 1.03 (n=110)	0.206	4.72 ± 1.06 (n=63)	4.58 ± 0.93 (n=63)	0.197	4.94 ± 1.12 (n=29)	4.61 ± 1 (n=29)	0.039
TG (mmol/L)	1.31 ± 0.84 (n=110)	1.19 ± 0.69 (n=110)	0.030	1.33 ± 0.9 (n=63)	1.5 ± 2.03 (n=63)	0.449	1.42 ± 0.79 (n=29)	1.29 ± 0.96 (n=29)	0.259
LDL-c (mmol/L)	2.88 ± 0.93 (n=110)	2.82 ± 0.89 (n=110)	0.402	2.79 ± 0.9 (n=63)	2.64 ± 0.82 (n=63)	0.124	2.92 ± 0.99 (n=29)	2.69 ± 0.88 (n=29)	0.099
HDL-c (mmol/L)	1.3 ± 0.33 (n=110)	1.31 ± 0.31 (n=110)	0.631	1.35 ± 0.34 (n=63)	1.32 ± 0.3 (n=63)	0.456	1.38 ± 0.31 (n=29)	1.34 ± 0.31 (n=29)	0.150
ApoB (g/L)	0.92 ± 0.24 (n=110)	0.91 ± 0.24 (n=110)	0.412	0.91 ± 0.23 (n=63)	0.90 ± 0.25 (n=63)	0.705	0.96 ± 0.21 (n=29)	0.96 ± 0.24 (n=29)	0.796
non-HDL-c (mmol/L)	3.46 ± 1.01 (n=110)	3.35 ± 0.98 (n=110)	0.148	3.38 ± 0.97 (n=63)	3.25 ± 0.87 (n=63)	0.225	3.57 ± 0.99 (n=29)	3.28 ± 0.92 (n=29)	0.049
LIP (mmol/L)	156.14 ± 303.68 (n=23)	156.29 ± 278.95 (n=23)	0.986	77.49 ± 75.35 (n=10)	83.04 ± 78.93 (n=10)	0.444	60.35 ± 24.68 (n=2)	42.60 ± 2.12 (n=2)	0.521
SBP (mmHg)	121.26 ± 12.75 (n=174)	120.38 ± 11.79 (n=174)	0.389	120.16 ± 12.85 (n=98)	119.6 ± 11.94 (n=98)	0.708	120.87 ± 12.11 (n=45)	119.49 ± 10.09 (n=45)	0.499
DBP (mmHg)	76.91 ± 9.38 (n=174)	76.44 ± 9.12 (n=174)	0.566	76.38 ± 9.47 (n=98)	74.86 ± 8.31 (n=98)	0.168	76.80 ± 9.41 (n=45)	77.16 ± 8.03 (n=45)	0.823
ALT (U/L)	20.65 ± 16.8 (n=168)	19.55 ± 13.2 (n=168)	0.355	20.25 ± 15.25 (n=88)	20.5 ± 13.32 (n=88)	0.863	19.91 ± 11.46 (n=43)	21.12 ± 18.55 (n=43)	0.633
AST (U/L)	21.04 ± 7.22 (n=168)	21.29 ± 7.59 (n=168)	0.671	20.78 ± 6.35 (n=88)	21.80 ± 7.36 (n=88)	0.201	21.26 ± 6.09 (n=43)	23.33 ± 12.34 (n=43)	0.177
ALB (g/L)	40.71 ± 4.36 (n=168)	40.53 ± 3.88 (n=168)	0.562	40.93 ± 4.77 (n=88)	40.36 ± 4.06 (n=88)	0.205	40.52 ± 5.01 (n=43)	40.4 ± 4.18 (n=43)	0.880
TP (g/L)	68.34 ± 5.99 (n=168)	67.79 ± 5.75 (n=168)	0.234	68.41 ± 6.44 (n=88)	67.63 ± 5.67 (n=88)	0.231	68.65 ± 5.97 (n=43)	67.64 ± 5.48 (n=43)	0.226
A/G	1.53 ± 0.33 (n=168)	1.53 ± 0.28 (n=168)	0.995	1.56 ± 0.38 (n=88)	1.52 ± 0.3 (n=88)	0.368	1.51 ± 0.41 (n=43)	1.52 ± 0.32 (n=43)	0.869
LAP (U/L)	29.71 ± 5 (n=112)	30.25 ± 5.01 (n=112)	0.047	29.36 ± 4.86 (n=63)	29.69 ± 5.57 (n=63)	0.340	29.41 ± 5.45 (n=31)	29.62 ± 5.14 (n=31)	0.672
GT (U/L)	24.17 ± 14.4 (n=121)	24.33 ± 14.97 (n=121)	0.789	24.98 ± 15.38 (n=70)	24.77 ± 16.11 (n=70)	0.838	27.85 ± 14.00 (n=35)	26.35 ± 12.68 (n=35)	0.318
GR (U/L)	56.34 ± 12.92 (n=119)	56.96 ± 13.46 (n=119)	0.340	54.24 ± 10.62 (n=62)	54.65 ± 11.74 (n=62)	0.682	53.3 ± 11.8 (n=28)	53.47 ± 13.1 (n=28)	0.912

(Continued)

10.3389/fendo.2022.985636

TABLE 3 Continued

Items	Baseline	Short term	p-Value	Baseline	Medium term	p-Value	Baseline	Long term	p-Value
DBIL (μmol/L)	4.19 ± 1.79 (n = 168)	4.16 ± 2.04 (n = 168)	0.761	4.13 ± 1.71 (n = 88)	4.08 ± 1.87 (n = 88)	0.769	4.09 ± 1.71 (n = 43)	4.15 ± 1.57 (n = 43)	0.826
IBIL (μmol/L)	8.72 ± 3.77 (n = 168)	8.47 ± 3.97 (n = 168)	0.336	8.75 ± 3.79 (n = 88)	8.42 ± 3.95 (n = 88)	0.326	9.19 ± 4.07 (n = 43)	8.96 ± 3.91 (n = 43)	0.694
TBIL (μmol/L)	13.01 ± 5.3 (n = 168)	12.64 ± 5.8 (n = 168)	0.287	12.94 ± 5.26 (n = 88)	12.51 ± 5.62 (n = 88)	0.357	13.29 ± 5.62 (n = 43)	13.10 ± 5.32 (n = 43)	0.819
RBC (10^{12}/L)	4.32 ± 0.62 (n = 164)	4.29 ± 0.62 (n = 164)	0.143	4.32 ± 0.54 (n = 85)	4.31 ± 0.56 (n = 85)	0.721	4.31 ± 0.56 (n = 39)	4.34 ± 0.55 (n = 39)	0.628
HGB (g/L)	128.06 ± 18.22 (n = 164)	127.06 ± 18.19 (n = 164)	0.140	127.21 ± 19.15 (n = 85)	127.46 ± 16.85 (n = 85)	0.843	127.23 ± 21.56 (n = 39)	128.49 ± 18.46 (n = 39)	0.476
WBC (10^9/L)	5.66 ± 1.69 (n = 164)	5.84 ± 2.12 (n = 164)	0.178	5.60 ± 1.64 (n = 85)	5.31 ± 1.58 (n = 85)	0.021	5.62 ± 1.64 (n = 39)	5.34 ± 1.47 (n = 39)	0.209
LY (10^9/L)	1.74 ± 0.59 (n = 164)	1.77 ± 0.66 (n = 164)	0.392	1.69 ± 0.58 (n = 85)	1.74 ± 0.57 (n=85)	0.337	1.66 ± 0.54 (n = 39)	1.68 ± 0.64 (n = 39)	0.794
PLT (10^9/L)	224.36 ± 56.79 (n=164)	222.84 ± 58.66 (n=164)	0.536	220.73 ± 57.45 (n=85)	212.55 ± 46.86 (n=85)	0.042	223.56 ± 64.26 (n = 39)	211.77 ± 52.94 (n = 39)	0.111

Data presented as mean ± standard deviation, or n (%).

abnormal blood glucose metabolism, that is, in addition to lowering blood glucose, it can also assist in the treatment of blood pressure and blood lipids, inhibit inflammation and improve immunity while treating high blood glucose.

Evaluation of WMT clinical therapeutic effect on blood glucose levels

All the enrolled patients were divided into high blood glucose group and normal blood glucose group according to blood glucose baseline. Patients were regrouped according to changes in blood glucose levels after 1-3 WMT treatments (Table 4). There were significant changes in blood glucose levels in the short term in patients with high blood glucose group. In the high blood glucose group, 72.22% returned to normal in the short term ($p < 0.001$), 57.14% returned to normal in the medium term ($p = 0.076$), and long term returned to normal is not significant ($p = 0.317$). Because the number of people is too small, there is no significant difference in the long term. Our data suggest that WMT can significantly change higher blood glucose levels in patients to normal levels in short term treatment; however, the efficacy of WMT remains to be explored. Our data show that WMT may significantly improve blood glucose levels after short term treatment, whereas blood glucose levels stabilize after medium and long term treatment.

Evaluation of the therapeutic effect of WMT on the ASCVD risk

According to ASCVD risk stratification, patients were divided into extremely high risk group, high risk group, medium risk group and low risk group. After WMT treatment, patients were regrouped into no risk changed group and the risk-changed group (Table 5). Acute coronary syndrome, coronary heart disease, stroke, and peripheral atherosclerosis were included in the extremely high risk group, and these patients were not reassigned after WMT and were not listed in Table 5.

In the high-risk group, the effects of short term and medium term WMT treatment were significant. Short term 25% and medium term 33.3% were classified as medium risk group or below ($p < 0.05$). In the medium risk group, the effects of short, medium and long term WMT treatment were not significant, but the number of people was reduced. In the ASCVD low risk group, this change was not statistically significant, suggesting that WMT does not increase the risk of ASCVD.

Discussion

To the best of our knowledge, this is one of the few clinical study to investigate the effects of WMT on patients with abnormal blood glucose metabolism, especially those with high blood glucose, in South China, indicating that regulating gut microbiota may be a new method for the treatment of abnormal blood glucose metabolism. These data show that WMT has a significant short and medium term effect on improving blood glucose in patients with high blood glucose, and at the same time, it has significant hypolipidemic and blood pressure-lowering effects on blood lipids and blood pressure in patients with high blood glucose. Overall, WMT significantly reduced the risk of high risk ASCVD in the short and medium term, and there was no significant difference between the medium and low

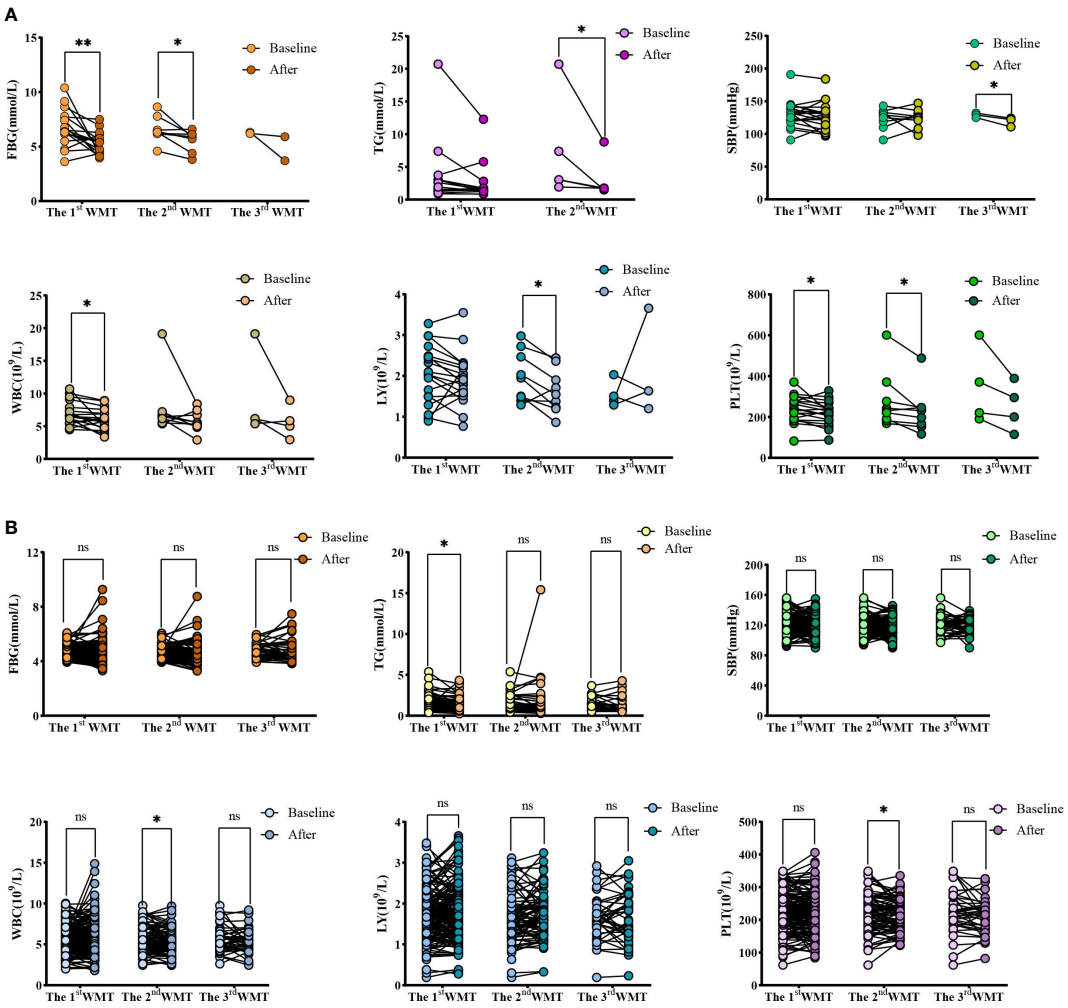

FIGURE 2
Changes of FBG, TG, SBP, WBC, LY and PLT levels after 1-3 times of washing and transplanting. **(A)** Changes of FBG, TG, SBP, WBC, LY and PLT in high blood glucose group; **(B)** Changes of FBG, TG, SBP, WBC, LY and PLT in normal blood glucose group. FBG, Fasting blood glucose; TG, Triglyceride; SBP, Systolic blood pressure; WBC, White blood cell; LY, Lymphocyte; PLT, Platelet. * indicates $p < 0.05$ ** indicates $p < 0.01$; ns, not significant.

risk groups, suggesting that WMT could reduce the short and medium term risk of ASCVD without increasing the risk of ASCVD.

Numerous studies have shown that gut microbiota disturbances may influence the progression of diabetes (32, 33). Patients with T2DM have a moderate dysbiosis between butyrate-producing and lactic acid bacteria (34). Furthermore, various metabolites, such as short chain fatty acids (SCFAs), produced by the gut microbiota differ significantly between T2DM and normal hosts (35). Studies have shown that ingestion of probiotics can effectively improve gut microbiota disturbances and relieve symptoms in diabetic patients, such as remodeling the formation of gut microbiota to improve or control the disease state (36). FMT is an approach to treat disease by rebuilding the microbiota (37). There is growing evidence that the therapeutic potential of FMT is based on an established clinical program that has become the first-line treatment for recurrent *Clostridium difficile* infections (38). However, understanding the impact of gut microbiota on metabolic disease is still in its infancy, and data on the effect of FMT on T2DM are still scarce. In our study, WMT had a significant short and medium term improvement in blood glucose in patients with high blood glucose. It is possible to restore gut microbiota balance to promote host homeostasis (39).

The potential effects of FMT on glucose homeostasis and insulin sensitivity in humans have been identified. FMT using lean donors was sufficient to improve glucose homeostasis in

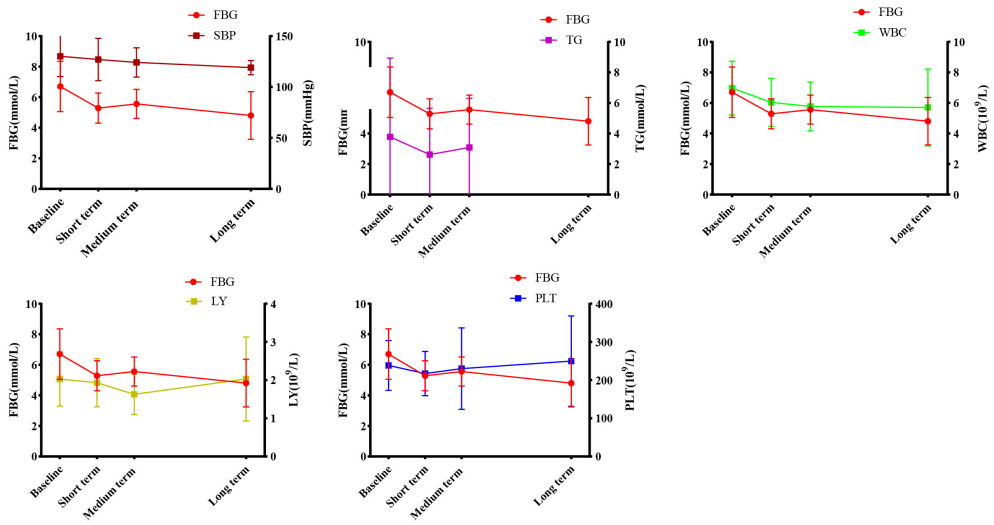

FIGURE 3
Correlation analysis of WMT on blood glucose regulation. FBG, Fasting blood glucose; TG, Triglyceride; SBP, Systolic blood pressure; WBC, White blood cell; LY, Lymphocyte; PLT, Platelet.

obese individuals, with a small decrease in HbA1c 6 weeks after FMT, which was associated with changes in gut microbiota (40). Another FMT double-blind placebo-controlled trial reported a slight improvement in HbA1c at 12 weeks (41). Our results for FBG and HbA1c showed a decreasing trend, providing further evidence for the hypoglycemic effect of WMT. As reported in the literature, FMT can show a restored phenotype following transfer of the donor's gut microbiota to the recipient (42). T2DM mice had reduced FI levels and improved HOMA-IR after reconstitution of their microbiota from normal mouse feces (17). Likewise, in a clinical trial, obese patients treated with FMT in lean healthy individuals showed positive changes in homeostasis model assessment of insulin sensitivity (HOMA-IS) (43). Our study did not observe a significant improvement in FI and HOMA-IR after WMT, although some studies showed that FMT significantly improved HOMA-IS (44). Our non-significant results may be due to the small sample size in our study, the lack of HOMA-IR indicators in many of our high blood glucose patients, and due to technical factors including the accuracy of the instrument, among others. For the current study, gut dysbiosis was associated with the development of insulin resistance and diabetes (42). The mechanism of gut microbiota-induced improvement in insulin resistance may be through altering body energy balance or reducing obesity induced by a high-fat diet. However, the exact mechanism needs to be fully explored.

FMT is associated with low-grade inflammation characterized by metabolic disturbances. Therapeutic FMT has

TABLE 4 Comprehensive clinical efficacy of short, medium and long term treatment on blood glucose levels.

Data periods	Before therapy (n)	Therapeutic effect base on blood glucose levels			
		Unchanged group (n)	Changed group (n, %)	X^2	p-Value
High blood glucose group					
Short term	18	5	13 (72.22%)	17.338	<0.001
Medium term	7	3	4 (57.14%)	3.150	0.076
Long term	2	0	2 (100%)	1.000	0.317
Normal blood glucose group					
Short term	154	149	5(3.36%)	3.253	0.071
Medium term	86	83	3 (4.65%)	1.375	0.244
Long term	42	37	5 (13.51%)	3.403	0.065

The definition of unchanged and changed of high blood glucose group were still high blood glucose group and changed to normal.
The definition of unchanged and changed of normal blood glucose were still normal and changed to high blood glucose group.

10.3389/fendo.2022.985636

TABLE 5 Effects of short, medium, and long term treatment on atherosclerotic cardiovascular disease risk classification.

Data periods	Before therapy (n)	Therapeutic effect base on ASCVD risk stratification			
		Unchangedgroup (n)	Changedgroup (n, %)	X^2	p-Value
High risk group					
Short term	24	18	6(25%)	4.792	0.029
Medium term	15	10	5(33.3%)	3.896	0.050
Long term	7	6	1(14.3%)	1.077	0.299
Medium risk group					
Short term	10	8	2(20%)	0.556	0.456
Medium term	6	5	1(16.7%)	1.091	0.296
Long term	5	4	1(20%)	1.111	0.292
Low risk group					
Short term	84	79	5(5.8%)	3.298	0.069
Medium term	44	43	1(2.3%)	1.011	0.315
Long term	19	17	2(10.5%)	0.528	0.468

The definition of unchanged of high-, medium-, and low-risk groups were still high-, medium-, and low-risk after WMT procedures, respectively.

been reported to reduce the secretion of inflammatory factors and trigger multiple immune-mediated signaling pathways in colitis (45). As mentioned in one study, transplantation of gut microbiota such as *Faecalibacterium prausnitzii* prevented inflammatory damage to the pancreas (46). These findings are consistent with our results, the WBC in the high blood glucose group after WMT showed a decreasing trend in the short, medium and long term, and there were significant differences in the short term, indicating that WMT may inhibit the inflammatory response. LY showed a significant downward trend in the medium term, indicating that WMT may have an immunomodulatory effect. IL-6 and TNF-α are pro-inflammatory cytokines with multiple functions that can directly act on islet cells and cause islet β-cell damage (47). Low-grade chronic inflammation caused by microbiota imbalance usually leads to islet structural damage and impaired islet β-cell function, and islet β-cell apoptosis is the underlying cause of islet structural damage. Therefore, FMT treatment of inflammatory response and apoptosis of islet β cells can reverse islet damage and dysfunction, which may be a method worth exploring.

T2DM patients often have one or more components of metabolic syndrome, such as hypertension, dyslipidemia, obesity, etc., which significantly increase the risk, progression speed and harm of T2DM complications. Comprehensive treatment should be based on the control of blood glucose, blood pressure, blood lipids and body weight, antiplatelet therapy and other lifestyle improvements. In our study, in addition to improving blood glucose, WMT has blood lipid-lowering and blood pressure-lowering effects in patients with high blood glucose, and has a significant reduction in platelets in the short and medium term, which is in line with the recommendations of antiplatelet therapy. We speculate that the improvement of abnormal blood glucose metabolism after WMT is due to the improvement of gut microbiota after WMT, which comprehensively regulates blood lipids, blood pressure, and platelets. The short term goal of diabetes treatment is to eliminate diabetes symptoms and prevent acute complications by controlling hyperglycemia and metabolic disorders. The long term goal of diabetes treatment is to prevent chronic complications, improve patients' quality of life and prolong life through good metabolic control. A scientific and reasonable T2DM treatment strategy should be comprehensive, including control of blood glucose, blood pressure, blood lipids, and body weight, antiplatelet therapy, and lifestyle improvements. Although there are several studies on WMT function, such as Liang et al. showed that WMT treatment can alter blood lipids in patients with hyperlipidemia and hypolipidemia without serious adverse events (48). Studies by Zhong et al. have shown that WMT has antihypertensive effects in hypertensive patients (49). Pan et al. showed that WMT significantly improved children with autism spectrum disorder, gastrointestinal symptoms and sleep disturbance, and reduced systemic inflammation (50). The mechanism of FMT-induced disease remission remains largely unexplained. Diabetic symptoms may be alleviated by synergistic effects between gut commensal microbiota after FMT treatment, or may trigger multiple immune-inflammatory processes and pathways.

Future research should focus on the bacterial species and functional changes associated with FMT treatment in diabetic patients and how FMT affects the metabolism of other organs in long term improvement. Due to the complexity of the gut microbiota, further studies should explore whether specific microbial species or communities in FMT are dedicated to the prevention and treatment of diabetes. This may provide a new perspective and reference. Many factors influence the outcome

of FMT, namely donor selection and preparation, sample handling, mode of administration, and colonization resistance (51). FMT-related AEs are a challenge for FMT applications. In most cases, mild gastrointestinal AEs were well tolerated by FMT (52). Our WMT project based on Zhang's criteria found no serious AEs during and after WMT. Zhang et al. prepared washed microbial flora by repeating centrifugation and suspension three times on the basis of an automatic purification system, which significantly reduced AEs (25). At present, the understanding of the effect of WMT on the gut microbiota on metabolic diseases is still in its infancy, and data on the effect of WMT on abnormal blood glucose metabolism are still lacking. This is the first large-scale retrospective trial of abnormal blood glucose metabolism in China, including high blood glucose group and normal blood glucose group. The clinical evidence of the effect of WMT on blood glucose metabolism has been established, which lays the foundation for subsequent studies on the effects of gut microbiota (53), metabolic markers (54), and diet (55) regulation on abnormal blood glucose metabolism. Taken together, these results suggest that restoring gut microbiota may serve as a promising treatment for abnormal blood glucose metabolism; however, the mechanism of action requires further investigation.

This study has several limitations. First, this study mainly focused on the analysis of clinical blood glucose metabolism, blood lipid metabolism, and liver function, etc. The gut microbiota metagenomics and metabolomics before and after WMT have not been evaluated. Therefore, the lowering effect of WMT on blood glucose and related microbiota is unclear. Second, the impact of patient compliance. A small number of patients did not undergo long term treatment after short and medium term treatment, and returned to the hospital at short or long intervals for evaluation of the long term benefit of WMT treatment. Therefore, more data are needed to confirm the long term efficacy of WMT in the treatment of abnormal blood glucose metabolism. Third, we did not consider potential confounding factors between the main symptoms of WMT treatment and glycemia. Although data show that WMT can improve abnormal blood glucose metabolism in the short and medium term, we need large-scale prospective studies to further validate our conclusions.In the future, we plan to conduct a large-sample prospective study to verify the effect of WMT on blood glucose metabolism.

Conclusion

WMT has a significant effect of improving blood glucose, and at the same time, it has a significant effect on reducing blood lipid and blood pressure in patients with high blood glucose. WMT reduces the short- and medium-term risk of ASCVD without increasing the long term risk of ASCVD. Therefore, the regulation of gut microbiota by WMT may provide a new clinical approach for the treatment of abnormal blood glucose metabolism.

Data availability statement

The original contributions presented in the study are included in the article/supplementary material. Further inquiries can be directed to the corresponding authors.

Ethics statement

The studies involving human participants were reviewed and approved by the Ethics Committee (No. 2017-98) in accordance with the Declaration of Helsinki at the First Affiliated Hospital of Guangdong Pharmaceutical University, Guangzhou, China. The patients/participants provided their written informed consent to participate in this study.

Author contributions

X-XH, Q-PW, and LW designed the concept of the study. M-QL, Y-TX, X-JL, QZ, W-YL, and J-TX collected and analyzed the data. TL and W-YL were the statistics consultant, QZ was the consultant for endocrinology. LW wrote the draft manuscript. All authors contributed to the article and approved the submitted version.

Funding

This study was supported by the Key Technologies R&D Program of Guangdong Province (2022B1111070006), the Natural Science Foundation of Guangdong Province (2019A1515010125), and the Department of Education of Guangdong Province (2021KCXTD025).

Acknowledgments

We sincerely thank all patients in the study and all funding agencies that supported the study.

Conflict of interest

The authors declare that the research was conducted in the absence of any commercial or financial relationships that could be construed as a potential conflict of interest.

Publisher's note

References

1. Lin X, Xu Y, Pan X, Xu J, Ding Y, Sun X, et al. Global, regional, and national burden and trend of diabetes in 195 countries and territories: An analysis from 1990 to 2025. *Sci Rep* (2020) 10(1):14790. doi: 10.1038/s41598-020-71908-9

2. Dwyer-Lindgren L, Mackenbach JP, van Lenthe FJ, Flaxman AD, Mokdad AH. Diagnosed and undiagnosed diabetes prevalence by county in the U.S., 1999–2012. *Diabetes Care* (2016) 39(9):1556–62. doi: 10.2337/dc16-0678

3. Cho NH, Shaw JE, Karuranga S, Huang Y, da Rocha Fernandes JD, Ohlrogge AW, et al. IDF diabetes atlas: Global estimates of diabetes prevalence for 2017 and projections for 2045. *Diabetes Res Clin Pract* (2018) 138:271–81. doi: 10.1016/j.diabres.2018.02.023

4. Diabetes Society of Chinese Medical Association. Guideline for the prevention and treatment of type 2 diabetes mellitus in China (2020 edition) (Part 1). *Chin J of Pract Intern Med* (2021) 41(8):668–95. doi: 10.19538/j.nk2021080106

5. Wang L, Gao P, Zhang M, Huang Z, Zhang D, Deng Q, et al. Prevalence and ethnic pattern of diabetes and prediabetes in China in 2013. *JAMA* (2017) 317 (24):2515–23. doi: 10.1001/jama.2017.7596

6. Jia W, Weng J, Zhu D, Ji L, Lu J, Zhou Z, et al. Society: Standards of medical care for type 2 diabetes in China 2019. *Diabetes/Metabolism Res Rev* (2019) 35(6): e3158. doi: 10.1002/dmrr.3158

7. The L. Diabetes: a dynamic disease. *Lancet* (2017) 389(10085):2163. doi: 10.1016/S0140-6736(17)31537-4

8. Saeedi P, Salpea P, Karuranga S, Petersohn I, Malanda B, Gregg EW, et al. Mortality attributable to diabetes in 20–79 years old adults, 2019 estimates: Results from the international diabetes federation diabetes atlas, 9th edition. *Diabetes Res Clin Pract* (2020) 162:108086. doi: 10.1016/j.diabres.2020.108086

9. Krentz AJ, Patel MB, Bailey CJ. New drugs for type 2 diabetes mellitus. *Drugs* (2008) 68(15):2131–62. doi: 10.2165/00003495-200868150-00005

10. Cani PD. Human gut microbiome: hopes, threats and promises. *Gut* (2018) 67(9):1716. doi: 10.1136/gutjnl-2018-316723

11. Clemente JC, Ursell LK, Parfrey LW, Knight R. The impact of the gut microbiota on human health: An integrative view. *Cell* (2012) 148(6):1258–70. doi: 10.1016/j.cell.2012.01.035

12. Sedighi M, Razavi S, Navab-Moghadam F, Khamseh ME, Alaei-Shahmiri F, Mehrtash A, et al. Comparison of gut microbiota in adult patients with type 2 diabetes and healthy individuals. *Microb. Pathog.* (2017) 111:362–9. doi: 10.1016/j.micpath.2017.08.038

13. Pedersen HK, Gudmundsdottir V, Nielsen HB, Hyotylainen T, Nielsen T, Jensen BAH, et al. Human gut microbes impact host serum metabolome and insulin sensitivity. *Nature* (2016) 535(7612):376–81. doi: 10.1038/nature18646

14. Zhao L, Zhang F, Ding X, Wu G, Lam Yan Y, Wang X, et al. Gut bacteria selectively promoted by dietary fibers alleviate type 2 diabetes. *Science* (2018) 359 (6380):1151–6. doi: 10.1126/science.aao5774

15. Fei N, Zhao L. An opportunistic pathogen isolated from the gut of an obese human causes obesity in germfree mice. *ISME J* (2013) 7(4):880–4. doi: 10.1038/ismej.2012.153

16. Zhang C, Yin A, Li H, Wang R, Wu G, Shen J, et al. Dietary modulation of gut microbiota contributes to alleviation of both genetic and simple obesity in children. *EBioMedicine* (2015) 2(8):968–84. doi: 10.1016/j.ebiom.2015.07.007

17. Wang H, Lu Y, Yan Y, Tian S, Zheng D, Leng D, et al. Promising treatment for type 2 diabetes: Fecal microbiota transplantation reverses insulin resistance and impaired islets. *Front Cell Infect Microbiol* (2020) 9:455. doi: 10.3389/fcimb.2019.00455

18. Bafeta A, Yavchitz A, Riveros C, Batista R, Ravaud P. Methods and reporting studies assessing fecal microbiota transplantation. *Ann Internal Med* (2017) 167 (1):34–9. doi: 10.7326/M16-2810

19. de Groot P, Scheithauer T, Bakker GJ, Prodan A, Levin E, Khan MT, et al. Donor metabolic characteristics drive effects of faecal microbiota transplantation on recipient insulin sensitivity, energy expenditure and intestinal transit time. *Gut* (2020) 69(3):502. doi: 10.1136/gutjnl-2019-318320

20. Qazi T, Amaratunga T, Barnes EL, Fischer M, Kassam Z, Allegretti JR. The risk of inflammatory bowel disease flares after fecal microbiota transplantation: Systematic review and meta-analysis. *Gut Microbes* (2017) 8(6):574–88. doi: 10.1080/19490976.2017.1353848

21. Allegretti JR, Kassam Z, Mullish BH, Chiang A, Carrellas M, Hurtado J, et al. Effects of fecal microbiota transplantation with oral capsules in obese patients. *Clin Gastroenterol Hepatol* (2020) 18(4):855–63. doi: 10.1016/j.cgh.2019.07.006

22. Kootte RS, Levin E, Salojärvi J, Smits LP, Hartstra AV, Udayappan SD, et al. Improvement of insulin sensitivity after lean donor feces in metabolic syndrome is driven by baseline intestinal microbiota composition. *Cell Metab* (2017) 26(4):611–619.e6. doi: 10.1016/j.cmet.2017.09.008

23. Cruz-Aguliar RM, Wantia N, Clavel T, Vehreschild MJGT, Buch T, Bajbouj M, et al. An open-labeled study on fecal microbiota transfer in irritable bowel syndrome patients reveals improvement in abdominal pain associated with the relative abundance of akkermansia muciniphila. *Digestion* (2019) 100(2):127–38. doi: 10.1159/000494252

24. Pamer EG. Fecal microbiota transplantation: Effectiveness, complexities, and lingering concerns. *Mucosal Immunol* (2014) 7(2):210–4. doi: 10.1038/mi.2013.117

25. Zhang T, Lu G, Zhao Z, Liu Y, Shen Q, Li P, et al. Washed microbiota transplantation vs. manual fecal microbiota transplantation: Clinical findings, animal studies and *in vitro* screening. *Protein Cell* (2020) 11(4):251–66. doi: 10.1007/s13238-019-00684-8

26. Zhang F. Fecal microbiota transplantation-standardization study: Nanjing consensus on methodology of washed microbiota transplantation. *Chin Med J* (2020) 133(19):2330–2. doi: 10.1097/CM9.0000000000000954

27. Mullish BH, Quraishi MN, Segal JP, McCune VL, Baxter M, Marsden GL, et al. The use of fecal microbiota transplant as treatment for recurrent or refractory clostridium difficile infection and other potential indications: Joint British society of gastroenterology (BSG) and healthcare infection society (HIS) guidelines. *Gut* (2018) 67(11):1920. doi: 10.1136/gutjnl-2018-316818

28. Matthews DR, Hosker JP, Rudenski AS, Naylor BA, Treacher DF, Turner RC. Homeostasis model assessment: Insulin resistance and β-cell function from fasting plasma glucose and insulin concentrations in man. *Diabetologia* (1985) 28 (7):412–9. doi: 10.1007/BF00280883

29. Williams B, Mancia G, Spiering W, Agabiti Rosei E, Azizi M, Burnier M, et al. Practice guidelines for the management of arterial hypertension of the European society of cardiology and the European society of hypertension: ESC/ESH task force for the management of arterial hypertension. *J Hypertens.* (2018) 36 (12):314–40. doi: 10.1080/08037051.2018.1527177

30. Chinese Cardiovascular Disease Prevention Guidelines (2017) Writing Group, Editorial Board of Chinese Journal of Cardiovascular Diseases. Chinese Guidelines for the prevention of cardiovascular diseases. *Chin J Cardiol* (2018) 46 (1):10–25. doi: 10.3760/cma.j.issn.0253-3758.2018.01.004

31. Chinese Medical Association General Practice Branch. Guideline for primary care of obesity: Practice version (2019). *Chin J Gen Pract* (2020) 19 (2):102–7. doi: 10.3760/cma.j.issn.1671-7368.2020.02.003

32. Nie Q, Chen H, Hu J, Fan S, Nie S. Dietary compounds and traditional Chinese medicine ameliorate type 2 diabetes by modulating gut microbiota. *Crit Rev Food Sci Nutr* (2019) 59(6):848–63. doi: 10.1080/10408398.2018.1536646

33. Saad MJA, Santos A, Prada PO. Linking gut microbiota and inflammation to obesity and insulin resistance. *Physiology* (2016) 31(4):283–93. doi: 10.1152/physiol.00041.2015

34. Qin J, Li Y, Cai Z, Li S, Zhu J, Zhang F, et al. A metagenome-wide association study of gut microbiota in type 2 diabetes. *Nature* (2012) 490 (7418):55–60. doi: 10.1038/nature11450

35. Salek RM, Maguire ML, Bentley E, Rubtsov DV, Hough T, Cheeseman M, et al. A metabolomic comparison of urinary changes in type 2 diabetes in mouse, rat, and human. *Physiol Genomics* (2007) 29(2):99–108. doi: 10.1152/physiolgenomics.00194.2006

36. Shen T-CD, Albenberg L, Bittinger K, Chehoud C, Chen Y-Y, Judge CA, et al. Engineering the gut microbiota to treat hyperammonemia. *J Clin Invest* (2015) 125(7):2841–50. doi: 10.1172/JCI79214

37. Lee P, Yacyshyn BR, Yacyshyn MB. Gut microbiota and obesity: An opportunity to alter obesity through faecal microbiota transplant (FMT). *Diabetes Obes Metab* (2019) 21(3):479–90. doi: 10.1111/dom.13561

38. Cammarota G, Ianiro G, Tilg H, Rajilić-Stojanović M, Kump P, Satokari R, et al. European Consensus conference on faecal microbiota transplantation in clinical practice. *Gut* (2017) 66(4):569. doi: 10.1136/gutjnl-2016-313017

39. Meslier V, Laiola M, Roager HM, De Filippis F, Roume H, Quinquis B, et al. Mediterranean Diet intervention in overweight and obese subjects lowers plasma cholesterol and causes changes in the gut microbiome and metabolome independently of energy intake. *Gut* (2020) 69(7):1258. doi: 10.1136/gutjnl-2019-320438

40. Rinott E, Youngster I, Yaskolka Meir A, Tsaban G, Zelicha H, Kaplan A, et al. Effects of diet-modulated autologous fecal microbiota transplantation on weight regain. *Gastroenterology* (2021) 160(1):158–173.e10. doi: 10.1053/j.gastro.2020.08.041

41. Yu EW, Gao L, Stastka P, Cheney MC, Mahabamunuge J, Soto MT, et al. Fecal microbiota transplantation for the improvement of metabolism in obesity: The FMT-TRIM double-blind placebo-controlled pilot trial. *PloS Med* (2020) 17 (3):e1003051. doi: 10.1371/journal.pmed.1003051

42. de Groot PF, Frissen MN, de Clercq NC, Nieuwdorp M. Fecal microbiota transplantation in metabolic syndrome: History, present and future. *Gut Microbes* (2017) 8(3):253–67. doi: 10.1080/19490976.2017.1293224

43. Aron-Wisnewsky J, Clément K, Nieuwdorp M. Fecal microbiota transplantation: A future therapeutic option for Obesity/Diabetes? *Curr Diabetes Rep* (2019) 19(8):51. doi: 10.1007/s11892-019-1180-z

44. Vrieze A, Van Nood E, Holleman F, Salojärvi J, Kootte RS, Bartelsman JFWM, et al. Transfer of intestinal microbiota from lean donors increases insulin sensitivity in individuals with metabolic syndrome. *Gastroenterology* (2012) 143 (4):913–916.e7. doi: 10.1053/j.gastro.2012.06.031

45. Burrello C, Garavaglia F, Cribiù FM, Ercoli G, Lopez G, Troisi J, et al. Therapeutic faecal microbiota transplantation controls intestinal inflammation through IL10 secretion by immune cells. *Nat Commun* (2018) 9(1):5184. doi: 10.1038/s41467-018-07359-8

46. Ganesan K, Chung SK, Vanamala J, Xu B. Causal relationship between diet-induced gut microbiota changes and diabetes: A novel strategy to transplant faecalibacterium prausnitzii in preventing diabetes. *Int J Mol Sci* (2018) 19 (12):3720. doi: 10.3390/ijms19123720

47. Park J, Decker JT, Smith DR, Cummings BJ, Anderson AJ, Shea LD. Reducing inflammation through delivery of lentivirus encoding for anti-inflammatory cytokines attenuates neuropathic pain after spinal cord injury. *J Controlled Release* (2018) 290:88–101. doi: 10.1016/j.jconrel.2018.10.003

48. Liang F, Lu X, Deng Z, Zhong HJ, Zhang W, Li Q, et al. Effect of washed microbiota transplantation on patients with dyslipidemia in south China. *Front Endocrinol* (2022) 13:827107. doi: 10.3389/fendo.2022.827107

49. Zhong HJ, Zeng HL, Cai YL, Zhuang Y-P, Liou YL, Wu Q, et al. Washed microbiota transplantation lowers blood pressure in patients with hypertension. *Front Cell Infect Microbiol* (2021) 11:679624. doi: 10.3389/fcimb.2021.679624

50. Pan ZY, Zhong HJ, Huang DN, Wu LH, He XX. Beneficial effects of repeated washed microbiota transplantation in children with autism. *Front Pediatr* (2022) 10:928785. doi: 10.3389/fped.2022.928785

51. Leshem A, Horesh N, Elinav E. Fecal microbial transplantation and its potential application in cardiometabolic syndrome. *Front Immunol* (2019) 10:1341. doi: 10.3389/fimmu.2019.01341

52. Wang SA, Xu MQ, Wang WQ, Cao XC, Piao MY, Khan S, et al. Systematic review: Adverse events of fecal microbiota transplantation. *PloS One* (2016) 11(8): e0161174. doi: 10.1371/journal.pone.0161174

53. Wu L, Xie X, Li Y, Liang T, Zhong H, Ma J, et al. Metagenomics-based analysis of the age-related cumulative effect of antibiotic resistance genes in gut microbiota. *Antibiotics* (2021) 10(8):1006. doi: 10.3390/antibiotics10081006

54. Wu L, Xie X, Liang T, Ma J, Yang L, Yang J, et al. Integrated multi-omics for novel aging biomarkers and antiaging targets. *Biomolecules* (2022) 12(1):39. doi: 10.3390/biom12010039

55. Liang T, Wu L, Xi Y, Li Y, Xie X, Fan C, et al. Probiotics supplementation improves hyperglycemia, hypercholesterolemia, and hypertension in type 2 diabetes mellitus: An update of meta-analysis. *Crit Rev Food Sci Nutr* (2021) 61 (10):1670–88. doi: 10.1080/10408398.2020.1764488

frontiers | Frontiers in Endocrinology

TYPE Original Research
PUBLISHED 07 October 2022
DOI 10.3389/fendo.2022.987081

OPEN ACCESS

EDITED BY
Si Jin,
Huazhong University of Science and Technology, China

REVIEWED BY
Yi Ma,
Peking University Third Hospital, China
Jizhong Shen,
Nanjing Drum Tower Hospital, China

*CORRESPONDENCE
Zhigang Zhao
zzgttyy@163.com

†These authors have contributed equally to this work

SPECIALTY SECTION
This article was submitted to Cellular Endocrinology, a section of the journal Frontiers in Endocrinology

RECEIVED 05 July 2022
ACCEPTED 21 September 2022
PUBLISHED 07 October 2022

CITATION
Li C, Guo S, Huo J, Gao Y, Yan Y and Zhao Z (2022) Real-world national trends and socio-economic factors preference of sodium-glucose cotransporter-2 inhibitors and glucagon-like peptide-1 receptor agonists in China.
Front. Endocrinol. 13:987081.
doi: 10.3389/fendo.2022.987081

Real-world national trends and socio-economic factors preference of sodium-glucose cotransporter-2 inhibitors and glucagon-like peptide-1 receptor agonists in China

Cao Li[1†], Shanshan Guo[1†], Jiping Huo[1], Yiming Gao[1,2], Yilong Yan[1,2] and Zhigang Zhao[1*]

[1]Department of Pharmacy, Beijing Tiantan Hospital, Capital Medical University, Beijing, China, [2]Department of Clinical Pharmacology, School of Pharmaceutical Sciences, Capital Medical University, Beijing, China

Backgrounds: Robust evidence have demonstrated the beneficial effect of Sodium-glucose cotransporter-2 inhibitors (SGLT2i) and glucagon-like peptide-1 receptor agonists (GLP-1RA) in T2D patients with cardiovascular diseases and chronic kidney disease. Multiple studies analyzed patterns and predictors of SGLT2i and GLP-1RA in the US, Europe and worldwide. However, there is no study about the utilization of these two classes of drugs in real-world in China.

Method: A total of 181743 prescriptions of SGLT2i and 59720 GLP-1RA were retrospectively pooled from Hospital Prescription Analysis Cooperation Project from 2018 to 2021. The social-economic characteristics of patients and prescribers, including age, gender, residency, hospital level, insurance type, department visited, and payment amount, were collected and analyzed to study trends and risk factors associated with preference among two antidiabetics.

Results: Annual number of prescriptions of SGLT2i significantly increased to approximately 140 folds, while GLP-1RA increased to about 6.5 folds. After adjustment for socio-economic information, several patients or physician characteristics were positively associated with the preference of GLP-1RA, including female gender (OR 1.581, 95% CI 1.528-1.635), residents in second-tier cities (OR 1.194, 95% CI 1.148-1.142), visiting primary or secondary hospital level (OR 2.387, 95% CI 2.268-2.512); while other factors were associated with the preference of SGLT2i, including older adults (OR 0.713, 95% CI 0.688-0.739), uncovered by insurance (OR 0.310, 95% CI 0.293-0.329), visiting other departments compared with endocrinology. In addition, the share of SGLT2i and GLP-1RA was low but in an increasing tendency.

Conclusions: SGLT2i and GLP-1RA prescription significantly increased from 2018 to 2021. The socio-economic risk factors in choosing SGLT2i or GLP-1RA highlight an effort required to reduce disparities and improve health outcomes.

KEYWORDS

SGLT2i, GLP-1RA, type 2 diabetics, cardiovascular diseases, chronic kidney disease

Introduction

With the development of economy and the growth of urbanization, the global prevalence of diabetes was approximately 10.5% in 2021 and is estimated to rise to 12.2% in 2045, resulting in serious health consequences and socio-economic problems (1). Patients with type 2 diabetes (T2D) are at elevated risk of cardiovascular disease (CVD) and chronic kidney diseases (CKD), which are the leading cause of morbidity and mortality (2). Recently several randomized controlled trials have demonstrated that two classes of glucose-lowering medications, glucagon-like peptide-1 receptor agonists (GLP-1RA) and sodium-glucose cotransporter-2 inhibitors (SGLT2i), have shown a significant protective effect on CVD or CKD in T2D patients (3–5). In addition, guidelines of the European Association for the Study of Diabetes (EASD) and the American Diabetes Association (ADA) have updated the major role of both SGLT2i and GLP-1RA in the management of T2D patients with reno- or cardio- complications (6).

As the approval of new classes of medications, pharmacotherapy of T2D has changed remarkably over the past 2 decades. For instance, monotherapy of GLP-1RA and SGLT2i increased to approximately 2-3 folds from 2015 to 2019 in the United States (7). A similar substantially increasing of these two medications was found in Europe, and the change even occurred before the published guidelines (8, 9). Although the new agent SGLT2i and GLP-1RA were already widely used globally, large country differences still exist due to the characteristics of patients and the capacity of financial systems (10).

In China, the prevalence of diabetic adults was estimated as 12.4% and higher than the global average (8.3%) (11). Importantly, the prevalence of adequate management was not significantly improved. The first GLP-1RA and SGLT2i were incorporated into the national medical insurance reimbursement list in late 2017 and 2020, respectively. To the best of our knowledge, large-scale study of these two classes of antidiabetics was not reported yet in China. Thus, the present study aims (1) to study prescription trends of GLP-1RA and SGLT2i; (2) to characterize socio-economic factors associated with the selection of these two classes of drugs from 2018 to 2021 in real-world.

Methods

Data sources

This study was designed as a retrospective cross-sectional study based on prescription data. Prescriptions were extracted from the Cooperation Project Database of Hospital Prescriptions (CPDHP), which has been extensively used for pharmacoepidemiology studies in China (12, 13). The CPDHP is a multi-institutional database consisting of prescription information obtained from 102 hospitals in 9 cities or provinces, including Shanghai, Hangzhou, Beijing, Tianjin, Shenyang, Zhengzhou, Harbin, Chengdu, and Guangzhou. A random sample of 10-day prescriptions in the above hospitals is selected quarterly each year, containing two non-consecutive Mondays to Fridays (except national holidays). Information in prescriptions were collected and unified in same format, including the sample city/province, patient number, gender, age, department, visit time, insurance type, generic drug name, hospital level, and payment amount. Furthermore, the personal information of patients and clinicians were masked in this project. The present study was approved by the ethics committee at Beijing Tiantan Hospital, Capital Medical University.

Study sample

In the present study, outpatient prescriptions that met the following criteria were included: (1) prescribed for patients aged over 18 years; (2) containing at least one SGLT2i or GLP-1RA; and (3) prescribed between 2018 and 2021. However, the prescriptions with missing age or sex were excluded.

Drug classes

Antidiabetics in this study were coded according to the World Health Organization Anatomical Therapeutic Chemical classification system, which were divided into two categories: (1) A10BJ, GLP-1RA: Exenatide, Liraglutide, Lixisenatide,

Dulaglutide, Semaglutide, Beinaglutide, and Loxenatide; (2) A10BK, SGLT2i: Dapagliflozin, Canagliflozin, Empagliflozin, and Ertugliflozin; this study only focuses on these two classes of antidiabetic agents.

Statistical analysis

Relative numbers of medications per year were calculated with the number of annual total prescriptions. Data were presented as means ± SD for continuous variables or as frequency (%) for categorical variables. Baseline characteristics between SGLT2i and GLP-1RA groups were analyzed using $\chi 2$ tests. A logistic regression model was performed to analyze patient and prescriber socio-economic characteristics to analyze preference of SGLT2i or GLP-1RA. All data were conducted and analyzed using Microsoft Excel and IBM SPSS Statistics (version 26; IBM Corporation, USA).

Results

Overall trends in utilization of SGLT2i and GLP-1RA

A total of 181743 prescriptions of SGLT2i and 59720 GLP-1RA were pooled from the outpatient of CPDHP database (Table 1). The annual number of prescriptions of SGLT2i dramatically increased to approximately 140 folds, while GLP-1RA increased to about 6.5 folds, from 2018 to 2021 (Figure 1; Table 1). With respect to the total annual medication expenditure of these two classes of antidiabetics, it showed a similar tendency with growth to 44 and 6.8 folds, respectively. In addition, the trends of gender and age in drug utilization were also analyzed. The proportion of females using SGLT2i decreased considerably from 45.5% in 2018 to 39.6% in 2021, while the use of GLP-1RA was steady (Figure 2A; Supplementary Tables S1, S2). The proportion of SGLT2i and GLP-1RA used in subjects aged 18-64 both decreased in the study period, from 76.0% to 58.7% and from 76.5% to 71.3% (Figure 2B; Supplementary Tables S1, S2).

Characteristics of study population using SGLT2i and GLP-1RA

Characteristics of subjects who used SGLT2i or GLP-1RA from 2018 to 2021 are presented in Table 1. The female gender was more likely to be prescribed GLP-1RA (48.1 vs 40.1%, $p = 0.001$) than SGLT2i. Subjects treated with SGLT2i were significantly older than those treated with GLP-1RA in both groups aged ≥65 and 18-64 (Table 1). The majority of patients are residents in robust economic first-tier cities of Beijing, Shanghai, and Guangzhou (Tables 1; Supplementary Tables S3, S4). Most SGLT2i (91.2%) and GLP-1RA (89.6%) were provided by tertiary hospitals other than primary or secondary ones. In terms of department/clinician visited, most patients received prescription from endocrinologists, cardiologists, nephrologists, general partitioners/internal medical (GP/IM) physicians (SGLT2i, 65.5%, 10.7%, 3.3%, 11.4%; GLP-1RA, 85.2%, 2.4%, 0.7%, 4.8%), respectively. In addition, approximately three-quarters population were covered by full or partial insurance, although some insurance information was missing.

Associated factors of selection on SGLT2i or GLP-1RA

To better understand associated socio-economic factors in choosing SGLT2i or GLP-1RA, the logistic regression model was used to determine the probable predictors (Table 2). Using

Table 1 Baseline characteristics of the study sample.

Characteristic	SGLT2i	GLP-1RA	P-value
Total	181743 (100)	59720 (100)	
Gender			0.001
Male	108893 (59.9)	30988 (51.9)	
Female	72850 (40.1)	28732 (48.1)	
Age (mean, SD)			0.001
18-64	52.5 (9.2)	48.3 (11.1)	
≥65	72.8 (6.6)	72.1 (6.4)	
Year			<0.001
2018	899 (0.5)	4539 (7.6)	
2019	4597 (2.5)	11271 (18.9)	
2020	51035 (28.1)	14157 (23.7)	
2021	125212 (68.9)	29753 (49.8)	
City Type			<0.001
First -tier	126467 (69.6)	38057 (63.7)	
Other	55276 (30.4)	21663 (36.3)	
Hospital Level			<0.001
Tertiary hospitals	165680 (91.2)	53503 (89.6)	
Primary or secondary	16063 (8.2)	6217 (10.4)	
Insurance Type			<0.001
Full or partial	133512 (73.5)	46249 (77.5)	
Self-pay	31830 (17.5)	6516 (10.9)	
Unknown	16401 (9.0)	6935 (11.6)	
Department Visited			<0.001
Endocrinology	119071 (65.5)	50867 (85.2)	
Cardiology	19452 (10.7)	1437 (2.4)	
Nephrology	5907 (3.3)	428 (0.7)	
GP/IM	20650 (11.4)	2890 (4.8)	
Others	16663 (9.2)	4098 (6.9)	
Payment (mean, SD)	157.2 (106.7)	690.0 (488.8)	<0.001

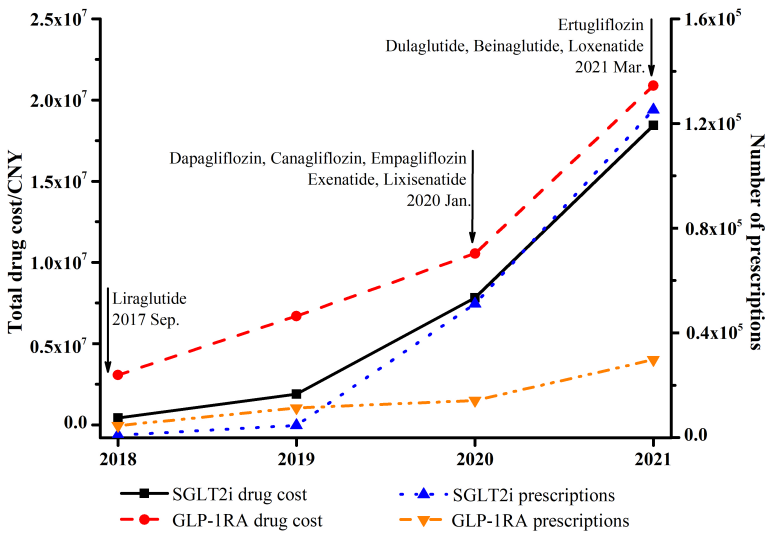

FIGURE 1
Total trends of expenditure and prescriptions of SGLT2i and GLP-1RA from 2018 to 2021.

adults aged from 18-64 as a reference, the odds ratio for SGLT2i (OR 0.713, 95% CI 0.688-0.739) increased along with age compared with GLP-1RA. The probability of using SGLT2i was lower in female (OR 1.581, 95% CI 1.528-1.635) gender than in male. Among the study periods, we found less use of GLP-1RA in 2019 (OR 0.618, 95% CI 0.561-0.681), 2020 (OR 0.451, 95% CI 0.410-0.495), and 2021 (OR 0.474, 95% CI 0.432-0.519) compared with 2018. In addition, self-pay patients had a significantly lower prevalence of using GLP-1RA (OR 0.310, 95% CI 0.293-0.329); in contrast, patients visiting primary or secondary hospitals (OR 2.387, 95% CI 2.268-2.512) had a significantly higher chance of receiving GLP-1RA.

Compared with endocrinologists, all other specialties including in cardiology (OR 0.109, 95% CI 0.099-0.120), nephrology (OR 0.306, 95% CI 0.261-0.358), GP/IM (OR 0.146, 95% CI 0.133-0.155) had a lower preference prescribing GLP-1RA to patients (Table 2). Worthy mentioning, although the proportion of two classes of drugs was low in the department of cardiology and nephrology, it showed an overall increasing tendency with SGLT2i (nephrology, 0.7% to 3.4%) and GLP-1RA from 2018 to 2021 (nephrology, 0.5% to 0.7%; cardiology, 0.7% to 3.2%), except stable tendency of SGLT2i in cardiology (10.8% to 11.0%, Figure 3; Supplementary Tables S1, S2).

Discussion

To the best of our knowledge, this is the first nationwide representative retrospective analysis of new cardio-reno beneficial antidiabetics in the real-world in mainland China. Our study comprehensively showed that (1) a substantial increase in the utilization of SGLT2i (140 folds) and GLP-1RA (6.5 folds) from 2018 to 2021 (Figure 1; Table 1); (2) various pharmacoeconomic and prescriber characteristics associated with the preference of SGLT2i or GLP-1RA: male, and self-pay patients are more likely to be treated with SGLT2i; while healthcare clinicians in primary or secondary hospitals, younger adults, endocrinologists prefer to prescribe GLP-1RA over SGLT2i (Table 2); (3) absolute number of prescriptions and proportion of new antidiabetics showed an overall increasing trend in the department of cardiology and nephrology (Figure 3; Supplementary Tables S1, S2).

A significant growth in the utilization and drug expenditure of SGLT2i and GLP-1RA was found in the 4-year study period. First of all, the decision of the National Medical Products Administration (NMPA) and the National Healthcare Security Administration (NHSA) had a substantial influence on the medication trends (Figure 1). After new antidiabetics GLP-1RA and SGLT2i were approved by NMPA, the first GLP-1RA (2017 Sep.) and SGLT2i (2020 Jan.) were reimbursed by national insurance lists in China. The overall trend is similar compared to the US (14), Europe (9), and other countries or continents worldwide (10) in previous studies. However, there were still some differences between China and US. For instance, increasing utilization of GLP-1RA was steeper and dramatic in China from 2018 (2nd year covered by national insurance) to 2021, compared with 2008 (2nd year included in Medicare) to 2011 (15, 16), this might be due to GLP-1RA was confirmed beneficial to CVDs patients was progressively proved in 2015 (17, 18). Second, all authoritative western and China guidelines (19–22)

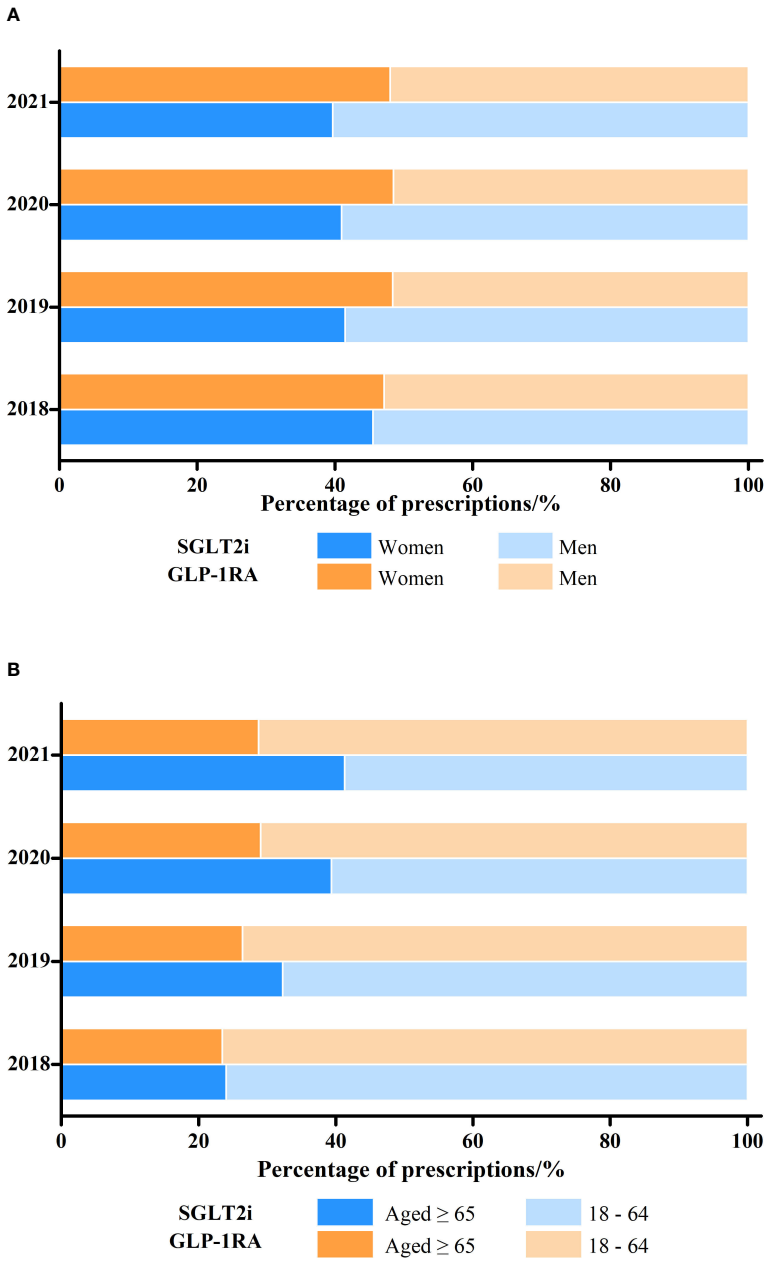

FIGURE 2
Changes in the proportion of SGLT2i and GLP-1RA prescriptions dispensed by **(A)** patient gender and **(B)** age, 2018-2021.

have strongly recommended the application of SGLT2i and GLP-1RA in diabetic patients with CVD complications. As heart failure indication of SGLT2i approved in 2022, presumable indication expansion of GLP-1RA, a predicable major increasing share of new antidiabetics and structure change of antihyperglycemic medication may take place in following years.

Our study revealed gender and age differences in the selection of new antidiabetics. The present study indicates that the female gender was more likely to be treated with GLP-1RA, and a prior study suggested that female patients had a higher chance of receiving GLP-1RA (23). The potential mechanism could be the utilization of GLP-1RA in gestational diabetes mellitus, a disease only harms women. Studies have indicated a potential beneficial

Table 2 The social-economic factors associated with selection of SGLT2i or GLP-1RA.

Characteristic	OR	95% CI	*P*
Gender			
Female	1.581	1.528-1.635	< 0.001
Age			
≥65	0.713	0.688-0.739	< 0.001
Year			
2018	ref		
2019	0.618	0.561-0.681	< 0.001
2020	0.451	0.410-0.495	< 0.001
2021	0.474	0.432-0.519	< 0.001
City Type			
First -tier	ref		
Other	1.194	1.148-1.242	< 0.001
Hospital Level			
Tertiary hospitals	ref		
Primary or secondary	2.387	2.268-2.512	< 0.001
Insurance Type			
Full or partial	ref		
Self-pay	0.310	0.293-0.329	< 0.001
Unknown	0.505	0.476-0.537	< 0.001
Department Visited			
Endocrinology	ref		
Cardiology	0.109	0.099-0.120	< 0.001
Nephrology	0.306	0.261-0.358	< 0.001
GP/IM	0.146	0.133-0.155	< 0.001
Others	0.612	0.575-0.651	< 0.001
Payment Amount	1.015	1.015-1.016	< 0.001

"ref" is abbreviated for reference.

effect of GLP-1RA on the female with different stages of gestational diabetes mellitus (24–26). In addition, polycystic ovary syndrome (PCOS), a common disease affecting up to 20% of women of reproductive age, was shown to be alternatively alleviated by GLP-1RA with clinical evidence (15, 27–29). Physiologically, GLP-1RA modulates mammalian hypothalamus, pituitary, gonads, ovaries, and has an anti-inflammatory and anti-fibrotic function. In the aspect of age, older adults had a higher chance of being prescribed SGLT2i. Clinical guidelines for elderly T2D in China recommend an escalation therapy for pharmacotherapy, and according to guideline for monotherapy of SGLT2i has no risk of hypoglycemia while GLP-1RA does not (30). Generally, older adults are more vulnerable to hypoglycemia, a condition sometimes even life-threatening. In addition, SGLT2i has one more recommendation of treating heart failure compared with GLP-1RA in older adults, and SGLT2i was showed more beneficial in renal outcomes (30, 31).

Economic factors could have a substantial influence on the selection of medications. Our results suggest that subjects without insurance coverage, and visiting tertiary hospitals were more frequently prescribed SGLT2i than GLP-1RA. The average payment of GLP-1RA (690.0 ± 488.8 CNY) was significantly higher than SGLT2i (157.2 ± 106.7 CNY). In the US, the relative high-cost affects that the new antidiabetics are most frequently prescribed to patients with private insurance and least to people with self-pay (32). The hospital level was classified as another economic factor, because the China health insurance system is different from developed western countries. Actually, the floating population, whom originally living in less developed cities or rural areas, leaving their hometown, working or seeking medical services in tertiary hospitals located in large first tier cities, normally has a lower income and more sensitive to drug price; whereas urban-resident patients visiting primary or secondary may have a better income status and financial affordability. Thus, the patient in different-tier cities might reflects the financial conditions. To be mentioned, although T2D prevalence was higher in urban cities, patients living in rural areas had excess mortality (33, 34). Higher costs might be barriers to dispensing new classes of antidiabetics for vulnerable patients, which might further lead to medical inequality (35, 36).

Clinicians in different departments play an important role in the selection of new hyperglycemia medications. Similar with prior studies (14, 37), our study suggests that cardiologists or nephrologists prefer prescribing SGLT2i over GLP-1RA compared to endocrinologists (Table 2). According to EASD/ADA guideline (38), SGLT2i is preferably recommended for reducing HF and/or CKD progression in cardiovascular outcomes trials (CVOTs), which could be the potential reason for more favorable in the department of cardiology and nephrology. As GLP-1RA was recently approved for treating obesity and evidences showed an effect of losing weight, overweight or obesity patients may visit department of endocrinology, and then treated by GLP-1RA. The substantial growth of SGLT2i and GLP-1RA was observed similarly in our study and US (37, 39); however, most prescriptions were dispensed in the department of endocrinology in China, but primary care/internal medicine physicians in the US. In addition, although robust evidence and guidelines have recommended new antidiabetics, patients meeting appropriate criteria still were not treated with them. Concerning one-third of T2D patients concomitant with CVD (40, 41) and almost 40% concomitant with CKD (16), the low prevalence of SGLT2i and GLP-1RA in endocrinology and nephrology makes them important candidates for significant clinical benefits.

In conclusion, the present nationwide real-world study highlights that SGLT2i and GLP-1RA prescription significantly increased from 2018 to 2021, which may contribute to substantial welfare for T2D patients with CVD or CKD. In addition, our results showed some patient socio-economic and prescriber characteristics are associated with the preference of SGLIT2i over GLP-1RA, including male gender, relative older age, patients vising tertiary hospitals, uncovered by insurance and department other than endocrinology, which means there is still a lot of work to reduce disparities, guarantee patient safety and improve health outcomes.

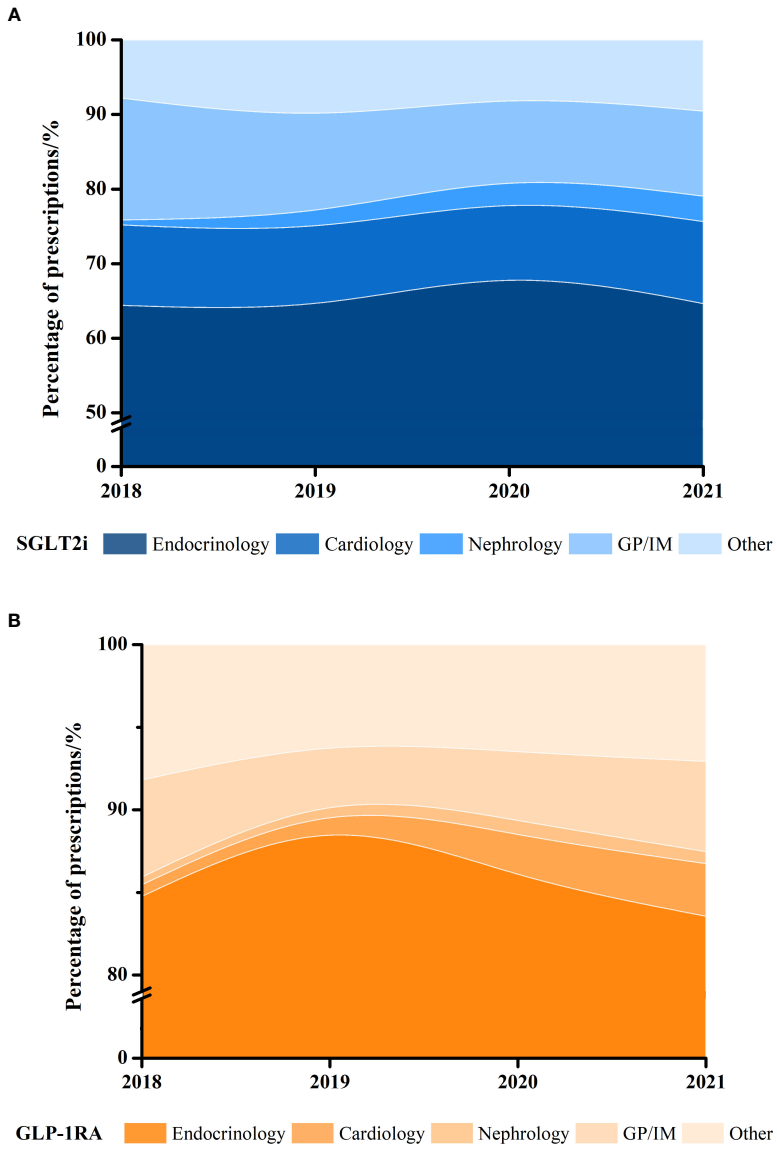

FIGURE 3
Proportion of yearly **(A)** SGLT2i and **(B)** GLP-1RA dispensed prescriptions in different clinical departments, 2018–2021.

Our study had some limitations. First, the present study only analyzed SGLT2i and GLP-1RA, and other information of antidiabetic medications was missing; it is unable to study the overall structure change of diabetic pharmacotherapy. Second, although the present study included a large number of cross-sectional samples, it should be cautious to apply the current conclusion to the general Chinese population, especially in less developed cities and rural areas. Third, since the co-prescribing information of medications and laboratory tests (glucose, HbA1c, *etc.*) was not accessed, it is unable to evaluate and track therapeutic and adverse effects.

Data availability statement

The original contributions presented in the study are included in the article/Supplementary Material. Further inquiries can be directed to the corresponding author.

Ethics statement

The studies involving human participants were reviewed and approved by Beijing Tiantan Hospital, Capital Medical

University. Written informed consent for participation was not required for this study in accordance with the national legislation and the institutional requirements.

Author contributions

CL, SG and ZZ conceived and designed the study. CL and SG wrote the manuscript. CL, SG, JH, YG, YY, and ZZ performed statistics and generated the figures and tables. All authors contributed to the revision of paper. All authors listed have made a direct and substantial contribution to the manuscript, and approved it for publication.

Funding

This work was supported by MiaoPu Project of Beijing Tiantan Hospital (2020MP07); Yangfan Project of Beijing Hospitals Authority (ZYLX201827); the National Key Research and Development Program (2016YFE0205400).

Conflict of interest

The authors declare that the research was conducted in the absence of any commercial or financial relationships that could be construed as a potential conflict of interest.

Publisher's note

Supplementary material

The Supplementary Material for this article can be found online at: https://www.frontiersin.org/articles/10.3389/fendo.2022.987081/full#supplementary-material

References

1. Sun H, Saeedi P, Karuranga S, Pinkepank M, Ogurtsova K, Duncan BB, et al. Idf diabetes atlas: Global, regional and country-level diabetes prevalence estimates for 2021 and projections for 2045. *Diabetes Res Clin Pract* (2022) 183:109119. doi: 10.1016/j.diabres.2021.109119

2. Patorno E, Htoo PT, Glynn RJ, Schneeweiss S, Wexler DJ, Pawar A, et al. Sodium-glucose cotransporter-2 inhibitors versus glucagon-like peptide-1 receptor agonists and the risk for cardiovascular outcomes in routine care patients with diabetes across categories of cardiovascular disease. *Ann Intern Med* (2021) 174 (11):1528–41. doi: 10.7326/M21-0893

3. Zelniker TA, Wiviott SD, Raz I, Im K, Goodrich EL, Bonaca MP, et al. Sglt2 inhibitors for primary and secondary prevention of cardiovascular and renal outcomes in type 2 diabetes: A systematic review and meta-analysis of cardiovascular outcome trials. *Lancet* (2019) 393(10166):31–9. doi: 10.1016/S0140-6736(18)32590-X

4. Kristensen SL, Rorth R, Jhund PS, Docherty KF, Sattar N, Preiss D, et al. Cardiovascular, mortality, and kidney outcomes with glp-1 receptor agonists in patients with type 2 diabetes: A systematic review and meta-analysis of cardiovascular outcome trials. *Lancet Diabetes Endocrinol* (2019) 7(10):776–85. doi: 10.1016/S2213-8587(19)30249-9

5. Neuen BL, Young T, Heerspink HJL, Neal B, Perkovic V, Billot L, et al. Sglt2 inhibitors for the prevention of kidney failure in patients with type 2 diabetes: A systematic review and meta-analysis. *Lancet Diabetes Endocrinol* (2019) 7(11):845–54. doi: 10.1016/S2213-8587(19)30256-6

6. Buse JB, Wexler DJ, Tsapas A, Rossing P, Mingrone G, Mathieu C, et al. 2019 Update to: Management of hyperglycemia in type 2 diabetes, 2018. a consensus report by the American diabetes association (Ada) and the European association for the study of diabetes (Easd). *Diabetes Care* (2020) 43(2):487–93. doi: 10.2337/dci19-0066

7. Heyward J, Christopher J, Sarkar S, Shin JI, Kalyani RR, Alexander GC. Ambulatory noninsulin treatment of type 2 diabetes mellitus in the united states, 2015 to 2019. *Diabetes Obes Metab* (2021) 23(8):1843–50. doi: 10.1111/dom.14408

8. Engler C, Leo M, Pfeifer B, Juchum M, Chen-Koenig D, Poelzl K, et al. Long-term trends in the prescription of antidiabetic drugs: Real-world evidence from the diabetes registry tyrol 2012-2018. *BMJ Open Diabetes Res Care* (2020) 8(1): e001279. doi: 10.1136/bmjdrc-2020-001279

9. Mardetko N, Nabergoj Makovec U, Locatelli I, Janez A, Kos M. Uptake of new antidiabetic medicines in 11 European countries. *BMC Endocr Disord* (2021) 21(1):127. doi: 10.1186/s12902-021-00798-3

10. Arnold SV, Tang F, Cooper A, Chen H, Gomes MB, Rathmann W, et al. Global use of Sglt2 inhibitors and glp-1 receptor agonists in type 2 diabetes. results from discover. *BMC Endocr Disord* (2022) 22(1):111. doi: 10.1186/s12902-022-01026-2

11. Dave CV, Schneeweiss S, Wexler DJ, Brill G, Patorno E. Trends in clinical characteristics and prescribing preferences for Sglt2 inhibitors and glp-1 receptor agonists, 2013-2018. *Diabetes Care* (2020) 43(4):921–4. doi: 10.2337/dc19-1943

12. Zhu Y, Qiao Y, Dai R, Hu X, Li X. Trends and patterns of antibiotics use in china's urban tertiary hospitals, 2016-19. *Front Pharmacol* (2021) 12:757309. doi: 10.3389/fphar.2021.757309

13. Wang Z, Wu X, Yu Z, Yu L. Utilization of drugs for attention-deficit hyperactivity disorder among young patients in China, 2010-2019. *Front Psychiatry* (2021) 12:802489. doi: 10.3389/fpsyt.2021.802489

14. Sangha V, Lipska K, Lin Z, Inzucchi SE, McGuire DK, Krumholz HM, et al. Patterns of prescribing sodium-glucose cotransporter-2 inhibitors for Medicare beneficiaries in the united states. *Circ Cardiovasc Qual Outcomes* (2021) 14(12): e008381. doi: 10.1161/CIRCOUTCOMES.121.008381

15. Kahal H, Abouda G, Rigby AS, Coady AM, Kilpatrick ES, Atkin SL. Glucagon-like peptide-1 analogue, liraglutide, improves liver fibrosis markers in obese women with polycystic ovary syndrome and nonalcoholic fatty liver disease. *Clin Endocrinol (Oxf)* (2014) 81(4):523–8. doi: 10.1111/cen.12369

16. Wu B, Bell K, Stanford A, Kern DM, Tunceli O, Vupputuri S, et al. Understanding ckd among patients with T2dm: Prevalence, temporal trends, and treatment patterns-nhanes 2007-2012. *BMJ Open Diabetes Res Care* (2016) 4(1): e000154. doi: 10.1136/bmjdrc-2015-000154

17. Pfeffer MA, Claggett B, Diaz R, Dickstein K, Gerstein HC, Kober LV, et al. Lixisenatide in patients with type 2 diabetes and acute coronary syndrome. *New Engl J Med* (2015) 373(23):2247–57. doi: 10.1056/NEJMoa1509225

18. Drucker DJ. The cardiovascular biology of glucagon-like peptide-1. *Cell Metab* (2016) 24(1):15–30. doi: 10.1016/j.cmet.2016.06.009

19. American Diabetes A. Cardiovascular disease and risk management: Standards of medical care in diabetes-2020. *Diabetes Care* (2020) 43(Suppl 1): S111–S34. doi: 10.2337/dc20-S010

20. Das SR, Everett BM, Birtcher KK, Brown JM, Januzzi JLJr., Kalyani RR, et al. 2020 Expert consensus decision pathway on novel therapies for cardiovascular risk reduction in patients with type 2 diabetes: A report of the American college of cardiology solution set oversight committee. *J Am Coll Cardiol* (2020) 76(9):1117–45. doi: 10.1016/j.jacc.2020.05.037

21. Cosentino F, Grant PJ, Aboyans V, Bailey CJ, Ceriello A, Delgado V, et al. 2019 Esc guidelines on diabetes, pre-diabetes, and cardiovascular diseases developed in collaboration with the easd. *Eur Heart J* (2020) 41(2):255–323. doi: 10.1093/eurheartj/ehz486

22. Cai C, Jia WP. [to promote the integration of prevention and treatment for the whole-course management of diabetes: Interpretation of the national guideline for the prevention and control of diabetes in primary care (2022)]. *Zhonghua Nei Ke Za Zhi* (2022) 61(7):713–6. doi: 10.3760/cma.j.cn112138-20220329-00222

23. Mishriky BM, Cummings DM, Powell JR. Cardiovascular benefits of glp-1ra and sglt-2i in women with type 2 diabetes. *Prim Care Diabetes* (2022) 16(3):471–3. doi: 10.1016/j.pcd.2022.03.012

24. Elkind-Hirsch KE, Paterson MS, Shaler D, Gutowski HC. Short-term sitagliptin-metformin therapy is more effective than metformin or placebo in prior gestational diabetic women with impaired glucose regulation. *Endocr Pract* (2018) 24(4):361–8. doi: 10.4158/EP-2017-0251

25. Vedtofte L, Bahne E, Foghsgaard S, Bagger JI, Andreasen C, Strandberg C, et al. One year's treatment with the glucagon-like peptide 1 receptor agonist liraglutide decreases hepatic fat content in women with nonalcoholic fatty liver disease and prior gestational diabetes mellitus in a randomized, placebo-controlled trial. *J Clin Med* (2020) 9(10):3213. doi: 10.3390/jcm9103213

26. Chen C, Huang Y, Dong G, Zeng Y, Zhou Z. The effect of dipeptidyl peptidase-4 inhibitor and glucagon-like peptide-1 receptor agonist in gestational diabetes mellitus: A systematic review. *Gynecol Endocrinol* (2020) 36(5):375–80. doi: 10.1080/09513590.2019.1703943

27. Salamun V, Jensterle M, Janez A, Vrtacnik Bokal E. Liraglutide increases ivf pregnancy rates in obese pcos women with poor response to first-line reproductive treatments: A pilot randomized study. *Eur J Endocrinol* (2018) 179(1):1–11. doi: 10.1530/EJE-18-0175

28. Rasmussen CB, Lindenberg S. The effect of liraglutide on weight loss in women with polycystic ovary syndrome: An observational study. *Front Endocrinol (Lausanne)* (2014) 5:140. doi: 10.3389/fendo.2014.00140

29. Han Y, Li Y, He B. Glp-1 receptor agonists versus metformin in pcos: A systematic review and meta-analysis. *Reprod BioMed Online* (2019) 39(2):332–42. doi: 10.1016/j.rbmo.2019.04.017

30. Chinese Elderly Type 2 Diabetes Prevention and Treatment of Clinical Guidelines Writing Group; Geriatric Endocrinology and Metabolism Branch of Chinese Geriatric Society; Geriatric Endocrinology and Metabolism Branch of Chinese Geriatric Health Care Society; Geriatric Professional Committee of Beijing Medical Award Foundation; National Clinical Medical Research Center for Geriatric Diseases (PLA General Hospital). Clinical guidelines for prevention and treatment of type 2 diabetes mellitus in the elderly in China (2022 edition). *Zhonghua Nei Ke Za Zhi* (2022) 61(1):12–50. doi: 10.3760/cma.j.cn112138-20211027-00751

31. Karagiannis T, Tsapas A, Athanasiadou E, Avgerinos I, Liakos A, Matthews DR, et al. Glp-1 receptor agonists and Sglt2 inhibitors for older people with type 2 diabetes: A systematic review and meta-analysis. *Diabetes Res Clin Pract* (2021) 174:108737. doi: 10.1016/j.diabres.2021.108737

32. Kitten AK, Kamath M, Ryan L, Reveles KR. National ambulatory care non-insulin antidiabetic medication prescribing trends in the united states from 2009 to 2015. *PloS One* (2019) 14(8):e0221174. doi: 10.1371/journal.pone.0221174

33. Wang L, Zhou B, Zhao Z, Yang L, Zhang M, Jiang Y, et al. Body-mass index and obesity in urban and rural China: Findings from consecutive nationally representative surveys during 2004-18. *Lancet* (2021) 398(10294):53–63. doi: 10.1016/S0140-6736(21)00798-4

34. Bragg F, Holmes MV, Iona A, Guo Y, Du H, Chen Y, et al. Association between diabetes and cause-specific mortality in rural and urban areas of China. *JAMA* (2017) 317(3):280–9. doi: 10.1001/jama.2016.19720

35. Shao H, Li P, Guo J, Fonseca V, Shi L, Zhang P. Socioeconomic factors play a more important role than clinical needs in the use of Sglt2 inhibitors and glp-1 receptor agonists in people with type 2 diabetes. *Diabetes Care* (2022) 45(2):e32–e3. doi: 10.2337/dc21-1800

36. Morton JI, Ilomki J, Magliano DJ, Shaw JE. Persistent disparities in diabetes medication receipt by socio-economic disadvantage in Australia. *Diabet Med* (2022) 39(9):e14898. doi: 10.1111/dme.14898

37. Adhikari R, Jha K, Dardari Z, Heyward J, Blumenthal RS, Eckel RH, et al. National trends in use of sodium-glucose cotransporter-2 inhibitors and glucagon-like peptide-1 receptor agonists by cardiologists and other specialties, 2015 to 2020. *J Am Heart Assoc* (2022) 11(9):e023811. doi: 10.1161/JAHA.121.023811

38. Davies MJ, D'Alessio DA, Fradkin J, Kernan WN, Mathieu C, Mingrone G, et al. Management of hyperglycemia in type 2 diabetes, 2018. a consensus report by the American diabetes association (Ada) and the European association for the study of diabetes (Easd). *Diabetes Care* (2018) 41(12):2669–701. doi: 10.2337/dci18-0033

39. Gilstrap LG, Blair RA, Huskamp HA, Zelevinsky K, Normand SL. Assessment of second-generation diabetes medication initiation among Medicare enrollees from 2007 to 2015. *JAMA Netw Open* (2020) 3(5):e205411. doi: 10.1001/jamanetworkopen.2020.5411

40. Einarson TR, Acs A, Ludwig C, Panton UH. Prevalence of cardiovascular disease in type 2 diabetes: A systematic literature review of scientific evidence from across the world in 2007-2017. *Cardiovasc Diabetol* (2018) 17(1):83. doi: 10.1186/s12933-018-0728-6

41. Weng W, Tian Y, Kong SX, Ganguly R, Hersloev M, Brett J, et al. The prevalence of cardiovascular disease and antidiabetes treatment characteristics among a Large type 2 diabetes population in the united states. *Endocrinol Diabetes Metab* (2019) 2(3):e00076. doi: 10.1002/edm2.76

frontiers | Frontiers in Endocrinology

TYPE Original Research
PUBLISHED 12 October 2022
DOI 10.3389/fendo.2022.1011383

OPEN ACCESS

EDITED BY
Qiulun Lu,
Nanjing Medical University, China

REVIEWED BY
Shan Lu,
Nanjing Medical University, China
Guanghong Jia,
University of Missouri, United States
Oscar Lorenzo,
Health Research Institute Foundation Jimenez Diaz (IIS-FJD), Spain

*CORRESPONDENCE
Sheng Li
shengli410@126.com;
lisheng@tjh.tjmu.edu.cn

SPECIALTY SECTION
This article was submitted to Cellular Endocrinology, a section of the journal Frontiers in Endocrinology

RECEIVED 04 August 2022
ACCEPTED 27 September 2022
PUBLISHED 12 October 2022

CITATION
Peng L, Zhu M, Huo S, Shi W, Jiang T, Peng D, Wang M, Jiang Y, Guo J, Men L, Huang B, Wang Q, Lv J, Lin L and Li S (2022) Myocardial protection of S-nitroso-L-cysteine in diabetic cardiomyopathy mice. *Front. Endocrinol.* 13:1011383. doi: 10.3389/fendo.2022.1011383

Myocardial protection of S-nitroso-L-cysteine in diabetic cardiomyopathy mice

Lulu Peng[1], Mengying Zhu[1], Shengqi Huo[1], Wei Shi[1], Tao Jiang[1,2], Dewei Peng[1], Moran Wang[1], Yue Jiang[1], Junyi Guo[1], Lintong Men[1], Bingyu Huang[1], Qian Wang[1], Jiagao Lv[1], Li Lin[1] and Sheng Li[1]*

[1]Division of Cardiology, Department of Internal Medicine, Tongji Hospital, Tongji Medical College, Huazhong University of Science and Technology, Wuhan, China, [2]Department of Geriatrics, Tongji Hospital, Tongji Medical College, Huazhong University of Science and Technology, Wuhan, China

Diabetic cardiomyopathy (DCM) is a severe complication of diabetes mellitus that is characterized by aberrant myocardial structure and function and is the primary cause of heart failure and death in diabetic patients. Endothelial dysfunction plays an essential role in diabetes and is associated with an increased risk of cardiovascular events, but its role in DCM is unclear. Previously, we showed that S-nitroso-L-cysteine(CSNO), an endogenous S-nitrosothiol derived from eNOS, inhibited the activity of protein tyrosine phosphatase 1B (PTP1B), a critical negative modulator of insulin signaling. In this study, we reported that CSNO treatment induced cellular insulin-dependent and insulin-independent glucose uptake. In addition, CSNO activated insulin signaling pathway and promoted GLUT4 membrane translocation. CSNO protected cardiomyocytes against high glucose-induced injury by ameliorating excessive autophagy activation, mitochondrial impairment and oxidative stress. Furthermore, nebulized CSNO improved cardiac function and myocardial fibrosis in diabetic mice. These results suggested a potential site for endothelial modulation of insulin sensitivity and energy metabolism in the development of DCM. Data from these studies will not only help us understand the mechanisms of DCM, but also provide new therapeutic options for treatment.

KEYWORDS

diabetic cardiomyopathy, glucose uptake, insulin signaling pathway, S-nitrosothiols, S-nitrosylation

Introduction

Type 2 diabetes mellitus (T2DM) is one of the most prevalent long-range metabolic disorders worldwide. It is currently spreading in an astonishing speed. From the International Diabetes Federation (IDF), it is estimated that the incidence of diabetes will reach 10.5% by 2021, up from 4.6% in 2000. By 2030, 578 million people are expected to be affected by diabetes, and 700 million people are expected by 2045 (1). Diabetic cardiomyopathy is a significant cause of morbidity and mortality in diabetic patients (2). The diagnosis of DCM is usually based on the presence of cardiac dysfunction but no hypertension or coronary artery disease in diabetic patients (3). Although many attempts have been made to research effective treatments for the long-term management of diabetic cardiomyopathy, the overall clinical results are still disappointing (4). To date, there remains an urgent need for effective treatment for diabetic cardiomyopathy.

Generally, three key pathophysiological factors (e.g., insulin resistance, endothelial dysfunction and metabolic disturbances in the myocardium) are believed to be involved in T2DM. Insulin signal transduction is a fundamental regulatory mode to ameliorate IR and myocardial energy metabolism. Through the regulation of this signaling pathway, a variety of physiological and pathological mechanisms can be improved, making it a very attractive treatment for T2DM complicated by heart failure. The insulin signal is turned on insulin binding to the insulin receptor to activate the MAPK and AKT pathways. On the other hand, insulin signaling is turned off by protein tyrosine phosphatases (PTPs), mainly PTP1B, dephosphorylation of insulin receptors and their substrates to downregulate signal transduction (5). PTP1B, an extensively expressed nonreceptor classical PTP, belongs to the class 1 PTPs (6). As required for PTP1B catalysis, the N-terminal domain contains nucleophilic residues Cys215 and Arg221. It regulates the activity of PTP1B through some posttranslational modifications (PTMs), such as phosphorylation, ER surface binding, oxidization, O-GlcNAcylation (7), sumoylation, S-nitrosylation (8) and sulfhydrylation, to perform the corresponding biological functions. Numerous PTP1B inhibitors have been reported, but few of them have been used in the clinic due to difficulties in discovering their potency *in vivo* (9). Therefore, finding a new inhibitor of PTP1B is extremely important.

Endothelial dysfunction (ED) is the mutual pathological mechanism of diabetes and cardiovascular diseases, which directly impacts the overall prognosis and survival (10). Under normal circumstances, endothelial cells maintain vascular homeostasis to maintain healthy vascular function. The endothelium mainly fights against diseases by regulating vascular tone, maintaining vascular wall permeability and antagonizing vascular inflammation (11). The endothelium lines the inner surface of vascular systems with squamous epithelial cells. A variety of mechanisms are involved in endothelial functions, including the regulation of vasodilation and contraction, thrombosis, immunity, and inflammation. Endothelial dysfunction eventually leads to vascular remodeling, myocardial remodeling, and cardiac dysfunction (12). Endothelial dysfunction is often an early pathophysiological feature of most cardiovascular diseases (CVDs) and an independent predictor of future cardiovascular prognosis (13). Clinically, the leading cause of the high morbidity of heart failure and poor prognosis in diabetic patients may be endothelial dysfunction (14). Nitric oxide (NO) plays a major role in endothelial function and is predominantly synthesized by endothelial NO synthase (eNOS). NO signaling regulates vasodilation and myocardial contraction to play a certain role in myocardial protection (15). In addition to canonical NO signaling, a recent meta-analysis of proteomic data suggested that cysteine S-nitrosylation was also a regulator of myocardial cell metabolism (16). S-nitroso-L-cysteine (CSNO) is the simplest endogenous S-nitrosothiol and is derived from eNOS. It exerts biological activity through the S-nitrosylation reaction, independent of NO. Previously, we reported that CSNO nitrosylated PTP1B to interfere with its binding to the substrate and inhibited its enzyme activity (17). In this study, we investigated the protective effect of SNO on the cardiac structure and function of DCM and reported the effect of SNO on cellular glucose uptake, the insulin signaling pathway and the potential mechanism of improving high glucose-induced injury to cardiomyocytes.

Materials and methods

Ethics statement

A committee of Tongji Medical College, Huazhong University of Science and Technology approved the use of wild-type C57BL/6J mice (male, 4 weeks and 15 g). All procedures were executed according to the National Institutes of Health Guide for the Care and Use of Laboratory Animals.

Animals and treatment

C57BL/6J mice (Shulaibao Biotech) were permitted to adapt to feed in the experimental environment for 2 weeks. The DCM model was developed by following a high-fat diet for 8 weeks and injecting STZ (150 mg/kg, Sigma–Aldrich, USA) intraperitoneally for 5 days. The control group was given the same amount of citrate buffer (vehicle) intraperitoneally and fed a normal diet. After 1 week, blood glucose measurements were monitored. Three consecutive random measurements of blood glucose above 16.7 mM were considered successful. The early treatment group (ET group) was administered nebulized CSNO (88 ppm for 20 minutes per day) when fed a high-fat diet, while

the late treatment group (LT group) was administerednebulized CSNO when the model was built.

Doppler echocardiography

Each group of mice was examined using echocardiography at week 2, and 16. 3% isoflurane mixed in 1 L/min 100% O_2 was used to induce anesthesia in mice, and 2% isoflurane mixed in 1 L/min 100% O_2 was used to maintain anesthesia. We averaged the cardiac parameters from at least three separate cardiac cycles. For echocardiographic operators, the grouping of mice was blinded.

Histological staining

Paraffin sections were prepared by agar preembedding myocardial tissue. The blocks were dyed with hematoxylin-eosin (HE), Sirius Red and Masson's trichrome. In addition, the area of myocardial cells was quantified by staining with wheat germ agglutinin (WGA). This staining was performed using standard protocols.

Cell culture

H9c2 myoblasts (ATCC, Manassas, U.S.) were cultured in Dulbecco's modified Eagle's medium (KeyGEN BioTECH, China) supplemented with 10% (v/v) fetal bovine serum (FBS, Gibco, Thermo Fisher Scientific, U.S.) and 1% (v/v) penicillin/streptomycin (Sangon, China) in an incubator (5% CO_2, humidified at 37°C). Cells were induced with high-glucose DMEM (33 mM) configured with anhydrous glucose for 48 h to simulate hyperglycemic conditions.

Determination of cell viability

The cells were seeded in 96-well plates at 5×10^3 cells per well. When the cells grew for approximately 12 h and adhered well, they were exposed to different concentrations of CSNO for 1 h. CCK8 assays were used to determine cell viability and growth. At a wavelength of 450 nm, the absorbance was detected by a spectrophotometer.

Glucose uptake assay

After treatment, the cells were coincubated with ^{3}H labeled 2- deoxyglucose (^{3}H-2-DOG). After washing the cells, the ^{3}H-2-DOG content in cardiomyocytes was measured by a scintillation counter, and glucose uptake was quantitatively detected.

Western blot

The treated cells and spilt cells were collected using RIPA lysis buffer (18). Equal amounts of protein were loaded on Bis-Tris SDS–PAGE (the concentration was determined by the molecular weight of protein) for gel electrophoresis. The band was transferred to PVDF membrane and combined with antibody overnight. The antibodies we used were as follows: p-Akt (CST, #4060, 1:1000), AKT (CST, #4685, 1:1000), p-IR (CST, #3021, 1:1000),IR (CST, #23413, 1:1000), IRS (CST, #95816, 1:1000), p-IRS (Sigma–Aldrich, ZRB09432, 1:1000), GLUT4 (CST, #2213, 1:1000), N-cadherin (CST, #13116, 1:1000), LC3B (CST, #3868, 1:1000), P62 (CST, #23214, 1:1000) and GAPDH (CST, #2118L). A prestained protein ladder (Thermo Scientific) and HRP-conjugated secondary antibodies were applied as well.

Real-time PCR

We conducted a quantitative PCR study as described in our recent publication (18). The primer sequences were as follows: Mouse ANP Forward 5'-ACCTGCTAGACCACCTGGAG-3', Reverse 5'-CCTTGGCTGTTATCGGTACCGG-3'. Mouse BNP Forward 5'-GAGGTCACTCCTATCCTCTGG-3', Reverse 5'-GCCATTTCCTCCGACTTTTCTC-3'. Mouse β-MHC Forward 5'-CCGAGTAGGTCAACAA-3', Reverse 5'-CTTCACGGGCACCCTTGGA-3'. Mouse COL-1 Reverse 5'-AGGCTTCAGTGGTTTGGATG-3', Reverse 5'-CACCAACAGCACCATCGTTA-3'. Mouse GAPDH'Forward 5'-GGTTGTCTCCTGCGACTTCA-3', Reverse 5'-TGGTCCAGGGTTTCTTACTCC-3'. To calculate fold changes in gene expression, ΔCt test = Ct of target genes in test groups - Ct of gapdh in test group and ΔCt con = Ct of target genes in control groups - Ct of gapdh in control group were first obtained. Next, the ΔCt test was normalized by ΔCt con. ΔΔCt = ΔCt test - ΔCt con. The final step is to calculate the difference in expression levels. Change fold = 2^(-ΔΔCt).

Plasma membrane separation experiment

A membrane protein extraction kit (Beyotime, China) was used to extract cell membrane proteins. The isolated protein was detected by western blot.

Measurement of ATP contents

The ATP levels were measured using an enhanced ATP assay kit (Beyotime S0027). The assays were performed

according to the instruction manual. A luminometer was used to measure the optical density of the mixture. Based on an ATP concentration-versus-absorptance standard curve, the ATP concentration was calculated.

Mitochondrial membrane potential assay

After cell treatment, the culture medium was removed and discarded. The cells were washed with preheated PBS 3 times. In accordance with the instructions provided, treated cells were incubated with 200 nM JC-1 (C2006, Beyotime) for 30 minutes at 37°C. The fluorescence of red and green was detected using a fluorescence microscope. MMP fluorescence intensity was assessed using ImageJ software. MMP =JC-1 polymer fluorescence intensity/JC-1 monomer fluorescence intensity.

Mitochondrial morphological measurement

A density of 1×10^5 cells/dish seeded in confocal dishes was treated with high glucose (33 mM) for 48 h and CSNO (50 μM) for 1 h. Three rinses with PBS were followed by 30 min of incubation with 200 nM MitoTracker® Red CMXRos (Thermo Fisher). Image capture of mitochondria was performed using confocal laser scanning microscopy (Eclipse-TI2, Nikon, Japan). An analysis of mitochondrial morphology was performed by using ImageJ with Mitochondrial Network Analysis (MiNA). The following three parameters were used to evaluate the morphology of the mitochondrial network: individuals of mitochondria, mitochondrial footprint and mean network size.

Measurement of cardiomyocyte size

After being exposed to high glucose (33 mM) for 48 h and CSNO (50 μM) for 1 h, H9c2 were fixed with 4% paraformaldehyde for 15 min. Following washing with TBST 3 times, the cells were blocked with a 10% solution of normal goat serum in PBS for 1 h. Then, the slides were incubated with 50 μg/mL phalloidin (AAT BioQuest, #23122) for 1 h away from light. DAPI counterstain (Sigma–Aldrich, MO, USA) was applied to the nuclei of each cell. Images capture of cell shape was performed by laser scanning confocal microscopy (Eclipse-TI2, Nikon, Japan).

Autophagic flux assay

Tandem mRFP-GFP-LC3 overexpression was achieved by infection of cells (a density of 1×10^5 cells/dish seeded in confocal dishes) with recombinant adenoviruses (Genechem, Shanghai, China) for 10 h after attachment. Fluorescence was checked by fluorescence microscopy to determine whether the virus had been transferred into the cells. After the virus was transferred into the cells, the cells were washed with PBS and cultivated in high-glucose for 48 h and CSNO for 1 h. Confocal laser scanning microscopy (Eclipse-TI2, Nikon, Japan) was used to capture autophagy flux images.

Statistical analysis

Data were expressed as an SEM average in triplicate. ImageJ software was used to quantitatively analyze the results of histological staining, WB and immunofluorescence. The statistical analysis and drawing were carried out using SPSS 21.0 software and GraphPad 8.0. We used one-way and two-way ANOVA to determine whether there were significant differences between the experimental groups. The threshold for statistical significance was $p < 0.05$.

Results

Effects of SNO on the metabolic parameters of diabetic mice

To study the impact of exogenous SNO *in vivo*, we nebulized CSNO. Experimental flow chart for the experiments is shown in Figure 1A. There was no obvious difference in body or heart weight among the groups (Figures 1B, C). However, the DCM group showed an increasd heart weight/body weight (HW/BW) ratio (Figure 1D). These data indicated that exogenous SNO ameliorated myocardial hypertrophy in diabetic mice. There were no significant differences between the 4 groups in heart rate (HR) (Figure 1E). Compared with the control group, the DCM group showed higher fasting blood glucose and random blood glucose. CSNO treatment decreased fasting blood glucose but had no obvious effect on random blood glucose (Figures 1F, G). As shown in Figure 1H, OGTT testing showed blood glucose levels of DCM mice spiked after glucose administration (15 min) and remained high after 120 min. The $AUC_{0-120\ minGlu}$ levels were significantly increased in the T2DM group after the dietary intervention start, while the ET group and LT group were lower (Figure 1I). These data indicate that exogenous SNO improved the glucose homeostasis of diabetic mice.

SNO ameliorated cardiac dysfunction in diabetic mice

DCM is diagnosed by detecting both structural and functional alterations in the left ventricle (LV) (19). Using M-mode echocardiography, we assessed the protective effect of

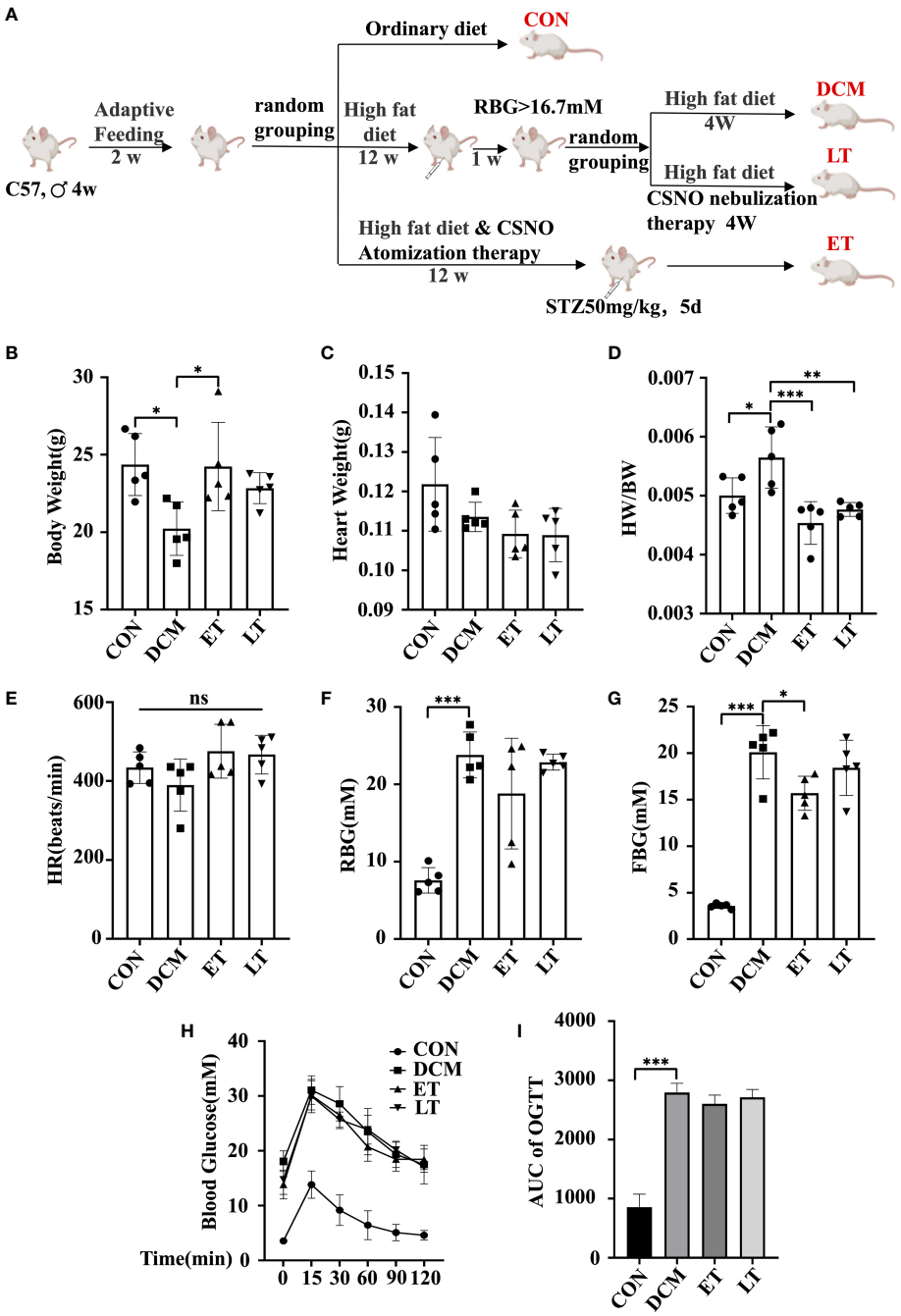

FIGURE 1
Mouse body weight, heart weight and blood glucose levels. **(A)** A flowchart showing the experimental process for modeling mice. **(B)** Body weight of mice. **(C)** Heart weight of mice. **(D)** Heart weight to body weight ratio (HW/BW). **(E)** Heart rate (HR). **(F)** Random body glucose(RBG). **(G)** Fasting blood glucose levels (FBG). **(H)** After fasting for 16 hours, mice were given glucose solution by gavage, and the corresponding blood glucose values were measured at different time points. The corresponding curve was drawn, namely, an oral glucose tolerance test (OGTT) curve. **(I)** The area under the curve (AUCglucose) was quantified. * represents $p < 0.05$; ** represents $p < 0.01$; *** represents $p < 0.001$. The "ns" symbol stands for "no significance".

exogenous SNO on the cardiac function of DCM mice. In comparison with the control group, a significant decrease in ejection fraction (EF) and fractional shortening (FS) was observed in DCM animals, which showed poor systolic dysfunction, indicating that DCM model was successfully developed. However, CSNO treatment markedly restored the aberrant myocardial parameters (Figures 2A, B). In addition, CSNO treatment reduced the E'/A' ratio and IVRT compared

with DCM mice, indicating that CSNO improved diastolic function (Figures 2C, D). Staining with HE, Masson's trichrome, Sirius red, and WGA was used to evaluate the changes in the myocardium in DCM mice. The results showed that DCM mice exhibited disarrayed cellular structures, ruptured myofibrils, increased fibrotic infiltration and obscured intercellular borders (Figures 2E–G). WGA staining showed increased cardiomyocyte size, and CSNO treatment reduced cardiomyocyte size (Figure 2H). All these anomaly variations were mitigated by CSNO treatment in the ET group and LT group. We also determined the mRNA expression levels of ANP, BNP, β-MHC, and col-1 by quantitative real-time PCR. Consistent with the results described previously, there was an ameliorative effect of CSNO on myocardial fibrosis and myocyte hypertrophy (Figures 2I–L).

SNO increased cellular glucose uptake

To investigate the effects of exogenous SNO on cardiomyocyte viability, H9c2 cells were exposed to CSNO at different concentrations for 1 h. As revealed in Figures 3A, B, 100 μM CSNO treatment or a lower concentration had no obvious effect on cytotoxicity. CSNO treatment significantly enhanced cell viability at low concentrations, and this effect was concentration dependent. A disturbance in glucose metabolism is the key point of the development of DCM. Although diabetic patients are in a hyperglycemic state, due to insulin resistance, the intake of glucose is insufficient. The cells are actually in a "hungry" state. Therefore, it is essential to restore insulin sensitivity and increase glucose intake to regulate glucose homeostasis. To test the effect of SNO on glucose uptake, cells were pretreated with different concentrations of CSNO with or without insulin. The results showed that CSNO alone increased glucose uptake in a dose-dependent manner (Figure 3C). In short, CSNO had an insulin-like effect. CSNO also increased glucose uptake in the presence of insulin, which indicated that CSNO increased insulin sensitivity (Figure 3D).

SNO enhanced GLUT4 translocation in cardiomyocytes

Life relies primarily on glucose as an energy source. GLUT4 is the dominant glucose transporter in the human heart (20). GLUT4 primarily resides in intracellular membrane compartments under basic conditions. A 10-to-20 fold increase in glucose transport into cardiomyocytes occurs when GLUT4 is translocated to the cell surface (21). The stimulation of myocardial glucose uptake induced by CSNO may be dependent on glucose transporter trafficking. In Figure 4A, the plasma membranes were separated and GLUT4 was measured. We detected that CSNO treatment not only promoted GLUT4 membrane translocation but also enhanced insulin-stimulated GLUT4 translocation.

SNO regulated the insulin signaling pathway in cardiomyocytes

Energy metabolism disorder and severe insulin resistance (IR) are the main pathological mechanisms of T2DM complicated with heart failure. Because of the great importance of the insulin signal transduction pathway in insulin resistance, we further elucidated the effect of CSNO on the insulin signaling pathway. According to the results, CSNO treatment upregulated the expression of phospho-IR, phospho-IRS1, and phospho-Akt in a concentration/time-dependent manner (Figures 4B, C). In Figure 4D, the results showed that CSNO not only activated insulin signaling without insulin, but also further enhanced the insulin-stimulated activation of insulin signaling pathway. In conclusion, CSNO activated the insulin signaling transduction.

SNO ameliorated high glucose-induced insulin resistance in cardiomyocytes

High glucose for 48 h is used to model insulin resistance. Glucose uptake is defective under insulin resistance conditions. Upon high glucose stimulation, a significant reduction in glucose uptake was observed. CSNO treatment increased glucose uptake (Figures 5A, B). In addition, we detected that CSNO significantly activated the insulin signaling pathway under insulin resistance (Figure 5C). In comparison with the control group, the membrane translocation of GLUT4 stimulated by insulin decreased in states of insulin resistance. However, CSNO facilitated GLUT4 translocation (Figure 5D).

SNO reversed high glucose-induced excessive autophagy in cardiomyocytes

Autophagy is a fundamental catabolic mode that plays a very important role in maintaining cellular metabolic homeostasis by degrading and recovering some harmful components. However, the excessive activation of autophagy leads to cell death as well (22). Light chain protein 3 (LC3) is a specific marker of autophagy initiation. The P62/SQSTM1 (sequetosome1) protein is a ubiquitin-binding protein involved in the degradation of autophagy-lysosome. The accumulation of P62 indicates impaired autophagy (23). In Figures 6A–C, high glucose induced autophagy, evidenced by an increase in LC3-I conversion to LC3-II and a decrease in P62. CSNO treatment reversed this condition. To further clarify the effect of CSNO on autophagy, we used the autophagy inhibitor, bafilomycin A1

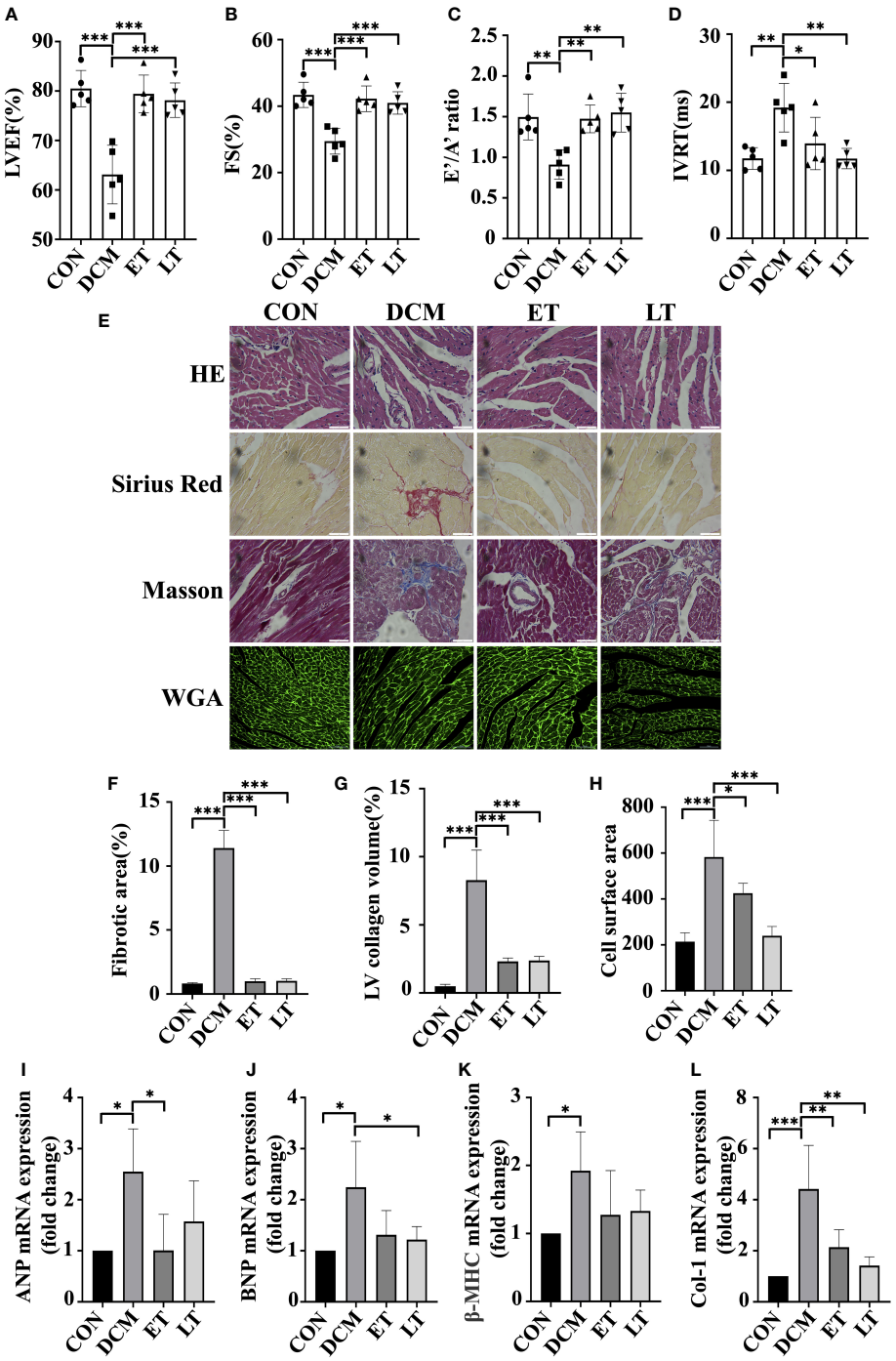

FIGURE 2
The effect of SNO on cardiac function in diabetic mice. Indices of cardiac systolic function, **(A)** Left ventricular ejection fraction (EF %). **(B)** Fractional shortening (FS %). Indices of cardiac diastolic function, **(C)** Early-to-late septal annulus motion in diastole (E'/A') and **(D)** Isovolumic relaxation time (IVRT). **(E)** HE staining, Sirius red staining, Masson trichrome staining and WGA staining of mouse hearts. Scale bar=50 mm. **(F)** The percentage of fibrotic area was quantified. **(G)** The percentage of LV collagen area was quantified. **(H)** Quantitative analysis of cardiac myocyte cross-sections. **(I-L)** Relative ANP, BNP, β-MHC and Col-1 mRNA expression normalized to GAPDH. * represents $p < 0.05$; ** represents $p < 0.01$; *** represents $p < 0.001$.

10.3389/fendo.2022.1011383

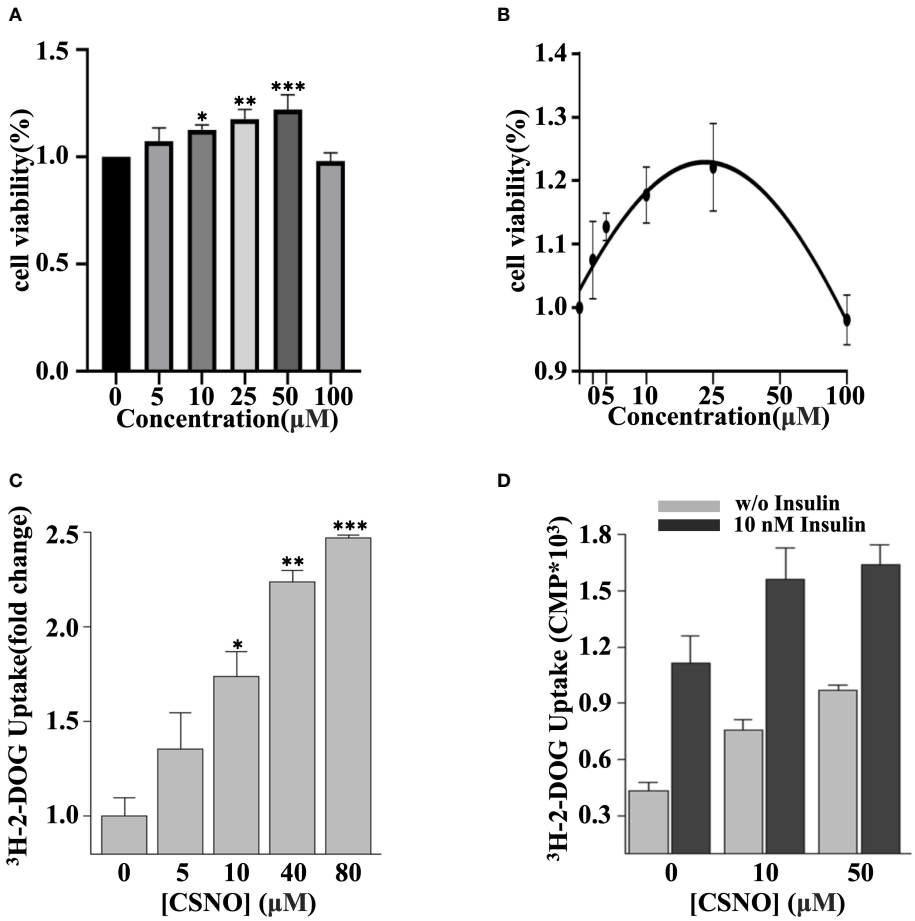

FIGURE 3
CSNO promoted cellular glucose uptake. **(A)** H9c2 cells were incubated with CSNO at different concentrations for 1 h. Cell viability was examined using a CCK8 kit. **(B)** The corresponding curve diagram of cell viability. **(C)** CSNO promoted cellular glucose uptake in a concentration-dependent manner. **(D)** CSNO increased insulin-dependent and noninsulin-dependent glucose uptake. * represents $p < 0.05$; ** represents $p < 0.01$; *** represents $p < 0.001$.

(Baf-A1). Baf-A1 is a lysosomal inhibitor that obstructs autophagy-lysosomal fusion and blocks autophagic flux. Baf-A1 alone caused the accumulation of LC3-II. Treatment with CSNO reduced the levels of LC3II, indicating that CSNO possibly played a role by inhibiting the formation of autophagosomes rather than blocking the degradation of autophagosomes (Figures 6D, E). We further used tandem fluorescent mRFP-GFP-LC3 adenovirus transfection to independently investigate the accumulation of typical autophagosomes and autolysosomes. When autophagosomes merge with lysosomes, GFP is quenched because of the acidic environment. Thus, green puncta represent autophagosomes, red puncta represent autolysosomes, yellow puncta (overlay of green and red) represent autophagosomes. Consistent with the previous results, high glucose stimulation significantly induced red puncta and yellow LC3-II puncta formation, supporting increased autophagic flux. CSNO restored autophagic flux by blocking autophagosome formation (Figures 6F, G).

SNO improved high glucose-induced mitochondrial function in cardiomyocytes

The major hallmark of diabetes is hyperglycemia, which perturbs the energy metabolic milieu. It impairs mitochondrial function and eventually leads to cardiac dysfunction. Compared with the control group, after high glucose stimulation for 48 h, the production of ATP decreased (Figure 7A), which may be related to mitochondrial destruction, and CSNO improved this

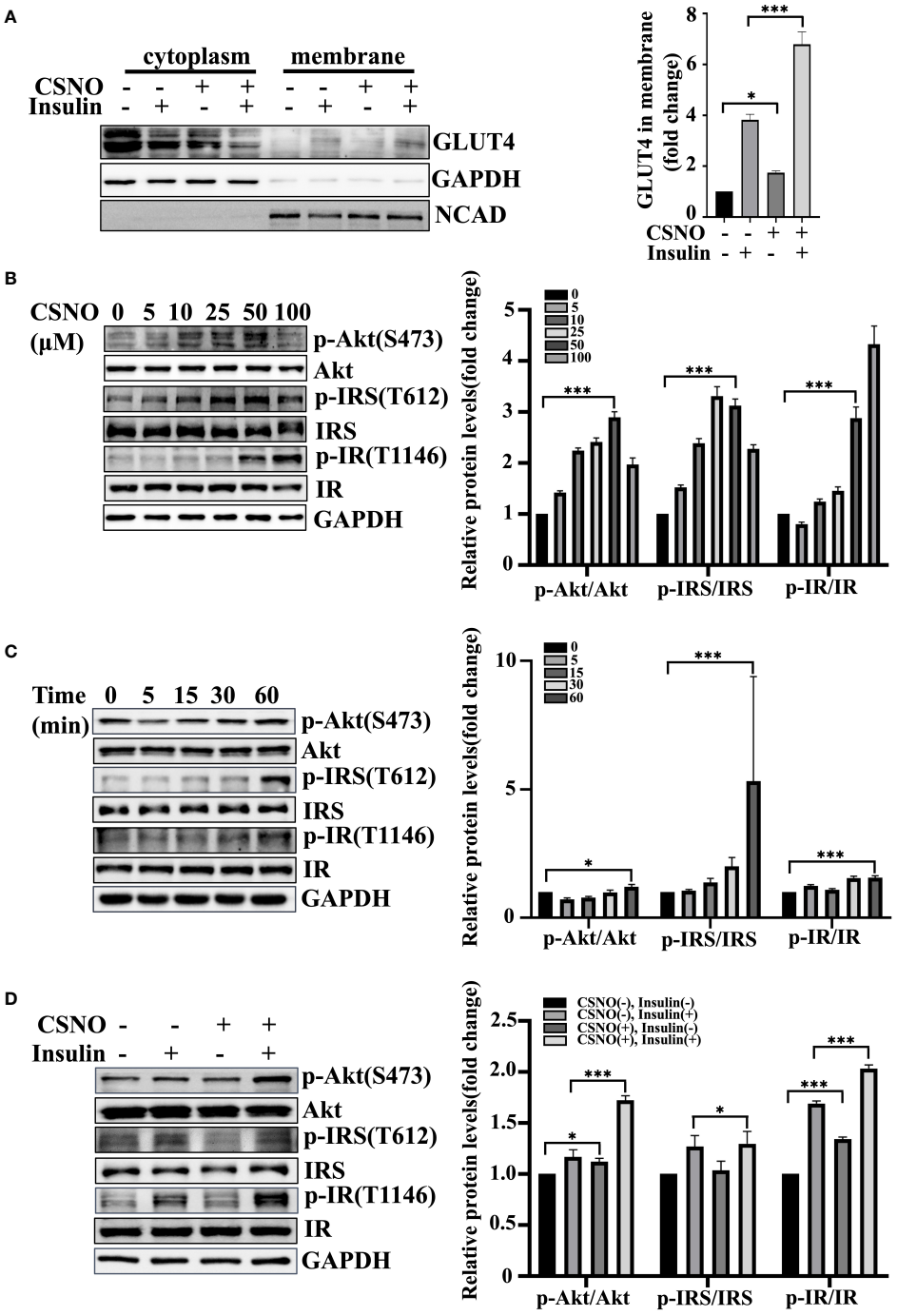

FIGURE 4
CSNO promoted GLUT4 membrane translocation and the insulin signaling pathway. **(A)** After the cytoplasm and cell membrane were separated, the expression of GLUT4 on membrane protein was detected. It was normalized to N-cadherin. **(B)** CSNO concentration-dependently activated the insulin signaling pathway in H9c2 cells. The expression level and phosphorylation level of Akt, IRS and IR were analyzed by Western blot. The protein band diagram and quantitative statistical diagram are shown. **(C)** CSNO time-dependently activated the insulin signaling pathway in H9c2 cells. The expression level and phosphorylation level of Akt, IRS and IR were analyzed by Western blot. The protein band diagram and quantitative statistical diagram are shown. **(D)** CSNO promoted activation of the insulin signaling pathway and further increased the effect of insulin on the insulin signaling pathway. The expression level and phosphorylation level of Akt, IRS and IR were analyzed by Western blot. The protein band diagram and quantitative statistical diagram are shown. * represents $p < 0.05$; *** represents $p < 0.001$.

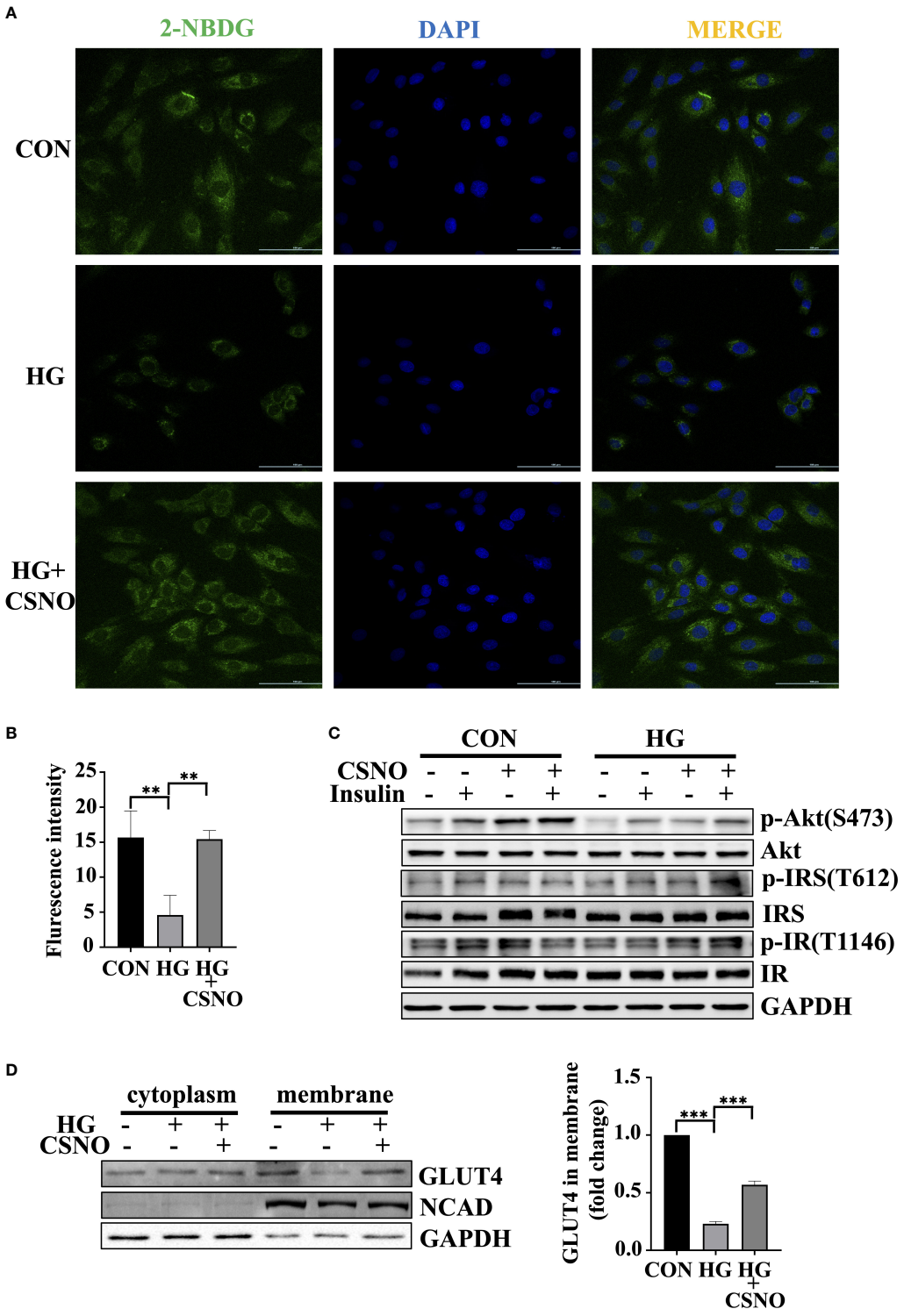

FIGURE 5
CSNO alleviated insulin resistance. **(A)** Glucose uptake was detected by fluorescence analysis of 2-NBDG uptake by cells. Scale bar=100 μm. **(B)** The statistical graph of fluorescence intensity which was analyzed with imageJ software. Scale bar=100 μm. **(C)** The expression level and phosphorylation level of Akt, IRS and IR were analyzed by Western blot. **(D)** After the cytoplasm and cell membrane were separated, the expression of GLUT4 on membrane protein was detected. It was normalized to N-cadherin. ** represents $p < 0.01$; ***represents $p < 0.001$.

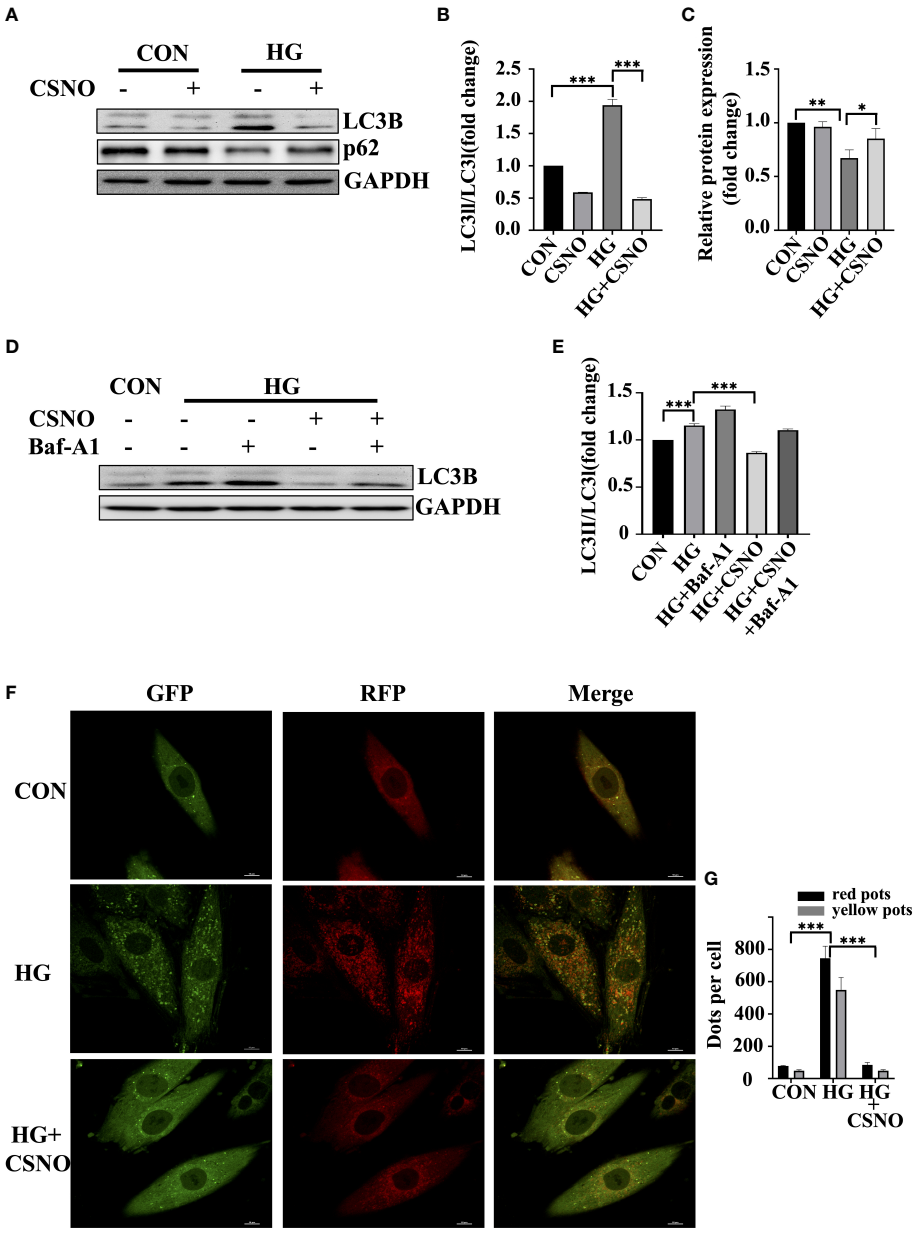

FIGURE 6
CSNO inhibited high glucose-induced excessive autophagy. **(A-C)** The expression levels of P62, LC3 II/I and GAPDH were analyzed by Western blot. The protein band diagram and quantitative statistical diagram are shown. **(D, E)** After adding the autophagy inhibitor Baf-A1,the expression of LC3 II/I and GAPDH was analyzed by Western blot. The protein band diagram and quantitative statistical diagram are shown. **(F)** An adenovirus expressing GFP-RFP-LC3 protein was used to detect autophagic flux. Scale bar=10 μm. **(G)** To quantify yellow and red LC3 dots per cell in each condition, Image-Pro Plus was used. * represents $p < 0.05$; ** represents $p < 0.01$; *** represents $p < 0.001$.

effect. To observe the changes in mitochondria, MitoTracker Red was used. Under normal conditions, healthy cells showed a tubular mitochondrial network. When cells were stimulated with high glucose, mitochondrial reticulation was destroyed. The mitochondria became spherical and more fragmented, indicating an increase in mitochondrial fission. Compared with the control group, we observed that the volume of mitochondria was smaller. CSNO improved the mitochondrial

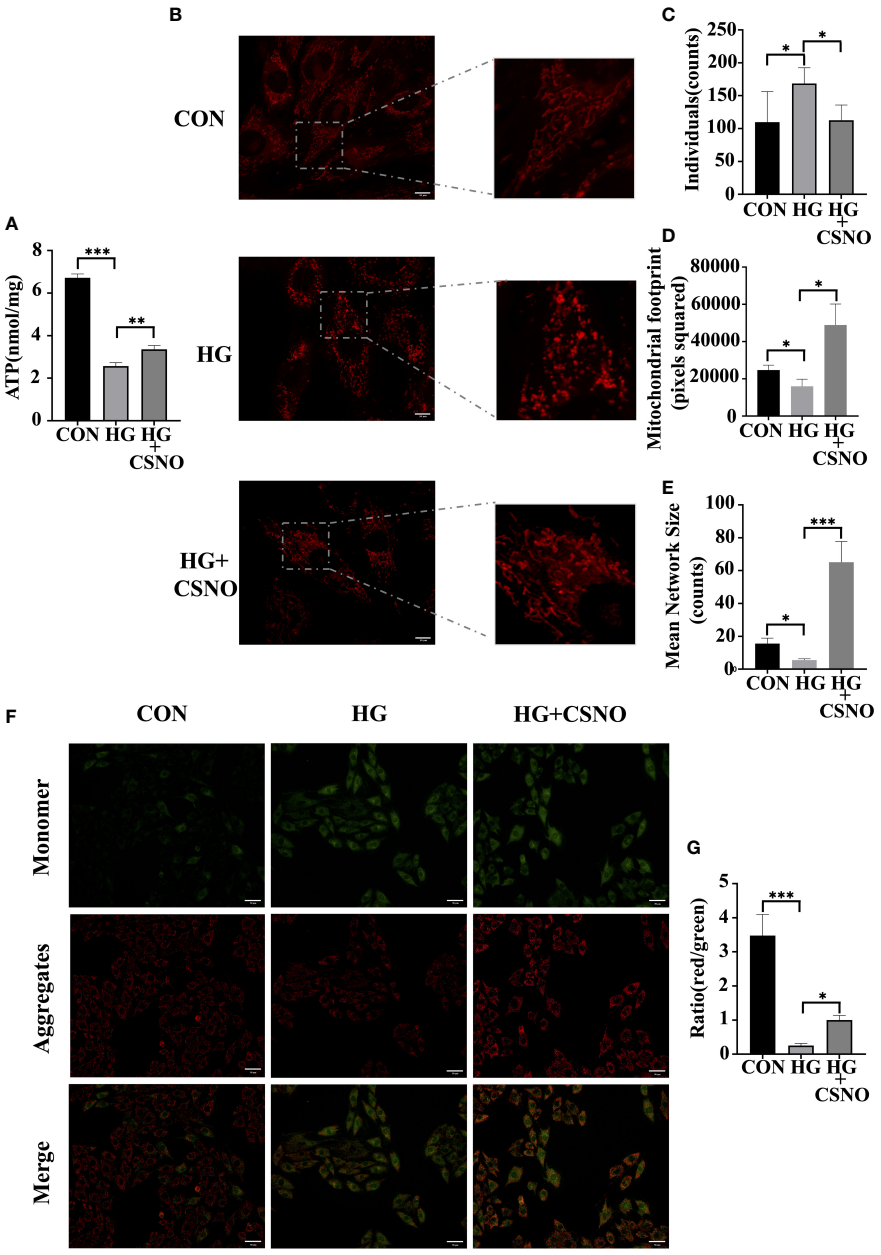

FIGURE 7
CSNO ameliorated high glucose-induced mitochondrial dysfunction. **(A)** ATP assay kits were used to determine cellular ATP levels. **(B)** Analysis of mitochondria stained with MitoTracker using confocal microscopy. Scale bar =10 μm. **(C-E)** MiNa in ImageJ was used to analyze the structural characteristics of the mitochondrial network, including individuals, mitochondrial footprint and mean network size. **(F)** Mitochondrial membrane potential (MMP) was determined by staining with JC1. JC-1 aggregates emit red fluorescence in healthy mitochondria with polarized inner mitochondria. As MMP dissipates, cytosolic monomers of JC-1 emit green fluorescence. Scale bar=50 μm. **(G)** A fluorescence ratio of red to green was used to calculate the MMP of cardiomyocytes for each group. * represents $p < 0.05$; ** represents $p < 0.01$; *** represents $p < 0.001$.

morphological changes and significantly increased the volume, indicating that CSNO promoted mitochondrial fission in high glucose-treated cardiomyocytes (Figures 7B–E).

Additionally, maintaining mitochondrial membrane permeability and mitochondrial function is also dependent on mitochondrial membrane potential (MMP). JC-1 cationic dye was used to detect MMP. Red fluorescence represents aggregates, green fluorescence represents monomers, and the ratio of aggregates to monomers is the MMP level. MMP levels were diminished in the high glucose-treated group, whereas MMP

levels were recovered with CSNO supplementation (Figures 7F, G).

SNO suppressed high glucose-induced oxidative stress in cardiomyocytes

Oxidative stress also serves as an important pathological mechanism of DCM. Mitochondrial dysfunction can also lead to excessive production of ROS. The imbalance between ROS production and elimination is referred to as oxidative stress. To determine whether CSNO affected oxidative stress, we used DHE staining to detect intracellular ROS. As shown in Figures 8A, B, under the stimulation of high glucose, the intracellular fluorescence intensity obviously increased, and the CSNO treatment group decreased, indicating that CSNO alleviated the oxidative stress caused by high glucose. It has been reported that oxidative stress is essential for the development of cell hypertrophy. We stained cells with fluorescently labeled phalloidin to observe cardiomyocyte size. We found that CSNO ameliorated high glucose-induced cell hypertrophy (Figures 8C, D).

Discussion

In our study, we found that an endogenous endothelial-derived SNO promoted glucose uptake in cells and increased insulin sensitivity. To the best of our knowledge, this has not been previously reported. Our results yield novel insight into how endothelial dysfunction may cause insulin resistance. Numerous studies have found that endothelial cells play an unexpected role in metabolic homeostasis, in addition to maintaining vascular homeostasis (15). In endothelial cells, GLUT1 is the primary glucose transporter. Chronic exposure to high glucose levels reduced endothelial GLUT1 expression to minimize the glucose transport rate in the heart (24). HIF1α in endothelial cells also played a role in glucose uptake, as

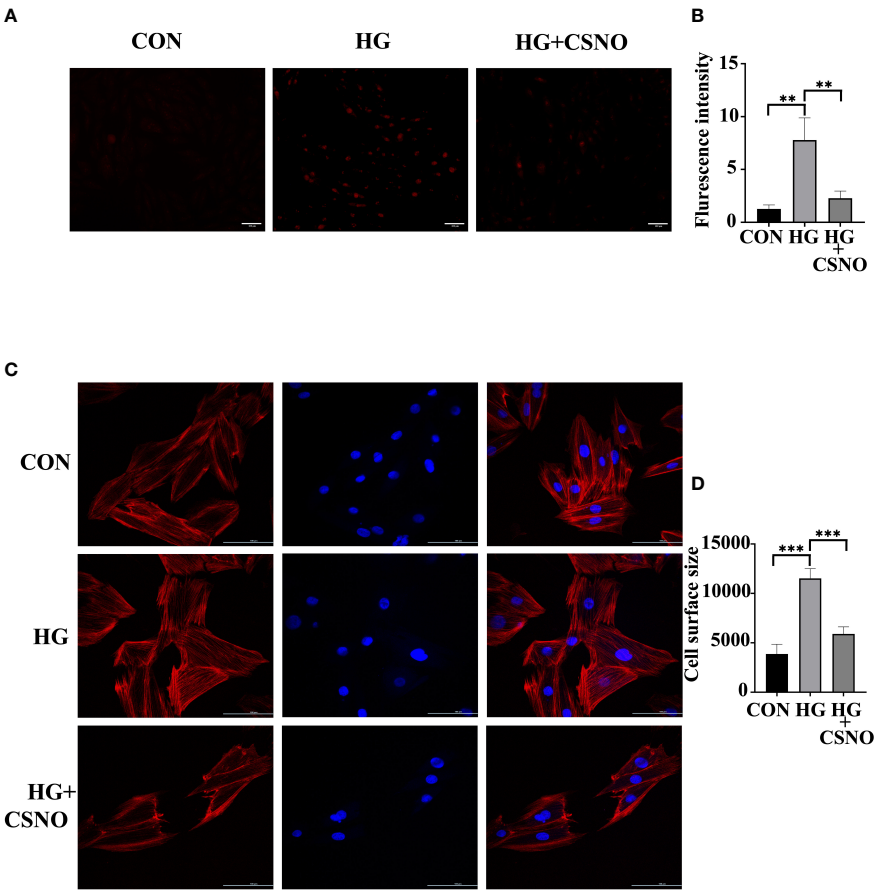

FIGURE 8
CSNO promoted high glucose-induced oxidative stress. **(A, B)** Analysis of reactive oxygen species (ROS) by dihydroethidium (DHE). Scale bar =100 μm. **(C, D)** The size of the cell was determined by detecting filaments of F-actin in the cell cytoskeleton using phalloidin. Scale bar=100 μm. ** represents $p < 0.01$; *** represents $p < 0.001$.

evidenced by endothelial-specific HIF1α knockout mice exhibiting reduced CSF/blood glucose ratios (25). Insulin improved insulin sensitivity and responsiveness of nonobese people through nitric oxide-dependent vasodilation in skeletal muscle (26). According to our study, endothelial SNO activated insulin signaling pathways and facilitated GLUT4 membrane translocation to improve glucose metabolism in cardiomyocytes. It was also believed that endothelial cells were responsible for maitaining metabolic homeostasis by secreting factors such as nitric oxide (NO), insulin-stimulating factors, growth factors, and enzymes (15). Our research revealed that SNO also had the potential to maintain metabolic homeostasis, which was previously unknown.

The mechanism of DCM has been extensively studied, including abnormal energy metabolism, abnormal subcellular composition and endothelial dysfunction (27). However, there is no specific pharmaceutical treatment at present. Many studies have shown that cardiac microvascular endothelial dysfunction often appears in the first stage of DCM and runs through the whole process (28). Creating specific modifications to target certain biomolecules on microvascular endothelial cells (MVECs) and myocardial cells exposed to high glucose stimulation has shown beneficial effects in clinical trials (29). In the heart, there is a close relationship between endothelial cells and cardiac myocytes. Many cardiac activity factors derived from the endothelium can regulate the activity of cardiac myocytes, such as endothelin -1 (ET-1), neuroregulatory protein 1 (NRG-1), nitric oxide (NO) and prostaglandins, as well as the recently reported angiopoietin, neuroregulatory protein 1 (NRG-1), apelin and dickkopf-3 (30). Zhao et al. proved that ET-1 maintained normal cardiac function and myocardial survival of mice by upregulating NF-κB signaling to reduce TNF-related apoptosis (31). Apelin regulated cardiomyocytes by binding its GPCR receptor APJ to antagonize the renin-angiotensin system (32). Prostaglandin I2 improved ET1-induced myocardial hypertrophy by activating IP prostaglandin-like receptor and cyclic adenosine monophosphate-dependent signal transduction in myocardial cells (33). NO maintained normal cardiac pump function by activating the NO/cGMP/PKG pathway. NO is mainly produced by eNOS. In-depth research has found that the endothelial relaxing factor produced by eNOS is not only NO gas but also sulfhydryl nitric oxide (SNO) combined with sulfhydryl (-SH). Our results showed that SNO not only activated the insulin signaling pathway, but also protected cardiomyocytes from the damage caused by high glucose by improving abnormal energy metabolism, mitochondrial dysfunction, excessive production of reactive oxygen species and excessive autophagy. *In vivo*, nebulization of SNO in diabetic mice effectively improved cardiac dysfunction and myocardial fibrosis. It also suggested that endothelial dysfunction played an important role in DCM. However, there is still a need for further exploration of the underlying mechanism.

SNO not only has the same biological characteristics as NO gas but also regulates protein function through S-nitrosylation of thiols, which is a posttranslational modification, while NO gas has no such function. Our previous study found that SNO from eNOS inhibited PTP1B activity. PTP1B is the major negative regulator of the insulin signaling pathway. Recently, increasing attention has been focused on targeting PTP1B inhibitors for T2DM treatment. However, they have not been used in the clinic and have just reached the stage of clinical trials due to some limitations related to the tissue-specific functions of PTP1B (34). Our results shed new light on finding endogenous PTP1B inhibitors instead of chemical synthesis. Different from synthetic compounds, SNO is an endogenous molecule that already exists *in vivo*. Besides the adverse reactions caused by high concentrations, the possibility of unpredictable toxicity and side effects is small. In addition, 50–80% homology between catalytic sites of PTP1B and other phosphatases limits the use of selective PTP1B inhibitors (35). However, unlike other tyrosine phosphatases, the amino acid sequence composition and special three-dimensional structure of PTP1B in its enzyme active site, especially the basic amino acid residues, Arg45, Lys116 and Lys210, are similar to C215 in the enzyme active site in the spatial structure. Therefore, the entropy value of the nucleophilic reaction with SNO is low, which gives SNO high specificity in inhibiting PTP1B (36). To bind to the highly charged catalytic sites of PTP1B, inhibitors should be charged with anions at physiological pH, but they often show limited cell permeability and low bioavailability (37) (38);. Our previous research proved that SNO entered into cells *via* LAT1 and LAT2 to exert its corresponding biological effects (39). Hence, SNO had the therapeutic potential as a PTP1B inhibitor. However, it is unclear whether the CSNO effect was solely dependent on PTP1B inhibition. Other mechanisms may also be involved, and further investigation is needed. Meanwhile, whether there are other metabolites of SNO playing a role in myocardial protective effects still needs further exploration.

In summary, the present study found that endothelium-derived SNO promoted cardiac function in DCM mice. We showed the facilitatory effect of SNO on glucose uptake, GLUT4 membrane translocation and the insulin signaling pathway. SNO protected cells against high glucose-induced damage through inhibition of oxidative stress and excessive autophagy and improvement of mitochondrial dysfunction. Together, our study provided new insight into the molecular mechanism behind DCM, with the potential to be used as a therapeutic target in the future.

Data availability statement

The original contributions presented in the study are included in the article/supplementary material. Further inquiries can be directed to the corresponding author.

Ethics statement

The animal study was reviewed and approved by TongJi Hospital Application for Ethical Approval for Research Involving Animals.

Author contributions

It was SL and LP who conceived and designed the study. The majority of the experiments were conducted and analyzed by LP, and the manuscript was written by LP. During experimentation and analysis of results, MZ, SH, WS, TJ, DP, MW, JG, LM provide guidance and advice. YJ, BH, QW assisted with the animal experiment. Reagents, equipment, and advice were provided by JL and LL. The manuscript was reviewed, edited, and feedback was provided by SL and LL. Final approval of the manuscript was obtained from all authors. All authors contributed to the article and approved the submitted version.

Funding

This work was supported by the National Natural Science Foundation of China [grant numbers 81974032, 82070396].

Conflict of interest

The authors declare that the research was conducted in the absence of any commercial or financial relationships that could be construed as a potential conflict of interest.

Publisher's note

All claims expressed in this article are solely those of the authors and do not necessarily represent those of their affiliated organizations, or those of the publisher, the editors and the reviewers. Any product that may be evaluated in this article, or claim that may be made by its manufacturer, is not guaranteed or endorsed by the publisher.

References

1. Saeedi P, Petersohn I, Salpea P, Malanda B, Karuranga S, Unwin N, et al. Global and regional diabetes prevalence estimates for 2019 and projections for 2030 and 2045: Results from the international diabetes federation diabetes atlas, 9(th) edition. *Diabetes Res Clin Pract* (2019) 157:107843. doi: 10.1016/j.diabres.2019.107843

2. Wang Y, Luo W, Han J, Khan ZA, Fang Q, Jin Y, et al. MD2 activation by direct AGE interaction drives inflammatory diabetic cardiomyopathy. *Nat Commun* (2020) 11:2148. doi: 10.1038/s41467-020-15978-3

3. Gulsin GS, Brady EM, Swarbrick DJ, Athithan L, Henson J, Baldry E, et al. Rationale, design and study protocol of the randomised controlled trial: Diabetes interventional assessment of slimming or training tO lessen inconspicuous cardiovascular dysfunction (the DIASTOLIC study). *BMJ Open* (2019) 9: e023207. doi: 10.1136/bmjopen-2018-023207

4. Guo R, Hua Y, Rogers O, Brown TE, Ren J, Nair S. Cathepsin K knockout protects against cardiac dysfunction in diabetic mice. *Sci Rep* (2017) 7:8703. doi: 10.1038/s41598-017-09037-z

5. Li T, Ma X, Fedotov D, Kjaerulff L, Frydenvang K, Coriani S, et al. Structure elucidation of prenyl- and geranyl-substituted coumarins in gerbera piloselloides by NMR spectroscopy, electronic circular dichroism calculations, and single crystal X-ray crystallography. *Mol (Basel Switzerland)* (2020) 25:1706. doi: 10.3390/molecules25071706

6. Popov D. Novel protein tyrosine phosphatase 1B inhibitors: interaction requirements for improved intracellular efficacy in type 2 diabetes mellitus and obesity control. *Biochem Biophys Res Commun* (2011) 410:377–81. doi: 10.1016/j.bbrc.2011.06.009

7. Zhao Y, Tang Z, Shen A, Tao T, Wan C, Zhu X, et al. The role of PTP1B O-GlcNAcylation in hepatic insulin resistance. *Int J Mol Sci* (2015) 16:22856–69. doi: 10.3390/ijms160922856

8. Hess DT, Stamler JS. Regulation by s-nitrosylation of protein post-translational modification. *J Biol Chem* (2012) 287:4411–8. doi: 10.1074/jbc.R111.285742

9. Sharma B, Xie L, Yang F, Wang W, Zhou Q, Xiang M, et al. Recent advance on PTP1B inhibitors and their biomedical applications. *Eur J med Chem* (2020) 199:112376. doi: 10.1016/j.ejmech.2020.112376

10. Ye H, He Y, Zheng C, Wang F, Yang M, Lin J, et al. Type 2 diabetes complicated with heart failure: Research on therapeutic mechanism and potential drug development based on insulin signaling pathway. *Front Pharmacol* (2022) 13:816588. doi: 10.3389/fphar.2022.816588

11. Boutagy NE, Singh AK, Sessa WC. Targeting the vasculature in cardiometabolic disease. *J Clin Invest* (2022) 132:e148556. doi: 10.1172/jci148556

12. Ren J, Wu NN, Wang S, Sowers JR, Zhang Y. Obesity cardiomyopathy: evidence, mechanisms, and therapeutic implications. *Physiol Rev* (2021) 101:1745–807. doi: 10.1152/physrev.00030.2020

13. Monteiro JP, Bennett M, Rodor J, Caudrillier A, Ulitsky I, Baker AH. Endothelial function and dysfunction in the cardiovascular system: the long non-coding road. *Cardiovasc Res* (2019) 115:1692–704. doi: 10.1093/cvr/cvz154

14. Sardu C, Paolisso P, Sacra C, Mauro C, Minicucci F, Portoghese M, et al. Effects of metformin therapy on coronary endothelial dysfunction in patients with prediabetes with stable angina and nonobstructive coronary artery stenosis: The CODYCE multicenter prospective study. *Diabetes Care* (2019) 42:1946–55. doi: 10.2337/dc18-2356

15. Pi X, Xie L, Patterson C. Emerging roles of vascular endothelium in metabolic homeostasis. *Circ Res* (2018) 123:477–94. doi: 10.1161/circresaha.118.313237

16. Lau B, Fazelinia H, Mohanty I, Raimo S, Tenopoulou M, Doulias PT, et al. Endogenous s-nitrosocysteine proteomic inventories identify a core of proteins in heart metabolic pathways. *Redox Biol* (2021) 47:102153. doi: 10.1016/j.redox.2021.102153

17. Li S, Whorton AR. Regulation of protein tyrosine phosphatase 1B in intact cells by s-nitrosothiols. *Arch Biochem biophys* (2003) 410:269–79. doi: 10.1016/s0003-9861(02)00696-3

18. Jiang T, Peng D, Shi W, Guo J, Huo S, Men L, et al. IL-6/STAT3 signaling promotes cardiac dysfunction by upregulating FUNDC1-dependent mitochondria-associated endoplasmic reticulum membranes formation in sepsis mice. *Front Cardiovasc Med* (2021) 8:790612. doi: 10.3389/fcvm.2021.790612

19. Wei J, Zhao Y, Liang H, Du W, Wang L. Preliminary evidence for the presence of multiple forms of cell death in diabetes cardiomyopathy. *Acta Pharm Sinica B* (2022) 12:1–17. doi: 10.1016/j.apsb.2021.08.026

20. Heitmeier MR, Payne MA, Weinheimer C, Kovacs A, Hresko RC, Jay PY, et al. Metabolic and cardiac adaptation to chronic pharmacologic blockade of facilitative glucose transport in murine dilated cardiomyopathy and myocardial ischemia. *Sci Rep* (2018) 8:6475. doi: 10.1038/s41598-018-24867-1

21. Szablewski L. Glucose transporters in healthy heart and in cardiac disease. *Int J Cardiol* (2017) 230:70–5. doi: 10.1016/j.ijcard.2016.12.083

22. Chen ZF, Li YB, Han JY, Wang J, Yin JJ, Li JB, et al. The double-edged effect of autophagy in pancreatic beta cells and diabetes. *Autophagy* (2011) 7:12–6. doi: 10.4161/auto.7.1.13607

23. Bjørkøy G, Lamark T, Pankiv S, Øvervatn A, Brech A, Johansen T. Monitoring autophagic degradation of p62/SQSTM1. *Methods enzymol* (2009) 452:181–97. doi: 10.1016/s0076-6879(08)03612-4

24. Kaiser N, Sasson S, Feener EP, Boukobza-Vardi N, Higashi S, Moller DE, et al. Differential regulation of glucose transport and transporters by glucose in vascular endothelial and smooth muscle cells. *Diabetes* (1993) 42:80–9. doi: 10.2337/diab.42.1.80

25. Huang Y, Lei L, Liu D, Jovin I, Russell R, Johnson RS, et al. Normal glucose uptake in the brain and heart requires an endothelial cell-specific HIF-1α-dependent function. *Proc Natl Acad Sci United States America* (2012) 109:17478–83. doi: 10.1073/pnas.1209281109

26. Baron AD, Steinberg HO, Chaker H, Leaming R, Johnson A, Brechtel G. Insulin-mediated skeletal muscle vasodilation contributes to both insulin sensitivity and responsiveness in lean humans. *J Clin Invest* (1995) 96:786–92. doi: 10.1172/jci118124

27. Nirengi S, Peres Valgas da Silva C, Stanford KI. Disruption of energy utilization in diabetic cardiomyopathy; a mini review. *Curr Opin Pharmacol* (2020) 54:82–90. doi: 10.1016/j.coph.2020.08.015

28. Khan ZA, Chakrabarti S. Endothelins in chronic diabetic complications. *Can J Physiol Pharmacol* (2003) 81:622–34. doi: 10.1139/y03-053

29. Feener EP, King GL. Endothelial dysfunction in diabetes mellitus: role in cardiovascular disease. *Heart failure monitor* (2001) 1:74–82.

30. Wang M, Li Y, Li S, Lv J. Endothelial dysfunction and diabetic cardiomyopathy. *Front Endocrinol* (2022) 13:851941. doi: 10.3389/fendo.2022.851941

31. Tongers J, Fiedler B, König D, Kempf T, Klein G, Heineke J, et al. Heme oxygenase-1 inhibition of MAP kinases, calcineurin/NFAT signaling, and hypertrophy in cardiac myocytes. *Cardiovasc Res* (2004) 63:545–52. doi: 10.1016/j.cardiores.2004.04.015

32. Ashley E, Chun HJ, Quertermous T. Opposing cardiovascular roles for the angiotensin and apelin signaling pathways. *J Mol Cell Cardiol* (2006) 41:778–81. doi: 10.1016/j.yjmcc.2006.08.013

33. Shinmura K, Tamaki K, Sato T, Ishida H, Bolli R. Prostacyclin attenuates oxidative damage of myocytes by opening mitochondrial ATP-sensitive k+ channels via the EP3 receptor. *Am J Physiol Heart Circulatory Physiol* (2005) 288:H2093–101. doi: 10.1152/ajpheart.01003.2004

34. Campos-Almazán MI, Hernández-Campos A, Castillo R, Sierra-Campos E, Valdez-Solana M, Avitia-Domínguez C, et al. Computational methods in cooperation with experimental approaches to design protein tyrosine phosphatase 1B inhibitors in type 2 diabetes drug design: A review of the achievements of this century. *Pharm (Basel Switzerland)* (2022) 15:866. doi: 10.3390/ph15070866

35. Teimouri M, Hosseini H, ArabSadeghabadi Z, Babaei-Khorzoughi R, Gorgani-Firuzjaee S, Meshkani R. The role of protein tyrosine phosphatase 1B (PTP1B) in the pathogenesis of type 2 diabetes mellitus and its complications. *J Physiol Biochem* (2022) 78:307-322. doi: 10.1007/s13105-021-00860-7

36. Barford D, Flint AJ, Tonks NK. Crystal structure of human protein tyrosine phosphatase 1B. *Sci (New York N.Y.)* (1994) 263:1397–404. doi: 10.1126/science.8128219

37. Thareja S, Aggarwal S, Bhardwaj TR, Kumar M. Protein tyrosine phosphatase 1B inhibitors: a molecular level legitimate approach for the management of diabetes mellitus. *Med Res Rev* (2012) 32:459–517. doi: 10.1002/med.20219

38. Tamrakar AK, Maurya CK, Rai AK. PTP1B inhibitors for type 2 diabetes treatment: a patent review (2011 - 2014). *Expert Opin Ther patents* (2014) 24:1101–15. doi: 10.1517/13543776.2014.947268

39. Li S, Whorton AR. Identification of stereoselective transporters for s-nitroso-L-cysteine: role of LAT1 and LAT2 in biological activity of s-nitrosothiols. *J Biol Chem* (2005) 280:20102–10. doi: 10.1074/jbc.M413164200

frontiers | Frontiers in Endocrinology

TYPE Original Research
PUBLISHED 12 October 2022
DOI 10.3389/fendo.2022.986131

OPEN ACCESS

EDITED BY
Ye Ding,
Georgia State University, United States

REVIEWED BY
Youzhi Zhang,
Hubei University of Science and Technology, China
Yang Gao,
Zhongshan Ophthalmic Center, Sun Yat-sen University, China

*CORRESPONDENCE
Xiaobo Xia
xbxia21@163.com
Lexi Ding
lexiding@csu.edu.cn

†These authors have contributed equally to this work

SPECIALTY SECTION
This article was submitted to Cellular Endocrinology, a section of the journal Frontiers in Endocrinology

RECEIVED 04 July 2022
ACCEPTED 26 September 2022
PUBLISHED 12 October 2022

CITATION
Wang C, An Y, Xia Z, Zhou X, Li H, Song S, Ding L and Xia X (2022) The neuroprotective effect of melatonin in glutamate excitotoxicity of R28 cells and mouse retinal ganglion cells. *Front. Endocrinol.* 13:986131. doi: 10.3389/fendo.2022.986131

The neuroprotective effect of melatonin in glutamate excitotoxicity of R28 cells and mouse retinal ganglion cells

Chao Wang[1,2,3†], Yaqiong An[1,2,3†], Zhaohua Xia[1,2,3], Xuezhi Zhou[1,2,3], Haibo Li[1,2,3], Shuang Song[4], Lexi Ding[1,2,3*] and Xiaobo Xia[1,2,3*]

[1]Eye Center of Xiangya Hospital, Central South University, Changsha, China, [2]Hunan Key Laboratory of Ophthalmology, Central South University, Changsha, China, [3]National Clinical Research Center for Geriatric Disorders, Xiangya Hospital, Central South University, Changsha, China, [4]Department of Social Medicine and Health Management, Xiangya School of Public Health, Central South University, Changsha, China

Glaucoma is the leading cause of irreversible blindness. The progressive degeneration of retinal ganglion cells (RGCs) is the major characteristic of glaucoma. Even though the control of intraocular pressure could delay the loss of RGCs, current clinical treatments cannot protect them directly. The overactivation of N-methyl-D-aspartic acid (NMDA) receptors by excess glutamate (Glu) is among the important mechanisms of RGC death in glaucoma progression. Melatonin (MT) is an indole neuroendocrine hormone mainly secreted by the pineal gland. This study aimed to investigate the therapeutic effect of MT on glutamate excitotoxicity of mouse RGCs and R28 cells. The Glu-induced R28 cell excitotoxicity model and NMDA-induced retinal injury model were established. MT was applied to R28 cells and the vitreous cavity of mice by intravitreal injection. Cell counting kit-8 assay and propidium iodide/Hoechst were performed to evaluate cell viability. Reactive oxygen species and glutathione synthesis assays were used to detect the oxidative stress state of R28 cells. Retina immunofluorescence and hematoxylin and eosin staining were applied to assess RGC counts and retinal structure. Flash visual-evoked potential was performed to evaluate visual function in mice. RNA sequencing of the retina was performed to explore the underlying mechanisms of MT protection. Our results found that MT treatment could successfully protect R28 cells from Glu excitotoxicity and decrease reactive oxygen species. Also, MT rescued RGCs from NMDA-induced injury and protected visual function in mice. This study enriches the indications of MT in the treatment of glaucoma, providing practical research ideas for its comprehensive prevention and treatment.

KEYWORDS

melatonin, glaucoma, NMDA, glutamate, oxidative stress, retinal ganglion cell

Introduction

Glaucoma is the leading cause of irreversible blindness in the world, and it is characterized by progressive degeneration of retinal ganglion cells (RGCs) and their axons, accompanied by visual field defects (1). The global prevalence of glaucoma in the 40- to 80-year-old population is estimated to be 3.5%. With the number and proportion of the elderly population increasing, 111.8 million people are expected to suffer from glaucoma by 2040 (2). At present, the management of glaucoma mainly focuses on the regulation of intraocular pressure (IOP) and slowing its progress (3). Many studies have shown that even controlling the increase in IOP cannot prevent the death of RGCs and progressive visual field defects (4–6). For patients with end-stage glaucoma, there is no effective neuroprotective method. Therefore, seeking effective optic neuroprotective medication for the treatment of glaucoma is necessary.

As an excitatory neurotransmitter, glutamate (Glu) exists widely in retinal neurons and is involved in the signal transmission between photoreceptors, bipolar cells, and RGCs through N-methyl-D-aspartic acid (NMDA) receptors (7, 8). In the pathological state of glaucoma, excess Glu between synapses cannot be effectively removed and can cause NMDA receptor overactivation, calcium overload in nerve cells, and oxidative stress damage, leading to the death of RCGs and degeneration, which is called glutamate excitotoxicity (8). Many studies have confirmed glutamate excitotoxicity to be among the important mechanisms of RGC death in glaucoma progression (9–11).

Melatonin (N-acetyl-5-methoxytryptamine, $C_{13}N_2H_{16}O_2$) is an indole neuroendocrine hormone mainly secreted by the pineal gland (12). The secretion of MT has a circadian rhythm. After night falls, the synthesize of MT increases, and the secretion level of MT in the body also increases accordingly, reaching a peak at 2-3 am in the morning. The level of MT at night directly affects the quality of sleep. As a classic antioxidant, MT can protect against oxidative stress damage through different mechanisms, including direct scavenging of reactive oxygen species (ROS), regulation of signaling pathways against oxidative stress, and upregulation of glutathione synthesis (GSH). In addition to MT, many of its metabolites also function as ROS scavengers (13). Through different mechanisms, MT can attenuate oxidative stress damage in lipids, proteins, DNA, and many tissues. Besides being secreted from the pineal gland, MT has also been found to be synthesized and released by many ocular structures, including the retina, ciliary body, lens, and Harderian gland in chickens (13, 14). Studies have shown that MT can exert neuroprotective effects through its anti-oxidative stress effect (15–17),, although its role in neuroprotective effects in glaucoma is still unclear.

In this study, we found that MT showed an effective neuroprotective effect against neuronal glutamate toxicity, and it significantly reduced NMDA-induced loss of RGCs. Moreover, MT treatment significantly reversed changes in the retinal transcriptome caused by NMDA. All these results highlight the potential value of MT as a potential medication for neuroprotection treatment in glaucoma.

Materials and methods

Cell culture and glutamate excitotoxicity model

Immortalized R28 cells (Key Laboratory of Ophthalmology, Xiangya Hospital, Central South University, Changsha, China) were maintained in low-glucose Dulbecco's modified Eagle's medium (11885084, Gibco, Carlsbad, USA) supplemented with 10% fetal bovine serum (FSP500, ExCell Bio, Jiangsu, China) and 1% penicillin-streptomycin (C100C5, NCM Biotech; Zhejiang, China) at 37°C with 5% CO_2. In the glutamate excitotoxicity model, cells were treated with L-Glutamate (ab120049, Abcam, Cambridge, UK) and incubated for 24 h.

Cell viability assay

Cell viability was measured by cell counting kit-8 (CCK-8; C6005, NCM Biotech). R28 cells were seeded in 96-well plates at a density of 5000 cells/well and cultured in a medium containing various concentrations of Glu (5, 10, 15, 20, 25 mM). After 24 h incubation, 10% CCK-8 was added and incubated at 37°C for 3h, as per the manufacturer's instructions. Absorbance was measured at 450 nm using a microplate reader. Meanwhile, propidium iodide (PI)/Hoechst was applied to calculate the R28 cell survival rate after Glu and MT (M5250, Sigma-Aldrich, St. Louis, MO, USA) were treated for 24 h; cells were stained using apoptosis and necrosis assay kit (C1056, Beyotime, Shanghai, China) and pictured using an optical microscope (Eclipse C1, Nikon, Tokyo, Japan).

ROS assay

Intracellular ROS were detected using a cellular ROS assay kit (ab113851; Abcam). The collected cells were digested with trypsin and then stained in culture media with 20 μM DCFDA and incubated for 30 minutes at 37°C. The cells were washed with 1× buffer after incubation and analyzed immediately with a flow cytometer. Forward and side scatter gates were established to exclude debris and cellular aggregates from the analysis. DCF was excited by the 488 nm laser and detected at 535 nm (typically FL1). The mean florescence intensity (MFI) were analyzed by Flowjo software version 10.0.7.

Reduced glutathione assay

A micro reduced GSH assay kit (BC1175, Solarbio, Beijing, China) was used to detect reduced GSH. A total of 5 million cells were collected and cleaned twice with PBS. The GSH extract was then added twice for repeated freeze–thaw (frozen in liquid nitrogen and dissolved in a 37°C water bath) and centrifuged at 8000 g for 10 min, and the supernatant was collected at 4°C. The GSH content was detected according to the instructions and standardized according to the number of cells.

Animals and NMDA-induced retinopathy mouse model

C57BL/6 mice (8 weeks old; Slaccas, Changsha, China) were fed with standard laboratory food and water in a comfortable environment with a 12 h light–dark cycle. All the experimental procedures were approved by the Institutional Animal Care and Use Committee (IACUC) of Central South University (Changsha, China). All mice were divided into Three groups: Sham (only acupuncture without injection), NMDA (20 mM), and MT (20 mM NMDA + 400 mM MT). All the mice were anesthetized with pentobarbital (1%, 80 mg/kg, intraperitoneal injection; Beijing Sanshu, China) and then operated on under a stereomicroscope. Oxybuprocaine hydrochloride (Santen Pharmaceuticals, Tokyo, Japan) was used to induce ocular surface anesthesia, and tropicamide phenylephrine (Santen Pharmaceuticals) was used to dilate the pupils. A 30 G needle was inserted into the vitreous cavity along the limbus and injected at a volume of 1 μL per eye. Tobramycin dexamethasone eye ointment (Alcon Inc, Geneva, Switzerland) was used to prevent infection after injection. The mice were euthanized 5 d after the injection, and their eyeballs were removed with tweezers for the follow-up research.

Flash visual-evoked potential analysis

Visual function was assessed by flash visual-evoked potential analysis (FVEP) 5 d after intravitreal injection, all after anesthesia. After 15 min of dark adaptation, the following 3 electrodes were fixed separately and inserted under the skin: ground electrode (ack), cathode (anterior bregma), and anode (occipital bone). After covering the contralateral eye, the images of both eyes were measured by a multifocal electroretinography recorder (GT-2008V-VI, Gotec, Chongqing, China) and recorded by Ganzfeld electrodiagnostic system (Gotec). The time of the flash is 100 ms. The first negative wave amplitude and first positive wave latencies were used to assess the visual function in mice.

Hematoxylin and eosin staining

The mice were euthanized 5 days after modeling, and their eyeballs were removed and fixed with an FAS eyeball fixator (G1109, Servicebio, Wuhan, China). The eyeballs were embedded in paraffin and cut into 4 μm vertical sections. Sections were stained with hematoxylin and eosin (H&E; G1120, Servicebio) according to the manufacturer's instructions and visualized using an optical microscope (Eclipse C1). CaseViewer software (3DHISTEC, Sysmex, Switzerland) was used to measure the thickness of the ganglion cell layer at distances of 300, 600, 900, 1200, and 1500 μm from the optic nerve center.

Retina immunofluorescence and RBPMS staining

The mice were euthanized 5 days after modeling, and their eyeballs were removed and fixed with 4% paraformaldehyde (G1101, Servicebio) fixation for 1 h, and the retinas were detached under a stereomicroscope. The retinas were sealed with 5% bovine serum albumin and 0.5% Triton-X100 in PBS for 1.5 h at room temperature, followed by incubation with primary antibody RBPMS (ab152101, Abcam) at 4°C overnight. They was cleaned with 0.5% Triton-X100 in PBS 4 times for 5 min each were then incubated with fluorescent-labeled secondary antibody away from light for 2 h at ambient temperature. The retinas were then viewed and pictured by optical microscope (Eclipse C1).

RNA sequencing

The mouse retinas were collected 5 days after NMDA intervention. Three individual retinas were treated as one sample, and each group contained 3 samples. RNA was isolated by total RNA kit (R6834-01, Omega Bio-Tek),. Total amounts and integrity of RNA were assessed using the RNA Nano 6000 assay kit of the Bioanalyzer 2100 system (Agilent Technologies, CA, USA). After RNA was converted to cDNA, the samples were sequenced by the Illumina NovaSeq 6000 at Novogene (Beijing, China). Genes with a fold-change ≥1.5 identified by edgeR and a false discovery rate <0.05 were considered differentially expressed (BMKCloud, http://www.biocloud.net/). Gene functional annotations were based on the Kyoto Encyclopedia of Genes and Genomes (KEGG, https://www.genome.jp/kegg/) and Gene Ontology (GO, http://www.geneontology.org/) databases.

Statistical analysis

SPSS 26.0 statistical software (IBM Corp., Armonk, NY, USA) was used for statistical analysis of all data. All data were presented as the mean ± standard deviation (SD). One-way analysis of variance (ANOVA) was used to assess the significance differences of cell viability, ROS, GSH, RGCs survival and FVEP results between groups. Repeated measures ANOVA was used to assess thickness of retinal ganglion cell

complex (GCC). Charts were built using GraphPad Prism 6.0 (GraphPad Inc., La Jolla, CA, USA). P value <0.05 was statistically significant.

Results

MT protects R28 cells from Glu-induced excitotoxicity

To investigate the appropriate concentration of Glu, R28 cells were treated with 5-25mM Glu at different concentrations for 24 h. CCK-8 assay results showed that cell viability decreased gradually with increasing Glu concentration in a concentration-dependent manner. Compared with the control group, 10 mM (47.90 ± 15.50%), 15 mM (26.41 ± 5.48%), 20 mM (5.41 ± 3.86%), 25 mM (4.73 ± 1.43%) significant decreased cell viability with Glu treatment for 24 h. (P <0.001, n = 4) (Figure 1A). In subsequent experiments, R28 cells were treated with 10 mM Glu for 24 h as the immobilization condition. Subsequently, we investigated the protective effect of different concentrations of MT on glutamate-induced excitotoxicity injury. The results showed that compared with the Glu group, the cell viability of the MT group was significantly increased with the increasing MT concentration. The cell viability reached 109.1 ± 6.9% when the concentration of MT was at 400 μM (P <0.001, n = 6) (Figure 1B), suggesting that MT has a protective effect on Glu-induced R28 cell damage, and the MT at concentration of 600 μM, 800 μM and 1000 μM also showed good protective effect (P <0.001, n = 6). Meanwhile, PI/Hoechst staining was used to confirm this view, and it was observed that R28 cells died more after 24 h of glutamate treatment, while MT saved this damage (Figure 1C). These results suggest that MT can protect R28 cells from glutamate-induced excitotoxicity.

MT protects R28 cells from Glu-induced oxidative stress

To investigate the effects of MT on Glu-induced oxidative stress in R28 cells, intracellular ROS and reduced GSH levels were detected. The results showed that ROS levels increased gradually over time after Glu treatment and peaked at 12 h (7.42 ± 0.52), and MT treatment could ameliorate the changes induced by Glu (3.67 ± 0.30, P <0.001, n = 3) (Figures 2A, B). At 24 h, MT was still protective (5.14 ± 0.43, P <0.01, n = 3), but this was not as significant as at 12 h (Figures 2A, B). Meanwhile, with the increase in Glu treatment time, the intracellular GSH level

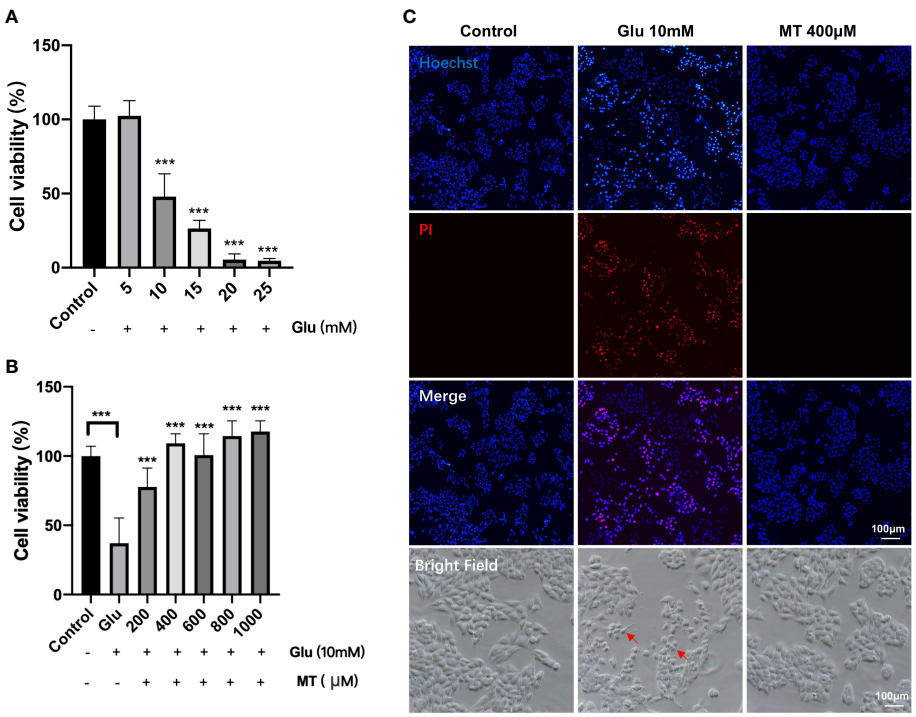

FIGURE 1
MT protects R28 cells from glutamate-induced excitotoxicity. **(A)** Effects of different concentrations of Glu on R28 cell viability after 24 h treatment. (n = 4) **(B)** Protective effect of different concentrations of MT on R28 cells treated with 10 mM glutamate for 24h. (n=6) **(C)** Pictures of R28 cells stained by PI and Hoechst. Red arrows: glutamate-induced excitotoxicity of R28 cells. Data are the mean ± SD; ***p < 0.001. Scale bar = 50 μm.

gradually decreased and reached its lowest at 24 h (0.20 ± 0.01, P <0.001, n = 3) (Figure 2C). However, the GSH level of the MT group was not significantly improved when compared with the Glu group (0.16 ± 0.02, P >0.05, n = 3) (Figure 2C).

MT protects against NMDA-induced retinal damage in mice

To further determine the protective effect of MT on retinal excitotoxicity, the thickness of GCC was measured after H&E staining, and RGCs were counted and quantitatively analyzed after being labeled with RBPMS by retinal immunofluorescence. H&E staining showed that the retinal GCC thickness of mice in the NMDA group was significantly thinner than that in the control group 5 days after intravitreal injection of NMDA (P <0.001, n = 4) (Figures 3A, B). MT treatment could effectively inhibit the thinning of the GCC layer caused by NMDA at 300, 600 and 900 μm from the optic nerve center (P <0.05, n = 4). Retinal immunofluorescence showed that the density of RGCs in the NMDA group was significantly lower than that in the control group, while the number of surviving RGCs in the MT group (1883.10 ± 124.63) was significantly better than that in the NMDA group (849.30 ± 47.10) but still lower than that in the control group (2694.60 ± 145.85, P <0.001, n = 4) (Figure 3C). These results suggest that MT has a protective effect on NMDA-induced retinal injury in mice.

MT protects visual function in mice

We also studied the effect of MT on electrophysiological activity of the retina and its protective effect on visual function in mice. The amplitude of N1 wave was decreased NMDA treatment (1.98 ± 0.76 μV) compared with control group (4.87 ± 1.10 μV), and MT increase amplitude of N1(4.85 ± 0.82 μV, P <0.001, n = 6).The latencies of P2 wave were prolonged 5 days after intravitreal injection in the NMDA group (115.42 ± 5.45 ms) compared with control group (84.83 ± 3.52 ms), and MT ameliorated this change (103.91 ±

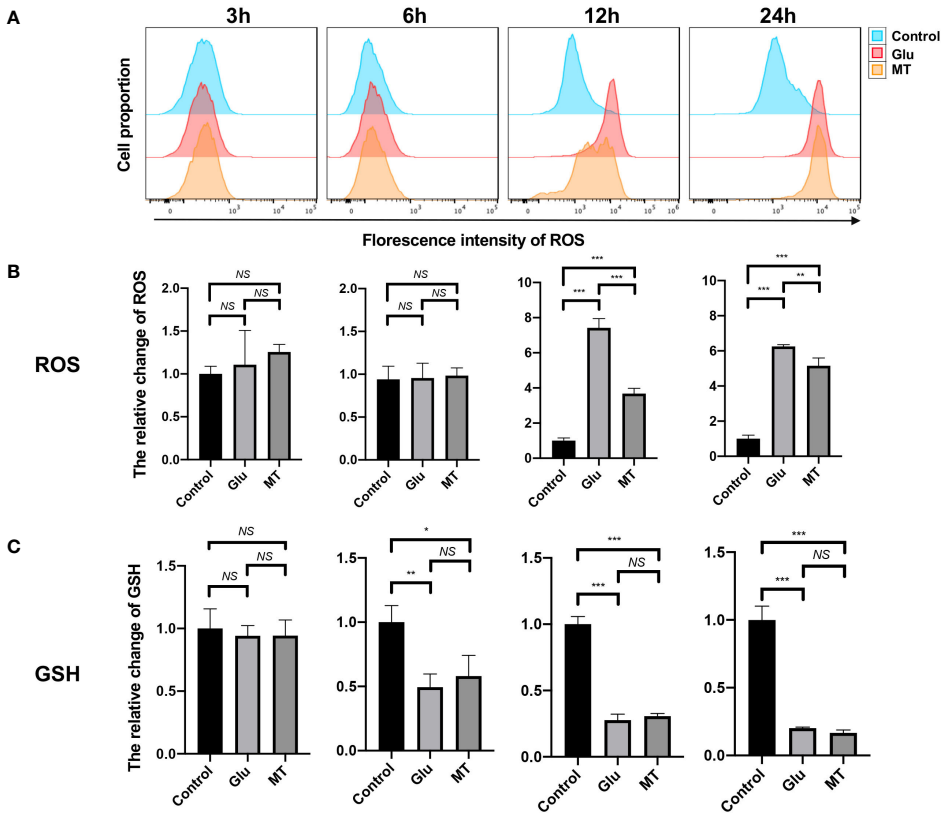

FIGURE 2
MT protects R28 cells from Glu-induced oxidative stress. **(A, B)** ROS levels increased gradually over time after glutamate treatment, and MT could ameliorate this change. (n = 3) **(C)** GSH levels decreased over time, but MT treatment could not rescue this change. (n = 3) Data are the mean ± SD; NS, No Significant, *p < 0.05, **p < 0.01, ***p < 0.001.

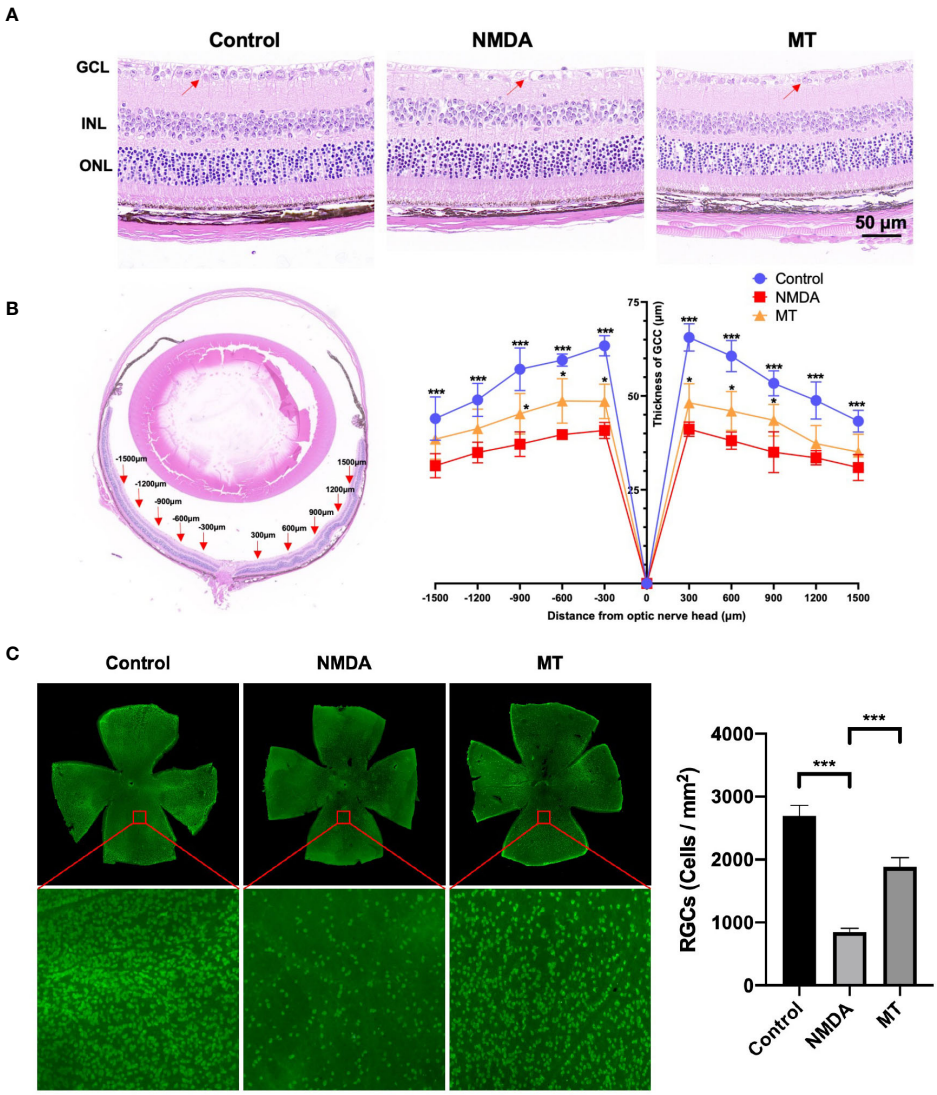

FIGURE 3
MT protects against NMDA-induced retinal damage in mice. **(A)** Images of H&E staining sections of mice retina at 5 days after intravitreal injection (Scale bar = 50 μm). Red arrows: RGCs. **(B)** At 5 days after intravitreal injection of NMDA, the GCC thickness of mice was measured ±300, ± 600, ± 900, ±1200, and ±1500 μm away from the optic nerve. (n=4) **(C)** Labeling of RGCs with RBPMS 5 days after intravitreal injection of NMDA. MT improved the density reduction of NMDA-induced RGC injury in mice (Scale bar = 100 μm). (n=4) Data are the mean ± SD; *p < 0.05, ***p < 0.001.

5.28, P <0.005, n = 6) (Figure 4). These results suggest that NMDA causes retinal dysfunction in mice, and MT can improve the visual conduction dysfunction induced by excitotoxicity.

MT ameliorated transcriptome abnormalities in NMDA-induced retinal injury

To investigate further the mechanism of the neuroprotective effects of MT on the retina, RNA sequencing analysis was performed. Compared with the control group, the NMDA-treated group had 1519 upregulated genes and 1663 downregulated genes. With the intervention of the MT, 139 genes were upregulated and 227 genes downregulated (Figure 5A). MT treatment mitigated the expression of approximately 49 upregulated genes and 57 downregulated genes induced by NMDA (Figure 5B). These genes included 5 neuroactive ligand-receptor interaction-related genes (Oprl1/Ptafr/Adcyap1r1/Lpar6/Crhr1), 3 PI3K-Akt signaling pathway-related genes (Col6a3/Lpar6/Gng4), and 3 calcium signaling pathway-related genes (Ptafr/Prkcg/Orai3). These results suggest that MT exhibits its neuroprotective effect by ameliorating retinal transcriptome abnormalities (Figure 5C).

10.3389/fendo.2022.986131

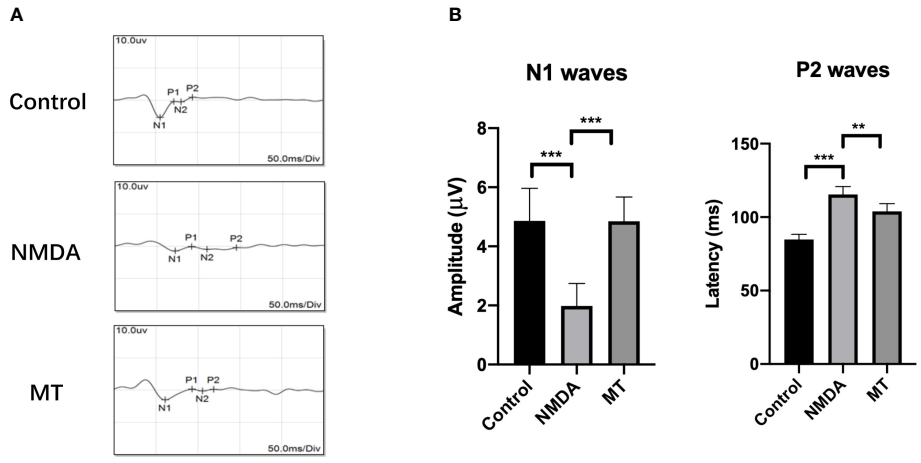

FIGURE 4
MT protects visual function in mice. **(A)** FVEP images of mice after intravitreal injection of NMDA 5 days. **(B)** The amplitude of N1 waves and the latencies of P2 waves of FVEPs in mice at 5 days after injection. (n = 6) Data are the mean ± SD; **p < 0.01, ***p < 0.001. Scale bar = 10.0 μV and 50 ms.

Analysis of differentially expressed genes in NMDA-treated and MT-treated mice retinas

KEGG and GO analyses were performed to densify the signaling pathway and biological process changes in the retina. We performed KEGG analysis on the differentially expressed genes in the control, NMDA, and MT groups. This indicated that the PI3K-Akt and MAPK signaling pathways were both crucial after NMDA intervention. After MT treatment, the PI3K-Akt and JAK-STAT pathways were involved in rescuing the injury induced by NMDA (Figure 6A). GO analysis results showed that the retinal biological process, cellular component, and molecular function were all altered by MT intervention. The differentially expressed genes were enriched in the biological process (Figure 6B).

Discussion

The characteristic death of RGCs is one of the most important features of glaucoma, which can cause irreversible visual field defects and seriously affect the life quality of patients (18, 19). Although many glaucoma medications have been applied in clinical treatment, their use for glaucomatous neuroprotection is still very limited, and there are no clear clinical outcomes (20, 21).

Many studies have shown a potential relationship between MT and glaucoma. Patients with glaucoma are often accompanied by sleep disturbances, anxiety, and depression, and studies have shown that glaucoma is also associated with disturbances in the rhythm of MT secretion (22, 23). Recent studies showed that urinary 6-sulfatoxymelatonin, the main metabolite of serum MT in glaucoma patients, is significantly lower than normal, suggesting the possibility of a circadian rhythm disturbance in glaucoma patients, which MT can restore (24).

Focusing on the eye, although MT can be secreted by various eye structures, and the aqueous humor also contains a certain concentration of MT (25), the role of MT in the eye is still unclear. Concentrations of MT have been shown to be 3 times higher in aqueous humor in patients with elevated IOP than in normal patients, and the same was also observed in a mouse model of glaucoma (26). Preoperative treatment with oral MT has been shown to reduce IOP in patients who have undergone cataract surgery (27). Animal models and clinical trials have also shown that MT and its analogs can reduce IOP (28, 29). Some studies have demonstrated that MT exerts antiapoptotic and neuroprotective effects on retinal neurons after hypoxia-ischemia and acute intraocular hypertension (30, 31). In our study, we established the classical NMDA-induced retinal injury model, which imitated the different mechanisms of RGC death in the pathogenesis of glaucoma. We found that MT has a significant protective effect on cellular Glu excitotoxicity both *in vivo* and *in vitro* and provides a supplement to the protective role of melatonin in the pathogenesis of different glaucoma.

We found that MT at a concentration of 400 μM had a 100% protective effect on Glu-induced cell excitotoxicity in R28 cells, and a high concentration of 1000 μM had no toxic effect on cells, confirming that MT is effective and safe. MT also showed a good neuroprotective effect *in vivo*. MT rescued NMDA-induced RGC loss and GCC thinning, and through the detection of FVEP, it was

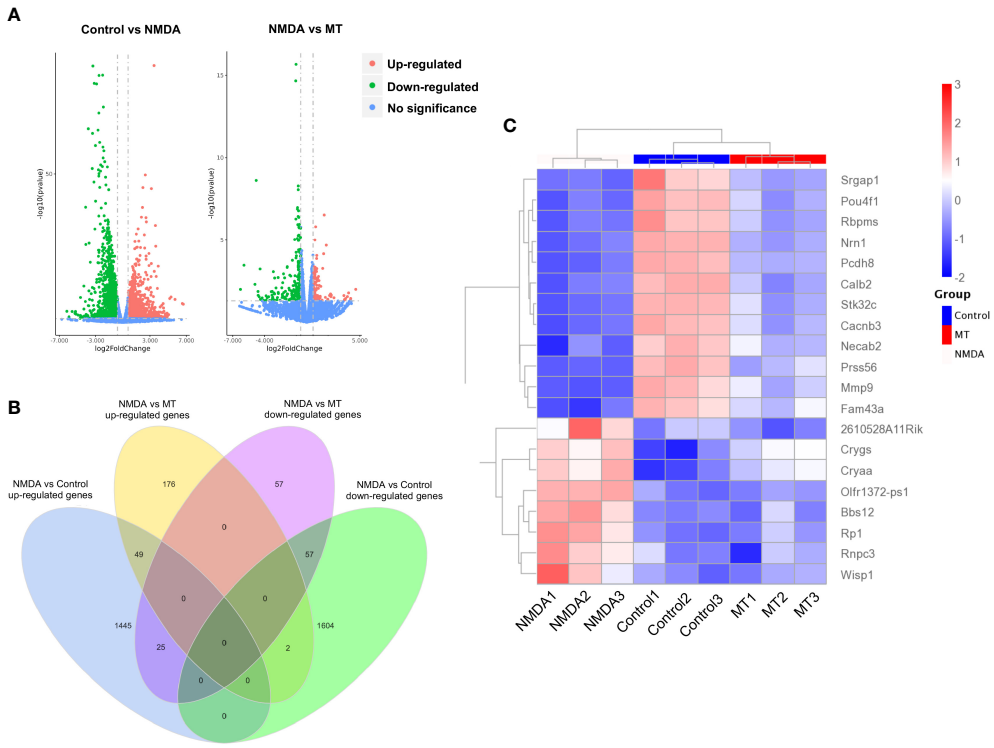

FIGURE 5
MT ameliorates retinal transcriptome abnormalities in NMDA-induced retinal injury. **(A)** Volcano plot of differentially expressed genes between control, NMDA, and MT groups. **(B)** Venn diagram shows the differentially expressed genes among the control, NMDA, and MT group. **(C)** The heat map shows MT-restored top 20 genes.

confirmed that melatonin can restore partial visual function in mice. As an endocrine hormone with strong anti-oxidative stress ability, MT has strong potential for the neuroprotection of glaucoma.

As a classic antioxidant, MT can effectively scavenge ROS and increase the content of intracellular GSH to resist oxidative stress injury (32). In our study, we found that after glutamate excitotoxicity injury, although MT had a significant protective effect on R28 and RGCs and a significant recovery of visual function in mice, it did not increase the content of GSH. As a common antioxidative product, its depletion is much greater than its synthesis in the glutamate excitotoxicity process. ROS was significantly higher than that in the Glu group at 24 h, but it still had a 5.16-fold increase compared to the control group. Therefore, we speculate that, in addition to the scavenging effect of MT on ROS, other mechanisms also play a key role in the process of neuroprotective effect.

To explore the mechanism of action of the neuroprotective effect of MT, we conducted RNA sequencing of the retina, and the sequencing results of this study found that MT rescued abnormal retinal transcriptome expression induced by NMDA. Through further gene enrichment, we found significant changes in the PI3K-AKT and MAPK signaling pathways in NMDA-induced retinal injury, and after MT treatment, different genes were enriched to the P13K-AKT and JAK-STAT signaling pathways. This is consistent with many of the studies that showed PI3K-AKT and MAPK to be involved in the occurrence and development of glaucoma and play an important role in the death of RGCs (33–36). Studies have also shown that RGCs are protected by intervening PI3K-AKT and JAK-STAT signaling pathways through regulating apoptosis, autophagy, and oxidative stress processes (37–41). In our study, sequencing results showed a neuroprotective effect, suggesting that MT may depend on the above pathways. However, the specific mechanism of action needs to be studied further.

Conclusion

This study explored the neuroprotective effects of MT on NMDA-reduced RGC death and Glu-induced R28 cell excitotoxicity. It found that MT successfully rescues RGCs from NMDA-reduced injury and protects visual function in

10.3389/fendo.2022.986131

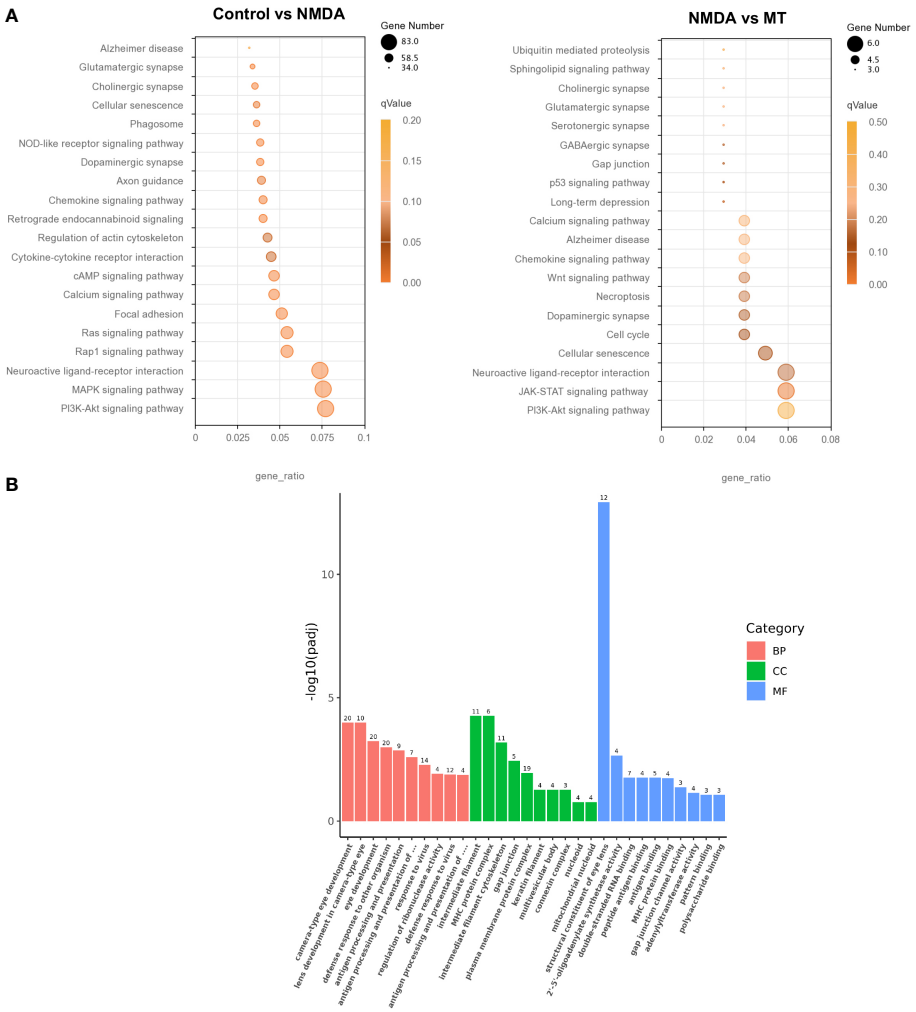

FIGURE 6
Analysis of differentially expressed genes in NMDA- and MT-treated mice retina. **(A)** KEGG analysis of differentially expressed genes between control, NMDA, and MT group. **(B)** Go analysis of differentially expressed genes between control, NMDA, and MT group in biological process (BP), cellular component (CC), and molecular function (MF).

mice. MT also protects R28 cells from Glu excitotoxicity and decreases ROS. RNA sequencing indicated that MT treatment repairs the abnormal transcriptome caused by NMDA, and PI3K-AKT and JAK-STAT signaling pathways may play an important role in this process. This study provides practical research ideas for the comprehensive prevention and treatment of glaucoma.

Data availability statement

The datasets presented in this study can be found in online repositories. The names of the repository/repositories and accession number(s) can be found here: https://www.ncbi.nlm.nih.gov/bioproject/, SRA PRJNA867307.

Ethics statement

The animal study was reviewed and approved by Institutional Animal Care and Use Committee (IACUC) of Central South University.

Author contributions

CW and YA wrote the first draft of the paper. XX and LD edited the paper. XX, LD and CW designed research. CW, YA performed laboratory research. ZX performed FVEP examination. XZ performed bioinformatics Analysis, CW, YA and SS analyzed data. All authors contributed to the article and approved the submitted version.

Funding

This study was financially supported by The National Key Research and Development Program of China (No.2020YFC2008205), The National Natural Science Foundation of China (No. 82171058, No.81974134 for XX, No.82070966 to LD, No.8210041510 to CW), Key R&D Plan of Hunan Province of China (No.2020SK2076 to XX), Science and Technology Innovation Program of Hunan Province (No.2021RC3026 to LD), Natural Science Foundation of Hunan Province (No.2021JJ41021 to CW) and China Postdoctoral Science Foundation (No.2021M693556 to CW).

Acknowledgments

We thank Lemeng Feng, Weizhou Fang, Shirui Dai, Cheng Zhang and Wulong Zhang for technical assistance. We thank Scribendi (https://www.scribendi.com/) for editing the English text of a draft of this manuscript.

Conflict of interest

The authors declare that the research was conducted in the absence of any commercial or financial relationships that could be construed as a potential conflict of interest.

Publisher's note

References

1. Weinreb RN, Aung T, Medeiros FA. The pathophysiology and treatment of glaucoma: a review. *JAMA* (2014) 311(18):1901–11. doi: 10.1001/jama.2014.3192

2. Tham YC, Li X, Wong TY, Quigley HA, Aung T, Cheng CY. Global prevalence of glaucoma and projections of glaucoma burden through 2040: a systematic review and meta-analysis. *Ophthalmology* (2014) 121(11):2081–90. doi: 10.1016/j.ophtha.2014.05.013

3. De Moraes CG, Liebmann JM, Levin LA. Detection and measurement of clinically meaningful visual field progression in clinical trials for glaucoma. *Prog Retin Eye Res* (2017) 56:107–47. doi: 10.1016/j.preteyeres.2016.10.001

4. Villasana GA, Bradley C, Ramulu P, Unberath M, Yohannan J. The effect of achieving target intraocular pressure on visual field worsening. *Ophthalmology* (2022) 129(1):35–44. doi: 10.1016/j.ophtha.2021.08.025

5. Manabe Y, Sawada A, Yamamoto T. Localization in glaucomatous visual field loss vulnerable to posture-induced intraocular pressure changes in open-angle glaucoma. *Am J Ophthalmol* (2020) 213:9–16. doi: 10.1016/j.ajo.2020.01.010

6. Cheung CY, Li SL, Chan PP, Chan NCY, Tan S, Man X, et al. Intraocular pressure control and visual field changes in primary angle closure disease: the CUHK PACG longitudinal (CUPAL) study. *Br J Ophthalmol* (2020) 104(5):629–35. doi: 10.1136/bjophthalmol-2019-314322

7. Thoreson WB, Witkovsky P. Glutamate receptors and circuits in the vertebrate retina. *Prog Retin Eye Res* (1999) 18(6):765–810. doi: 10.1016/s1350-9462(98)00031-7

8. Shen Y, Liu XL, Yang XL. N-methyl-D-aspartate receptors in the retina. *Mol Neurobiol* (2006) 34(3):163–79. doi: 10.1385/MN:34:3:163

9. Du J, Cleghorn W, Contreras L, Linton JD, Chan GC, Chertov AO, et al. Cytosolic reducing power preserves glutamate in retina. *Proc Natl Acad Sci U.S.A.* (2013) 110(46):18501–6. doi: 10.1073/pnas.1311193110

10. Teuchner B, Dimmer A, Humpel C, Amberger A, Fischer-Colbrie R, Nemeth J, et al. VIP, PACAP-38, BDNF and ADNP in NMDA-induced excitotoxicity in the rat retina. *Acta Ophthalmol* (2011) 89(7):670–5. doi: 10.1111/j.1755-3768.2009.01828.x

11. Guo X, Zhou J, Starr C, Mohns EJ, Li Y, Chen EP, et al. Preservation of vision after CaMKII-mediated protection of retinal ganglion cells. *Cell* (2021) 184 (16):4299–4314 e12. doi: 10.1016/j.cell.2021.06.031

12. Cipolla-Neto J, Amaral FGD. Melatonin as a hormone: New physiological and clinical insights. *Endocr Rev* (2018) 39(6):990–1028. doi: 10.1210/er.2018-00084

13. Reiter RJ, Mayo JC, Tan DX, Sainz RM, Alatorre-Jimenez M, Qin L. Melatonin as an antioxidant: under promises but over delivers. *J Pineal Res* (2016) 61(3):253–78. doi: 10.1111/jpi.12360

14. Wiechmann AF, Summers JA. Circadian rhythms in the eye: the physiological significance of melatonin receptors in ocular tissues. *Prog Retin Eye Res* (2008) 27(2):137–60. doi: 10.1016/j.preteyeres.2007.10.001

15. Wilkinson D, Shepherd E, Wallace EM. Melatonin for women in pregnancy for neuroprotection of the fetus. *Cochrane Database Syst Rev* (2016) 3:CD010527. doi: 10.1002/14651858.CD010527.pub2

16. Melhuish Beaupre LM, Brown GM, Goncalves VF, Kennedy JL. Melatonin's neuroprotective role in mitochondria and its potential as a biomarker in aging, cognition and psychiatric disorders. *Transl Psychiatry* (2021) 11(1):339. doi: 10.1038/s41398-021-01464-x

17. Aridas JD, Yawno T, Sutherland AE, Nitsos I, Wong FY, Hunt RW, et al. Melatonin augments the neuroprotective effects of hypothermia in lambs following perinatal asphyxia. *J Pineal Res* (2021) 71(1):e12744. doi: 10.1111/jpi.12744

18. Fry LE, Fahy E, Chrysostomou V, Hui F, Tang J, van Wijngaarden P, et al. The coma in glaucoma: Retinal ganglion cell dysfunction and recovery. *Prog Retin Eye Res* (2018) 65:77–92. doi: 10.1016/j.preteyeres.2018.04.001

19. Almasieh M, Wilson AM, Morquette B, Cueva Vargas JL, Di Polo A. The molecular basis of retinal ganglion cell death in glaucoma. *Prog Retin Eye Res* (2012) 31(2):152–81. doi: 10.1016/j.preteyeres.2011.11.002

20. Naik S, Pandey A, Lewis SA, Rao BSS, Mutalik S. Neuroprotection: A versatile approach to combat glaucoma. *Eur J Pharmacol* (2020) 881:173208. doi: 10.1016/j.ejphar.2020.173208

21. Guymer C, Wood JP, Chidlow G, Casson RJ. Neuroprotection in glaucoma: recent advances and clinical translation. *Clin Exp Ophthalmol* (2019) 47(1):88–105. doi: 10.1111/ceo.13336

22. Gubin D, Neroev V, Malishevskaya T, Cornelissen G, Astakhov SY, Kolomeichuk S, et al. Melatonin mitigates disrupted circadian rhythms, lowers intraocular pressure, and improves retinal ganglion cells function in glaucoma. *J Pineal Res* (2021) 70(4):e12730. doi: 10.1111/jpi.12730

23. Gubin D, Weinert D. Melatonin, circadian rhythms and glaucoma: current perspective. *Neural Regener Res* (2022) 17(8):1759–60. doi: 10.4103/1673-5374.332149

24. Yoshikawa T, Obayashi K, Miyata K, Saeki K, Ogata N. Decreased melatonin secretion in patients with glaucoma: Quantitative association with glaucoma severity in the LIGHT study. *J Pineal Res* (2020) 69(2):e12662. doi: 10.1111/jpi.12662

25. Viggiano SR, Koskela TK, Klee GG, Samples JR, Arnce R, Brubaker RF. The effect of melatonin on aqueous humor flow in humans during the day. *Ophthalmology* (1994) 101(2):326–31. doi: 10.1016/s0161-6420(94)31332-7

26. Alkozi H, Sanchez-Naves J, de Lara MJ, Carracedo G, Fonseca B, Martinez-Aguila A, et al. Elevated intraocular pressure increases melatonin levels in the aqueous humour. *Acta Ophthalmol* (2017) 95(3):e185–9. doi: 10.1111/aos.13253

27. Ismail SA, Mowafi HA. Melatonin provides anxiolysis, enhances analgesia, decreases intraocular pressure, and promotes better operating conditions during cataract surgery under topical anesthesia. *Anesth Analg* (2009) 108(4):1146–51. doi: 10.1213/ane.0b013e3181907ebe

28. Pescosolido N, Gatto V, Stefanucci A, Rusciano D. Oral treatment with the melatonin agonist agomelatine lowers the intraocular pressure of glaucoma patients. *Ophthal Physiol Opt* (2015) 35(2):201–5. doi: 10.1111/opo.12189

29. Martinez-Aguila A, Fonseca B, Bergua A, Pintor J. Melatonin analogue agomelatine reduces rabbit's intraocular pressure in normotensive and hypertensive conditions. *Eur J Pharmacol* (2013) 701(1-3):213–7. doi: 10.1016/j.ejphar.2012.12.009

30. Huang R, Xu Y, Lu X, Tang X, Lin J, Cui K, et al. Melatonin protects inner retinal neurons of newborn mice after hypoxia-ischemia. *J Pineal Res* (2021) 71(1): e12716. doi: 10.1111/jpi.12716

31. Zhang Y, Huang Y, Guo L, Zhang Y, Zhao M, Xue F, et al. Melatonin alleviates pyroptosis of retinal neurons following acute intraocular hypertension. *CNS Neurol Disord Drug Targets* (2021) 20(3):285–97. doi: 10.2174/1871527319666201012125149

32. NaveenKumar SK, Hemshekhar M, Jagadish S, Manikanta K, Vishalakshi GJ, Kemparaju K, et al. Melatonin restores neutrophil functions and prevents apoptosis amid dysfunctional glutathione redox system. *J Pineal Res* (2020) 69(3): e12676. doi: 10.1111/jpi.12676

33. Galindo-Romero C, Vidal-Villegas B, Asis-Martinez J, Lucas-Ruiz F, Gallego-Ortega A, Vidal-Sanz M. 7,8-dihydroxiflavone protects adult rat axotomized retinal ganglion cells through MAPK/ERK and PI3K/AKT activation. *Int J Mol Sci* (2021) 22(19). doi: 10.3390/ijms221910896

34. Xi X, Chen Q, Ma J, Wang X, Xia Y, Wen X, et al. Acteoside protects retinal ganglion cells from experimental glaucoma by activating the PI3K/AKT signaling pathway *via* caveolin 1 upregulation. *Ann Transl Med* (2022) 10(6):312. doi: 10.21037/atm-22-136

35. Ye MJ, Meng N. Resveratrol acts *via* the mitogen-activated protein kinase (MAPK) pathway to protect retinal ganglion cells from apoptosis induced by hydrogen peroxide. *Bioengineered* (2021) 12(1):4878–86. doi: 10.1080/21655979.2021.1954742

36. Yu H, Zhong H, Li N, Chen K, Chen J, Sun J, et al. Osteopontin activates retinal microglia causing retinal ganglion cells loss *via* p38 MAPK signaling pathway in glaucoma. *FASEB J* (2021) 35(3):e21405. doi: 10.1096/fj.202002218R

37. Zhao N, Shi J, Xu H, Luo Q, Li Q, Liu M. Baicalin suppresses glaucoma pathogenesis by regulating the PI3K/AKT signaling *in vitro* and in vivo. *Bioengineered* (2021) 12(2):10187–98. doi: 10.1080/21655979.2021.2001217

38. Xu K, Li S, Yang Q, Zhou Z, Fu M, Yang X, et al. MicroRNA-145-5p targeting of TRIM2 mediates the apoptosis of retinal ganglion cells *via* the PI3K/AKT signaling pathway in glaucoma. *J Gene Med* (2021) 23(11):e3378. doi: 10.1002/jgm.3378

39. DeParis S, Caprara C, Grimm C. Intrinsically photosensitive retinal ganglion cells are resistant to n-methyl-D-aspartic acid excitotoxicity. *Mol Vis* (2012) 18:2814–27.

40. Luo JM, Cen LP, Zhang XM, Chiang SW, Huang Y, Lin D, et al. PI3K/akt, JAK/STAT and MEK/ERK pathway inhibition protects retinal ganglion cells *via* different mechanisms after optic nerve injury. *Eur J Neurosci* (2007) 26(4):828–42. doi: 10.1111/j.1460-9568.2007.05718.x

41. Vigneswara V, Akpan N, Berry M, Logan A, Troy CM, Ahmed Z. Combined suppression of CASP2 and CASP6 protects retinal ganglion cells from apoptosis and promotes axon regeneration through CNTF-mediated JAK/STAT signalling. *Brain* (2014) 137(Pt 6):1656–75. doi: 10.1093/brain/awu037

frontiers | Frontiers in Endocrinology

TYPE Original Research
PUBLISHED 14 October 2022
DOI 10.3389/fendo.2022.1011669

OPEN ACCESS

EDITED BY
Chengqi Xu,
Huazhong University of Science and Technology, China

REVIEWED BY
Haoxiao Zheng,
Southern Medical University, China
Osama Althunibat,
Al-Hussein Bin Talal University, Jordan

*CORRESPONDENCE
Yanbo Shi
shiyanbocas@163.com

†These authors have contributed equally to this work and share first authorship

SPECIALTY SECTION
This article was submitted to Cellular Endocrinology, a section of the journal Frontiers in Endocrinology

RECEIVED 04 August 2022
ACCEPTED 27 September 2022
PUBLISHED 14 October 2022

CITATION
Du S, Shi H, Xiong L, Wang P and Shi Y (2022) Canagliflozin mitigates ferroptosis and improves myocardial oxidative stress in mice with diabetic cardiomyopathy. *Front. Endocrinol.* 13:1011669. doi: 10.3389/fendo.2022.1011669

Canagliflozin mitigates ferroptosis and improves myocardial oxidative stress in mice with diabetic cardiomyopathy

Shuqin Du[1,2,3,4†], Hanqiang Shi[1,2†], Lie Xiong[1,2], Ping Wang[3] and Yanbo Shi[1,2*]

[1]Central Laboratory of Molecular Medicine Research Center, Jiaxing Traditional Chinese Medicine (TCM) Hospital Affiliated to Zhejiang University of Traditional Chinese Medicine, Jiaxing, China, [2]Jiaxing Key Laboratory of Diabetic Angiopathy Research, Jiaxing, China, [3]School of Pharmacy, Zhejiang University of Technology, Hangzhou, China, [4]School of Medicine, Jiaxing University, Jiaxing, China

Canagliflozin (Cana), an anti-diabetes drug belongs to sodium-glucose cotransporter 2 inhibitor, is gaining interest because of its extra cardiovascular benefits. Ferroptosis is a new mode of cell death, which can promote the occurrence of diabetic cardiomyopathy (DCM). Whether Cana can alleviate DCM by inhibiting ferroptosis is the focus of this study. Here, we induced DCM models in diabetic C57BL6 mice and treated with Cana. Meanwhile, in order to exclude its hypoglycemic effect, the high glucose model in H9C2 cells were established. In the *in vivo* study, we observed that Cana could effectively alleviate the damage of cardiac function in DCM mice, including the increasing of lactate dehydrogenase (LDH) and cardiac troponin I (cTnI), the alleviating of myocardial fiber breakage, inflammation, collagen fiber deposition and mitochondrial structural disorder. We evaluated reactive oxygen species (ROS) levels by DCFH-DA and BODIPY 581/591 C11, *in vitro* Cana reduced ROS and lipid ROS in H9C2 cells induced by high glucose. Meanwhile, JC-1 fluorochrome assay showed that the decreased mitochondrial membrane potential (MMP) was increased by Cana. Furthermore, the inhibitory effects of Cana on myocardial oxidative stress and ferroptosis were verified *in vivo* and *in vitro* by protein carbonyl (PCO), malondialdehyde (MDA), superoxide dismutase (SOD), catalase (CAT), glutathione (GSH). As a key inducer of ferroptosis, the deposition of total iron and Fe^{2+} can be inhibited by Cana both *in vivo* and *in vitro*. In addition, western blot results indicated that the expression of ferritin heavy-chain (FTN-H) was down-regulated, and cystine-glutamate antiporter (xCT) was up-regulated by Cana in DCM mice and cells, suggesting that Cana inhibit ferroptosis by balancing cardiac iron homeostasis and promoting the system Xc^-/GSH/GPX4 axis in DCM. These findings underscore the fact that ferroptosis plays

10.3389/fendo.2022.1011669

an important role in the development and progression of DCM and targeting ferroptosis may be a novel strategy for prevention and treatment. In conclusion, Cana may exert some of its cardiovascular benefits by attenuating ferroptosis.

KEYWORDS

canagliflozin, sodium-glucose cotransporter 2 inhibitor, ferroptosis, mitochondria, diabetic cardiomyopathy, lipid peroxidation

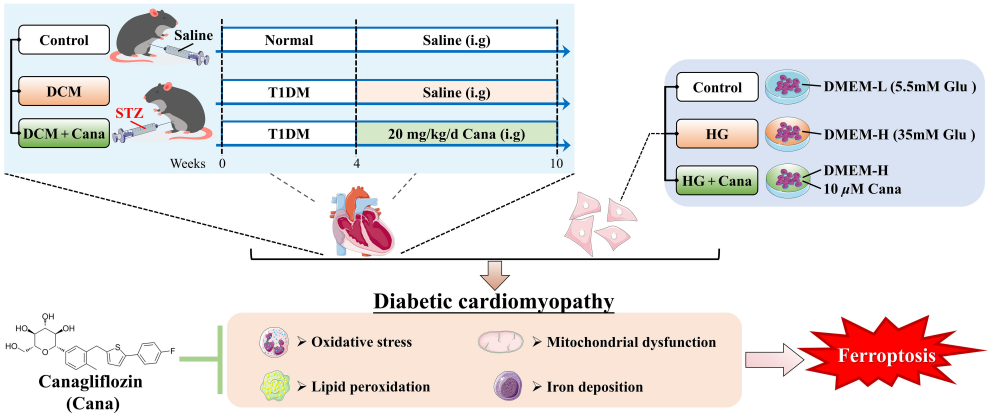

GRAPHICAL ABSTRACT
Canagliflozin mitigates ferroptosis and improves myocardial oxidative stress in mice with diabetic cardiomyopathy.

Introduction

Diabetes is a metabolic disease characterized by chronic hyperglycemia. Long-term hyperglycemia will aggravate the damage of the patient's systemic tissues and organs, leading to a variety of serious complications. It is reported that the probability of cardiovascular disease in diabetic patients is 2-3 times higher than that in non-diabetic patients (1), and diabetic cardiovascular disease has become an important factor causing death and disability in diabetic patients. Among them, diabetic cardiomyopathy (DCM) is a diabetic based disease that occurs in the absence of other cardiac dysfunction and eventually leads to heart failure. However, the pathogenesis of DCM has not been fully elucidated. Because of the complexity and harmfulness, the prevention and treatment of the disease is imminent.

As an essential trace element in almost all living organisms, iron plays a critical role in maintaining normal physiological function. During the past decades, more and more attention has been paid to the iron overload related diseases. In diabetes, persistent high blood glucose and insulin resistance can cause a vicious circle by altering cellular metabolism, promoting the accumulation of peroxidation and the death of cells. So far, diabetes has been verified to be associated with abnormal iron metabolism. For example, systemic iron overload can contribute to abnormal glucose metabolism and the onset of type 2 diabetes (T2DM) (2) and aggravate insulin resistance (3). Furthermore, it is confirmed that ferroptosis, a programmed cell death which characterized by iron-dependent accumulation of lethal lipid peroxidation (4), is involved in cognitive impairment and diabetic endothelial dysfunction in type I diabetes mellitus (T1DM) (5, 6). In particularly, a growing number of evidence supports that maintenance of iron homeostasis is essential for proper cardiac function since the iron accumulation will induce ferroptosis and leading to the damage and dysfunction of myocardial tissues (7). Recently, Cai group (8) identified the role of ferroptosis in DCM, and reported that Nrf2 activation by sulforaphane inhibited ferroptosis and prevented DCM, suggesting that it is feasible to treat DCM by inhibiting ferroptosis. Due to the limited regenerative capacity of the myocardium in mammalian adult hearts, inhibition of cardiomyocyte death might be one of the important ways to alleviate DCM (9). Taken together, taking ferroptosis as the

starting point may provide a new strategy for the prevention and control of DCM.

Canagliflozin (Cana), a hypoglycemic drug of sodium-glucose cotransporter 2 inhibitor (SGLT2i), has shown promising anti-cardiovascular effect in multicenter clinical randomized double-blind studies, which can reduce the risk of cardiovascular death or hospitalization for heart failure in diabetic patients and non-diabetic patients (10, 11). Meanwhile, Cana have shown the ability to attenuate oxidative stress and improve myocardial function by suppressing apoptosis, promoting antioxidant and anti-inflammatory pathways (11, 12). At present, the protective effects of Cana on the heart have been gradually revealed in various myocardial injuries, such as autoimmune myocarditis (13), myocardial lipotoxicity (12) and even isoprenaline-induced cardiotoxicity (14). In addition, a recent study reported that Cana may exert its cardiovascular benefits partly *via* its mitigation of ferroptosis (15), which is similar to the effect of empagliflozin (16), another SGLT2i. These studies provide clues that regulating ferroptosis may play an important role in the cardioprotective effects of SGLT2is. However, the cardioprotective mechanisms of Cana against DCM remain unclear and still need to be further explored.

Here, we aimed to determine whether the SGLT2i Cana plays a role in protection against ferroptosis in DCM *in vivo* and *in vitro*. We addressed this question using our established *in vivo* model of DCM induced by diabetic mice and high glucose induced H9C2 cells injury model *in vitro* to explore the potential mechanism of Cana in the treatment of DCM.

Method

Animals' treatment

Male C57BL/6J mice aged 6-8 weeks with weights of 18-20 g were obtained from the Slack Laboratory Animal Co., Ltd. (Shanghai, China). Production license number: SCXK (Shanghai) 2017-0005. The mice were kept in the Experimental Animal Center of Zhejiang University of Technology under specific-pathogen-free (SPF) environment (room temperature 22 ± 2°C, humidity 55 ± 5%, 12 h light/12 h dark cycle), with unrestricted access to food and water. Experiments were carried out according to the Guideline for the Care and Use of Laboratory Animals published by the National Institute of Health, USA. All experimental procedures were approved by the Animal Experimental Ethics Committee of Zhejiang University of Technology (Animal experimental research plan No. 20220317021).

Mice were allowed to acclimatize in the laboratory environment for 1 week before the beginning of the experiment. DCM model establishment: The mice were given a single intraperitoneal injection of 150 mg/kg 1% streptozotocin (STZ, V900890, Sigma, USA, dissolved in 0.1 mol/L sodium citrate buffer, pH = 4.4 - 4.6) (17, 18). Mouse blood from the tail vein was collected in each group of the model mice and tested by glucose meter (Accu-Chek® Performa test strips, Roche, Accu-Chek® Performa Combo, Roche, USA) on day 3, 5 and 7 after injection. The mice with random blood glucose levels ≥ 16.7 mmol/L were considered as diabetic models, and then kept for 4 weeks to induce DCM. Randomization was used to divide the mice into three groups (n = 8 per group): (1) CON group: mice were administered intragastrically with saline only. (2) DCM group: DCM model mice were treated with saline for 6 weeks. (3) DCM + Cana group: DCM model mice were treated with 20 mg/kg/d canagliflozin (15, 19, 20) (C126191, Aladdin, China) for 6 weeks. On the last day, electrocardiogram examination was performed after the drug intervention, then all animals were weighted and sacrificed, heart tissues were removed freshly and aseptically for measurements.

Cells treatment

H9C2 rat cardiomyocytes were obtained from the National Infrastructure of Cell Line Resource (1101RAT-PUMc000219). H9C2 were cultured in DMEM medium with 5.5 mmol/L glucose (11885084, Gibco, USA), 10% fetal bovine serum (FBS, 10100147, Gibco, USA) and 100 U/mL penicillin-100 μg/mL streptomycin sulfate (B540732, Sangon, China) at 37° C under 5% CO_2. According to the literature (4, 21, 22), in this research, high glucose was defined as 35 mmol/L was used to intervene H9C2 cardiomyocytes for 24 h to establish a DCM model *in vitro* study.

H9C2 cells were divided into three groups: (1) CON group: H9C2 cells were cultured with DMEM medium containing 5.5 mmol/L glucose. (2) HG group: H9C2 cells were cultured with DMEM medium containing 35 mmol/L glucose. (3) HG + Cana group: H9C2 cells were cultured with DMEM medium containing 35 mmol/L glucose and a final concentration of 10 μM canagliflozin. After 24 h of treatment, the H9C2 cells in each group were measured for related indexes.

Electrocardiogram

The mice were anesthetized using 3% sodium pentobarbital (50 mg/kg), and then fixed on a table in the supine position. Subcutaneous needle electrodes were connected to the mice for the limb lead at position II and electrocardiograms were recorded using the Power Lab 26 T data acquisition systems (AD, China). The ECG parameters PP interval, PR interval, RR interval, QRS interval and heart rate were recorded.

Collection of blood and tissue samples

At the end of the medical intervention, the mice were anesthetized using 3% sodium pentobarbital (50 mg/kg). Blood was collected through pericardiocentesis and then centrifuged at 4500 g (4°C) for 15 min to separate serum. Serum was stored at -80°C until analysis. Cardiac tissues were collected, the left ventricle tissues of the hearts were fixed in a 4% paraformaldehyde (E672002, Sangon, China) or 2.5% glutaraldehyde (A17876, Alfa Aesar, USA) for subsequent histopathology analysis and transmission electron microscopy (TEM). The remaining tissue samples were rapidly frozen with liquid nitrogen and stored at -80°C for futher examination.

Histopathology

The left ventricle tissues of the hearts were fixed in 4% paraformaldehyde (E672002, Sangon, China) for 48 h and embedded in paraffin, 5 μm sections were cut longitudinally and stained with hematoxylin and eosin (HE) to evaluate the pathological changes of myocardial tissue. Masson trichrome staining and Sirus red staining were used to observe the deposition of collagen in myocardial tissue. Image J software (https://imagej.nih.gov/ij/) was used for quantitatively analysis the degree of myocardial fibrosis.

Transmission electron microscopy

The left ventricle tissue was fixed in 2.5% glutaraldehyde (A17876, Alfa Aesar, USA). After fixation, dehydration, and impregnation, samples were embedded into epoxy resins and acrylic resins, 1 μm-thick sections were cut on an ultramicrotome with glass knives, then myofilament and mitochondria were observed by transmission electron microscope (Hitachi H-7500, Japan).

Cell viability assay

Cell viability was assessed using Cell Counting Kit-8 (CCK-8 kit, E606335, Sangon, China). Briefly, H9C2 cells were seeded into 96-well plates at 2×10^3/well. After overnight adhesion, H9C2 cells were starved for 6 h by serum-free medium to sync the cell cycle, and then cells were exposed to different concentrations (0.5, 2.5, 5, 10, 20, 40 μM) of Cana for 24 h. Subsequently, 10 μL CCK-8 solution was added to each well and incubated for 2 h at 37°C. The absorbance at 450nm was measured by a multiskan spectrum (Multiskan GO, Thermo, USA).

Biochemical analysis

All kits used in the determination of cTnI, MDA, PCO, GSH, ATP, Fe^{2+}, total iron and glucose contents are listed as below: mouse cardiac troponin I (cTnI) assay kit (ML989022-J, Enzyme-Linked Biotechnology, China), malondialdehyde (MDA) content assay kit (BC0025, Solarbio, China), protein carbonylation (PCO) assay kit (ML076345, Enzyme-Linked Biotechnology, China), reduced glutathione (GSH) content assay kit (D799614, Sangon, China), ATP assay kit (S0026, Beyotime, China), ferrous ion colorimetric assay kit (E-BC-K304-S, Elabsciences, China), total iron colorimetric assay kit (E-BC-K772-M, Elabsciences, China) and glucose assay kit with O-toluidine (S0201M, Beyotime, China). All experiments were performed according to the manufacturers' instructions, and measured by multiskan spectrum (Multiskan GO, Thermo, USA), luminometer (GloMax 20/20, Promega, USA) or spectrophotometer (Quick Drop, Molecular Devices, USA), respectively.

Detection of enzyme activities

The methods of activities assay of LDH, CAT, SOD, GSH-Px were listed as following: lactate dehydrogenase (LDH) activity assay kit (D799208, Sangon, China), catalase (CAT) activity assay kit (D799598, Sangon, China), total superoxide dismutase (SOD) assay kit with WST-8 (S0101S, Beyotime, China) and total glutathione peroxidase (GSH-Px) assay kit with NADPH (S0058, Beyotime, China). All experiments were performed according to the manufacturers' instructions, and measured by Multiskan Spectrum (Multiskan GO, Thermo, USA).

Fluorescence staining assay

Superoxide production, lipid peroxidation and MMP were detected using 2',7'-dichlorofluorescein diacetate (DCFH-DA, 35845, Sigma, USA), BODIPY 581/591 C11 (D3861, Thermo, USA) and JC-1 fluorochrome (C2006, Beyotime, China) respectively. H9C2 cells were seeded in 6-well plates at 10×10^4/well. After the treatments as described in section of "Cells treatment", H9C2 cells were washed twice with PBS, followed by incubation with 5 μM DCFH-DA, 2 μM BODIPY 581/591 C11 or 5 μM JC-1 for 30 min at 37°C in darkness, then the cells were washed three times with PBS or JC-1 staining buffer, respectively. Finally, fluorescence was measured using inverted fluorescence microscope (Axio Observer D1, ZEISS, Germany), and the fluorescence intensity of each group was analyzed by using Image J software (https://imagej.nih.gov/ij/).

Quantitative PCR

Total RNA was extracted from cardiac tissues or H9C2 cells by using Trizol lysate (9109, Takara, Japan), and subjected to reversely transcribed into cDNA using PrimeScript™ RT Master Mix (RR036Q, Takara, Japan) according to the manufacturers' instructions. The qPCR assay was performed on Real-Time PCR system (7500, ABI, USA) with 95° C for 30 s, 1 cycle: 95° C for 5 s, 60° C for 34 s, 40 cycles (RR820, Takara, Japan). GAPDH was used as internal reference gene, the primer sequences were listed in Table 1. The relative gene expressions were determined using the $2^{-\Delta\Delta Ct}$ method.

Western blotting

Western blotting analyses of cardiac tissue and H9C2 cells were performed as described. Briefly, total proteins of heart tissues or H9C2 cells were extracted with RIPA lysis buffer (R0020, Solarbio, China) containing protease inhibitor (04693116001, Roche, Germany). Then protein concentration was quantified by the BCA protein assay kit (C503051, Sangon, China). 30 μg of total protein samples from different groups were first electrophoresed through 10% SDS-PAGE gels and then transferred onto the nitrocellulose membranes (F619511, Sangon, China). After blocked with 5% skim milk in TBST at room temperature for 1 h, membranes were washed and incubated with the following primary antibodies overnight (as shown in Table 2). Washed with TBST, followed by incubated with corresponding HRP-conjugated secondary antibodies at room temperature for 2 h. The target bands were subsequently detected with chemiluminescent (ECL) Kit (D601039, Sangon, China) and chemiluminescent imaging system (5200 multi, Tanon, China).

Statistical analysis

Measurement data were expressed as the mean ± standard deviation and analyzed by SPSS software (version 23.0, USA). Statistical comparisons were performed using one-way ANOVA. $P < 0.05$ was considered statistically significant.

TABLE 1 qPCR Primer sequences.

Gene	Forward sequence (5'- 3')	Reverse sequence (5'- 3')	ProductSize (bp)
Rat_TfR1	CGGCTACCTGGGCTATTGTA	TTCTGACTTGTCCGCCTCTT	84
Rat_FPN	TCCTGGGCTTCGACTGTATC	CAAGTGAAGGCCACAGTTCC	124
Rat_FTN-H	GGCTGAATGCAATGGAGTGT	TCTTGCGTAAGTTGGTCACG	186
Rat_SLC7A11	GGTGGTGTGTTTGCTGTCT	AGAGGAGTGTGCTTGTGGA	101
Rat_GPX4	AATTCGCAGCCAAGGACATC	GGCCAGGATTCGTAAACCAC	170
Rat_GAPDH	CAATCCTGGGCGGTACAACT	TACGGCCAAATCCGTTCACA	162
Mouse_TfR1	TTGGGTAGTTGGAGATTGCC	TGAGGTCTTTGGCTTCTGGT	247
Mouse_FPN	AAGCGGCCCACACTAAGAAA	AGGCAATGTCCCATGTTGGT	237
Mouse_FTN-H	CATCAACCGCCAGATCAACC	GTCATCACGGTCTGGTTTCTTTAT	220
Mouse_SLC7A11	GGCACCGTCATCGGATCAG	CTCCACAGGCAGACCAGAAAA	100
Mouse_GPX4	CGCGATGATTGGCGCT	CACACGAAAACCCCTGTACTTATCC	175
Mouse_GAPDH	GAAGGGCTCATGACCACAG	AGATCCACGACGGACACATT	221

TfR1, transferrin receptor 1; FPN, ferroportin; FTN-H, ferritin heavy-chain; SLC7A11, Solute carrier family 7 member 11; GPX4, glutathione peroxidase 4; GAPDH, glyceraldehyde-3-phosphate dehydrogenase.

TABLE 2 The antibodies and dilution ratio.

Antibodies	Reacts with	Dilution ratio	Cat No	Manufacturers
anti-TfR1	Rat, Mouse	1:1000	ab84036	Abcam/UK
anti-FPN1	Rat, Mouse	1:500	ab58695	Abcam/UK
anti-FTN-H	Rat, Mouse	1:1000	ab75973	Abcam/UK
anti-GPX4	Rat, Mouse	1:1000	ab125066	Abcam/UK
anti-xCT	Rat, Mouse	1:1000	ab175186	Abcam/UK
anti-GAPDH	Rat, Mouse	1:10000	ab181602	Abcam/UK
HRP labeled Goat anti rabbit IgG (H + L)		1:50000	BK-R050	Bioker/China

TfR1, transferrin receptor 1; FPN, ferroportin; FTN-H, ferritin heavy-chain; xCT, cystine-glutamate antiporter; GPX4, glutathione peroxidase 4; GAPDH, glyceraldehyde-3-phosphate dehydrogenase.

Result

Cana attenuates myocardial injury in DCM mice

To investigate the therapeutic effect of Cana on myocardial injury in diabetes, mouse model of DCM was established. At the end of the experiment, the basic state and cardiac function of mice in these groups were faithfully recorded (Table 3). Mice in DCM group showed obvious diabetic symptoms such as elevated blood glucose, polydipsia, polyphagia, and weight loss. The results of ECG showed that significant slowing of heart rate accompanied by overt prolongation of RR interval, PP interval, and PR interval were present in DCM mice. At the same time, LDH and cTnI, both markers of cardiac injury, were also significantly increased in DCM mice, indicating that DCM indeed occurred. In contrast, the mice treated with Cana recovered both diabetic symptoms and cardiac function, although blood glucose levels remained higher than in controls. All these results indicated that Cana could alleviate diabetic myocardial injury in DCM mice.

Cana inhibits diabetic myocardial tissues fibrosis and oxidative stress

Pathological staining was used to further verify the degree of myocardial injury in mice. HE staining showed (Figure 1A) that myocardial fibers were intact and aligned in CON group, but disorganized or even fractured in the DCM group (yellow arrow). Besides, necrosis or inflammatory cells were increased, and the myocardial striations became blurred in DCM mice. In DCM + Cana group, myocardial fiber disorder was improved, and necrosis or inflammatory cells were obviously reduced. The increasing of collagen fibers in myocardial tissues were observed by Masson staining and Sirius red staining. As shown in Figures 1A-C, compared with CON group, many collagen fibers were deposited in myocardial tissues of DCM mice (black arrow), which was significantly alleviated after Cana treatment.

Next, we measured the level of oxidative stress, an inducer of DCM, in the myocardium of each group of mice. Compared with CON group, the contents of MDA and PCO in the myocardium of DCM mice were significantly increased (Figures 1D, E), while the activities of antioxidant enzymes SOD and CAT were obviously decreased (Figures 1F, G). And after treatment with Cana, the biochemical parameters of oxidative stress in DCM mice were improved, including the decrease of MDA and PCO (Figures 1D, E), and the increase of CAT (Figure 1G). These results suggested Cana exerted an anti-oxidative stress effect here.

Cana mitigates mitochondrial damage and ferroptosis in DCM mice

TEM was applied to observe the changes of mitochondrial morphology and structure in myocardial tissues. The ultrastructure was obviously changed in myocardial tissues of DCM mice, the myofilaments were fragmented, the mitochondria were swollen, part of the outer membrane was ruptured, and the mitochondrial cristae were disappeared or broken (Figure 2A). However, the disturbance of mitochondrial structure in DCM + Cana group was effectively improved, the swollen mitochondria were less, the mitochondrial inner and outer membranes were intact, and the number of mitochondrial cristae increased (Figure 2A). Correspondingly, the insufficiency of ATP level in myocardial tissues of DCM mice was partially improved after Cana treatment (Figure 2B), which reflected that Cana could reduce mitochondrial damage and protect mitochondrial function to a certain extent.

TABLE 3 Basic characteristics of mice in each group at the end of experiment.

	CON	DCM	DCM + Cana
Blood glucose (mmol/L)	8.90 ± 0.47	31.28 ± 3.58***	18.26 ± 1.09###
Body weight (mg)	29.45 ± 2.26	17.34 ± 2.31***	20.11 ± 1.34n.s.
Food intake (g/24 h)	12.28 ± 0.34	24.83 ± 3.44***	15.12 ± 1.64###
Water intake (mL/24 h)	33.6 ± 1.62	116.82 ± 13.59***	81.50 ± 18.93#
RR interval (ms)	135 ± 8.94	171 ± 11.14***	155 ± 10.00#
HR (bpm)	446 ± 28.49	328 ± 39.38***	388 ± 22.86#
PP interval (ms)	122 ± 14.70	158 ± 6.32***	140 ± 7.48#
PR interval (ms)	36 ± 4.15	71 ± 19.08***	56 ± 4.90#
QRS interval (ms)	28 ± 2.45	32 ± 4.00n.s.	30 ± 3.16n.s.
LDH (U/mg tissue)	3.56 ± 1.01	21.32 ± 1.54***	1.91 ± 0.20###
cTnI (pg/mL)	11.65 ± 0.88	18.33 ± 1.86**	14.67 ± 1.04#

Data are expressed as mean ± standard deviation (n = 8). HR, heart rate; LDH, lactate dehydrogenase; cTnI, mouse cardiac troponin I. (*: P<0.05; **: P<0.01; ***: P<0.001; compared with CON group; #: P< 0.05; ##: P<0.01; ###: P<0.001; compared with DCM group; n.s.: no significance.)

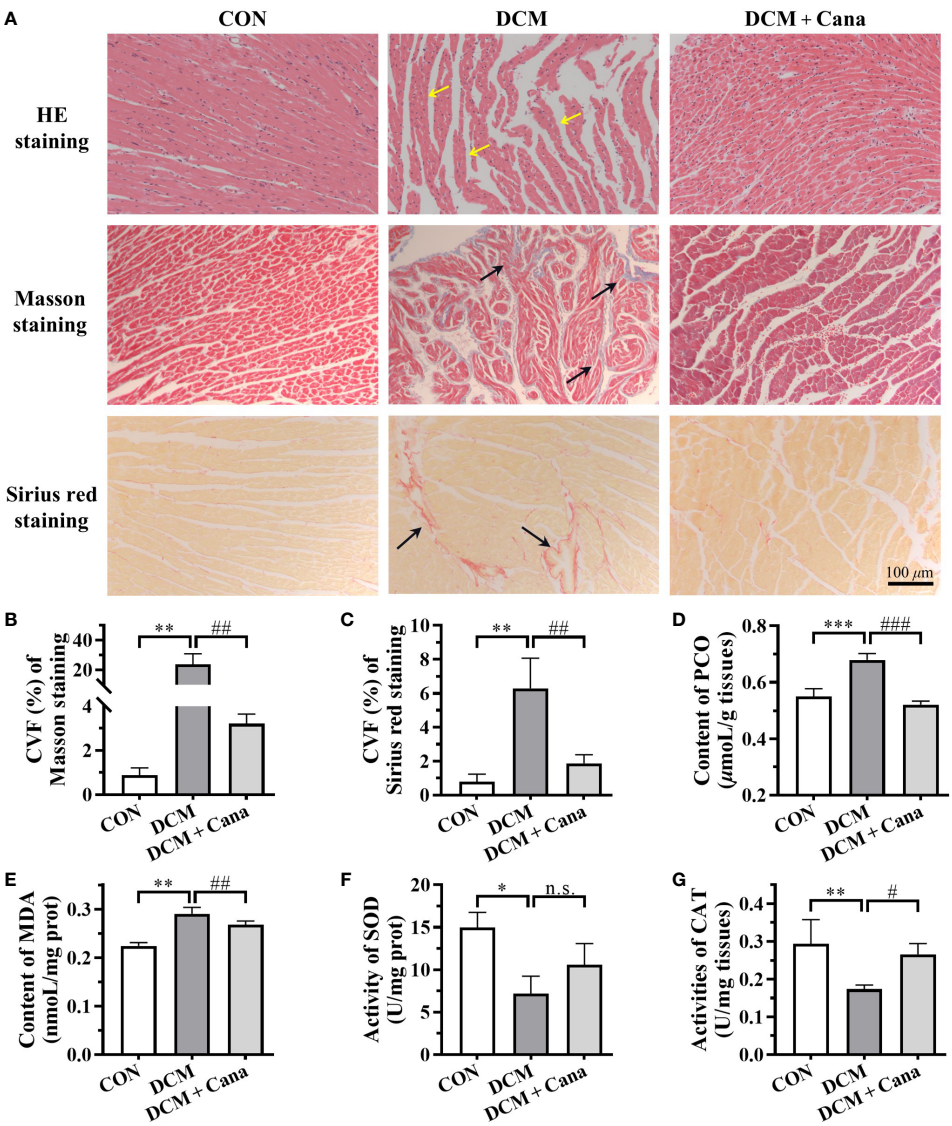

FIGURE 1
Canagliflozin inhibits oxidative stress and fibrosis in diabetic myocardial tissue **(A)** Pathological staining results of myocardial tissues (Scale bar: 100 μm). **(B)** CVF of Masson staining. **(C)** CVF of Sirus red staining. Contents of **(D)** PCO and **(E)** MDA, activities of **(F)** SOD and **(G)** CAT in myocardial tissues. CVF, collagen volume fraction; PCO, protein carbonyl; MDA, malondialdehyde; SOD, superoxide dismutase; CAT, catalase. (*: $P < 0.05$; **: $P < 0.01$; ***: $P < 0.001$; compared with CON group; #: $P < 0.05$; ##: $P < 0.01$; ###: $P < 0.001$; compared with DCM group; n.s.: no significance.).

Since the homeostasis metabolism of cardiac iron was closely related to heart disease, we examined key factors associated with iron metabolism and ferroptosis. In DCM mice, we found that the contents of total iron (Figure 2C) and Fe^{2+} (Figure 2D), and the expression of transferrin receptor 1 (TfR1) and ferritin heavy-chain (FTN-H) (Figures 2F, G) were significantly increased. Meanwhile, the content of GSH (Figure 2E) and the expression of ferroportin (FPN) and cystine-glutamate antiporter (xCT) (Figures 2F, G) were significantly reduced in DCM mice compared to normal mice. After the treatment of Cana, the contents of total iron (Figure 2C) and Fe^{2+} (Figure 2D), and the expression of TfR1 and FTN-H (Figures 2F, G) were all obviously lower, while the content of GSH (Figure 2E) and the expression of xCT (Figures 2F, G) were both significantly increased in DCM mice. But the protein level of glutathione peroxidase 4 (GPX4) showed no difference in the myocardial tissues between DCM group and DCM + Cana group (Figure 2G). These assays testified that ferroptosis indeed exist in DCM mice and Cana could inhibit ferroptosis by balancing iron homeostasis and increasing xCT expression.

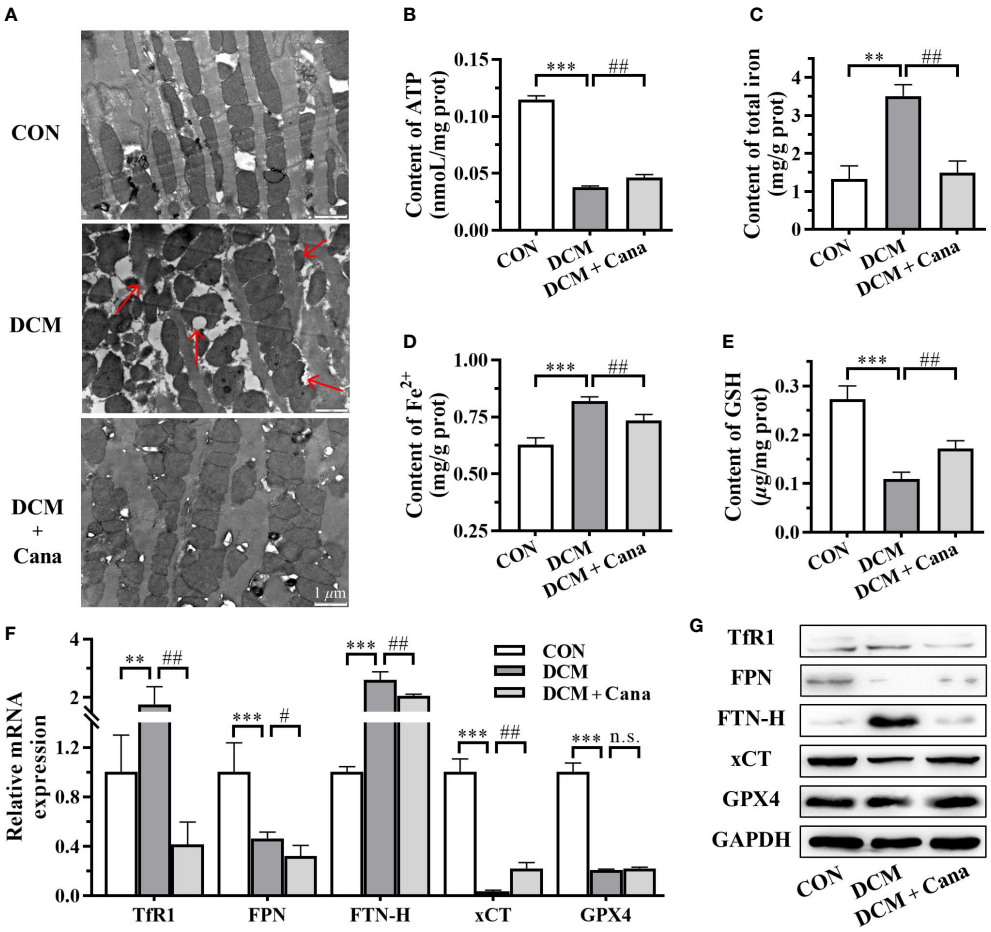

FIGURE 2
Canagliflozin inhibits mitochondrial damage and ferroptosis in diabetic mice. **(A)** Morphological and structural observation of mitochondria in myocardial tissues (Scale bar: 1 μm). Contents of **(B)** ATP; **(C)** total iron; **(D)** Fe^{2+} and **(E)** GSH in myocardial tissues. **(F)** Transcriptional level and **(G)** protein level of iron metabolism and ferroptosis related genes examined by qPCR and western blotting assay. ATP, adenosine triphosphate; GSH, glutathione; TfR1: transferrin receptor 1; FPN, ferroportin; FTN-H, ferritin heavy-chain; xCT, cystine-glutamate antiporter; GPX4, glutathione peroxidase 4; GAPDH, glyceraldehyde-3-phosphate dehydrogenase. (**: P<0.01; ***: P<0.001; compared with CON group; #: P<0.05; ##: P<0.01; compared with DCM group; n.s.: no significance.)

Cana alleviates high glucose injury of cardiomyocytes without hypoglycemic effect

Based on animal experiments, we further investigated the effect and mechanism of Cana in protecting H9C2 cells against high glucose injury. Firstly, H9C2 cells were treated with different concentrations of Cana (0.5, 2.5, 5, 10, 20, 40 μM) for 24 h with high glucose medium, and the cell viability was detected by CCK-8 kit. The result showed that, due to high glucose injury, the cell viability of H9C2 cells in HG group decreased by about 20% compared to normal cells. And compared with HG group, Cana could effectively improve the viability of H9C2 cells in a dose-dependent manner at a certain concentration range (0.5-10 μM) (Figure 3A). Therefore, 10 μM Cana with the best inhibitory effect on high glucose injury was selected for subsequent study.

Given the hypoglycemic effect of Cana in mice, the changes of intracellular glucose content with or without Cana were examined. Interestingly, our result found that Cana failed to effectively reduce the glucose level in H9C2 cells (Figure 3B), which may be related to tissue specificity as well as duration of action. In conclusion, Cana may have a non-hypoglycemic way to alleviate the high glucose injury of cardiomyocytes.

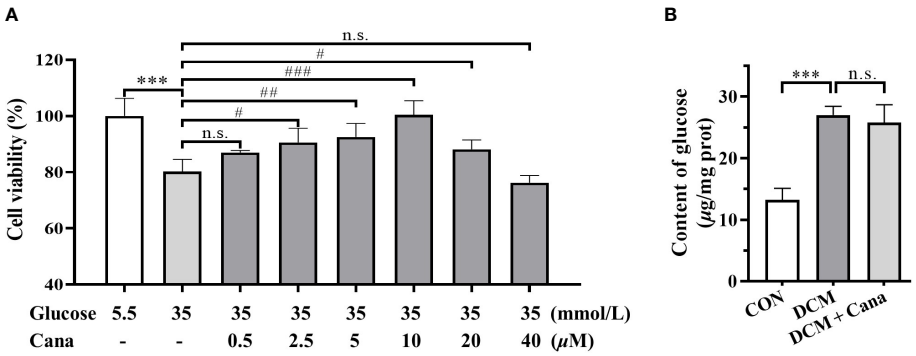

FIGURE 3
Canagliflozin alleviates high glucose injury of cardiomyocytes by non-hypoglycemic way. **(A)** Effects of high concentration of glucose and different concentrations of canagliflozin on the cell viability of H9C2 cells. **(B)** Content of glucose in H9C2 cells of each group. (***: P<0.001; compared with CON group; #: P< 0.05; ##: P<0.01; ###: P<0.001; compared with HG group; n.s.: no significance.).

Cana improves oxidative stress and mitochondrial damage induced by high glucose

To determine the effect of Cana on oxidative stress in cardiomyocytes, the levels of ROS, PCO, SOD, and CAT in H9C2 cells were measured. As shown in Figures 4A–E, ROS Level and PCO content were significantly higher, whereas SOD and CAT activities were significantly declined in HG group cells than in CON. Like those in animal experiments, Cana could reverse the oxidative stress induced by high glucose by reducing intracellular ROS (Figures 4A, B) and PCO level (Figure 4C), and increasing intracellular antioxidant enzymes activities (Figures 4D, E).

As the main organelle of energy metabolism and ROS production, mitochondria play an important role in cardiomyocytes. In our study, it was found that high glucose intervention in H9C2 cells resulted in a decrease in MMP (Figures 4F, G) and ATP production (Figure 4H), leading to mitochondrial damage. Moreover, the high glucose-induced reduction in MMP (Figures 4F, G) and ATP production (Figure 4H) could be ameliorated by Cana. These results manifested that Cana had an antioxidant effect as well as a protective function of mitochondria.

Cana mitigates ferroptosis induced by high glucose in cardiomyocytes

Since Cana maintained myocardial iron homeostasis in DCM mice, we further examined iron metabolism in H9C2 cells. After high glucose induction, iron deposition also observed in H9C2 cells, such as the increase of total iron (Figure 5D) and Fe^{2+} contents (Figure 5E) as well as FPN and FTN-H expression (Figures 5H, I). Although the mRNA expression of TfR1 was higher in HG group, the TfR1 protein level represented little difference in these three groups (Figures 5H, I). And after the intervention of Cana, the deposition of iron induced by high glucose was significantly reduced (Figures 5D, E, H, I).

The occurrence of ferroptosis is often accompanied by excessive accumulation of intracellular lipid peroxidation. C11-BODIPY staining showed that the level of oxC11-BODIPY was significantly increased in HG group compared with CON group (Figures 5A, B). At the same time, the increase of intracellular MDA level (Figure 5C) also reflected that high glucose induction increased the level of lipid ROS in cells of HG group. Furthermore, the system Xc^-/GSH/GPX4 axis, a crucial pathway against lipid peroxidation and ferroptosis, was as well suppressed in HG group (Figures 5F–I). Among them, the high expression of xCT mRNA might be compensatory. After Cana intervention, the levels of GSH, GSH-Px and xCT expression inhibited by high glucose were effectively restored (Figures 5F–I), resulting in a decrease in lipid peroxidation and inhibition of ferroptosis. The results demonstrate that Cana ameliorated ferroptosis by regulating iron metabolism and system Xc^-/GSH/GPX4 axis, which is consistent with the animal results.

Discussion

Iron is an essential trace element in almost all living organisms, as it is involved in many important biological processes such as energy and metabolism, being critical for maintaining body homoeostasis. The evidence to date suggests that the maintenance of iron homeostasis is essential for proper cardiac function (7). When iron overload occurs in cardiomyocytes, the labile forms of iron enter the mitochondria and injure cells *via* oxidative damage, resulting

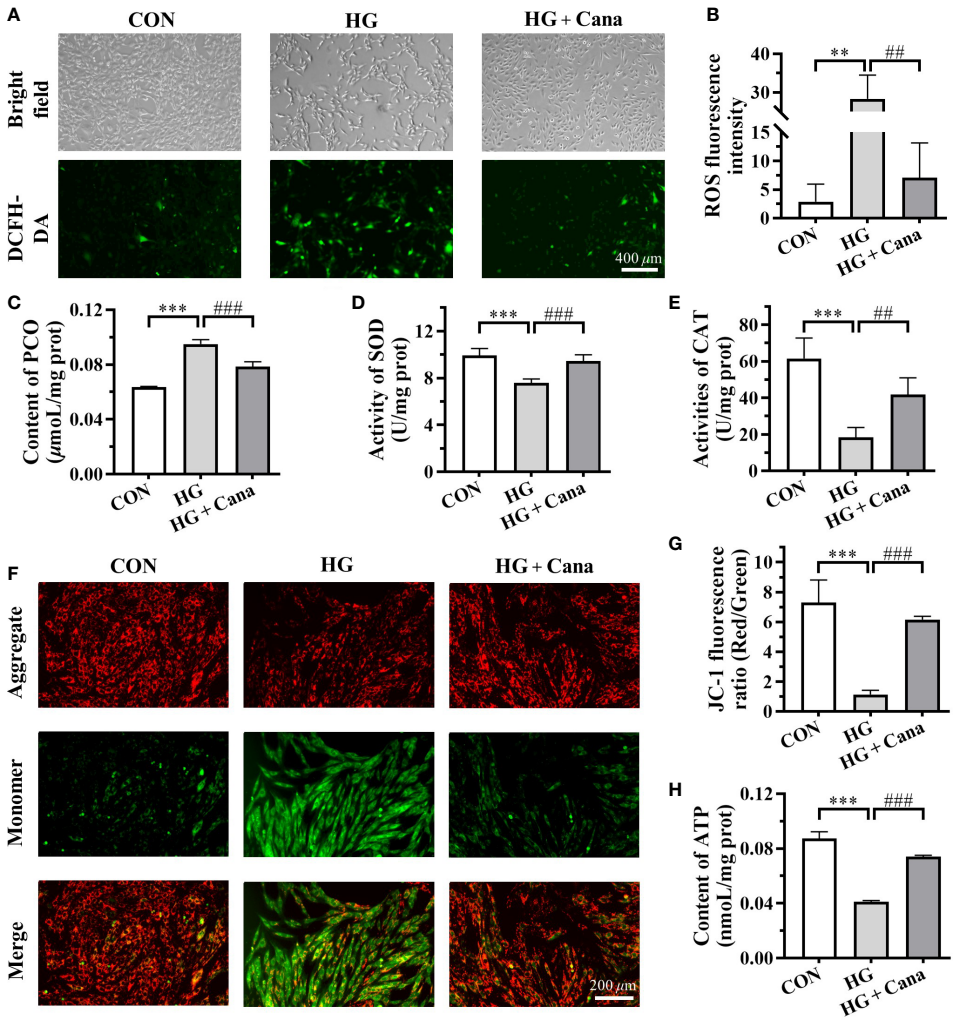

FIGURE 4
Canagliflozin improves oxidative stress and mitochondrial damage induced by high glucose. **(A)** The images and **(B)** fluorescence intensity of intracellular ROS stained by DCFH-DA (Scale bar: 400 μm). **(C)** Content of PCO; Activities of **(D)** SOD and **(E)** CAT in H9C2 cells of each group. **(F)** The images and **(G)** JC-1 fluorescence ratio of MMP analyzed by JC-1 kit (Scale bar: 200 μm). **(H)** Content of ATP. ROS, reactive oxygen species; PCO, protein carbonyl; SOD, superoxide dismutase; CAT, catalase; MMP, mitochondrial membrane potential; ATP, adenosine triphosphate. (**: P<0.01; ***: P<0.001; compared with CON group; ##: P<0.01; ###: P<0.001; compared with HG group.).

in heart diseases (23). Further research confirmed that the pathogenic mechanisms of iron overload-induced cardiomyopathy is directly driven by ferroptosis (24), a new form of programmed cell death that was characterized by the overwhelming, iron-dependent accumulation of lethal lipid peroxidation (25). Additionally, an increasing number of evidence show that ferroptosis is also involved in the development of many cardiovascular diseases. As supported, ferroptosis inhibitors Vitamin E and coenzyme Q10 can protect the myocardium in diabetic animals by attenuating oxidative stress (26, 27), which indicated that ferroptosis is more likely to be involved in DCM. Recently, some direct evidences have been found to support the point that ferroptosis plays an essential role in the pathogenesis of DCM, but the exact mechanisms underlying this process are not clear. An interesting study demonstrated that T1DM-induced autophagy inhibition may activate Nrf2-mediated ferroptosis in cardiomyocytes, thereby contributing to the progression of DCM (9). Conversely, Cai group (8) identified that inhibition of ferroptosis prevented the development of myocardial dysfunction in the heart of T2DM mice and Nrf2 activation sulforaphane suppressed ferroptosis and prevented DCM by upregulating ferritin and xCT levels. Different from apoptosis, which mainly occurs at the early stage of DCM and decreases with the progression of DCM (28, 29),

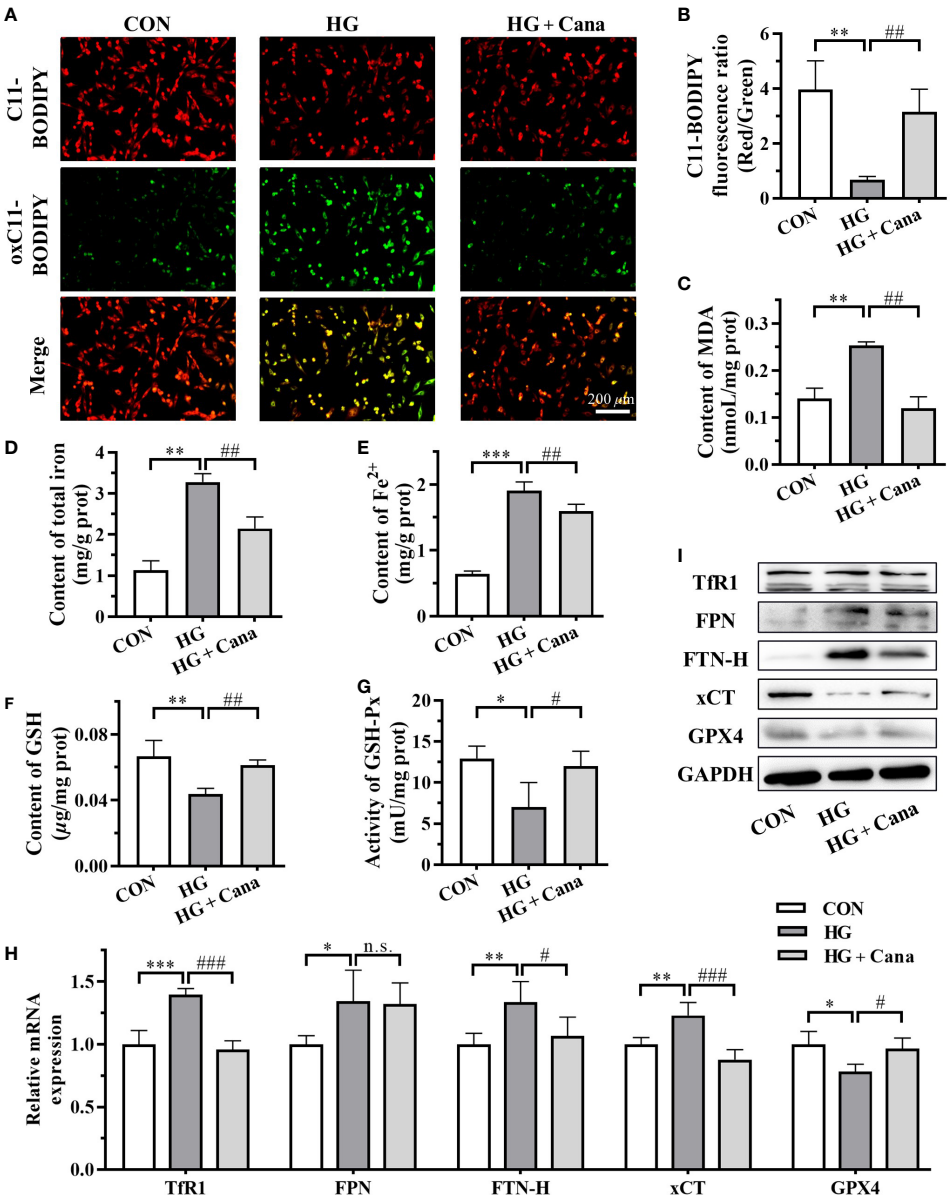

FIGURE 5
Cana mitigates ferroptosis induced by high glucose in cardiomyocytes. **(A)** The images and **(B)** C11-BODIPY fluorescence ratio of lipid ROS (Scale bar: 200 μm). C11-BODIPY represents the level of staining with the probe (unoxidized), while oxC11- BODIPY (oxidized) represents the level of lipid ROS. Contents of **(C)** MDA, **(D)** total iron and **(E)** Fe^{2+} in H9C2 cells. **(F)** Content of GSH; **(G)** Activity of GSH-Px in H9C2 cells. **(H)** Transcriptional level and **(I)** protein level of ferroptosis related genes examined by qPCR and western blotting assay. ROS: reactive oxygen species; MDA: malondialdehyde. ROS, reactive oxygen species; MDA, malondialdehyde; GSH, glutathione; GSH-Px, glutathione peroxidase; FTN-H, ferritin heavy-chain; xCT, cystine-glutamate antiporter; GPX4, glutathione peroxidase 4; GAPDH, glyceraldehyde-3-phosphate dehydrogenase. (*: P<0.05; **: P<0.01; ***: P<0.001; compared with CON group; #: P<0.05; ##: P<0.01; ###: P<0.001; compared with HG group; n.s.: no significance.).

ferroptosis seems to be more important at the later stage of DCM (8). Therefore, targeting ferroptosis may serve as a feasible therapeutic approach for DCM prevention.

SGLT2is are a class of oral antidiabetic drugs that promote urinary glucose excretion by inhibiting renal proximal tubules from reabsorbing glucose, thus reducing blood glucose levels. Several large-scale randomized clinical trials have demonstrated that SGLT2is can improve cardiovascular outcomes in patients with or without DM (11, 30). These benefits have long moved beyond its role as antidiabetic drugs, which bring SGLT2is to the forefront. Recent studies have also found that SGLT2is can modulate iron metabolism and maintain body iron

homeostasis as well as cardiac iron homeostasis (31, 32). Here, the role of ferroptosis in protecting myocardial function by SGLT2is has attracted more and more attention. As the first SGLT2i approved by FDA, Cana has been reported to be the most effective in preventing hospitalization for heart failure compared with other SGLT2is (33).

Several studies have manifested that Cana can regulate mitochondrial function *via* PPARα or AMPK-Sirt1-Pgc-1α signalling pathway (34). Meanwhile, as mentioned previously, Cana has several cardioprotective effects. Kondo et al (35) demonstrated for the first time that Cana suppressed myocardial NADPH oxidase activity and improved NOS coupling *via* SGLT1/AMPK/Rac1 signalling, leading to global anti-inflammatory and anti-apoptotic effects in the human myocardium. In experimental autoimmune myocarditis, Cana treatment markedly alleviated cardiac inflammation and improved cardiac function (13). And Cana also shown protective effects on diabetic hearts by inhibiting the mTOR/HIF-1α pathway to attenuate lipotoxicity in cardiomyocytes (20). Despite its cardioprotective effect is effective against isoprenaline-induced cardiomyocyte injury (14), but not for pirarubicin-induced cardiomyocyte injury (36). So further in-depth study is needed. Notably, a recent study reported that Cana exert its cardiovascular benefits partly *via* its mitigation of ferroptosis in a rodent model of HFpEF (15), which provide a new idea for the research of SGLT2is in heart disease, even DCM. So far, the cardioprotective mechanisms of Cana on DCM are not fully clear and needs to be further studied.

In our study, DM mice and H9C2 cells, a widely used cell line for the study of cardiac diseases (37), were used to establish DCM models *in vivo* and *in vitro*. Although Cana showed hypoglycemic effects in DCM mice, it did not appear to affect cardiomyocytes in the short term (24 h). In other studies, it was also mentioned that the cardioprotective effect of Cana may be independent of its hypoglycemic activity (38). Thus, there may be a non-hypoglycemic way of Cana to alleviate the high glucose injury of cardiomyocytes. Oxidative stress has been proved to play a significant role in the process of diabetes and its complications (39). Consistent with previous research (40, 41), hyperglycemia or high glucose did aggravate oxidative stress and induce cardiomyocytes injury in DM mice and H9C2 cells, indicating that the DCM model had been successfully established. In addition, the increase of total iron and Fe^{2+} contents and FTN-H expression reflected the occurrence of iron deposition in DCM models. *In vivo*, iron metabolism also regulated by hepcidin (31), which may account for the differences between animals and cells. At the same time, we noted a significant increase in MDA level with a remarkably decrease in GSH level in DCM models. As the substrate of GPX4, GSH not only play an antioxidant role but also participate in the occurrence of ferroptosis (42). The high level of MDA, one of the most important products of lipid peroxidation, reflected intracellular lipid ROS excessive accumulation. Besides, the fluorescence intensity of oxC11-BODIPY in H9C2 cells was dramatically increased after high glucose induction, which also proved that there were excessive lipid ROS in the cells. Hence, based on the fact that excess Fe^{2+} and lipid ROS exist, the main characteristics of ferroptosis, we hypothesized that ferroptosis does occur in the DCM models. In our study, Cana treatment mitigated ferroptosis by inhibiting myocardial oxidative stress and iron overload *in vitro* and *in vivo*. Moreover, in terms of morphological and structural changes, cells undergoing ferroptosis can be observed in TEM for mitochondrial abnormalities such as swelling, density changes and outer membrane rupture (25). These changes were indeed appeared in the cardiac tissue of DCM mice in our study, and Cana treatment ameliorated the damage of mitochondrial. All of these data indicated that ferroptosis may be one of the pathogeneses in DCM and Cana was able to palliate from ferroptosis to protect myocardial cells.

At the cellular level, the initiation and execution of ferroptosis are controlled by the pathways involved in iron, amino acids and lipid metabolism. Briefly, iron, transported into cells by TfR1, is either stored in FTN-H or exported by FPN. The excess cellular iron, particularly Fe^{2+}, can react directly with cellular oxidants to produce cytotoxic hydroxyl radicals *via* the Fenton reaction, which in turn promotes ferroptosis (7). The system Xc^-/GSH/GPX4 axis is the main cellular pathway to protect cells from undergoing ferroptosis by catalyzing toxic lipid hydroperoxides into nontoxic lipid alcohols under normal physiological conditions (43). To initially explore the mechanism by which Cana alleviates ferroptosis, we performed an analysis of ferroptosis-related gene expression. Results showed when DCM occurred, system Xc^-/GSH/GPX4 axis was suppressed, especially the xCT expression, while TfR1 and FTN-H were overexpressed. Similar results have also been found in myocardial tissue of mice with T2DM-induced DCM and rats with HFpEF (15). And after the treatment of Cana, the changes of these genes were partly reversed. Based on current evidences, we conclude that Cana may regulate ferroptosis to modify DCM by balancing cardiac iron homeostasis and overexpressing xCT (Figure 6). Further, it has been reported that Cana can activate AMPK/Nrf2/ATF4 pathway and inhibit p53 expression (44, 45). Nuclear factor erythroid 2-related factor 2 (Nrf2) and activating transcription factor 4 (ATF4) activated xCT expression by interacting with its promoter, while the deubiquitination of histone H2B by p53 inhibited xCT expression (46). For TfR1, Cana has been reported to inhibit mechanistic target of rapamycin (mTOR) (20), and the inhibition of mTOR could mediate the degradation of TfR1 mRNA through tristetraprolin (TTP). However, the relationship and specific mechanism of Cana in regulating iron metabolism and system Xc^-/GSH/GPX4 axis still need to be studied in depth, which will be the focus of our next attention.

The efficacy of SGLT2is as an adjuvant for insulin therapy in patients with T1DM has been verified in several clinical trials

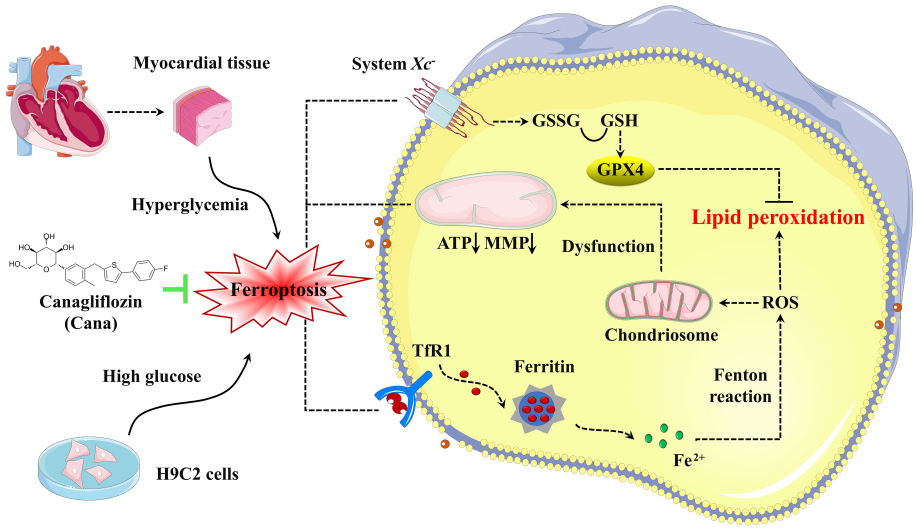

FIGURE 6
Schematic illustration of Cana alleviating ferroptosis in diabetic cardiomyopathy. High glucose, as pivotal pathogenic factors of DCM, inhibit the expression of SLC7A11 and promote the expression of TfR1, which in turn decrease the GSH levels and increase the labile iron levels, respectively. These alterations lead to increased lipid peroxidation and cardiomyocyte ferroptosis, which then initiates cardiac dysfunction, eventually leads to the DCM. Cana promotes upregulation of SLC7A11 and downregulation of TfR1 and FTN-H, which protect the cardiomyocytes from ferroptosis. TfR1, transferrin receptor 1; ROS, Reactive Oxygen Species; GSSG, oxidized glutathione; GSH, glutathione; GPX4, glutathione peroxidase 4; MMP, mitochondrial membrane potential; ATP, adenosine triphosphate.

(47, 48). Despite the potential benefits in people with T1DM, current researches on Cana mainly focus on T2DM. And rare relevant studies have identified the role of Cana in the treatment of T1DM induced cardiomyopathy. Our animal experiment found that Cana can really control blood glucose and diabetic symptoms in T1DM mice, and even attenuated myocardial injury through non-hypoglycemic way. Hence, Cana is a promising agent as an adjuvant for insulin therapy in the prevention and treatment of DCM. However, its potential mechanism and clinical safety need further exploration.

Data availability statement

The original contributions presented in the study are included in the article/supplementary material. Further inquiries can be directed to the corresponding author.

Ethics statement

Experiments were carried out according to the Guideline for the Care and Use of Laboratory Animals published by the National Institute of Health, USA. All experimental procedures were reviewed and approved by the Animal Experimental Ethics Committee of Zhejiang University of Technology (Animal experimental research plan No. 20220317021).

Author contributions

SD, HS, LX, PW and YS conceived and designed this research. SD performed experiments, analyzed data, and drafted the manuscript. All authors interpreted results of experiments. HS, LX, YS provided help on the edition of figures. HS, YS and LX edited and revised the manuscript. All authors contributed to the discussion, read and approved the final manuscript. All authors contributed to the article and approved the submitted version.

Funding

This work was supported by grants from Medicine and Health Science and Technology Plan Projects of Zhejiang Province (YS, 2020PY029), Science and Technology

Innovation Special Project of Jiaxing Science and Technology Bureau (YS, 2020AY30003), Zhejiang Provincial Health Science and Technology Program of Traditional Chinese Medicine (YS, 2021ZB283) and Jiaxing Key Laboratory of Diabetic Angiopathy.

Acknowledgments

The authors thank Prof. Zhu-FY, Prof. Wang-B and Prof. Tai-Y (Electron Microscope Platform, Medical Research Center of Zhejiang Chinese Medicine University, Hangzhou, China) for providing the technical support of TEM; Prof. Chen-Y, Prof. Wang-SF (Experimental Animal Center of Zhejiang University of Technology, Hangzhou, China) for providing the technical support of electrocardiogram.

Conflict of interest

The authors declare that the research was conducted in the absence of any commercial or financial relationships that could be construed as a potential conflict of interest.

Publisher's note

References

1. Bhagani H, Nasser SA, Dakroub A, El-Yazbi AF, Eid AA, Kobeissy F, et al. The mitochondria: A target of polyphenols in the treatment of diabetic cardiomyopathy. *Int J Mol Sci* (2020) 21(14):4962. doi: 10.3390/ijms21144962

2. Guo X, Zhou D, An P, Wu Q, Wang H, Wu A, et al. Associations between serum hepcidin, ferritin and hb concentrations and type 2 diabetes risks in a han Chinese population. *Br J Nutr* (2013) 110(12):2180–5. doi: 10.1017/S0007114513001827

3. Altamura S, Mudder K, Schlotterer A, Fleming T, Heidenreich E, Qiu R, et al. Iron aggravates hepatic insulin resistance in the absence of inflammation in a novel db/db mouse model with iron overload. *Mol Metab* (2021) 51:101235. doi: 10.1016/j.molmet.2021.101235

4. Ma H, Li Y, Hou T, Li J, Yang L, Guo H, et al. Sevoflurane postconditioning attenuates Hypoxia/Reoxygenation injury of cardiomyocytes under high glucose by regulating HIF-1α/MIF/AMPK pathway. *Front Pharmacol* (2020) 11:624809. doi: 10.3389/fphar.2020.624809

5. Hao L, Mi J, Song L, Guo Y, Li Y, Yin Y, et al. SLC40A1 mediates ferroptosis and cognitive dysfunction in type 1 diabetes. *Neuroscience* (2021) 463:216–26. doi: 10.1016/j.neuroscience.2021.03.009

6. Luo EF, Li HX, Qin YH, Qiao Y, Yan GL, Yao YY, et al. Role of ferroptosis in the process of diabetes-induced endothelial dysfunction. *World J Diabetes* (2021) 12(2):124–37. doi: 10.4239/wjd.v12.i2.124

7. Fang X, Ardehali H, Min J, Wang F. The molecular and metabolic landscape of iron and ferroptosis in cardiovascular disease. *Nat Rev Cardiol* (2022) 4:1–17. doi: 10.1038/s41569-022-00735-4

8. Wang X, Chen X, Zhou W, Men H, Bao T, Sun Y, et al. Ferroptosis is essential for diabetic cardiomyopathy and is prevented by sulforaphane *via* AMPK/NRF2 pathways. *Acta Pharm Sin B* (2022) 12(2):708–22. doi: 10.1016/j.apsb.2021.10.005

9. Zang H, Wu W, Qi L, Tan W, Nagarkatti P, Nagarkatti M, et al. Autophagy inhibition enables Nrf2 to exaggerate the progression of diabetic cardiomyopathy in mice. *Diabetes* (2020) 69(12):2720–34. doi: 10.2337/db19-1176

10. Radholm K, Figtree G, Perkovic V, Solomon SD, Mahaffey KW, de Zeeuw D, et al. Canagliflozin and heart failure in type 2 diabetes mellitus: Results from the CANVAS program. *Circulation* (2018) 138(5):458–68. doi: 10.1161/CIRCULATIONAHA.118.034222

11. Jardine MJ, Zhou Z, Mahaffey KW, Agarwal R, Bakris G, Bajaj HS, et al. Renal, cardiovascular, and safety outcomes of canagliflozin by baseline kidney function: A secondary analysis of the CREDENCE randomized trial. *J Am Soc Nephrol* (2020) 31(5):1128–39. doi: 10.1681/ASN.2019111168

12. Wang X, Wang Z, Liu D, Jiang H, Cai C, Li G, et al. Canagliflozin prevents lipid accumulation, mitochondrial dysfunction, and gut microbiota dysbiosis in mice with diabetic cardiovascular disease. *Front Pharmacol* (2022) 13:839640. doi: 10.3389/fphar.2022.839640

13. Long Q, Li L, Yang H, Lu Y, Yang H, Zhu Y, et al. SGLT2 inhibitor, canagliflozin, ameliorates cardiac inflammation in experimental autoimmune myocarditis. *Int Immunopharmacol* (2022) 110:109024. doi: 10.1016/j.intimp.2022.109024

14. Hasan R, Lasker S, Hasan A, Zerin F, Zamila M, Chowdhury FI, et al. Canagliflozin attenuates isoprenaline-induced cardiac oxidative stress by stimulating multiple antioxidant and anti-inflammatory signaling pathways. *Sci Rep* (2020) 10(1):14459. doi: 10.1038/s41598-020-71449-1

15. Ma S, He LL, Zhang GR, Zuo QJ, Wang ZL, Zhai JL, et al. Canagliflozin mitigates ferroptosis and ameliorates heart failure in rats with preserved ejection fraction. *Naunyn Schmiedebergs Arch Pharmacol* (2022) 395(8):945–62. doi: 10.1007/s00210-022-02243-1

16. Quagliariello V, De Laurentiis M, Rea D, Barbieri A, Monti MG, Carbone A, et al. The SGLT-2 inhibitor empagliflozin improves myocardial strain, reduces cardiac fibrosis and pro-inflammatory cytokines in non-diabetic mice treated with doxorubicin. *Cardiovasc Diabetol* (2021) 20(1):150. doi: 10.1186/s12933-021-01346-y

17. Cai L, Wang Y, Zhou G, Chen T, Song Y, Li X, et al. Attenuation by metallothionein of early cardiac cell death *via* suppression of mitochondrial oxidative stress results in a prevention of diabetic cardiomyopathy. *J Am Coll Cardiol* (2006) 48(8):1688–97. doi: 10.1016/j.jacc.2006.07.022

18. Bilim O, Takeishi Y, Kitahara T, Arimoto T, Niizeki T, Sasaki T, et al. Diacylglycerol kinase zeta inhibits myocardial atrophy and restores cardiac dysfunction in streptozotocin-induced diabetes mellitus. *Cardiovasc Diabetol* (2008) 7:2. doi: 10.1186/1475-2840-7-2

19. Suga T, Kikuchi O, Kobayashi M, Matsui S, Yokota-Hashimoto H, Wada E, et al. SGLT1 in pancreatic alpha cells regulates glucagon secretion in mice, possibly explaining the distinct effects of SGLT2 inhibitors on plasma glucagon levels. *Mol Metab* (2019) 19:1–12. doi: 10.1016/j.molmet.2018.10.009

20. Sun P, Wang Y, Ding Y, Luo J, Zhong J, Xu N, et al. Canagliflozin attenuates lipotoxicity in cardiomyocytes and protects diabetic mouse hearts by inhibiting the mTOR/HIF-1α pathway. *iScience* (2021) 24(6):102521.

21. Cao R, Fang D, Wang J, Yu Y, Ye H, Kang P, et al. ALDH2 overexpression alleviates high glucose-induced cardiotoxicity by inhibiting NLRP3 inflammasome activation. *J Diabetes Res* (2019) 21:4857921. doi: 10.1155/2019/4857921

22. Zhuang XD, Hu X, Long M, Dong XB, Liu DH, Liao XX, et al. Exogenous hydrogen sulfide alleviates high glucose-induced cardiotoxicity via inhibition of leptin signaling in H9c2 cells. *Mol Cell Biochem* (2014) 391(1-2):147–55. doi: 10.1007/s11010-014-1997-3

23. Berdoukas V, Coates TD, Cabantchik ZI. Iron and oxidative stress in cardiomyopathy in thalassemia. *Free Radic Biol Med* (2015) 88:3–9. doi: 10.1016/j.freeradbiomed.2015.07.019

24. Fang X, Wang H, Han D, Xie E, Yang X, Wei J, et al. Ferroptosis as a target for protection against cardiomyopathy. *Proc Natl Acad Sci U.S.A.* (2019) 116(7):2672–80. doi: 10.1073/pnas.1821022116

25. Dixon SJ, Lemberg KM, Lamprecht MR, Skouta R, Zaitsev EM, Gleason CE, et al. Ferroptosis: an iron-dependent form of nonapoptotic cell death. *Cell* (2012) 149(5):1060–72. doi: 10.1016/j.cell.2012.03.042

26. Shirpoor A, Salami S, Khadem-Ansari MH, Ilkhanizadeh B, Pakdel FG, Khademvatani K, et al. Cardioprotective effect of vitamin e: rescues of diabetes-

induced cardiac malfunction, oxidative stress, and apoptosis in rat. *J Diabetes Complications* (2009) 23(5):310–6. doi: 10.1016/j.jdiacomp.2008.02.009

27. Huynh K, Kiriazis H, Du XJ, Love JE, Jandeleit-Dahm KA, Forbes JM, et al. Coenzyme Q10 attenuates diastolic dysfunction, cardiomyocyte hypertrophy and cardiac fibrosis in the db/db mouse model of type 2 diabetes. *Diabetologia* (2012) 55(5):1544–53. doi: 10.1007/s00125-012-2495-3

28. Guo R, Liu W, Liu B, Zhang B, Li W, Xu Y, et al. SIRT1 suppresses cardiomyocyte apoptosis in diabetic cardiomyopathy: An insight into endoplasmic reticulum stress response mechanism. *Int J Cardiol* (2015) 191:36–45. doi: 10.1016/j.ijcard.2015.04.245

29. Zhang M, Zhang L, Hu J, Lin J, Wang T, Duan Y, et al. MST1 coordinately regulates autophagy and apoptosis in diabetic cardiomyopathy in mice. *Diabetologia* (2016) 59(11):2435–47. doi: 10.1007/s00125-016-4070-9

30. Suzuki Y, Kaneko H, Okada A, Itoh H, Matsuoka S, Fujiu K, et al. Comparison of cardiovascular outcomes between SGLT2 inhibitors in diabetes mellitus. *Cardiovasc Diabetol* (2022) 21(1):67. doi: 10.1186/s12933-022-01508-6

31. Ghanim H, Abuaysheh S, Hejna J, Green K, Batra M, Makdissi A, et al. Dapagliflozin suppresses hepcidin and increases erythropoiesis. *J Clin Endocrinol Metab* (2020) 105(4):57. doi: 10.1210/clinem/dgaa057

32. Ferrannini E, Murthy AC, Lee YH, Muscelli E, Weiss S, Ostroff RM, et al. Mechanisms of sodium-glucose cotransporter 2 inhibition: Insights from Large-scale proteomics. *Diabetes Care* (2020) 43(9):2183–9. doi: 10.2337/dc20-0456

33. Wei XB, Wei W, Ding LL, Liu SY. Comparison of the effects of 10 GLP-1 RA and SGLT2 inhibitor interventions on cardiovascular, mortality, and kidney outcomes in type 2 diabetes: A network meta-analysis of large randomized trials. *Prim Care Diabetes* (2021) 15(2):208–11. doi: 10.1016/j.pcd.2020.08.017

34. Wei D, Liao L, Wang H, Zhang W, Wang T, Xu Z, et al. Canagliflozin ameliorates obesity by improving mitochondrial function and fatty acid oxidation *via* PPARα *in vivo* and *in vitro*. *Life Sci* (2020) 247:117414. doi: 10.1016/j.lfs.2020.117414

35. Yang X, Liu Q, Li Y, Tang Q, Wu T, Chen L, et al. The diabetes medication canagliflozin promotes mitochondrial remodelling of adipocyte *via* the AMPK-Sirt1-Pgc-1α signalling pathway. *Adipocyte* (2020) 9(1):484–94. doi: 10.1080/21623945.2020.1807850

36. Shi H, Zeng Q, Wei Y, Yang H, Tang H, Wang D, et al. Canagliflozin is a potential cardioprotective drug but exerts no significant effects on pirarubicininduced cardiotoxicity in rats. *Mol Med Rep* (2021) 24(4):703.

37. Xue F, Cheng J, Liu Y, Cheng C, Zhang M, Sui W, et al. Cardiomyocyte-specific knockout of ADAM17 ameliorates left ventricular remodeling and function in diabetic cardiomyopathy of mice. *Signal Transduct Target Ther* (2022) 7(1):259. doi: 10.1038/s41392-022-01054-3

38. Lim VG, Bell RM, Arjun S, Kolatsi-Joannou M, Long DA, Yellon DM., et al. SGLT2 inhibitor, canagliflozin, attenuates myocardial infarction in the diabetic and nondiabetic heart. *JACC Basic Transl Sci* (2019) 4(1):15–26. doi: 10.1016/j.jacbts.2018.10.002

39. Wang Y, Feng F, He W, Sun L, He Q, Jin J, et al. miR-188-3p abolishes germacrone-mediated podocyte protection in a mouse model of diabetic nephropathy in type I diabetes through triggering mitochondrial injury. *Bioengineered* (2022) 13(1):774–88. doi: 10.1080/21655979.2021.2012919

40. Ding M, Feng N, Tang D, Feng J, Li Z, Jia M, et al. Melatonin prevents Drp1-mediated mitochondrial fission in diabetic hearts through SIRT1-PGC1α pathway. *J Pineal Res* (2018) 65(2):e12491.

41. Li L, Luo W, Qian Y, Zhu W, Qian J, Li J, et al. Luteolin protects against diabetic cardiomyopathy by inhibiting NF-kappaB-mediated inflammation and activating the Nrf2-mediated antioxidant responses. *Phytomedicine* (2019) 59:152774. doi: 10.1016/j.phymed.2018.11.034

42. Ingold I, Berndt C, Schmitt S, Doll S, Poschmann G, Buday K, et al. Selenium utilization by GPX4 is required to prevent hydroperoxide-induced ferroptosis. *Cell* (2018) 172(3):409–22. doi: 10.1016/j.cell.2017.11.048

43. Doll S, Proneth B, Tyurina YY, Panzilius E, Kobayashi S, Ingold I, et al. ACSL4 dictates ferroptosis sensitivity by shaping cellular lipid composition. *Nat Chem Biol* (2017) 13(1):91–8. doi: 10.1038/nchembio.2239

44. Wang S, Ding Y, Dong R, Wang H, Yin L, Meng S. Canagliflozin improves liver function in rats by upregulating asparagine synthetase. *Pharmacology* (2021) 106(11-12):606–15. doi: 10.1159/000518492

45. Song Z, Zhu J, Wei Q, Dong G, Dong Z. Canagliflozin reduces cisplatin uptake and activates akt to protect against cisplatin-induced nephrotoxicity. *Am J Physiol Renal Physiol* (2020) 318(4):F1041–52. doi: 10.1152/ajprenal.00512.2019

46. Tu H, Tang LJ, Luo XJ, Ai KL, Peng J. Insights into the novel function of system xc- in regulated cell death. *Eur Rev Med Pharmacol Sci* (2021) 25(3):1650–62.

47. Bayeva M, Khechaduri A, Puig S, Chang HC, Patial S, Blackshear PJ, et al. mTOR regulates cellular iron homeostasis through tristetraprolin. *Cell Metab* (2012) 16(5):645–57. doi: 10.1016/j.cmet.2012.10.001

48. Goyal I, Sattar A, Johnson M, et al. Adjunct therapies in treatment of type 1 diabetes. *J Diabetes* (2020) 12(10):742–53. doi: 10.1111/1753-0407.13078

Frontiers in Endocrinology

Explores the endocrine system to find new therapies for key health issues The second most-cited endocrinology and metabolism journal, which advances our understanding of the endocrine system. It uncovers new therapies for prevalent health issues such as obesity, diabetes, reproduction, and aging.

Discover the latest Research Topics

See more →

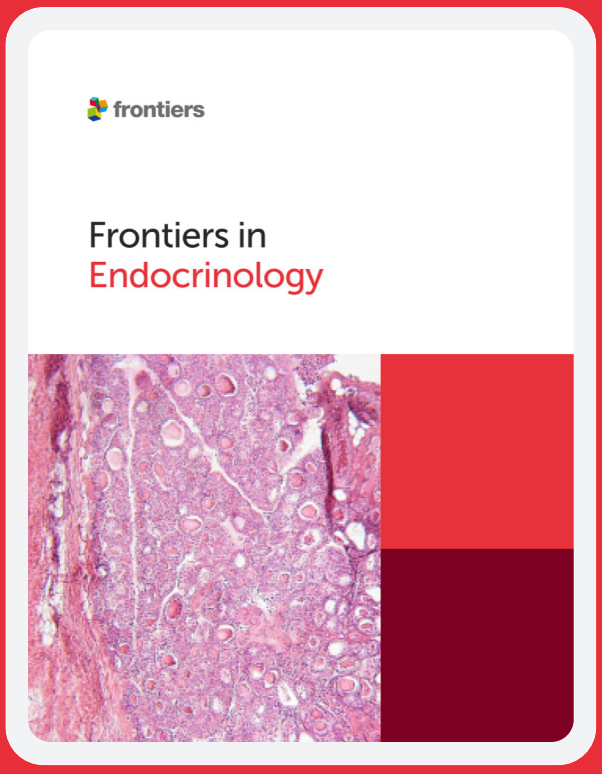

Frontiers

Avenue du Tribunal-Fédéral 34
1005 Lausanne, Switzerland
frontiersin.org

Contact us

+41 (0)21 510 17 00
frontiersin.org/about/contact